이학박사학위논문

mRNA-단백질 상호작용에 대한 시계열 분석

Time-resolved profiling of mRNA-protein interaction through the mRNA life cycle

2023년 8월

서울대학교 대학원

생명과학부

엄부연

이학박사학위논문

mRNA-단백질 상호작용에 대한 시계열 분석

Time-resolved profiling of mRNA-protein interaction through the mRNA life cycle

2023년 8월

서울대학교 대학원

생명과학부

엄부연

Time-resolved profiling of mRNA-protein interaction through the mRNA life cycle

Advisor: Professor V. Narry Kim

Submitting a doctoral thesis of philosophy
August, 2023

Graduate School of Seoul National University
School of Biological Sciences
Buyeon Um

Confirming the doctoral thesis written by Buyeon Um
June, 2023

Chair	Yoo-Sun Noh	(seal)
Vice Chair	Vic Narry Kim	(seal)
Examiner	Yoosik Kim	(seal)
Examiner	Hyeshik Chang	(seal)
Examiner	Hyun-Woo Rhee	(seal)

Abstract

Time-resolved profiling of mRNA-protein interaction through the mRNA life cycle

Buyeon Um
School of Biological Sciences
The Graduate School
Seoul National University

mRNAs continually change their protein partners throughout their life cycle, yet our understanding of mRNA-protein complexes (mRNPs) is limited by a lack of temporal information. Here, we present time-resolved mRNA interactome data by combining pulse metabolic labeling with photoactivatable ribonucleoside, UVA crosslinking, poly(A)+ RNA isolation, and mass spectrometry. This approach allows the quantification of over 700 mRNA-binding proteins (mRBPs) across ten distinct time points.

The chronological orders of RNA binding were consistent with the known functions, subcellular localizations and protein-protein interactions of the RBPs. Stress granule proteins were found to be enriched in "aged" mRNPs, implying their roles in the terminal stages of the mRNA life cycle. Many late binding RBPs were previously known as viral RBPs, suggesting their regulatory activities on viruses. We also built a computational model to systematically identify RBPs with unexpected binding dynamics based on their Gene Ontology annotations, indicating that they may have some unknown functions. We identify numerous mRBPs with unexpected dynamics, implying undiscovered functions and regulatory mechanisms. For data exploration, we have developed a web application available at chronology.rna.snu.ac.kr. By introducing a time dimen-

sion, this study offers a unique resource and insights into mRNP remodeling.

Keywords: mRNA; RNA-binding proteins; mRNP remodeling; Time-resolved mRNA interactome

Student ID: 2017-28623

Contents

List of Figures

List of Tables

Nomenclature

3' UTR	3' untranslated region
4sU	4-thio-uridine
5' UTR	5' untranslated region
6sG	6-thioguanosine
BP	Biological process
CC	Cellular component
CDS	coding sequence
GO term	Gene ontology term
hnRNP	heterogeneous nuclear ribonucleoprotein
HPLC	High-performance liquid chromatography
LC-MS	liquid chromatography and mass spectrometry
MCA	multiple corresponcence analysis
mRBP	mRNA-binding protein
mRNP	mRNA-protein complex
NMD	nonsense mediated decay

PABP	poly(A) binding protein
PAR-crosslinking	Photoactivatable ribonucleoside (PAR)-enhanced crosslinking
PPI	protein-protein interaction
RBD	RNA binding domain
RIC	RNA interactome capture
RIP	RNA immunoprecipitation
SG	stress granule
vRBP	viral RNA binding protein

1. Introduction

1.1 Life cycle of mRNA and its protein complexes

The life cycle of eukaryotic mRNA involves several distinct stages: transcription, pre-mRNA processing, nuclear export, translation, and decay. After transcription by RNA polymerase II, mRNA undergoes several processing steps, including 5´ capping, splicing, 3´ end cleavage, and polyadenylation. Once processed, the mRNA is exported from the nucleus to the cytoplasm. In the cytoplasm, mRNAs interact with translational initiation factors, facilitating 40S ribosome complex recruitment. After translation, poly(A) tail of mRNA is shortened by deadenylases. Following deadenylation, the mRNA can be subjected to decapping, exposing the mRNA to degradation (66) (Figure 1.1).

In each stage, mRNA interacts with a specific set of RNA binding proteins (RBPs) to form mRNA-protein complexes (mRNPs) (66; 52). These RBPs govern the activity, localization, and stability of mRNA, and influence its transition to the subsequent stage of the life cycle. Therefore, unveiling the stage-specific repertoire of RBPs is vital for understanding mRNA regulation.

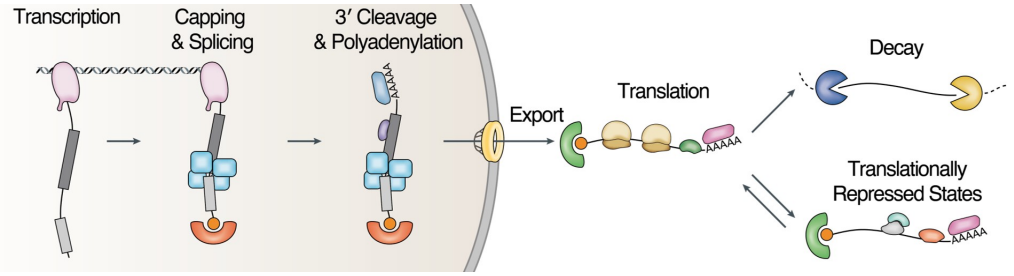

Figure 1.1 Life cycle of mRNA.

Since mRNP was first observed in the 1950s, many researchers have biochemically purified mRNPs and discovered core mRNP components, such as cap-binding proteins, heterogeneous nuclear ribonucleoproteins (hnRNPs), serine/arginine-rich (SR) splicing factors, and poly(A) binding proteins (PABPs) (22; 15; 66).

1.2 RNA interactome capture (RIC)

Studies have explored the interaction between mRNAs and RBPs comprehensively, employing high-throughput approaches such as the RNA interactome capture (RIC) (Figure 1.2). In RIC experiments, RNA-protein partners are first crosslinked either with UV light or chemical crosslinkers, followed by RNP enrichment methods such as oligo-dT capture, protein extraction, liquid chromatography and mass spectrometry (LC-MS) (10; 5). MS-based techniques collectively reported more than 6000 human proteins as potential RBPs (11), and it is believed that the human genome encodes at least 1,542 RBPs (24). These methods have been applied to numerous biological contexts, revealing the diverse biological roles of RBPs (69; 23; 57; 87).

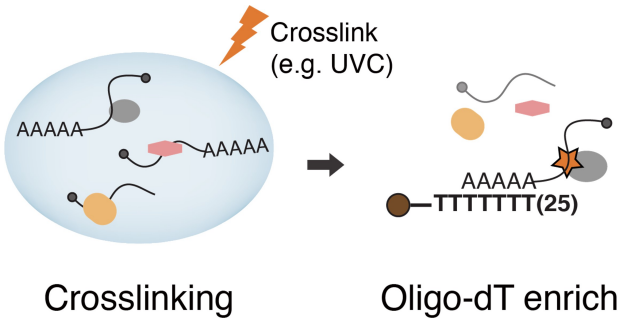

Figure 1.2 RNA interactome capture (RIC).

1.3 Photoactivatable Ribonucleoside (PAR) -enhanced crosslinking

PAR-crosslinking, also known as Photoactivatable Ribonucleoside-enhanced crosslinking, is a technique utilized to investigate RNA-protein interactions. Unlike crosslinking methods that use short-wavelength UV light, PAR-crosslinking employs modified ribonucleosides, such as 4-thio-uridine (4sU) and 6-thioguanosine (6sG), which can be photoactivated by UV light more efficiently. This photoactivation leads to the formation of covalent crosslinks between the RNA and the proteins in close proximity (Figure 1.3).

The photoactivatable ribonucleosides, such as 4sU, are specifically excited by long-wavelength UV light, typically around 365nm, which is in the UVA light range. Natural nucleotides are not excited by this wavelength. When the photoactivatable ribonucleosides are exposed to UVA light, the sulphur atom within them is released, forming photoadducts with amino acid side chains of nearby proteins. Amino acids with aromatic rings, such as phenylalanine, tyrosine, and tryptophan, as well as other amino acids like lysine and cysteine, can undergo PAR-crosslinking. The loss of the sulphur atom in 4sU during crosslinking causes the crosslinked 4sU to be recognized as a C during reverse transcription (4).

By employing PAR-crosslinking, researchers can capture and identify RNA-protein interactions in a spatially and temporally controlled manner. The technique

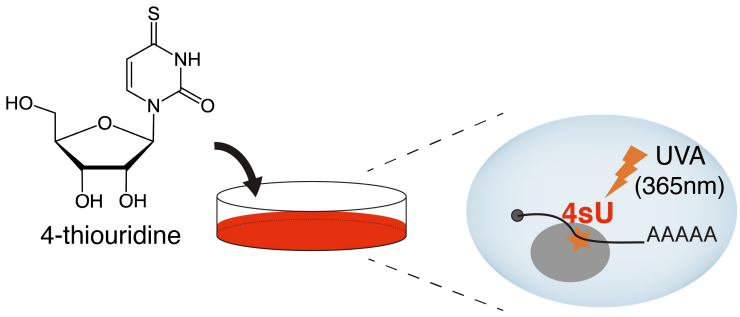

Figure 1.3 Photoactivatable Ribonucleoside-enhanced crosslinking.

enables the study of dynamic RNA-protein interactions, providing valuable insights into the roles of specific proteins in RNA-related processes (5).

2. Chronological profiling of mRNA-protein interaction

2.1 Background

While the previous approaches greatly advanced our knowledge of RNA-protein interactions, their limitation lies in providing unsynchronized mixed pools of mRNPs without temporal resolution. Since mRNPs involved in distinct stages of the mRNA life cycle (e.g. co-transcriptional processing vs. translating) are expected to be fundamentally different from each other, there is a need to collect and analyze mRNPs specific to each stage. Time-resolved profiling would help reveal the compositional changes in mRNPs throughout the mRNA life cycle, offering a more comprehensive understanding of RBP functions. An earlier study examined nascent RNPs by using 5-ethynyluridine labeling followed by click chemistry-based RNA capture, but this approach mainly yielded proteins bound to abundant noncoding RNAs and had a limited temporal resolution (0.5, 2, and 16 hours) (6).

In this study, we aimed to investigate the remodeling of mRNPs over time by developing a time-resolved RNA interactome capture technique. We enriched mRNAs of specific "ages" using pulse-chase metabolic labeling with 4sU and selective crosslinking under 365 nm light (UVA) across 10 time points (28; 42). This longitudinal analysis revealed the RNA binding dynamics of 734 mRBPs. We further integrated these temporal RNA interaction data with subcellular localization, protein-protein interaction, RNA granule formation, viral RNA interaction, and gene ontology data to identify RBPs with as-yet-unknown functions and provide new insights into mRNP remodeling. The chronological data of mRNA-protein interaction from this study can be accessed at: https://chronology.rna.snu.ac.kr/

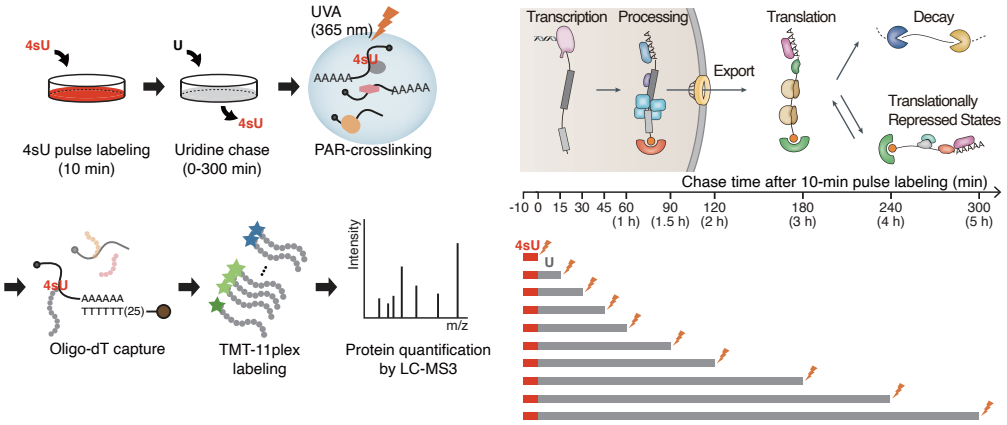

Figure 2.1 Experimental scheme. (A) Schematic of modified RIC for time-resolved mRNP capture. (B) Design of high-temporal resolution mRNP pulse-chase labeling using 4sU and U nucleosides.

2.2 Results

2.2.1 Time-resolved mRNA interactome profiling using RIC with 4sU pulse-labeling

To identify RBPs that associate with mRNAs at specific time points following RNA synthesis, I employed a pulse-labeling approach (Figure 2.1). HeLa cells were metabolically labeled with 4sU for 10 minutes, which is the shortest period yielding sufficient amounts of crosslinked materials needed for our proteomic analyses. This short duration of labeling did not notably affect cell viability (data not shown) or the transcriptome as determined by RNA-seq (Figure 2.2). After a washing procedure and chasing with unmodified uridine until the required time points, cells were exposed to UVA irradiation (365 nm) to induce photoactivatable ribonucleoside (PAR)-enhanced crosslinking between 4sU-labeled RNA and its associated proteins. We selected ten time points, spanning from 0 to 5 hours (0, 15, 30, 45, 60, 90, 120, 180, 240, and 300 min), which likely cover most stages of the mRNA life cycle, considering the median half-life of human mRNAs is 3.4 hours (average half-life, 6.9 hours) (73). For control, we omitted 4sU labeling ("no-4sU") to identify non-specific proteins and assess background levels.

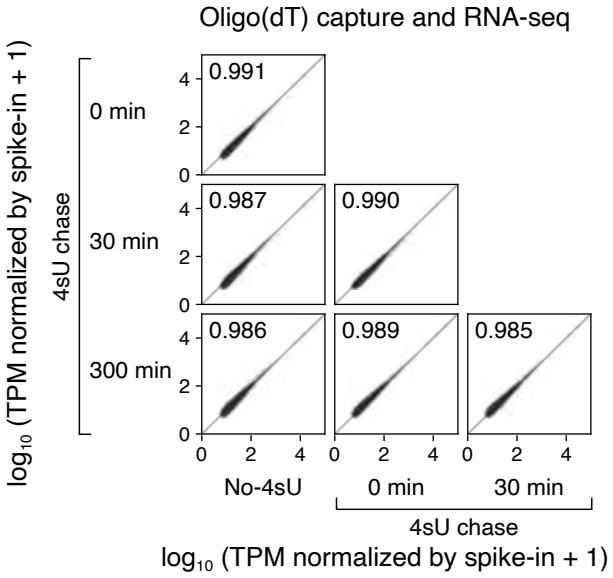

Figure 2.2 mRNA expression was not influenced substantially by 10-min 4sU treatment, as analyzed by RNA-seq. "No-4sU" refers to the oligo(dT) captured RNA population from unlabeled cells. The "4sU chase (0, 30, 300 min)" category corresponds to the oligo(dT) captured RNA populations from cells that were pulse-labeled with 4sU for 10 minutes and then chased with unmodified uridine for the respective time period. The Pearson's correlation coefficient for each sample-sample pair is indicated. The thin gray line represents the line of identity (y=x).

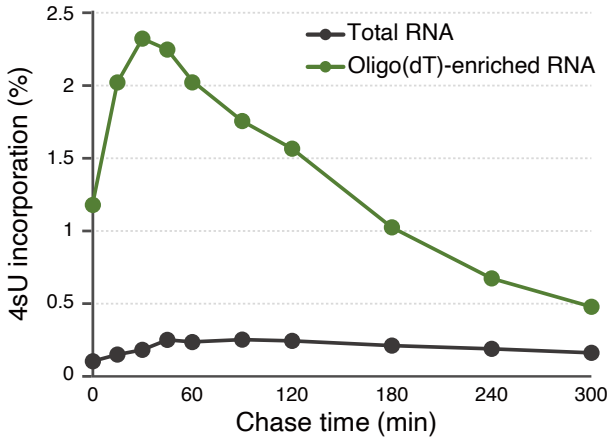

Figure 2.3 Proportion of 4sU relative to total U as measured by HPLC after single nucleotide digestion, using total RNA (black) or oligo(dT)-enriched RNA (green).

To estimate the 4sU incorporation rate under our conditions, I digested RNA into single nucleosides and analyzed them by high-performance liquid chromatography (HPLC) (Figure 2.3).[1] Immediately after the 10-minute labeling period (chase time=0 min), 4sU constituted approximately 1.2% of total uridines in the oligo(dT)-captured RNAs. The 4sU fraction increased to 2.3% within the next 30 minutes, likely because of residual intracellular 4sU and delayed phosphorylation of 4sU into 4sUTP (16). Subsequently, this 4sU fraction decreased likely because of intron removal and decay of labeled transcripts. These findings suggest that our pulse-chase conditions labeled approximately 2% of uridine residues, which corresponds to about ten 4sU incorporated per an mRNA molecule of 2 kb. Labeling occurs within a relatively narrow time window of about 30-40 minutes, without substantially affecting cell physiology.

Silver-staining of captured proteins revealed a peak at 30 min point, which gradually decreased over time, mirroring the pattern of 4sU incorporation into RNA (Figure 2.4). Protein bands were barely visible in the unlabeled negative control, indicating robust enrichment of PAR-crosslinked RBPs. The seized

[1] HPLC were performed by Dr. Yongwoo Na

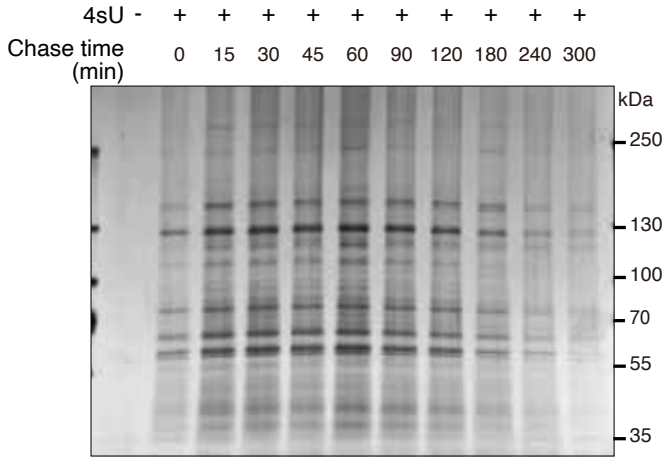

Figure 2.4 Silver staining visualizing the proteins eluted in the RIC experiments.

proteins were digested with trypsin, labeled with TMT 11-plex, and analyzed using LC-MS3 (74; 76). Protein quantities from triplicate samples were tested for enrichment against the unlabeled control (Figure 2.5).[2]

We determined "confidently quantified RBPs" based on two criteria: enrichment over unlabeled control and reproducibility across replicates (Figure 2.6 and Methods). This analysis yielded 801 confidently quantified proteins. To examine the specificity of our method in identifying RBPs, we compared our confidently quantified proteins with previously identified RBPs (11). More than 90% (734/801) of the confidently quantified proteins from our study were previously reported as mRNA interactors, and >80% of them were annotated with "RNA binding" Gene Ontology (GO) term (Figure 2.7). Regarding domains, we found 58 Pfam domains significantly enriched over all human proteins at a false discovery rate (FDR) of 1% (19) (Figure 2.8 and Methods). The majority of these enriched domains (35 out of 58), such as RRM, Helicase C, DEAD, and KH, have been experimentally verified as RNA binding domains (RBDs) or enriched in previous

[2]Jeesoo Kim generated the LC-MS3 data. All the bioinformatic analyses were done by Dr. Yeon Choi

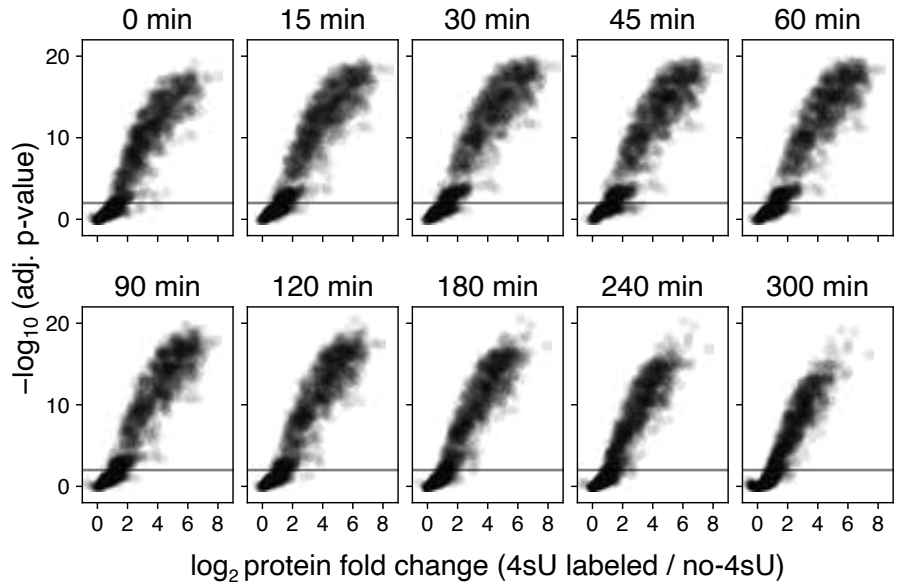

Figure 2.5 Volcano plots of protein differential expression, between no-4sU and 4sU labeled samples. The protein quantities were measured as TMT reporter ion intensities in triplicate. Fold changes between the no-4sU and 4sU-labeled samples were calculated, log2 transformed, and then averaged to obtain the log2 fold changes. P-values were determined using the DEqMS R library and adjusted by the Benjamini-Hochberg method.

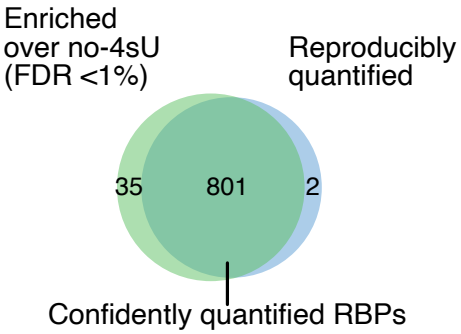

Figure 2.6 Venn diagram showing the number of proteins enriched over the control (no-4sU) and of those that are reproducibly quantified.

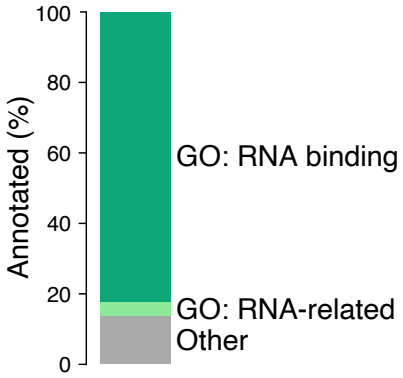

Figure 2.7 Gene Ontology (GO) annotations of the confidently quantified RBPs (n=801). RNA-related GO term was defined as any GO term containing 'RNA'.

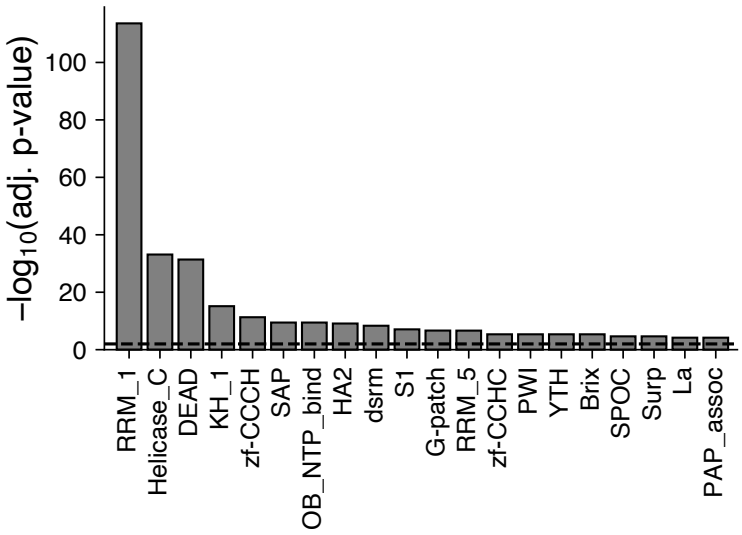

Figure 2.8 Top 20 enriched Pfam protein domains among the confidently quantified proteins (n=801). P-values were calculated by Fisher's exact test and adjusted by Benjamini-Hochberg method. Dashed line indicates an adjusted p-value of 0.01.

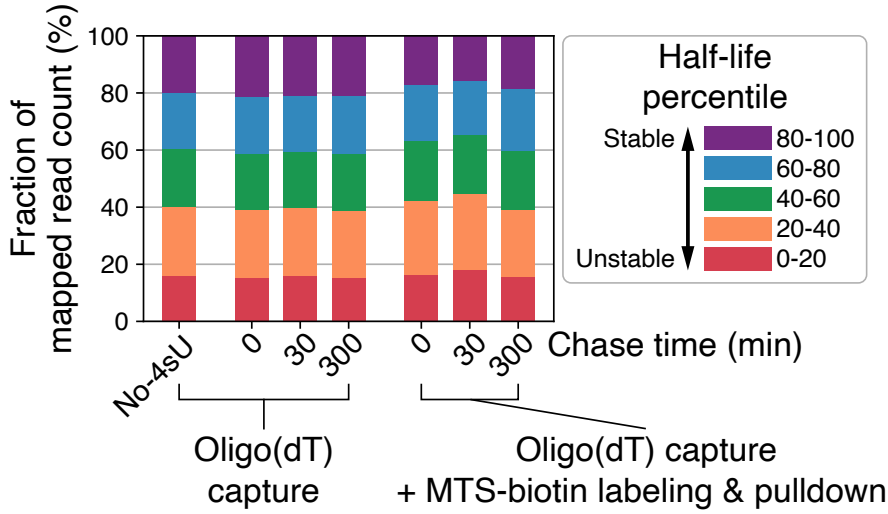

Figure 2.9 Fraction of RNA-seq read counts mapped to mRNAs within each half-life range. mRNA half-lives in HeLa cells were determined by (73). "Oligo(dT)" refers to the same RNA-seq experiments used in panel (A). "Oligo(dT) capture + MTS-biotin labeling & pulldown" means that the olido(dT) captured RNAs were subsequently treated with methylthiosulfonate-biotin, which labels 4sU, and precipitated with streptavidin beads.indicates RNAs labeled by 4sU for 10 minutes and then chased with unmodified uridine, which resembles the mRNA population captured in our RIC experiment. For these samples, oligo(dT) capture followed by methylthiosulfonate-biotin (MTS-biotin) pulldown was applied, to enrich the 4sU labeled RNAs.

RIC studies (10) (Table 2.1). Collectively, these results indicate that our method successfully captured RBPs.

To monitor the differences in the captured RNA populations over time, I performed RNA-seq on oligo(dT)-captured RNAs with an extra precipitation step which isolates 4sU-labeled RNAs. Comparing chase times 0 and 300 min (Figure 2.9), we observed only a modest reduction (from 16.5% to 15.5% in read proportion) of of unstable mRNAs (bottom 20% in half-life) and a slight increase (from 17.1% to 18.6% in read proportion) of stable mRNAs (top 20% in half-life).

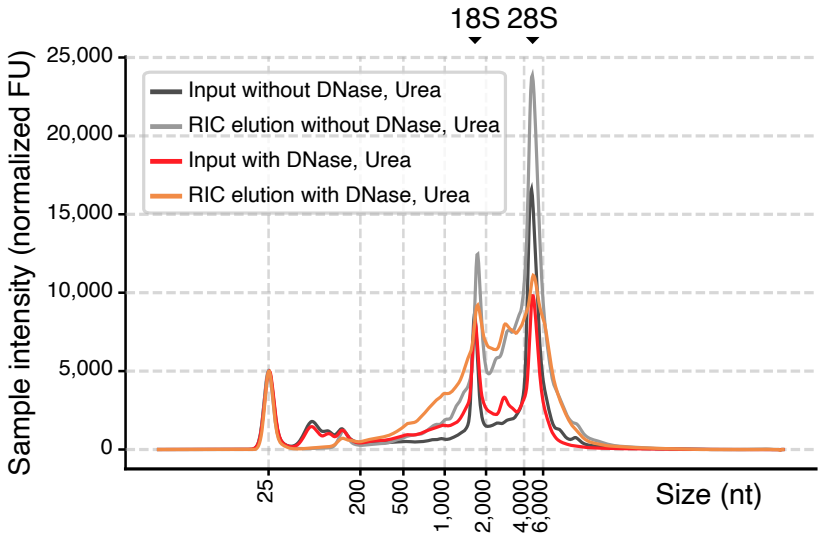

Figure 2.10 Electrophoreogram graphs of RNAs obtained using the conventional RNA interactome capture (RIC) method (without DNase treatment or urea lysis) and the modified RIC method (with DNase treatment and urea lysis), analyzed by Tapestation 4150. The input sample refers to the total RNA extracted using Trizol with or without DNase and urea, and used for RIC. FU indicates fluorescence units. Black triangles indicate the size of 18S and 28S rRNAs.

The majority (97.5%) of genes observed at 0 min remained detectable until 300 min (TPM>1), indicating that our experimental conditions represent the majority of mRNA species although we do not exclude a possibility that differential mRNA decay rates influence the mRBP repertoire over time to some extent.

Our RNA-seq data also showed that some RNAs with oligo(A) tails such as mitochondrial mRNAs and long noncoding RNAs, as well as abundant RNAs were partially precipitated (Figures 2.10 and 2.11) although our method enriched poly(A)+ mRNAs via oligo(dT) capture under a stringent condition with 4M urea and DNase treatment. Our list of RBPs contains 65 mitochondrial RBPs and 65 noncoding RNA-related proteins with established roles in snoRNA and rRNA

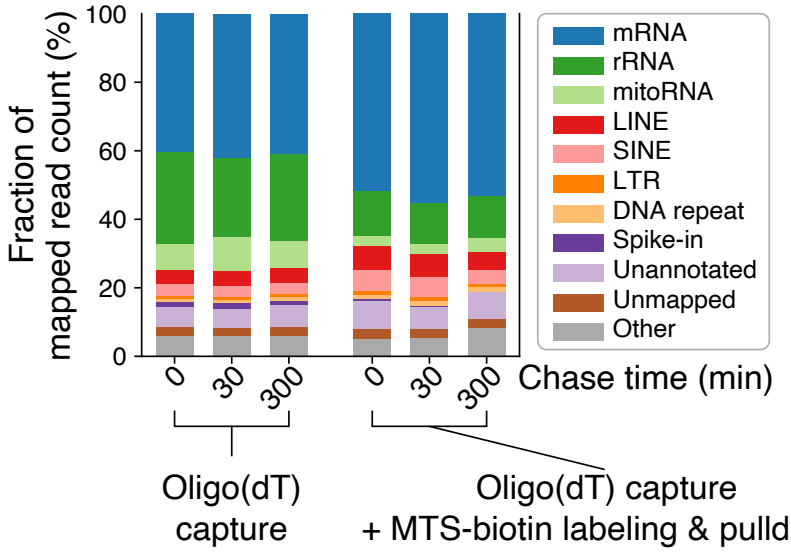

Figure 2.11 Fraction of RNA-seq read counts mapped to each RNA class. "Oligo(dT)" and "MTS-biotin labeling & pulldown + oligo(dT) capture" are the same as in 2.9.

processing. While their RNA binding dynamics may provide interesting insights into the noncoding RNA biogenesis pathways, and they could potentially have roles in the mRNA pathway, we excluded these proteins from further analysis due to our study's focus on nuclear genome-encoded mRNAs.

2.2.2 High-resolution profiling of RNA-binding dynamics

To investigate the mRNA binding dynamics of each RBP, we merged normalized protein quantities using a univariate spline (Figure 2.12). We defined the "peak binding time" for each RBP as the moment when the spline curve hits its maximum (Figure 2.12). This approach facilitated a quantitative comparison of the binding dynamics among RBPs. It should be noted that this "peak binding time" is actually delayed by approximately 30 minutes from the true maximal binding time due to the persistence of 4sU labeling after washing, as mentioned above.

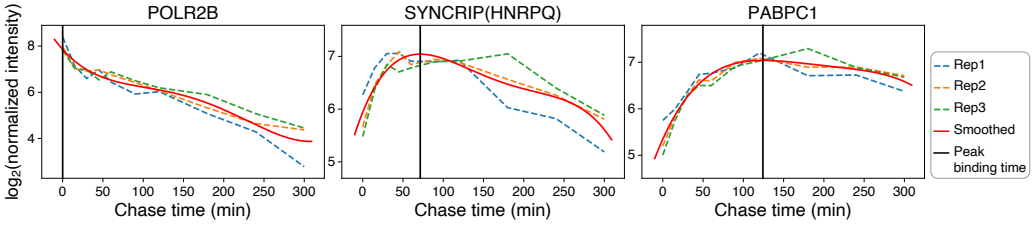

Figure 2.12 Processing of the mRNA binding dynamics from triplicated TMT intensities. Initially, the protein quantity of the no-4sU sample was subtracted from the quantity in the given sample at each time point to eliminate background levels. Subsequently, quantities from triplicates were normalized to achieve equal total quantities, and merged using a univariate spline. The peak binding time was determined from the resulting spline curve.

I initially examined representative RBPs with well-established roles (Figure 2.13). Subunits of RNA polymerase II (POLR2A and POL2R2B) exhibited the highest level of interaction at chase time 0 min, then swiftly declined, along with other transcription-related factors such as SUPT5H, SSRP1, SCAF8 (Figure 2.13A). Subsequently, pre-mRNA processing factors involved in 5´ capping, splicing, and 3´ end processing emerged (Figure 2.13B). Notably, some of the 3´ cleavage and polyadenylation factors (such as CSTF3, CSTF2T, and FIP1L1) are recruited even earlier than cap binding protein CBP20 (also known as NCBP2) and splicing factors. This concurs with the notion that premature 3´ cleavage and transcriptional termination are pervasive, and that short transcripts are extensively produced (35). Promoter-proximal polyadenylation sites are frequent in the antisense orientation from the promoter, leading to the generation of upstream short antisense transcripts (3), which may also partially explain the early association of the 3´-processing factors in our experiment.

The binding of the nuclear export factor (NXF1) and the TRanscription-EXport complex (TREX) components aligned with the replacement of nuclear PABP (PABPN1) by cytoplasmic PABPs (PABPC1 and PABPC4), reflecting mRNP remodeling during nuclear export (Figure 2.13C and 2.14). Translation factors like EIF4G and PABPC bind to mRNA between 1.5 and 4 hours (Figure

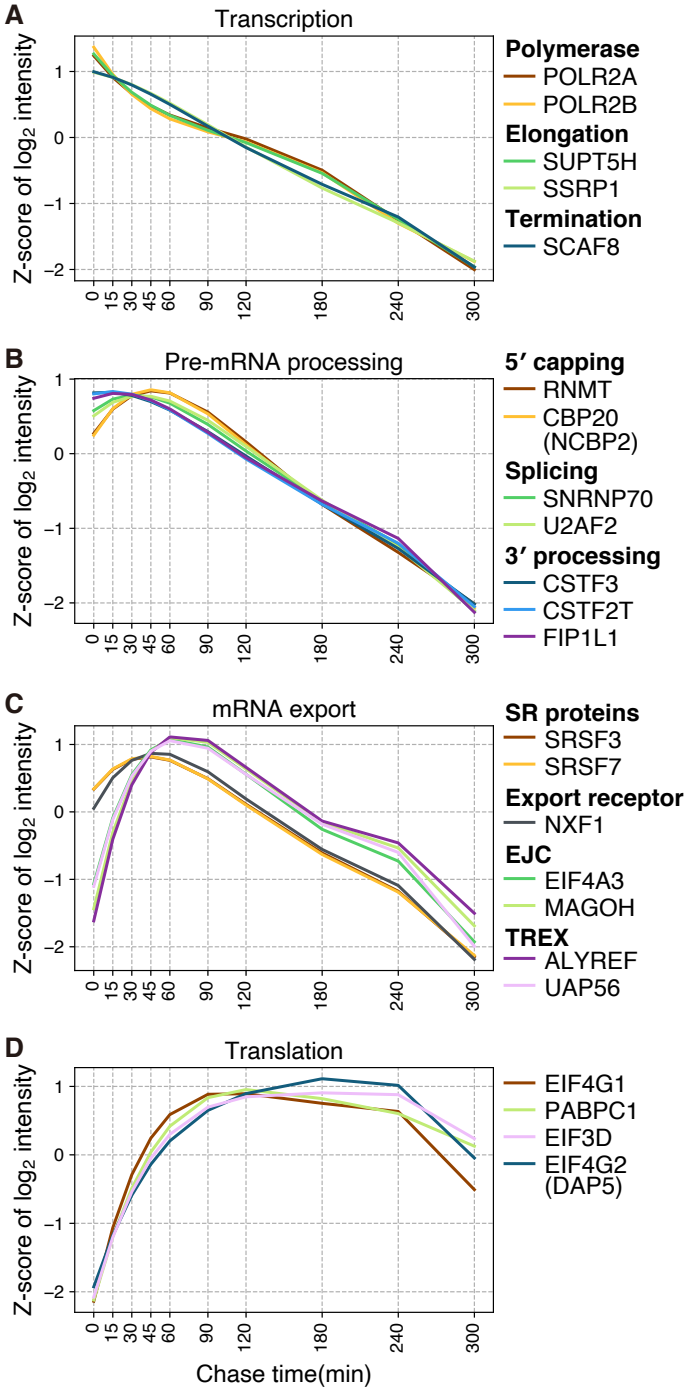

Figure 2.13 (A-D) mRNA binding dynamics of RBPs known to participate in mRNA transcription (A), pre-mRNA processing (B), mRNA nuclear export (C), and translation (D).

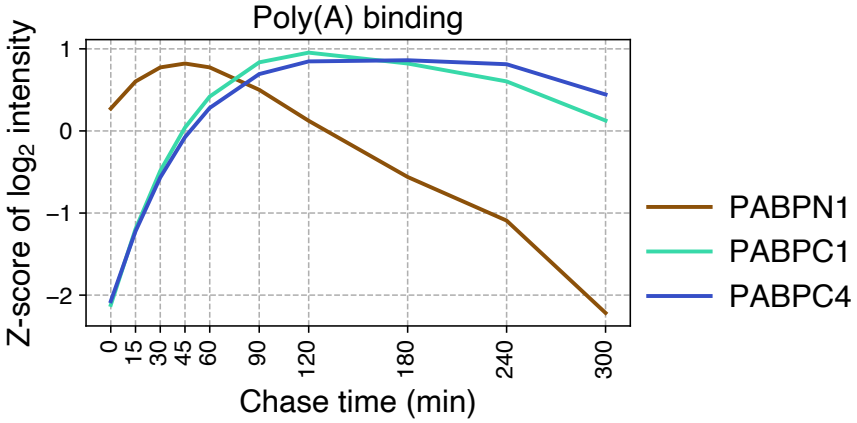

Figure 2.14 mRNA binding dynamics of poly(A) binding proteins

2.13D). The canonical cap binding protein in the cytoplasm, EIF4E, was not detected, possibly due to its low abundance and low crosslinkability. An alternative cap binding protein, EIF3D, was detected alongside its cofactor EIF4G2/DAP5, exhibiting slightly delayed dynamics compared with EIF4G, which may reflect their preferential binding to aged mRNAs or stable mRNAs.

The high temporal resolution of our data allowed us to observe even subtle differences in RNA interaction. For instance, HnRNPs and SR proteins, which bind and regulate pre-mRNAs, showed strikingly similar dynamics (Figures 2.15 and 2.16), indicating their primary function as general constituents of nuclear pre-mRNPs, even though some can shuttle between the nucleus and cytoplasm. One notable exception was HNRPQ (also known as hnRNP Q or SYNCRIP), detected at a substantially later time point than the other hnRNPs. This observation supports previous findings that HNRPQ/SYNCRIP modulates mRNA translation and decay (68; 82) (Figure 2.15). Furthermore, the core components of the exon junction complex (EJC) such as EIF4A3, RBM8A/Y14, and MAGOH precede CASC3/MLN51/BTZ, which is not essential for EJC formation and is mainly located in the cytoplasm, and PYM1, which functions in EJC recycling in the cytoplasm (63) (Figure 2.17).

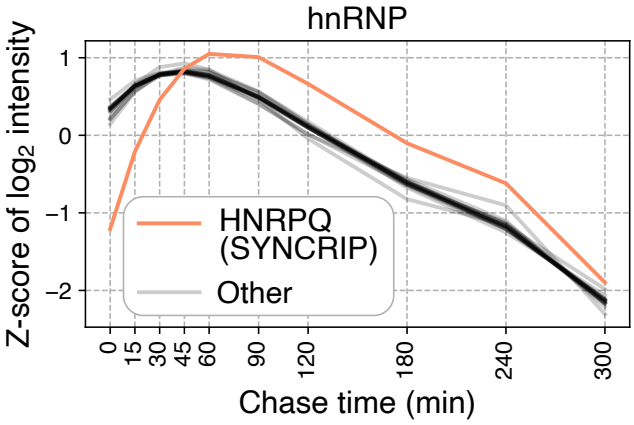

Figure 2.15 mRNA binding dynamics of hnRNP proteins

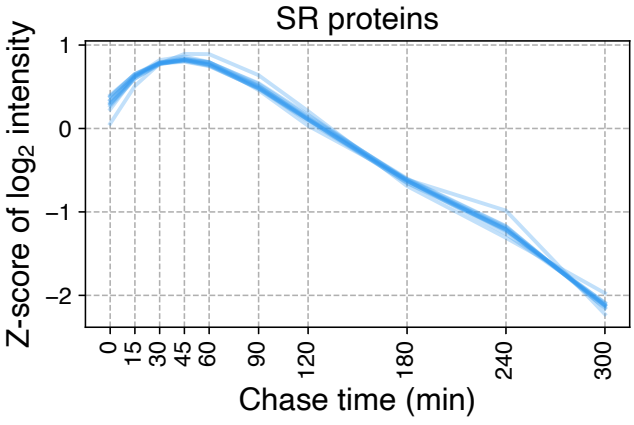

Figure 2.16 mRNA binding dynamics of SR proteins

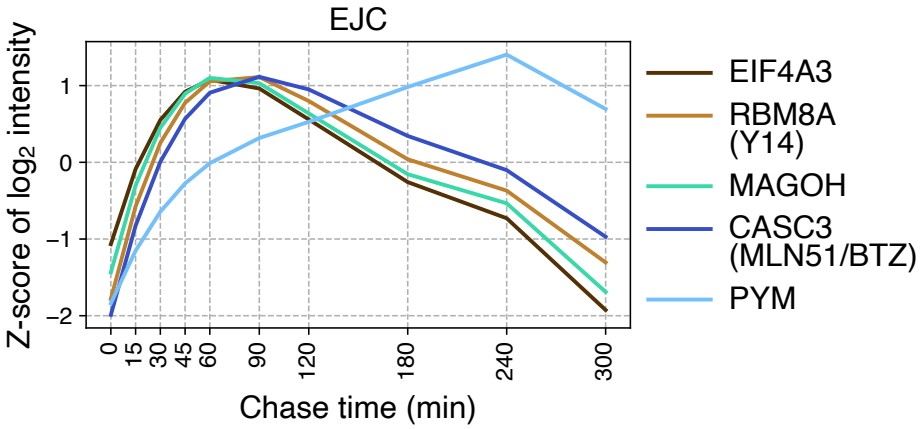

Figure 2.17 mRNA binding dynamics of EJC proteins

Moreover, proteins involved in splicing demonstrated a cascade of RNA association/dissociation (Figure 2.18), overall consistent with the known sequence of spliceosome assembly/disassembly, starting with the U1 and U2 snRNP components and proteins recruited to A complex, followed by the U4/U6.U5 tri-snRNP components and proteins recruited to B, B_{act}, and C complexes (Figure 2.18). Factors involved in m6A modification present another notable example of dynamic mRNA interaction (Figure 2.19); the nuclear writer complex components (RBM15 and ZC3H13) are followed by the nuclear reader (YTHDC1), nuclear eraser (ALKBH5), and cytoplasmic readers (e. g. YTHDC2, YTHDF1, YTHDF2, and YTHDF3) (21; 34) (Figure 2.19).

Our data also show the mRNA binding dynamics of proteins associated with human diseases; for instance, TDP43, EWS, TAF15, FUS, and hnRNPA1 implicated in Amyotrophic Lateral Sclerosis (Figure 2.20).

For validation, I conducted Western blotting analyses on RBPs detected in our analyses (Figure 2.21). Consistent with the mass spectrometry data, a pol II subunit POLR2 was detected primarily at the earliest time point, while nuclear RBPs such as hnRNPA1, SRSF7, PABPN, and TDP-43 peaked at 30–60 min, followed by the shuttling export factor ALYREF and subsequently by cytosolic

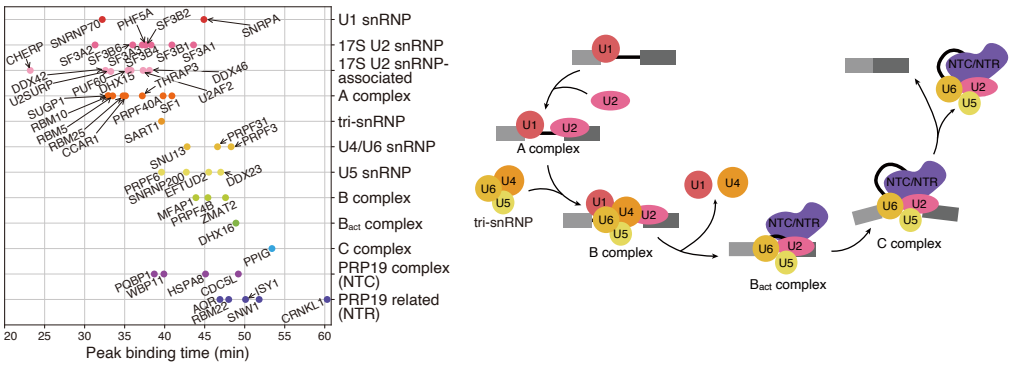

Figure 2.18 Peak binding times of splicing machinery proteins. For visualization, only the proteins quantified in all three replicates are shown. (Right) Schematic diagram of pre-mRNA splicing.

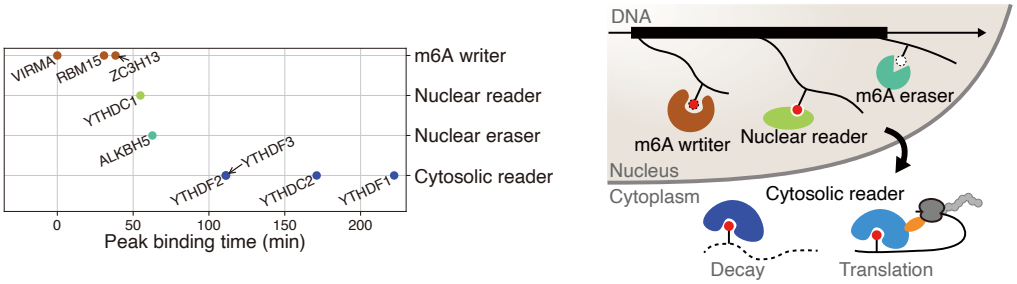

Figure 2.19 Peak binding times of m6A RNA modification-related proteins. Check Figure S3F for the known functions of m6A RNA modification-related proteins. (Right) Schematic diagram of m6A RNA modification

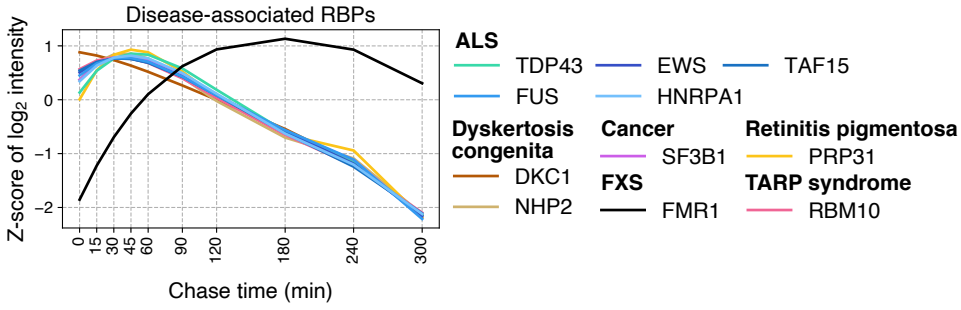

Figure 2.20 mRNA binding dynamics of RBPs associated with human diseases.

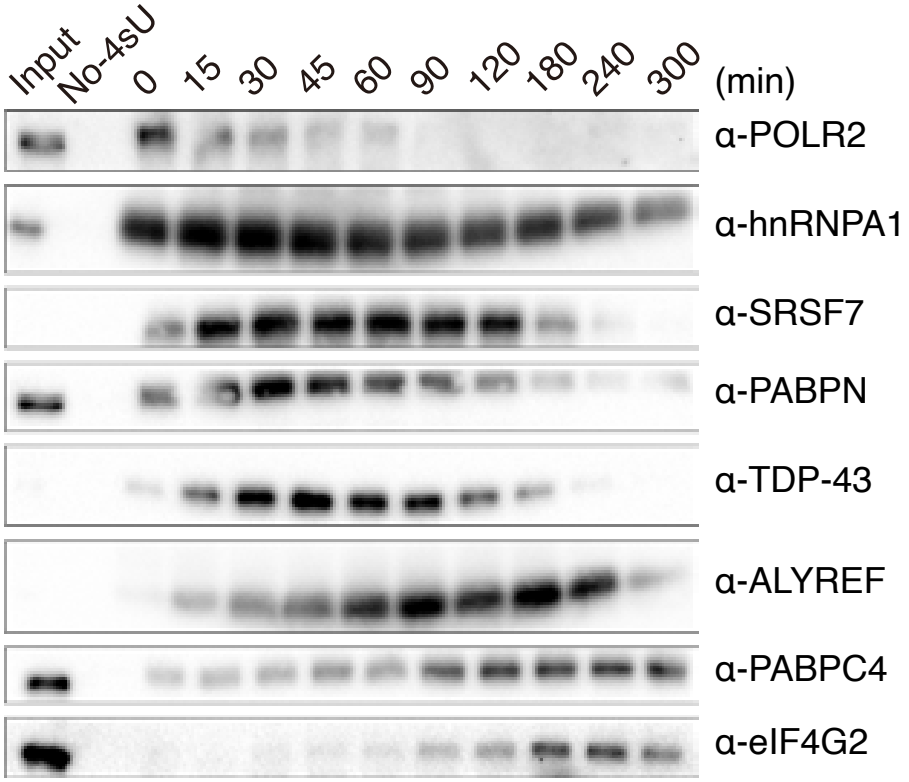

Figure 2.21 Validation by western blotting. Input represents 0.01% of the lysate that is used in the 0 min RIC sample. No-4sU means the RIC elution sample obtained from unlabeled cells.

translation factors, PABPC4 and EIF4G2. Thus, our dataset successfully reflects the known localizations and functions of the representative RBPs.

2.2.3 Clustering analysis of RBPs

To categorize mRBPs according to their temporal RNA-binding dynamics, we executed k-means clustering, utilizing z-score-normalized log2 protein intensity and peak binding time (Figure 2.22 and Table 2.2 ; also see Methods). "Biological process" (BP) GO term analyses revealed unique enrichment within each cluster (2)(Figure 2.23). Cluster I frequently displays transcription-related terms, whereas cluster II is enriched with pre-mRNA processing and splicing related terms. Export-related terms are observed in cluster III, whereas clusters IV and V were significantly associated with translation and nonsense mediated decay (NMD). Clusters VI and VII were enriched with translation regulation, stress granule (SG), and RNA decay terms.

Orthogonally, we calculated the mean peak binding time of the proteins within a given GO term group. Proteins with transcription-related terms show the earliest mean peak binding times (Figure 2.24, shown in x-axis) and belonged mainly to clusters I or II (Figure 2.24, indicated by colors). Proteins with processing-related terms and translation-related terms followed in the anticipated order. We repeated this test on "cellular component (CC)" GO terms to monitor the temporal changes in mRNP organizations (Figure 2.25). Proteins with "RNA polymerase complex" and "transcription elongation factor complex" terms were detected initially, followed by proteins with "cleavage and polyadenylation complex" and spliceosome-related terms. Proteins with translation-related terms (e.g. polysome, EIF4F complex, EIF3 complex) and decay/mRNA storage-related terms (e.g. P-body) took longer to bind to mRNA. Both BP and CC term analyses suggested that the transition from nuclear to cytoplasmic processes occurs at around 60-100 minutes and between clusters IV and V. Considering the inevitable lag period of approximately 30 minutes in our labeling scheme, this transition time aligns with the time required for mRNA export (30-40 minutes) (33; 53).

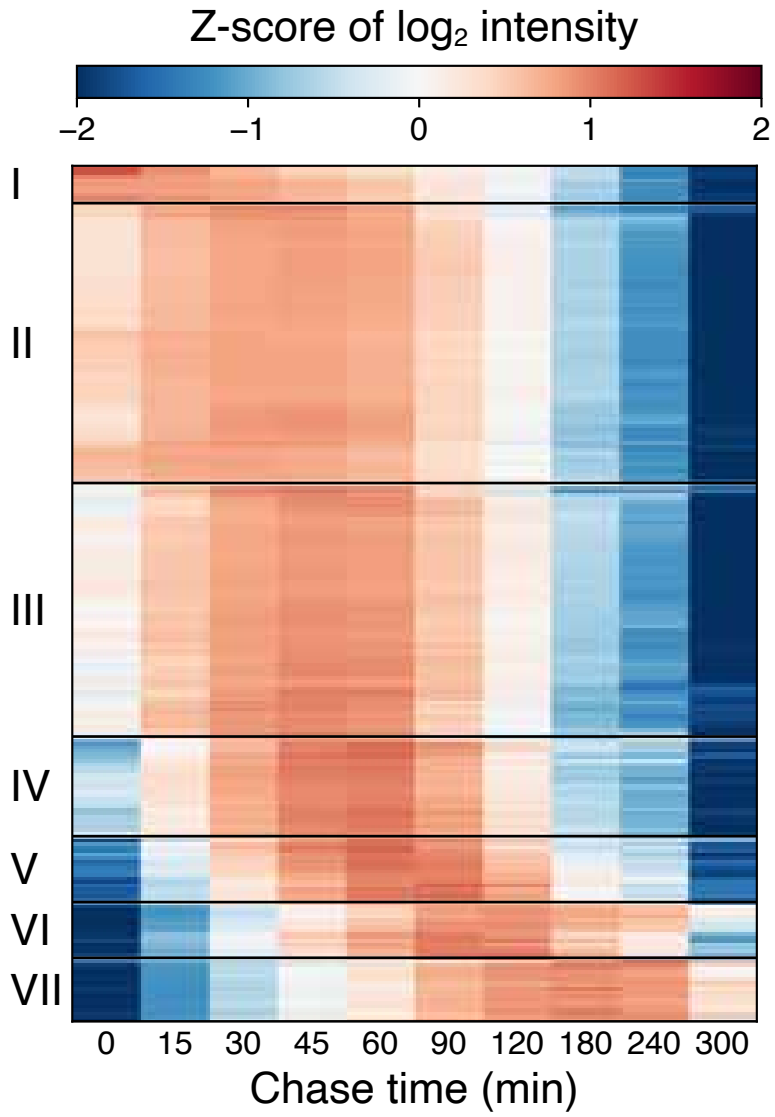

Figure 2.22 Clustering analysis based on mRNA binding dynamics. Each row of the heatmap represents the z-score normalized mRNA binding dynamics of a protein. Out of 801 confidently quantified proteins, 734 proteins that were previously reported as mRNA binders were used for clustering analysis. Mitochondrial mRNA binders (n=65) and potential non-coding RNA binders (n=65, e.g. ribosomal proteins, snoRNA binders) were excluded from this and following analyses (see methods for the list).

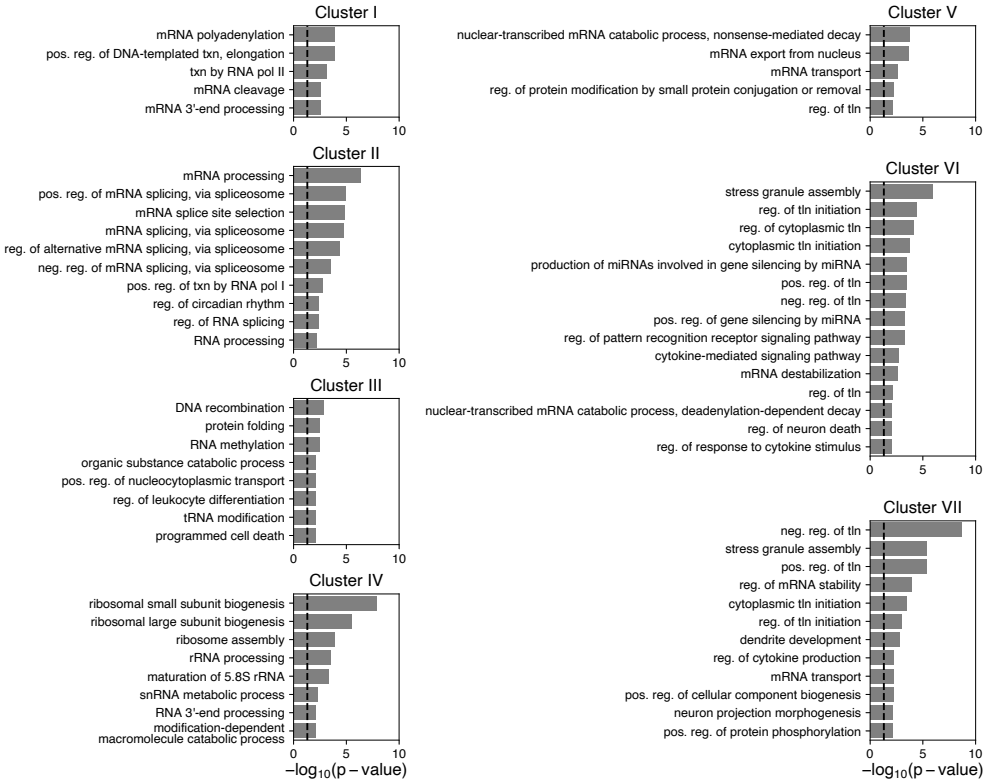

Figure 2.23 GO: BP term enrichment analysis on each cluster, using TopGO R library. For the background group for the enrichment test, all proteins identified (FDR 1%) in this study were included. pos.: positive, neg.: negative, txn: transcription, tln: translation, reg.: regulation.

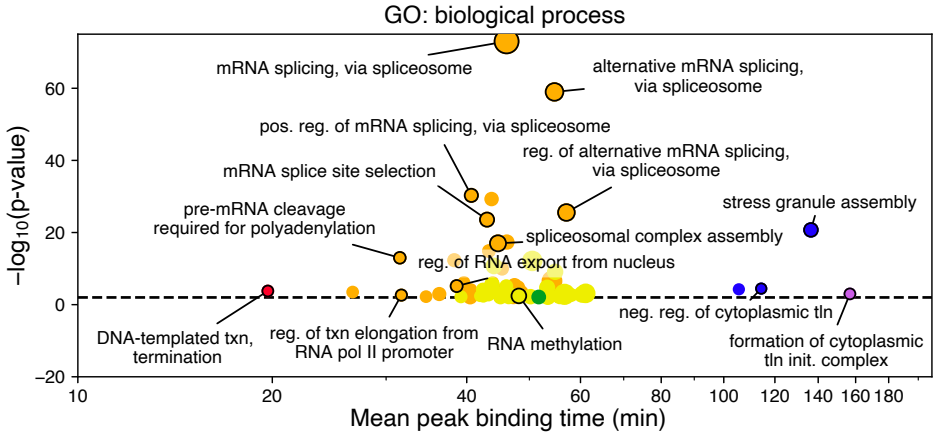

Figure 2.24 Bubble plot showing the mean peak binding time (x-axis) of the RBPs sharing the same GO : biological process (BP) terms. The significance of similarity in mRNA binding dynamics of the RBP group sharing the same terms are shown in y-axis, as p-values derived from two-sided Mann-Whitney U test on the Euclidean distances between proteins with the same GO annotations vs. those between proteins without the same GO annotations. Dashed line indicates P=0.01. To reduce the over-representation of general (higher level) GO terms, the elim algorithm described in (2) was applied during the p-value calculation. Color code indicates the most frequently occuring cluster among the RBPs annotated with each GO term. Area of each circle is proportional to the number of RBPs annotated with each GO.

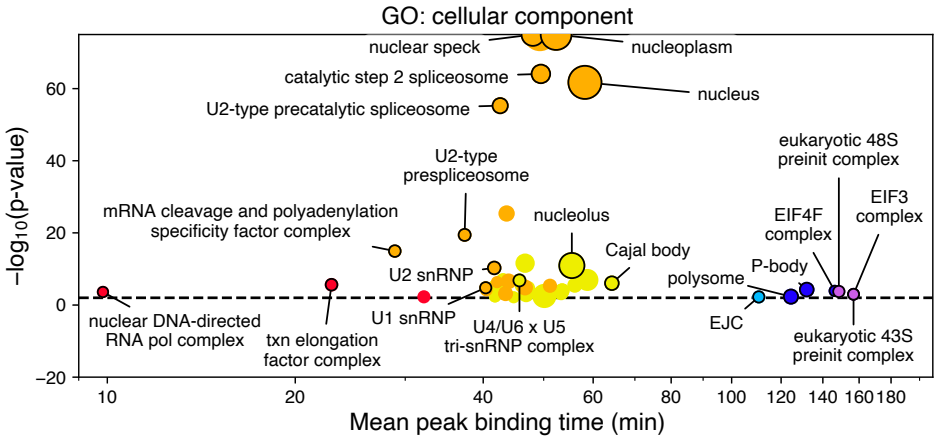

Figure 2.25 The same as 2.24 except for using GO: cellular component.

Comparing our data with protein localization data from the Human Protein Atlas (HPA), based on immunofluorescence staining (75), we found that proteins in cluster I are predominantly nuclear and that the fraction of nuclear proteins decreases gradually in later clusters (Figure 2.26). We also cross-referenced proximity labeling-based localization data (26) and found that most early binders are associated with chromatin, nucleoplasm, nuclear body, paraspeckles and/or spliceosomal complexes, while late binders are primarily in cytoplasmic RNP granules (Figure 2.27).

Next, we examined the enhanced crosslinking and immunoprecipitation followed by high-throughput sequencing (eCLIP) data from the ENCODE project, which revealed protein interaction sites on transcripts for 85 and 76 RBPs in K562 and HepG2 cells, respectively (80; 79; 81). We calculated the proportion of eCLIP peaks mapped to the intron, 5´ untranslated region (5' UTR), coding sequence (CDS), and 3´ UTR (Figure 2.28). Although some clusters are not represented well by the eCLIP data, we observed an overall consistent pattern from both cell lines. Early binders in clusters I, II, and III bind mainly to intronic regions, indicating their major role in the pre-mRNA complex. In contrast, late binders in clusters V, VI, and VII exhibited fewer eCLIP peaks in introns and large number of peaks in CDS and 3´ UTR, consistent with their role in mature mRNA complexes.

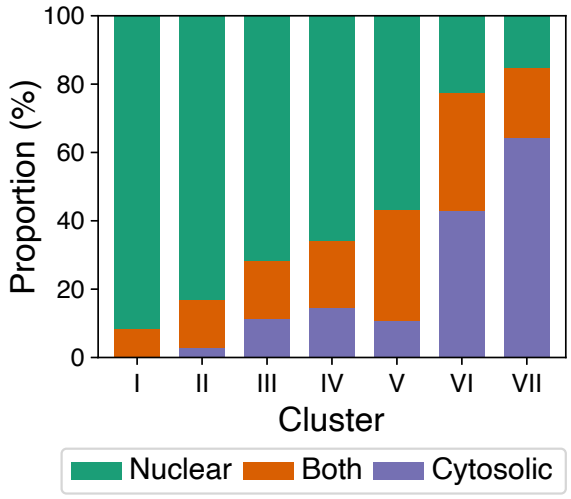

Figure 2.26 Proportion of nuclear and cytosolic proteins in each cluster, according to the annotation in HumanProteinAtlas.

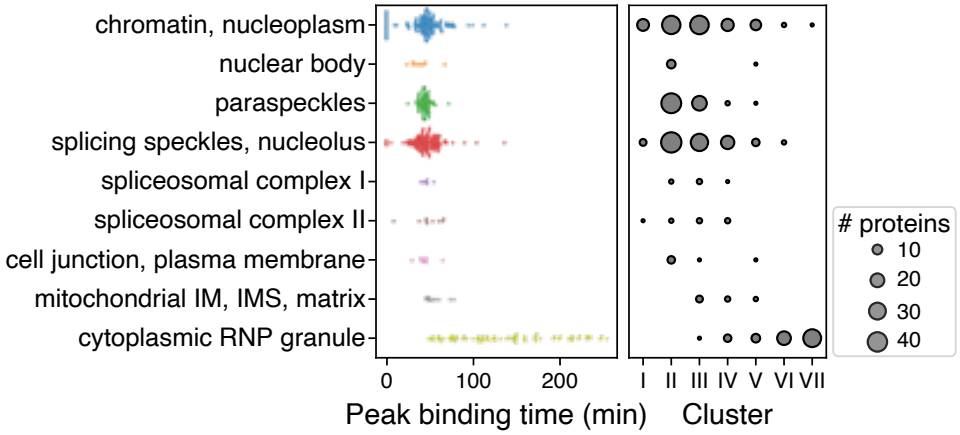

Figure 2.27 Beeswarm plot (left) and dot plot (right) of subcellular localization of RBPs. The y-axis of both plots indicates proximity-labeling based prediction of subcellular location, provided by the HumanCellMap. The x-axis of the left plot shows the peak binding time of each protein, and the x-axis of the right plot represents the cluster of each circle. The radius of each circle in the right plot is proportional to the number of proteins belonging to each category.

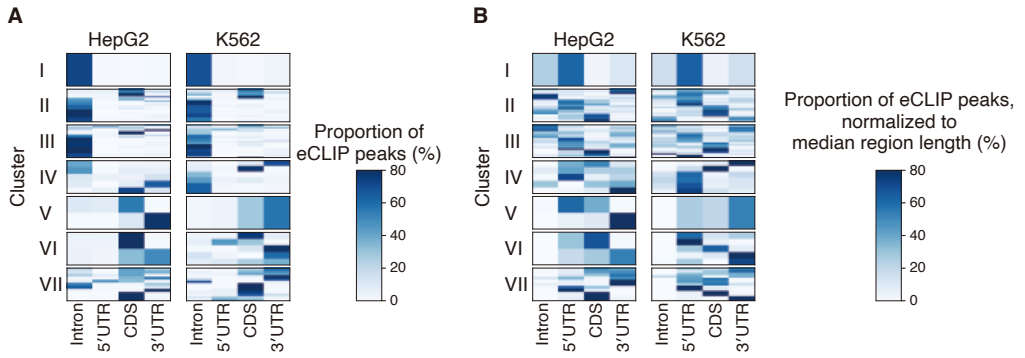

Figure 2.28 (A) Location of eCLIP peaks of 76 RBPs in HepG2 and 85 RBPs in K562, which overlap between our data and the ENCODE data. (B) Density of eCLIP peaks in intronic regions, 5' UTR, CDS, and 3' UTR. Density was calculated by normalizing the raw read proportion by the length of the intron, 5' UTR, CDS, and 3' UTR of highly expressed genes (TPM>10). Prior to normalization, eCLIP peaks that do not overlap with any protein coding gene were removed. The lengths used for normalization are as follows: intron: 21603 (K562) and 22541 (HepG2), 5´ UTR: 124 (K562) and 123 (HepG2), CDS: 1212 (K562) and 1237.5 (HepG2), and 3´ UTR: 959.5 (K562) and 979 (HepG2).

Notably, some late binders in cluster VI and VII are preferentially associated with CDS, suggesting that they may arrive after ribosome is cleared away from CDS, potentially forming translationally inert complexes on aged mRNAs. Thus, the eCLIP analyses further demonstrate the validity of our time-resolved mRNA interactome data, reflecting the mRNP life cycle.

2.2.4 Protein-protein interactions in mRNP complexes

Our data presents a comprehensive interactome of direct RNA binders. However, RNPs also contain proteins that associate via protein-protein interactions (PPI), contributing to the RNP function (48; 12). To extend the temporal map of RNP, we incorporated indirect RNA binders by merging our data with PPI information and generating a PPI network, using the RBPs identified in our study as seeds (Figure 2.29). This extended PPI network enriches our understanding of time-resolved RNP components.

Our analysis also showed PPIs between direct RNA binders identified in this study. Proteins within the same cluster tend to interact frequently with each other (2.29, shown in color). By measuring the number of PPIs between the seed proteins, we confirmed that the frequency of PPIs within the same cluster or between neighboring clusters (particularly clusters VI and VII) were significantly higher than randomly selected protein pairs (Figure 2.30A). Similar patterns were observed when we included proteins interacting indirectly via one neighbor (Figure 2.30B). These results suggest that proteins interacting with each other bind to mRNAs at similar time points, via PPIs as well as RNA-protein interactions, collectively forming stage-specific RNP complexes. To statistically validate this result orthogonally, we quantified temporal differences in mRNA binding by calculating the Euclidean distance of RNA binding dynamics between protein pairs (see Methods). Protein pairs with physical interaction evidence showed similar RNA binding dynamics, resulting in small Euclidean distances, compared to non-interacting protein pairs (Figure 2.31). Additionally, we cross-examined known protein complexes ("CORUM complexes") (25), by comparing the Euclidean distances of mRNA binding dynamics. RBPs within the same

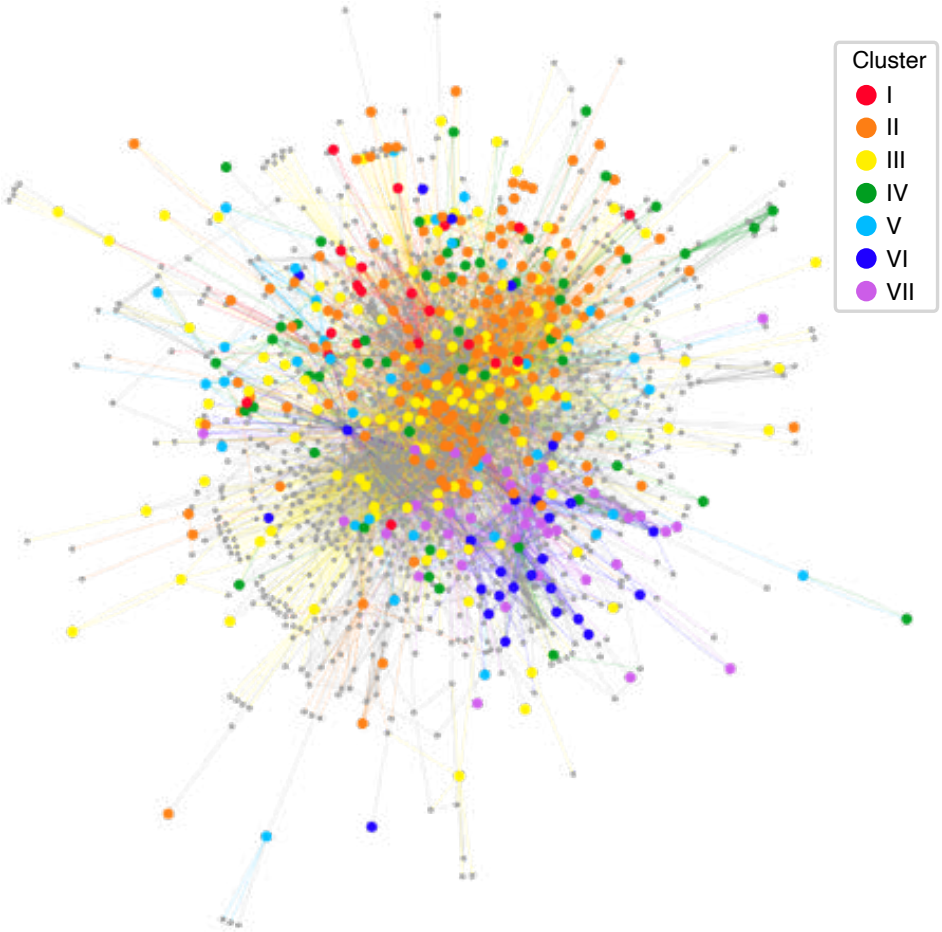

Figure 2.29 A protein-protein interaction (PPI) network of direct RBPs found in this study (color-coded to indicate their respective clusters) and their interactors. A graph with the largest number of connected proteins (n=1620) was chosen for visualization.

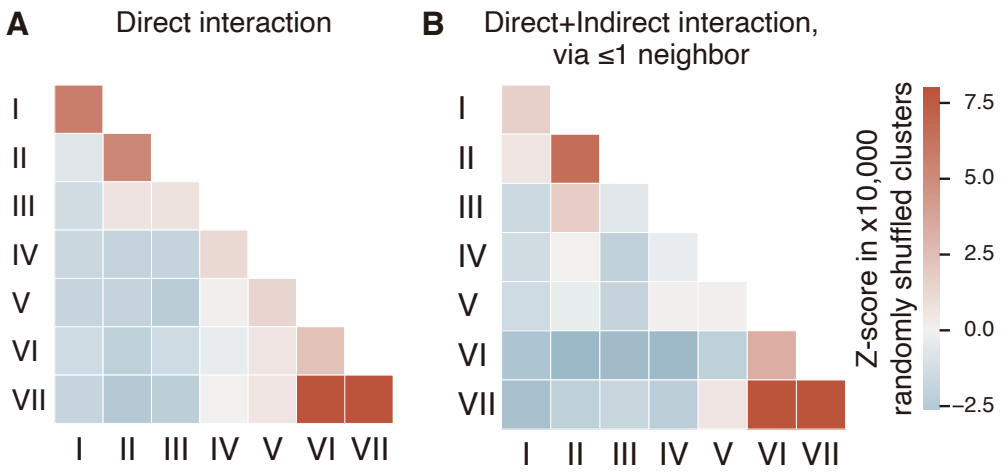

Figure 2.30 (A) PPIs within and between clusters. To calculate the normalized enrichment of PPIs, z-scores were calculated through 10,000 iterations of randomly shuffling clusters. This generated null distributions for PPI counts, from which the z-scores were derived. (B) PPIs within and between clusters. Same analysis as (A), except for using direct PPIs as well as indirect PPIs via one neighbor protein interactor.

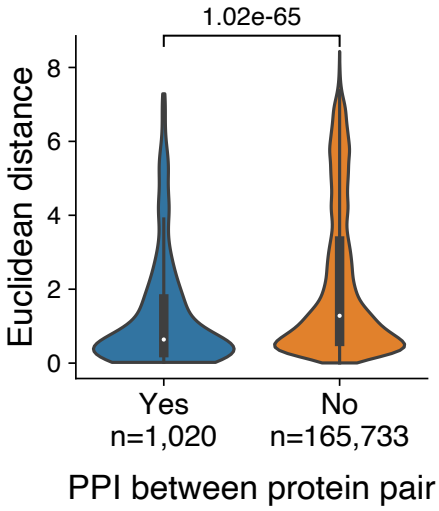

Figure 2.31 Violin plots visualizing the dissimilarities in terms of mRNA binding dynamics (represented by Euclidean distances, y-axis) between protein pairs that interact or do not interact. Box plots inside the violin plots show the median (center dot), first and third quartiles (lower and upper box limits, respectively), and 1.5 times the interquartile range (whiskers). P-value was calculated by the two-sided Mann-Whitney U test.

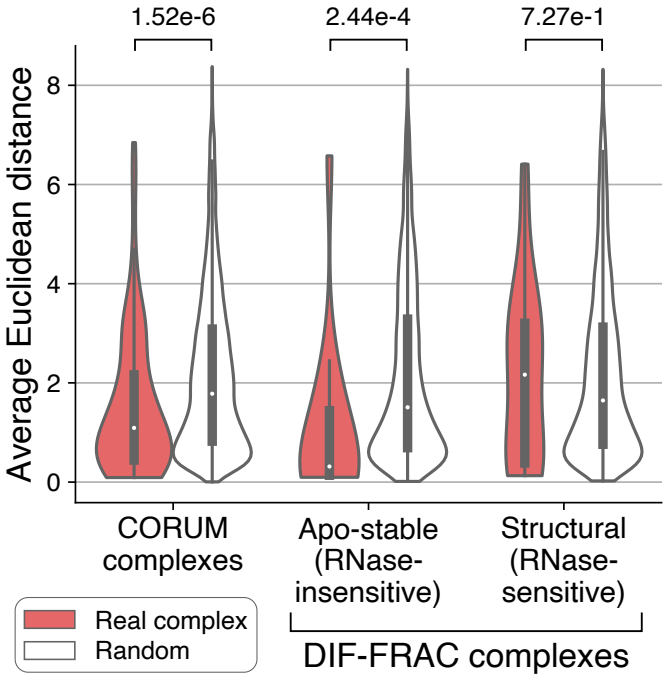

Figure 2.32 Violin plots of average Euclidean distances of mRNA binding dynamics, per protein complex. P-values were calculated by the two-sided Mann-Whitney U test. Mini box plots inside the violin plot indicate the same quantile range as (C). CORUM: all protein complexes in the CORUM database. DIF-FRAC complexes: RNA binding protein complexes, defined by (48).

complexes (Figure 2.32, left, red) displayed significantly lower Euclidean distances in RNA binding dynamics compared to randomly selected proteins (2.32, left, white), indicating that the components of these complexes join the mRNPs at similar temporal stages. Another earlier study grouped mRNP complexes ("DIF-FRAC" complexes) (48) into two groups based on RNase-sensitivity: "apo-stable" RNPs (RNase-insensitive; RNA-independent) and "structural" RNPs" (RNase-sensitive; RNA-dependent). Notably, apo-stable RNP components demonstrated significantly smaller Euclidean distances in RNA dynamics compared to random protein sets (2.32, middle), while structural RNP components did not (2.32, right).

Thus, proteins interacting with each other independently of RNA may join mRNP simultaneously as a pre-formed complex.

Overall, PPI and mRNA binding dynamics are in good agreement, indicating that proteins interacting with each other constitute stage-specific RNPs. However, some RBPs display markedly different dynamics from their PPI partners, represented by large Euclidean distances (Figure 2.33 and Table 2.3). The discrepancy between mRNA binding dynamics and PPI information implies that these RBPs may be multifunctional and/or have unidentified functions. For instance, a late binder MOV10 (cluster VII) has been reported to interact with both early binders (such as XRN2) and late binders (such as UPF1, STAU2, and IGFBPs) (Figure 2.34). Although MOV10 targets 3´ UTR regions and associates with regulators of mRNA stability and translation, it is also known to bind introns and interact with splicing factors (37; 20). The RNA binding time revealed in this study suggests that the majority of MOV10 molecules act in the late stage of the mRNA life cycle, at least under our experimental conditions.

2.2.5 Aged mRNPs and RNA granules

It was unanticipated that the late clusters were highly enriched with GO terms related to 'cytoplasmic RNP granules' and 'stress granule (SG) assembly' (Figures 2.24, and 2.27), even though I did not expose the cells to any stressors. When I performed immunofluorescence imaging using a G3BP1 antibody, a known SG marker, no visible foci were detected (Figure 2.35), indicating that SGs were not formed under our experimental conditions.

We examined the proteins interacting with G3BP1 ("G3BP1 protein interactome") (49), discovering that about 49% and 63% of cluster VI and VII proteins, respectively, overlap with G3BP1 interactors (Figure 2.36). The majority of these proteins have been reported to bind to G3BP1 independently of stress (49), suggesting that naturally aged mRNPs are similar to SGs in the protein composition.

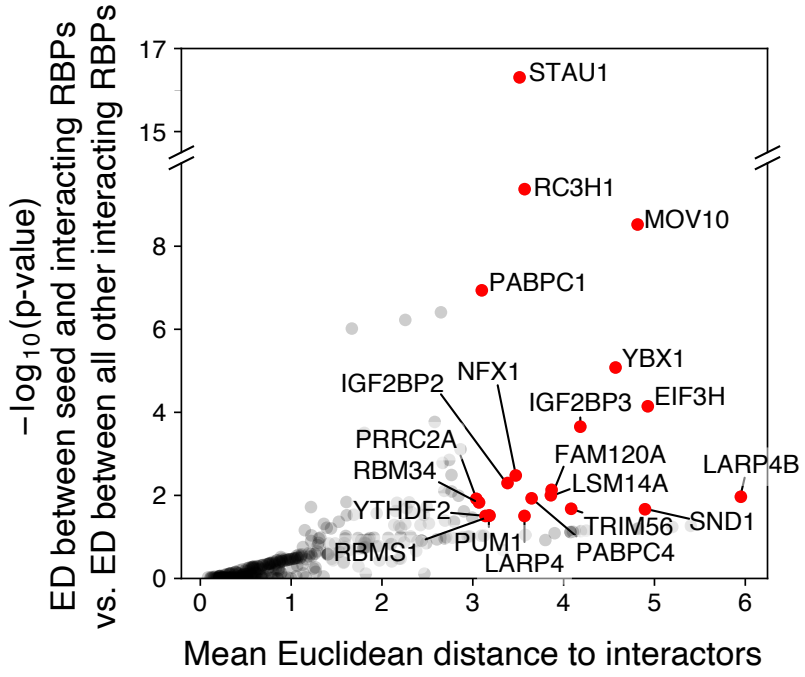

Figure 2.33 Scatter plot illustrating differential mRNA binding dynamics between RBPs and their protein interactors. The x-axis shows the average Euclidean distances (ED) of mRNA binding dynamics for a seed protein and its interactors. The y-axis represents differential p-values, comparing the ED between the seed protein and its interactors to the ED between other pairs of interacting proteins. P-values were calculated using the one-sided Mann-Whitney U test. RBPs meeting $P<0.05$ and mean Euclidean distance to interactors >3 are marked in red on the plot.

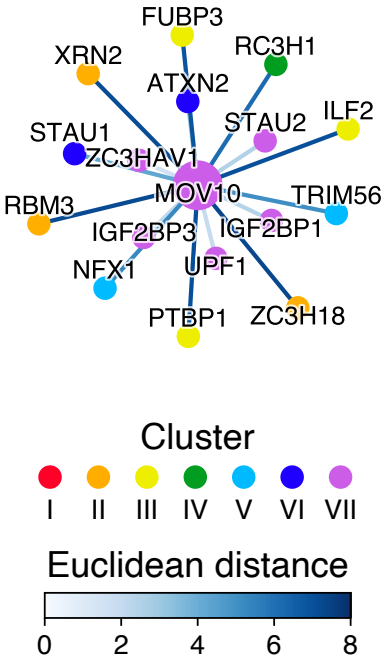

Figure 2.34 Euclidean distances between mRNA binding dynamics of MOV10 and its interactors. Edge colors represent the Euclidean distance between mRNA binding dynamics of two proteins. Protein nodes are colored according to their assigned cluster.

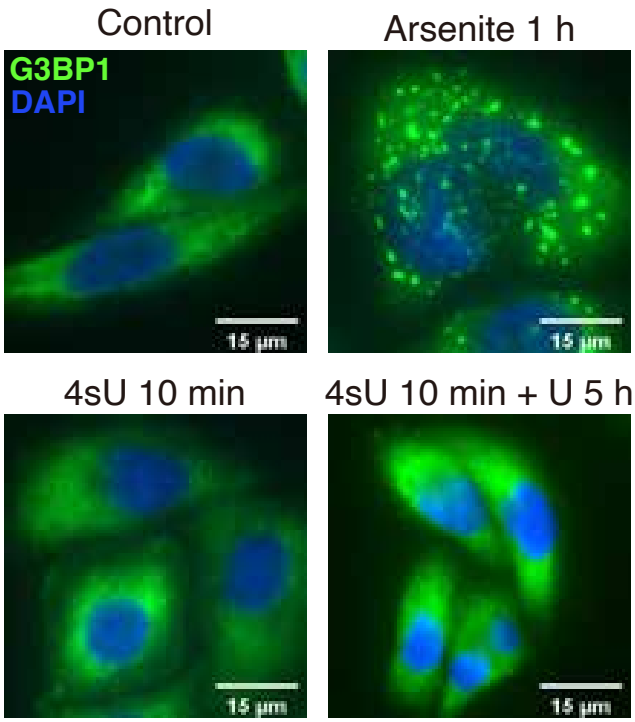

Figure 2.35 Immunofluorescence against G3BP1 (green) and DAPI (blue) in HeLa cells. Sodium arsenite treatment was used as a control for SG formation.

Figure 2.36 Proportion of stress-dependent (purple) or stress-independent (orange) G3BP1 interactors in each cluster. The list of G3BP1 protein interactors were from (49).

To validate our findings, we conducted 4sU pulse-labeling, UVA crosslinking, poly(A) RNA capture, and western blotting analyses on late binders which are known to localize to SGs (Figure 2.37). Our data confirm that LARP1, FMR1, IGF2BP3, and G3BP1 are indeed captured at late time points.

We further compared our RBPs with those known to localize to SGs and P-bodies (86; 85; 32). Remarkably, 67% and 74% of cluster VI and VII proteins were annotated as SG proteins, respectively, while PB proteins are not strongly enriched in late clusters (Figure 2.38A and Table 2.4).Furthermore, 26% of cluster VII proteins were annotated as the regulators of SG formation as well as the structural core proteins of SG (Figure 2.38B). Out of 36 proteins previously reported as SG regulators and core proteins, 16 proteins belong to cluster VI and VII (Figure 2.38C).

We observed frequent PPIs within and between clusters VI and VII (Figure 2.30). The majority of these interacting proteins in clusters VI and VII are indeed SG proteins, while those not participating in the interaction networks are

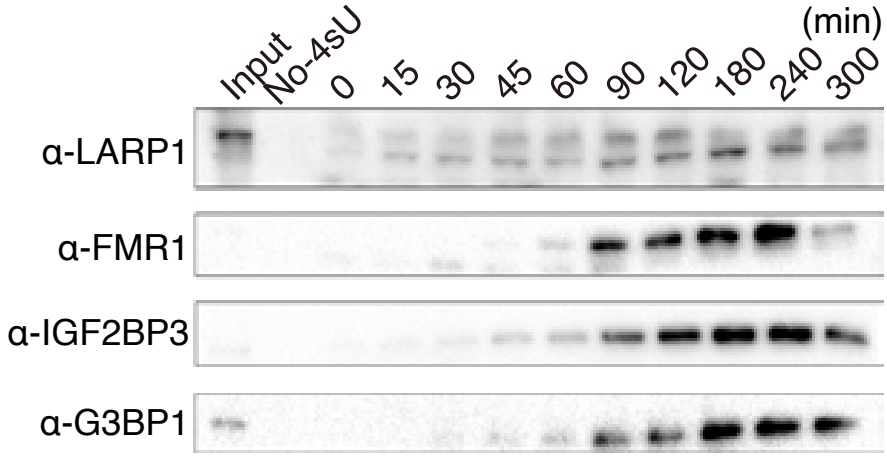

Figure 2.37 Validation of mRNA binding dynamics of SG proteins by western blotting. Input means 0.01% of lysate from chase time 0 min. No-4sU indicates the RIC elution sample obtained from unlabeled cells.

predominantly non-SG proteins (Figure 2.39). The considerable overlap between the SG proteome and late mRNPs, along with the frequent PPIs among late binders, suggests that late mRBPs may form submicroscopic RNP condensates with similar properties to SGs, which might be natural process of mRNA aging under unstressed conditions.

2.2.6 Interaction between viral RNAs and late binders

RNA viruses interact with a wide range of host RBPs for viral proliferation and immune evasion (31). Proteomics-based approaches have identified a large number of viral RNA binding proteins (vRBPs) (45; 56; 43; 38). Most of the vRBPs have also been reported as host RNA interactors. In line with this, 354 of RBPs found in our study have previously been described as vRBPs (Figure 2.40 and Table 2.4).

All temporal clusters contain vRBPs; however, we observed marked enrichment of vRBPs among late binders, most notably in cluster VII (Figure 2.40B). This enrichment is not solely attributed to the cytosolic localization of late binders,

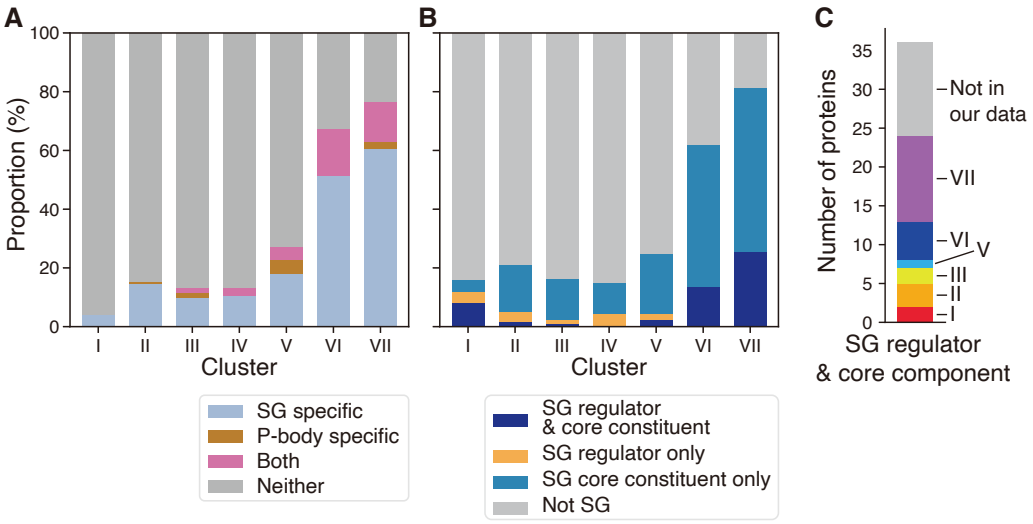

Figure 2.38 (A) Proportion of SG and P-body proteins in each cluster. Tier-1 SG and P-body list of RNA granule database (v1.0) was utilized. (B) Proportion of SG regulators (necessary for SG formation, identified by genetic screening) and SG core proteins (enriched in SG pull-down proteome) in each cluster. SG regulator and SG core protein lists were obtained from (85). (C) Number of SG proteins that belong to different temporal clusters. SG regulator and SG core protein were from (85).

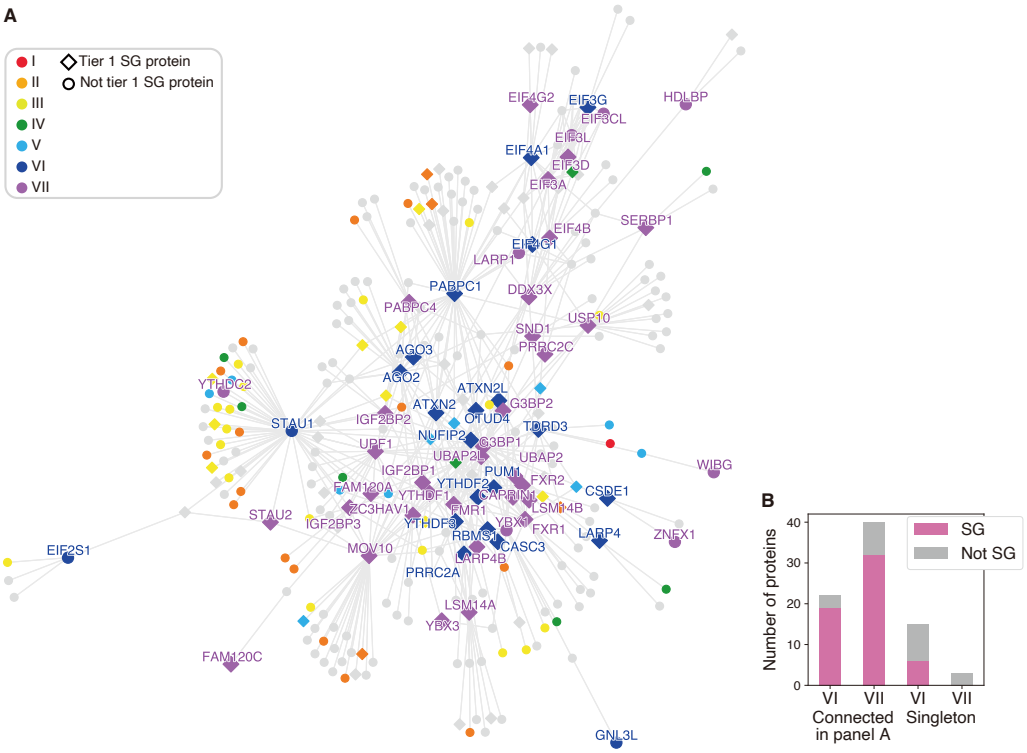

Figure 2.39 (A) Interaction network map of proteins belonging to cluster VI, cluster VII, and their interactors (n=298). SG core proteins are marked as square nodes. Gene names of cluster VI and VII proteins are marked above their respective nodes. (B) The number of SG and non-SG proteins among the connected cluster VI, VII proteins in (A) and not connected (singleton) cluster VI, VII proteins.

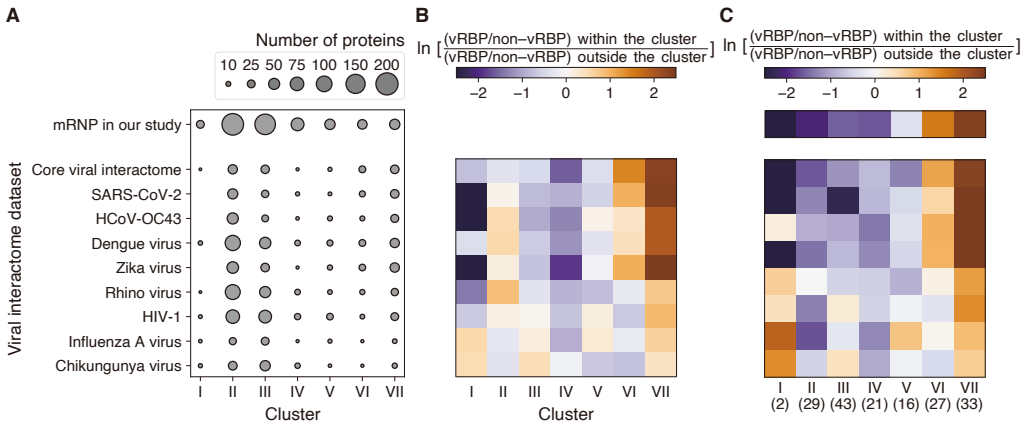

Figure 2.40 (A) Number of mRBPs found in viral RBPs, per each cluster. (B) Enrichment of vRBPs in each cluster, measured in log odds ratio. (C) Enrichment of vRBPs in each cluster, measured in log odds ratio, as in (B). But, unlike (B), we used only cytosolic proteins (annotated in HumanProteinAtlas) in this analysis. Numbers below the clusters indicate the number of cytosolic proteins, which include those located in both nucleus and cytosol and those restricted in the cytosol. Used vRBP dataset: Core viral interactome: (31); SARS-CoV-2: sgRNA, (45); HCoV-OC43: sgRNA at 36 hours post infection, (45); Dengue virus, Zika virus, Rhinovirus: (56); HIV-1: All splice variant captures, (43); Influenza A virus: (38); Chikungunya virus: 1 hour post infection, without interferon, (38)

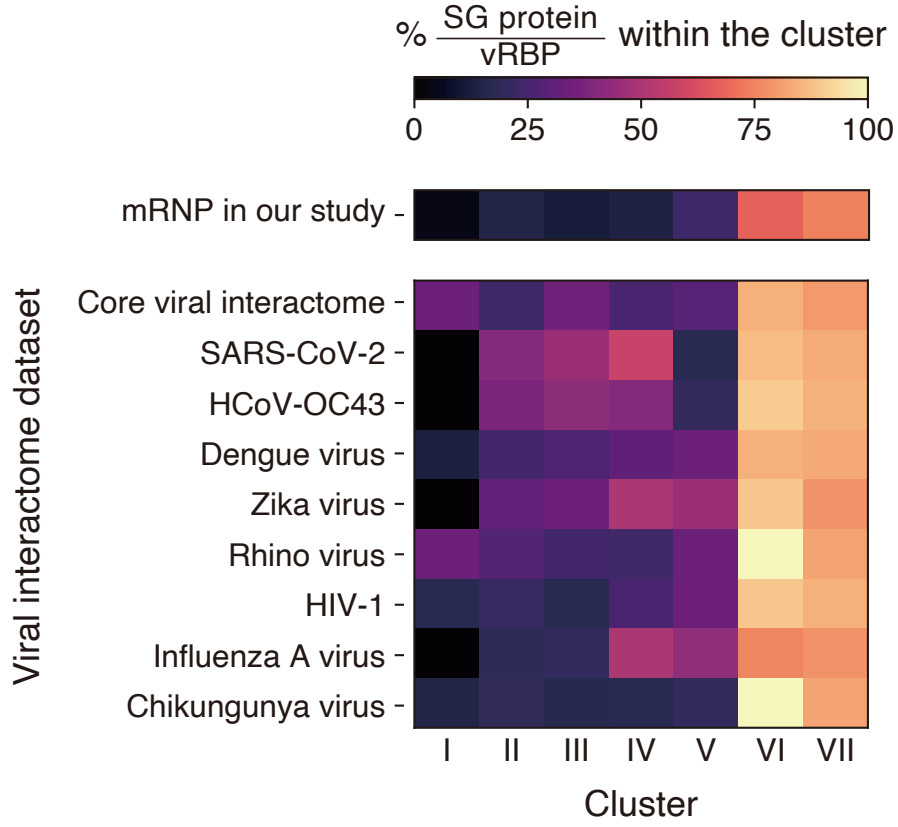

Figure 2.41 Proportion of SG proteins among viral RBPs, per each cluster.

as the same analysis restricted to the cytosolic proteins also exhibited higher enrichment in cluster VI and VII (Figure 2.40C). Transcripts of coronaviruses (SARS-CoV-2 and HCoV-OC43) and flaviviruses (dengue virus and zika virus) showed particularly strong enrichment with late clusters. We also noticed that SG proteins frequently appeared among vRBPs in the cluster VI and VII (Figure 2.41). This pattern mirrors the host mRNA interactome, but the SG protein proportion among vRBPs was higher than that in the host mRNA interactome across all clusters (Figure 2.41). The intersection of cluster VII, SG, and vRBP includes well-known antiviral proteins DDX3X and ZC3HAV1 (ZAP). These observations support the notion that the granule-forming late binders may play a

role in antiviral defense by sequestering viral RNAs, while some of them may be repurposed by viruses to facilitate viral proliferation (55; 7).

2.2.7 Systemic identification of RBPs with unexpected RNA binding dynamics

While mRNA binding dynamics generally align well with previously reported features, some RBPs display significant discrepancies between their RNA binding times and known functions, localizations, and PPIs. This suggests that these RBPs may possess yet-undiscovered functions. To systematically identify RBPs with unexpected dynamics, we developed a regression method that predicts mRNA binding dynamics based on annotated characteristics (Figure 2.42; for detailed information, please refer to the Methods section). We compiled a gene-GO term table that includes the RBPs identified in this study along with their corresponding GO term annotations. Due to the redundancy of certain GO terms (e.g. 'RNA binding' and 'nucleic acid binding'), we applied multiple correspondence analysis (MCA) to compress the information into a lower dimension. Subsequently, with the MCA-converted GO annotations, we fitted a ridge regression model to predict the z-score of a given RBP's quantity at each time point.

The coefficient of determination (R2) between the observed and expected z-scores at each time point ranged 0.55–0.79 (Figure 2.43). To understand which specific GO terms our regression model relied on, we calculated each GO term's contribution to the expected z-score (Table 2.5). For early timepoints (0–15 min), top positive contributors were GO terms related to transcription or splicing, while GO terms related to translation or cytoplasmic localization were the top negative contributors at these time points. At 1.5 hours, NMD was one of the positive contributors, whereas transcription and splicing-related terms contributed negatively. In later time points (3–5 hr), translation or cytoplasmic localization-related GO terms were the top positive contributors. Despite the overall high performance of our prediction model on well-annotated RBPs (Figure 2.44), we observed some RBPs with substantial differences between the expected and observed mRNA binding dynamics (Table 2.6 and Figure 2.45). Undercharacterized RBPs, sparsely

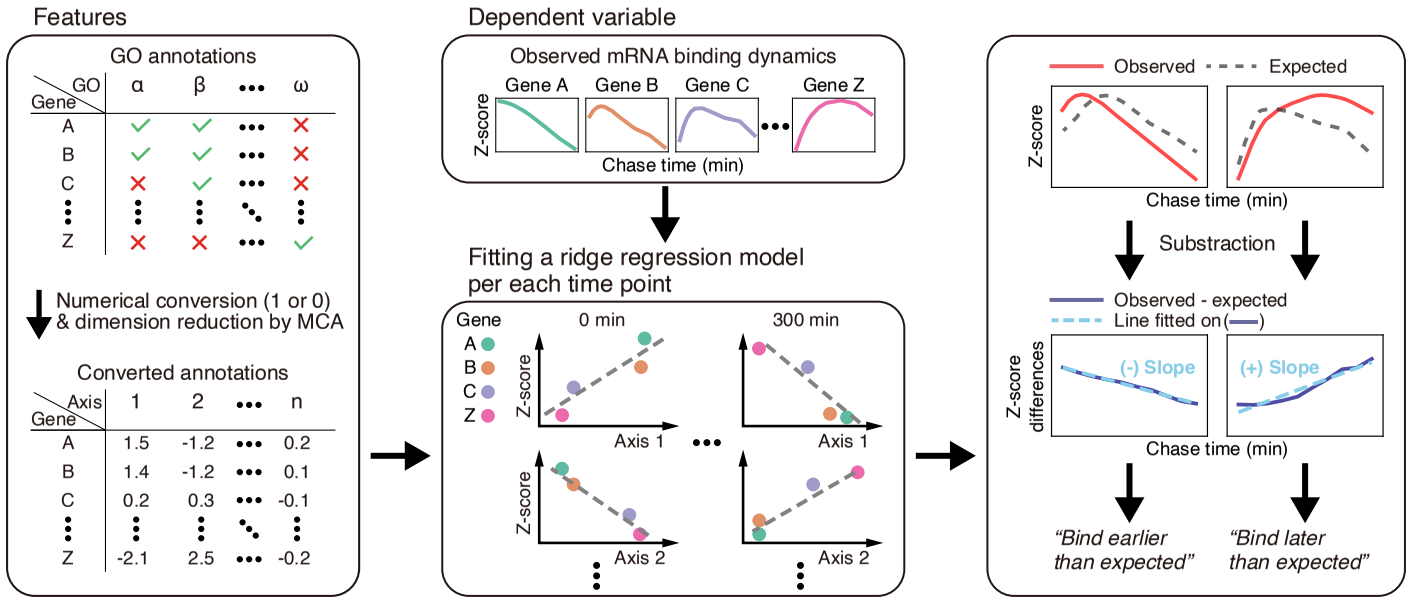

Figure 2.42 Schematic of the mRNA binding dynamics prediction model based on GO-term annotations. The gene-GO term table is encoded to numbers and transformed to the lower dimensions, by the Multiple Correspondence Analysis (MCA, left column). For each time point, a ridge regression model is fitted to find the relationship between the MCA-converted GO annotations and z-score normalized intensities. Model fitting was repeated for all 10 time points (middle column). The difference between the observed and expected values reveals RBPs that bind earlier or later than predicted (right column).

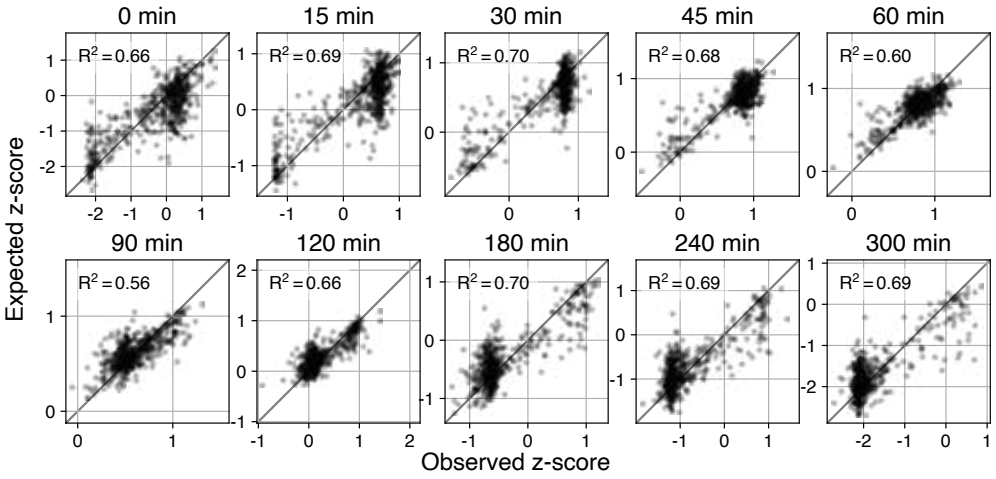

Figure 2.43 Comparison of the expected and observed z-scores at each time point. The coefficient of determination (R2) between two values is marked on each plot.

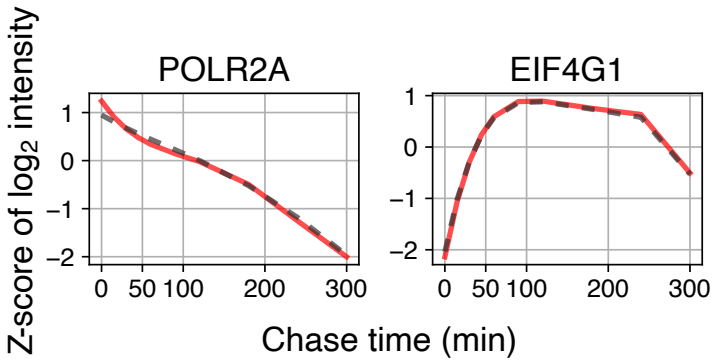

Figure 2.44 Observed and expected mRNA binding dynamics of well-studied RBPs, POLR2A and EIF4G1.

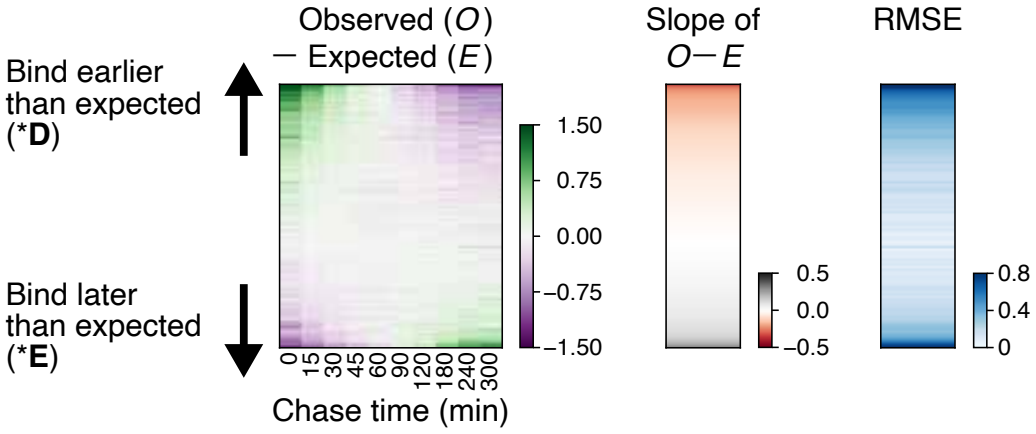

Figure 2.45 RBPs are sorted by the slope of the observed-minus-expected z-scores. RMSE: Root Mean Square Error

covered in literature, generally displayed high prediction errors (Figure 2.46). We sorted RBPs based on the difference between the expected and observed dynamics (Figure 2.47). RBPs at the top or bottom of this list bind to mRNA earlier or later than our model predicts. For example, LSM14B, FAM120A, and FAM120C, which are poorly studied and associated with only a few GO terms ("ribonucleoprotein complex", "mRNA binding", "RNA binding", "regulation of translation"), were predicted as an intermediate binder (class V), but they actually associate with mRNAs at very late time points (cluster VII) (Figure 2.48). Thus, our temporal RNA interaction data supplement current knowledge and assist in functional studies on under-characterized RBPs.

2.2.8 CCDC86 as cytoplasmic mRNA binding protein

To validate the discrepancy between the predicted mRNA binding dynamics and the observed behavior, we focused on CCDC86. Previous studies have reported the nuclear localization of CCDC86, particularly in the nucleoli (78), leading to the prediction of its early association with mRNA (Figure 2.49). It has also been suggested that CCDC86 may be involved in ribosome biogenesis based on its domain architecture, which includes a coiled-coil domain and a Cgr1-like domain.

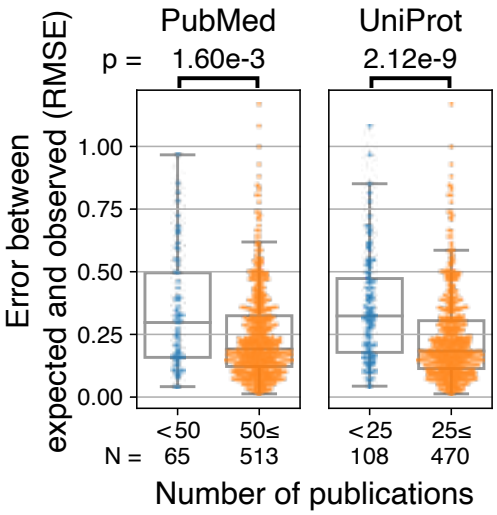

Figure 2.46 Box plots and beeswarm plots of root-mean-square-errors (RMSEs) between the observed and expected dynamics, for the RBPs with small or large number of publications. The number of publications were acquired from PubMed and UniProt web sites. Box plots show the median (center line), first and third quartiles (lower and upper box limits, respectively), and 1.5 times the interquartile range (whiskers). P-values were derived by the two-sided Mann-Whitney U test.

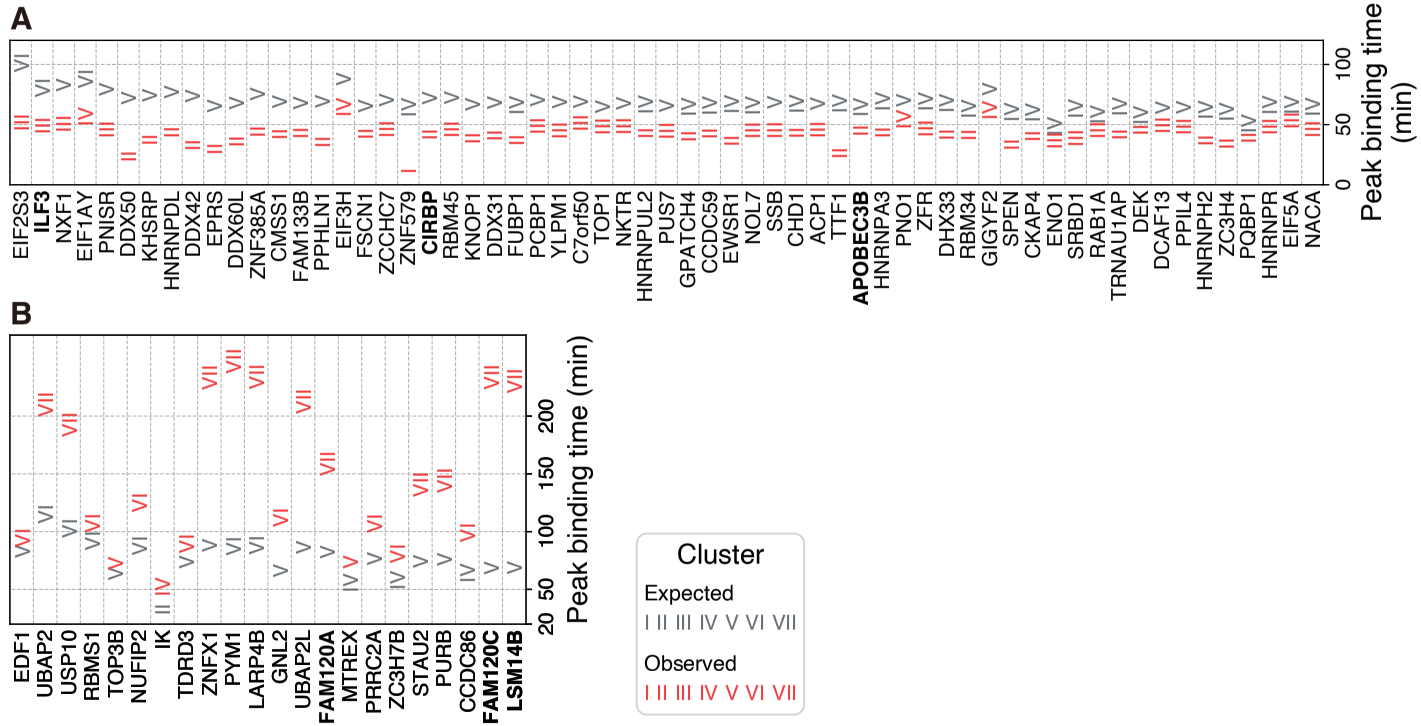

Figure 2.47 Unexpected early (A) or late (B) binders. Shown are RBPs whose slope of the observed-minus-expected z-score is higher than 0.15 or lower than -0.15.

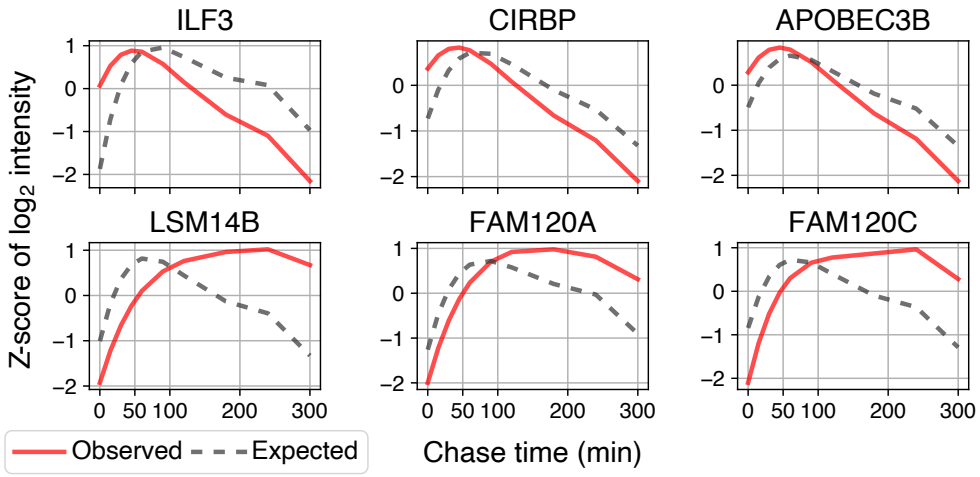

Figure 2.48 Observed and expected mRNA binding dynamics of selected RBPs.

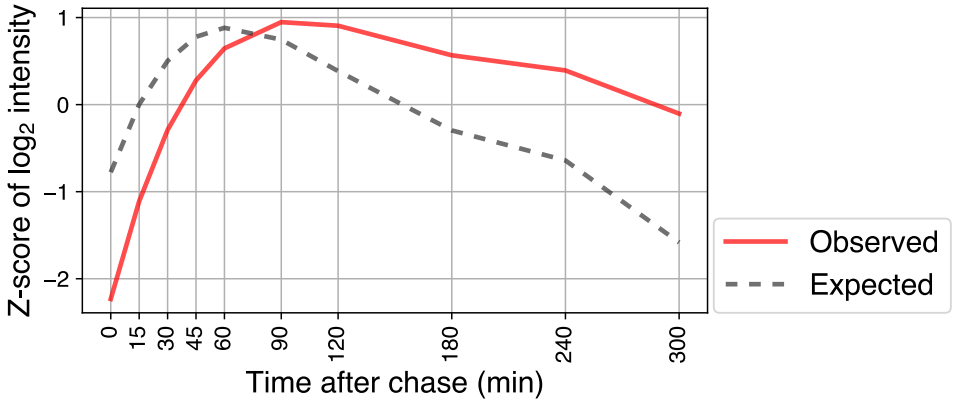

Figure 2.49 Observed and expected mRNA binding dynamics of CCDC86.

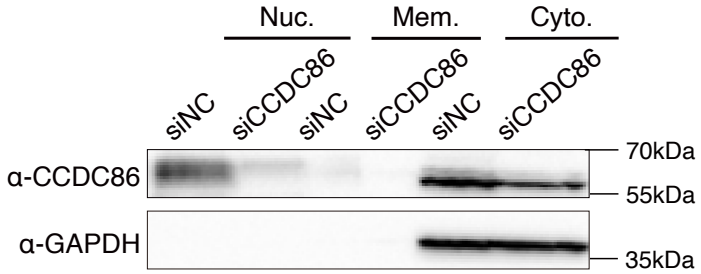

Figure 2.50 Western blotting of the subcellular fractionation after CCDC86 knockdown. HeLa cell was knockdowned with siCCDC86 for 48 hrs.

Cgr1, a yeast protein with nucleolar localization, plays a role in large subunit biogenesis through regulation of pre-rRNA processing in yeast (54). Another study based on Perturb-seq also suggested that CCDC86 is involved in ribosome biogenesis (62).

However, contrary to the initial prediction, our findings demonstrated that CCDC86 interacts with cytoplasmic mRNA until late time points (cluster VI), suggesting potential unknown functions in the cytoplasm. First, we performed cell fractionation experiments, confirming the presence of CCDC86 in both the nucleus and cytoplasm (Figure 2.50). Furthermore, RNA immunoprecipitation (RIP) experiments showed mRNA enrichment in the CCDC86 IP samples compared to the IgG control, even after EDTA treatment, which dissociates ribosomes from mRNA, indicating that the interaction is not mediated by ribosomes (Figure 2.51). Of note, RNA-seq analysis following CCDC86 knockdown revealed a limited number of significantly differentially expressed mRNAs (~200) (Figure 2.52). These findings suggest that CCDC86 may have a minimal impact on mRNA expression levels and stability. Notably, CCDC86 is not the only ribosome biogenesis factor that exhibits late mRNP binding. Proteins such as LSG1, GNL2, SDAD1, and SERBP1, found in clusters VI and VII, are known to be located in the nucleolus and influence rRNA processing (70). LSG1, GNL2, and SDAD1 function as 60s ribosome nuclear export factors, while SERBP1 is involved in mRNA 3´-UTR binding and mRNA stability regulation. These examples illustrate

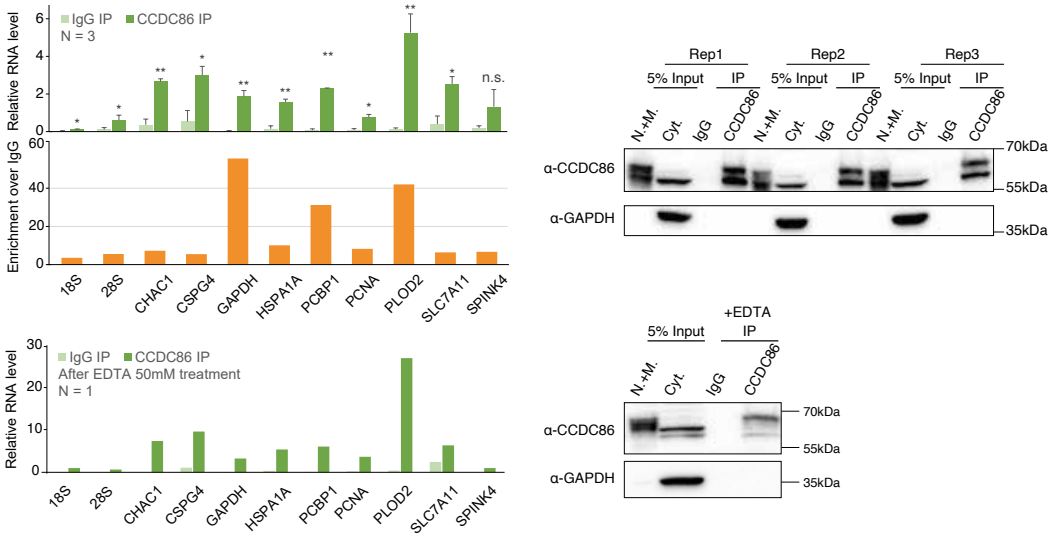

Figure 2.51 RIP-qPCR for CCDC86 in the cytoplasmic fraction. (right) Western blotting of RIP for CCDC86. (below) Same experiment except EDTA was treated in final 50mM. After immunoprecipitation (IP) of CCDC86 from the cytoplasmic fraction, one-fourth of the sample was used for Western blot analysis, while the remaining sample was subjected to RNA isolation using TRIzol for subsequent qPCR analysis. The relative abundance of various mRNAs, along with rRNAs, compared to 1% of input lysate, is shown in the graph. Data are represented as mean ± SD (n = 3 independent experiments). Spike-in RNA used in RNA isolation step was used for normalization. $*p < 0.05$ and $**p < 0.001$, two-sided Student's t test. N.+M. : nuclear and membrane fraction, Cyt.: cytosolic fraction.

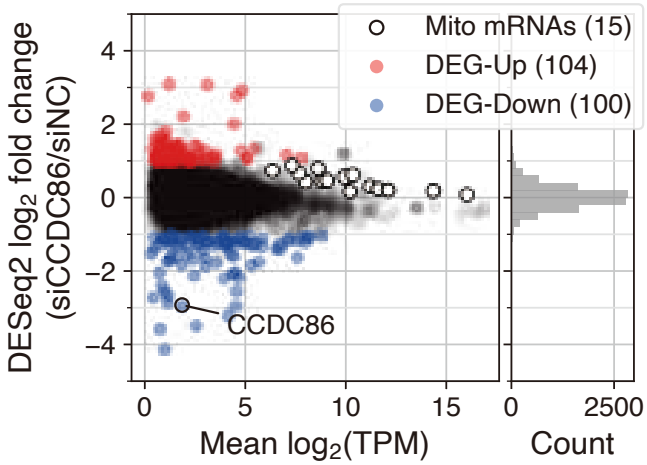

Figure 2.52 Knockdown RNA-seq was performed for CCDC86 in HeLa cell line. Red and blue dots indicate significantly up- or down-regulated genes (FDR 5% and |log2 fold change| > 1). The histogram in the right panel shows the distribution of log2 fold changes. NC: negative control, DEG: differentially expressed genes, TPM: transcripts per million.

how certain RBPs can act as both nuclear rRNA-related factors and cytosolic mRNA regulators. Further studies are required to unravel the specific functions of CCDC86 in mRNA regulation during the later stages of their life cycle, extending beyond its known involvement in pre-rRNA biogenesis.

2.2.9 Studying late binding RBPs can provide valuable insights into the state of mRNA between translation and decay

FAM120A was previously known as an mRNA transport factor, which contradicts its late mRNA binding pattern as observed in our study (Figure 2.48) (44; 71). Recent papers have reported conflicting roles of FAM120A in miRNA targeting, with one study suggesting enhancement (Kim et al.) and another indicating suppression (36), further adding to the controversy surrounding its function. However, when we performed FAM120A knockdown in HepG2, K562, and HeLa cells, only a small number of mRNAs (<200) showed significant changes, suggesting that its major function may not be directly related to general mRNA stability control, at

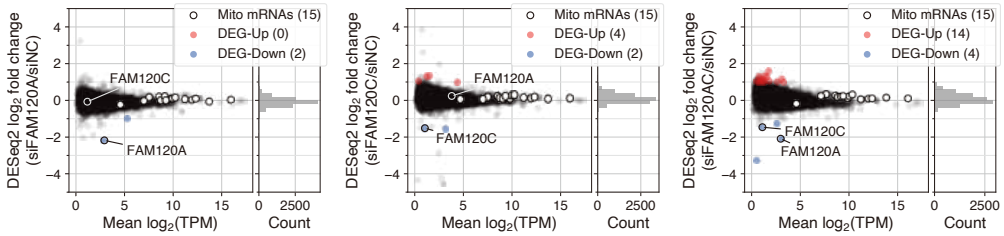

Figure 2.53 Knockdown RNA-seq was performed for FAM120A, FAM120C, and both (FAM120A/C) in HeLa, K562, and HepG2 cell lines. K562 and HepG2 data were re-analyzed from the ENCODE shRNA-seq dataset. Red and blue dots indicate significantly up- or down-regulated genes (FDR 5% and |log2 fold change| > 1). The histogram in the right panel shows the distribution of log2 fold changes. NC: negative control, DEG: differentially expressed genes, TPM: transcripts per million.

least under normal conditions (Figure 2.53). Additionally, FAM120A knockdown did not affect overall protein production, as observed in the SUnSET assay which labels only nascent peptides with puromycin (Figure 2.54) (64).

To address the possibility of functional compensation between FAM120A and its close paralog FAM120C, which also exhibited a late binding pattern, we conducted a double knockdown of FAM120A and FAM120C. However, this double knockdown only minimally affected mRNA levels and global protein translation (Figure 2.53 and 2.54). These findings suggest that the functions of FAM120A and FAM120C may not be essential for general mRNA stability control or translation regulation.

Previous discussions on the final stages of the mRNA life cycle have primarily focused on mRNA translation and decay. However, the presence of several late binding RBPs with limited impact on mRNA stability or translation raises the possibility of an unknown processing step between translation and decay in the mRNA life cycle. Furthermore, our findings regarding the interaction of old mRNAs with the stress-independent G3BP1 interactome suggest a potential association between these RBPs and mRNAs in a state prior to decay, where

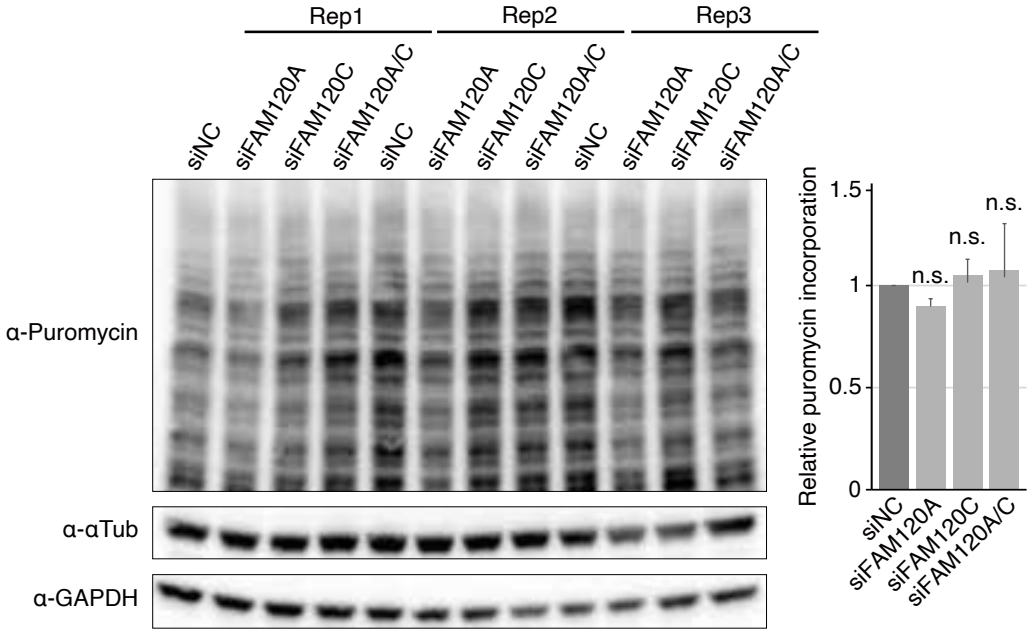

Figure 2.54 Western blot image of SUnSET analysis after FAM120A and FAM120C KD. The incorporation of puromycin was detected by anti-puromycin blot. -Tubulin and GAPDH immunoblots were used as loading controls. The graph show quantitative representation of puromycin incorporation observed in WB (right). Data are represented as mean ± SD (n = 3 independent experiments). n.s. not significant, paired two-sided Student's t-test.

translation is no longer occurring. Conducting additional research on late binding RBPs that do not significantly affect mRNA stability or translation will contribute to our understanding of the state of mRNA prior to decay. Such investigations may provide valuable hints about the intermediate states of mRNA between translation and decay.

2.3 Discussion

The current study utilized an oligo(dT) capture method to analyze poly(A)+ mRNAs. Although we successfully enriched mRNAs using stringent conditions, the RNA pool also contains oligoadenylated mitochondrial mRNAs, poly(A)+ long noncoding RNAs, and contaminants from other noncoding RNA species like rRNAs. Hence, we have excluded RBPs with well-established functions in noncoding RNA pathways from our analyses. Also note that our protocol depletes mRNAs that either lack a poly(A) tail (such as nascent transcripts or replication-dependent histone mRNAs) or possess very short poly(A) tails (such as decay intermediates). Thus, the RBPs quantified in this study may not fully represent co-transcriptional processing factors or decay factors. Future studies might consider using organic phase separation-based methods to capture RNPs, although this could introduce its own limitations due to a lack of RNA specificity (60; 77). Furthermore, because our approach targeted bulk mRNAs with various half-lives, the proportion of stable mRNAs modestly increased over time (Figure 2.9), enriching RBPs that preferentially associate with stable mRNAs. Finally, our bulk analyses do not account for gene-specific regulatory mechanisms. To circumvent all these limitations, future studies should aim to isolate and analyze gene-specific mRNPs using specific antisense oligos as baits. This presents a major technical challenge due to the low concentration of individual mRNA species. In the meantime, temporal gene-specific analyses of more abundant RNAs, such as rRNAs and snRNAs, could be a more attainable goal and may offer valuable insights into the complex processes of ribosome biogenesis and spliceosome biogenesis.

This study introduces the first longitudinal proteomic analysis of mRNPs with a high temporal resolution. Although numerous studies have been performed for decades to assign the functions and localizations of RBPs, from which the temporal sequence of mRNA binding has been inferred, direct and quantitative evidence has not been available at the proteomic level. The high resolution of our data allows us to detect even subtle differences in mRNA binding dynamics, establishing the chronological orders of RNA-protein interactions throughout the mRNA life cycle. We observe the nascent transcripts collected at 0 min chase time are associated with pol II subunits and transcription factors, some 3´ processing factors, and an m6A writer subunit VIRMA, revealing the initial pre-mRNP complex undergoing (or becoming committed to) the earliest events of co-transcriptional processing and modification. These early recruits are quickly followed by the other 3´ processing factors, hnRNPs, SR proteins, splicing factors, and spliceosome components (U1/U2 followed by tri-snRNPs). Additional proteins join the assemblage, featuring capping-related proteins and nuclear export factors. Several translation-related factors known to interact with ribosomes appear at this stage possibly due to partial rRNA contamination, while the majority of ribosomal proteins and translation factors emerge later. Posttranscriptional regulators, such as AGO proteins and YTHDF proteins, appear in clusters VI and VII. Other proteins implicated in translational repression, such as FMR1, and mRNA destabilization, like UPF1, are found in the final stage.

This temporal sequence generally aligns with the known locations of RBPs. Early binders are predominantly nuclear proteins, while late binding groups are highly enriched with cytoplasmic proteins. Late binders in cluster VII frequently overlap with SG proteome, which includes FMR1/FXR1/FXR2, G3BP1/2, UPF1, MOV10, DDX3X, YBX1/3, LSM14A/B, STAU2, PURA/B, IGF2BP1/2/3, UBAP2/UBAP2L, FAM120A/C, LARP1/4B, SND1, and ZC3HAV1. One can envision that these proteins bind to old mRNAs, forming submicroscopic SG-like small condensates. Given that some of these proteins are implicated in translational repression and decay, this aged mRNP complex may be in a “retired” state, in which mRNAs are less active translationally compared to those in “younger”

mRNPs. Because SG formation per se does not prevent translation (51), the assembly of the SG proteins on old mRNAs is likely to be a consequence, rather than a cause, of the natural process of "translational retirement." Whether or not this complex is indeed less active in translation, what triggers the changes in mRNP composition, and if liquid-liquid phase separation is involved, will be interesting topics for future studies. It is also noteworthy that this very late binding group is highly enriched with proteins that bind to viral transcripts, particularly those from coronaviruses and flaviviruses, with positive-sense single-stranded RNA genomes, whose structures are similar to those of cellular mRNAs. It will be interesting to investigate the functions of these vRBPs in viral infection.

Our experiments yielded some unexpected results. For instance, we detected pol II and 3´ end processing proteins among the earliest binders. Considering our experimental design which is based on oligo(dT) capture, their presence was unanticipated as they are supposed to function before the polyadenylation step. However, a recent report offers a potential explanation for these results: pol II and nascent transcripts readily incorporate into RNP complexes in nuclear matrix, where poly(A) tailed pre-mRNAs are held for further processing steps (72). Another intriguing observation involves the nuclear export factor NXF1. EJC components, SR proteins (SRSF3/SRp20 and SRSF7/9G8), and a TREX component (ALYREF/THOC4) have been reported to recruit NXF1 to promote mRNA export (41; 30; 88). However, our current data show that NXF1 is recruited soon after SR proteins but before EJC and TREX (Figure 2.13). This suggests that NXF1 might be recruited via direct RNA binding and/or assisted by early binders such as SR proteins. While we do not exclude the possibility that EJC and TREX also contribute to NXF1 recruitment, our results indicate a necessity to reassess the mechanisms of mRNA export.

To systematically identify RBPs with unanticipated binding dynamics, we trained a machine learning model to predict mRNA binding dynamics from GO annotations. This model was then applied to screen under-characterized RBPs by comparing the observed and expected dynamics. We found numerous RBPs that bind to mRNA earlier or later than expected, revealing proteins with

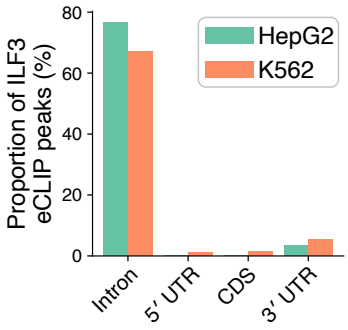

Figure 2.55 Proportions of ILF3 eCLIP peaks that are mapped to intron, 5´ UTR, CDS, and 3´ UTR regions. Both the HepG2 (green) and K562 (orange) eCLIP data are from the ENCODE project.

potentially unknown functions or multiple functions. For instance, we discovered ILF3 (also known as NF90) as an early binder belonging to cluster III. ILF3 has been implicated in various processes such as transcription, microRNA maturation, pre-mRNA splicing, RNA export, translation, and mRNA degradation (9; 27). However, recent eCLIP experiments showed a high proportion of intron peaks (Figure 2.55), suggesting ILF3's binding to pre-mRNAs rather than mature mRNAs. This observation aligns with our data and suggests a role of ILF3 mainly in pre-mRNA processing. Moreover, CIRBP (also termed hnRNP A18), which has been described as a regulator of mRNA stabilization and translational activation (84; 83), was identified as a cluster II protein in our study. CIRBP is predominantly found in the nucleus but partially relocates to the cytoplasm under stress conditions (13). Our dynamics data supports a nuclear function for CIRBP at least under the condition used in this study. The annotation-based prediction method and the temporal RNA binding information will provide a useful resource for further studies on these RBPs.

To foster community access to our data, we developed an interactive web application available at https://chronology.rna.snu.ac.kr. This platform enables the search for specific RBPs via their UniProt accessions or gene symbols. For each RBP, we provide detailed and comprehensive information on mRNA binding

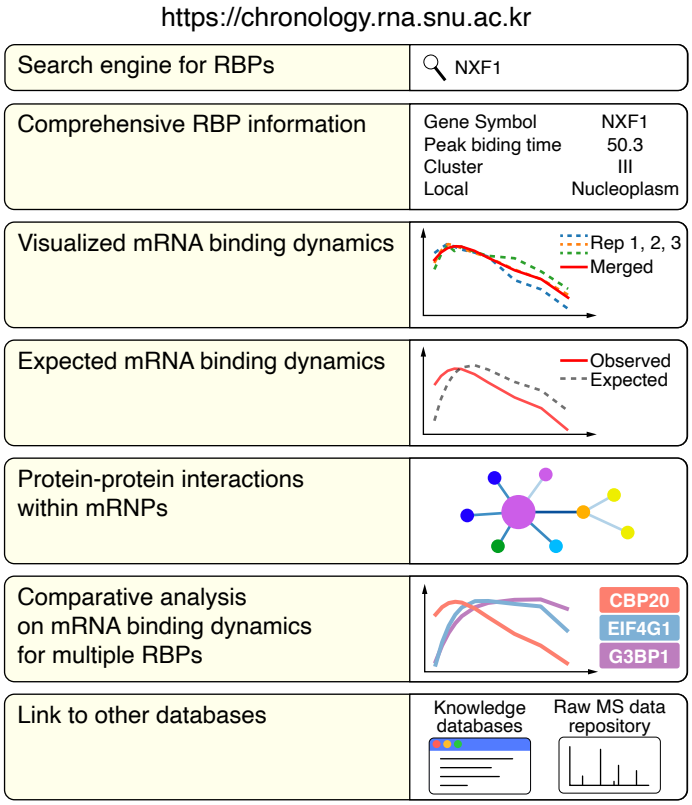

Figure 2.56 . A web application aiding community access to mRNA binding dynamics, accessible at https://chronology.rna.snu.ac.kr.

dynamics, subcellular localization, GO-based prediction of mRNA binding dynamics, and protein interactors within mRNPs. Furthermore, our web application allows researchers to compare the mRNA binding dynamics of multiple RBPs of interest and create combined line plots of the mRNA binding dynamics (Figure 2.56).

The methodology used in this study is readily adaptable to other biological contexts, provided that pulse-labeling and UVA cross-linking are feasible. For instance, a loss-of-function study could be combined to explore a gene's function in mRNP remodeling. Given that some RBPs are associated with genetic disorders (e.g. ALS caused by the defective TDP-43), examining the impact of

their mutations in disease models could yield intriguing results. One could also scrutinize the effects of pharmacological inhibitors/agonists on the mRNA life cycle. Investigating the molecular effects of splicing or translation inhibitors, currently under clinical trials or in use for cancer and genetic diseases, could be enlightening (18; 65; 46; 8). Moreover, mRNP profiling under stress conditions could reveal alterations in mRNP remodeling in cells coping with stressors such as amino acid deprivation, ER stress, heat shock, viral infection, and inflammation, adding new dimensions to the understanding of gene regulation.

2.4 Methods and Materials

Capture of the pulse-labeled RNA interactome

HeLa cells were maintained in DMEM (Welgene) supplemented with 9% FBS (Welgene, cat#S001-01) and cultured at 37°C with 5% CO2. Four 150mm dishes were used for each time point sample. For pulse-labeling, cells were incubated with 0.5mM 4sU (Sigma-Aldrich, cat#T4509) for 10 min. After washing three times with PBS, cells were incubated with DMEM supplemented with 1mM uridine until UVA irradiation. A "no-labeling" sample which was also irradiated with UVA was used as a negative control. After incubation with the uridine supplemented DMEM for a certain designated incubation time (0-5 h), the pulse-labeled cells were washed with cold PBS and irradiated with 365nm UV for 0.45J/cm2. After crosslinking, cells were immediately harvested and treated with TURBO DNaseI at 37°C for 30 min. The 2X lysis buffer (40mM Tris-HCl pH 7.5, 1M LiCl, 1% LiDS wt/vol, 1% NP40 wt/vol, 2mM EDTA, 10mM DTT, 8M Urea) were added to lyse the DNase treated cells. Lysates were homogenized by passing the lysate with a 21G needle. After measuring the amount of total protein with BCA assay, samples containing equal amounts of proteins (15mg) were used for RNA interactome capture (RIC). RIC was performed as in previous papers (10) with the following modifications. Oligo d(T) bead (NEB, cat#S1419S), which was washed with lysis/binding buffer (20mM Tris-HCl pH 7.5, 500mM LiCl, 0.5% LiDS wt/vol, 0.5% NP40 wt/vol, 1mM EDTA, 5mM DTT, 4M Urea), was added to the lysate

and incubated at room temperature for an hour. Beads were collected with the magnet, and the supernatant ("flowthrough") was transferred to a new tube and stored at 4°C for the additional capture (see below). The collected beads were washed once with lysis/binding buffer followed by two washes with wash buffer 1 (20 mM Tris-HCl pH 7.5, 500 mM LiCl, 0.1% LiDS wt/vol, 0.5% NP40 wt/vol, 1 mM EDTA, and 5 mM DTT), wash buffer 2 (20 mM Tris-HCl pH 7.5, 500 mM LiCl, 0.5% NP40 wt/vol, 1 mM EDTA, and 5 mM DTT), and wash buffer 3 (20 mM Tris-HCl pH 7.5, 200 mM LiCl, 1 mM EDTA and 5 mM DTT). For elution, beads were resuspended in 300 ul of elution buffer (20 mM Tris-HCl pH 7.5, 1 mM EDTA) and incubated for 3 min at 65°C with agitation before the supernatant containing eluted proteins was transferred to a fresh tube and stored. The elution step was repeated. The beads and the flowthrough from the first capture step were mixed to capture the residual RNPs remaining in the flowthrough. The incubation, wash, and elution steps were repeated, and the eluted proteins were combined with the eluted proteins from the first round.

Peptide sample preparation and TMT labeling for quantitative proteomics analysis

RNA-binding proteome samples collected via oligo(dT) bead pull down were first concentrated to 80 µl using speed-vac (Concentrator plus, Eppendorf) and then reduced with 20 mM dithiothreitol (DTT) (Sigma-Aldrich) at 37℃ for 1h. The samples were placed onto 30kDa molecular weight cut off (MWCO) filter (Amicon 30kDa, Merck Millipore) along with the 200 µl of urea buffer (8 M urea in 25 mM HEPES buffer, pH 8.5), followed by centrifugation at 15,000×g for 15 min at 24℃. Each sample was then reconstituted with 200 µl of the urea buffer and centrifuged again (twice). The samples were then alkylated with 200 µl of 80mM iodoacetamide (Sigma-Aldrich) in the urea buffer and incubated at 37℃ for 1 hour in the dark, followed by centrifugation. Each sample was then washed with 200 µl of the urea buffer twice and with 200 µl of 25 mM HEPES buffer (pH 8.5) twice. 100 ng of trypsin (~1:50 w/w, based on the estimation from TIC area) in 200 µl of HEPES buffer was added to each sample and incubated at 37℃ for

overnight. Samples were then centrifuged and the collected flow-throughs were concentrated to 40 µl using the speed-vac. Total of 11 samples were labeled with the TMT11plex reagents following the protocol provided by the manufacturer (Thermo Fisher). TMT labeled samples were combined and desalted using the C18 SPE cartridge (Supelco) and the elute from the cartridge was completely dried using the speed-vac and reconstituted with 50 µl of 10 mM ammonium bicarbonate (ABC) buffer.

A concatenated mid-pH (pH 8) RPLC off-line fractionation was carried out at micro-scale for multidimensional LC-MS3 analysis to improve the quantitative profiling depth. For micro-scale fractionation, a RPLC capillary column (320 µm i.d. x 55 cm) was in-house packed with Jupiter C18 beads (Phenomenex, 3 µm). The 50 µl of combined TMT11-labeled peptide sample was loaded onto the capillary column. A linear gradient of solvent A (10 mM ABC in water, pH 8) and solvent B (10 mM ABC in 90% acetonitrile) was applied on nanoAcquity (Waters) at a flow rate of 7 µL/min; 2% solvent B isocratic for initial 14 min, 2 to 10% solvent B for following 2 min, 10 to 40% solvent B for next 56 min. The eluent was automatically concatenated into 6 fractions using TriVersa NanoMate (Advion) and reconstituted with 25 mM ABC buffer for further LC-MS3 analysis.

Liquid chromatography and tandem mass spectrometry (LC-MS3) analysis

The TMT11-labeled 6 fractions were analyzed using an Orbitrap Eclipse via MS3 mode (Thermo Fisher Scientific) coupled with nanoAcquity UPLC system (Waters), which was equipped with an in-house packed trap (150 µm i.d. x 3 cm) and analytical column (75 µm i.d. x 100 cm) using 3 µm of Jupiter C18 particle (Phenomenex). During the analysis, the analytical capillary column was heated at 45°C with the column heater (Analytical Sales and Services). A linear gradient of solvent A (water with 0.1% formic acid) and solvent B (acetonitrile with 0.1% formic acid) was applied at a flow rate of 300 nl/min as follows: 5 to 8% solvent B for initial 10 min, 8 to 35% solvent B for next 195 min. Total run time for the SPS-MS3 analysis were 220 min with the following set up for MS acquisition; Full

MS scans (m/z 400–1600) were acquired at a resolution of 120k (at m/z 200) with 4E5 of AGC target value and 50 ms of ITmax. Selected precursor ions were first isolated at 0.7 Th of isolation window and subjected to HCD fragmentation for MS2 scans in orbitrap at a resolution of 15k (ITmax 60 ms, AGC 5E4 and NCE 30%). The 10 most intense MS2 fragment ions were synchronously isolated in ion trap for final HCD MS3 scans at a resolution of 50k and 0.4 Th of isolation width (AGC 13E5, ITmax 150 ms, and NCE 65%). Overall 3 s of cycle time was applied. The mass spectrometry proteomics data have been deposited to the ProteomeXchange Consortium via the PRIDE (58) partner repository with the dataset identifier PXD039054.

LC-MS3 data processing for peptide identification

For all proteome data analysis, canonical protein sequences (SwissProt) of UniProt human reference proteome UP000005640 (last modified on Dec 3th, 2018, 20303 proteins were included) was used. Pig trypsin (UniProt accession P00761) and the cRAP (common Repository of Adventitious Proteins) protein sequences version 2012.01.01 (http://www.thegpm.org/crap/index.html) were appended to the search space, to mark the peptides from the common contaminant proteins. To estimate peptide level FDR, decoy sequences were generated by reversing target protein sequences. The RAW format LC-MS3 data file was first converted into mzXML format using msconvert (ProteoWizard version 3.0.1908, (1)) with the following parameters: --ignoreUnknownInstrumentError --mzXML --filter "peakPicking true [1,2]" --filter "msLevel 1-2". Then, peak count filtering (≥ 20 peaks), charge suggestion (within range +1 - +7) and mzXML to MGF conversion was done by MzXML2Search (v5.2.0) with the following parameters: -mgf -B0 -T20000 -c1-7 -P20. Resulting MGF files were subjected to the MS-GF+ (v2020.07.02, (40)) for peptide identification at the search tolerance 10ppm. For MS-GF+ search, we set carbamidomethylation of cysteine and TMT labeling of peptide N-terminus/Lysine as static modification, and oxidation of methionine and acetylation of protein N-terminus as variable modification. Also, -m 3 option was set for the HCD fragmentation.

Total RNA analysis

For comparison between conventional RIC and our modified RIC method described above, one 150mm dish of HeLa cells were harvested and lysed with RIC lysis/binding buffer (20mM Tris-HCl pH 7.5, 500mM LiCl, 0.5% LiDS wt/vol, 0.5% NP40 wt/vol, 1mM EDTA, 5mM DTT). After the RIC procedure described above, RNA was isolated from the elution. For total RNA isolation from inputs, 1 ml of TRIzol (Invitrogen) was added to 2.5% of input lysates (which is about 50 ul). The rRNA ratio was estimated by usingTapestation RNA screen tape.

Measuring 4sU labeling efficiency

HeLa cells were pulse-labeled with 0.5 mM 4sU for 10 min and used directly for RNA purification to obtain total RNA population or used for oligo(dT) enrichment. During RNA purification with TRIzol, DTT was added to aqueous phase in the final 0.1 mM and total RNA was eluted in 1 mM DTT solution to prevent oxidation of the 4sU labeled RNA. For oligo(dT) enriched RNA samples, 5 mM DTT was added to the elution buffer after RIC. Single nucleoside digestion was performed as previously described (29). Nucleoside samples prepared from each experimental condition was reconstituted in 50 µl of solvent A (200 mM triethylammonium acetate) and loaded onto a BEH C18 column (2.1 mm i.d. x 300 mm, 1.7 µm particle) (Waters) coupled with the 1290 Infinity UHPLC system (Agilent) and the column heater was set at 25℃. A linear gradient of solvent A and solvent B (90 % methanol) was applied at a flow rate of 100 µl/min as follows: 100% isocratic solvent A for initial 5 min, 0 to 20% solvent B for 20 min, 20 to 30% solvent B for 20 min, 30 to 90% solvent B for 10min, and 90 to 0% solvent B for 2 min, followed by isocratic 100% solvent A for 33 min. UV absorbance at 260 nm and 330 nm were monitored. U and 4sU standards were separately analyzed or mixed 1:1 ratio, each diluted with equal amount of 400 mM triethylammonium acetate to make final concentration as 200 mM, and analyzed to determine the respective elution time based on the UV signal detection at 260 nm and 330 nm. Relative amount of U and 4sU nucleoside in each sample was estimated based

on the UV signal, area under the curve, obtained by 260 nm and 330 nm UV detection at the respective elution time point.

Pulse-labeled RNA sequencing and data processing

One 150 mm culture dish of HeLa cell for each time point was used for the experiment. Followed by 10 min of 4-thiouridine labeling, cells were harvested after incubation for 0 min, 30 min, and 5 hrs of uridine supplemented media. As a negative control, a no-4sU-labeled sample was also prepared. Cells were harvested without UV crosslinking and then treated with DNaseI. For spike-in RNAs, in vitro transcribed non-human RNAs were prepared with or without 4sU and then polyadenylated with ePAP (NEB). After adding spike-in RNAs to the same amount of lysate, the RIC protocol described above was used to enrich poly(A) RNA in the lysate except elution buffer (20 mM Tris-HCl pH 7.5, 1 mM EDTA, and 1mM DTT). The eluted samples were precipitated with ethanol. Enrichment of 4sU labeled RNA was performed based on the previously described protocol (17) with the following alterations. 50ug of poly(A) enriched RNAs were used for MTS-pulldown. MTS-biotin was diluted in N,N-Dimethylformamide (Sigma, cat#227056). RNAs were incubated with diluted MTS-biotin at room temperature for 2 hrs and purified with RNAclean XP (Beckman, cat#A63987). Dynabeads MyOne Streptavidin C1 (Invitrogen, cat#65002) were washed with nuclease-free water and high salt buffer (10 mM Tris, 1 mM EDTA, 100 mM NaCl, 0.05 % Tween-20 wt/vol) and then blocked with blocking buffer (10 mM Tris, 1 mM EDTA, 100 mM NaCl, 0.05 % Tween-20 wt/vol, 5 ug/ul glycogen) for an hour at room temperature. Biotinylated RNAs were heated at 65°C for 10 min and placed on ice. 10X High salt buffer was added to RNA solution to make it 1X concentration, and pre-washed beads were added to RNAs. Biotinylated RNA and streptavidin beads were incubated in dark for 15 min. The first supernatants were kept as flow-through. After washing beads with high salt buffer three times, 4-thiouridine labeled RNAs were eluted from beads with elution buffer (100 mM DTT, 5% 2-Mercaptoethanol, 20 mM HEPES pH 7.6, 1 mM EDTA, 100 mM NaCl, 0.05% Tween-20 wt/vol). RNA-seq libraries were constructed using MGIEasy

RNA Directional Library Prep Kit V2.0 (MGI, cat#1000006385) and sequenced by paired-end run on MGI sequencer.

The initial parts of sequence analysis were done by using Cutadapt version 3.0 (Martin). For 5´ and 3´ end of each read, the low-quality bases below Phred quality of 30 were trimmed. After trimming, 3´ adaptor sequences of both the first and second read of each pair were removed (Table 2.7). Read pairs with any read shorter than 70 bases were removed after trimming and adopter clipping. To get the readcount for each gene and spike-in, a transcript reference was build based on spike-in sequences (Table 2.7), UCSC Genome Browser hg38 RefGene annotation (downloaded on February 20, 2020), and hg 38 genome, by RSEM (v1.3.1) (47). Pre-mRNA transcript models were also generated and added to the transcript reference by in-house software, since un-spliced mRNAs might be included in the early stage mRNPs. The read pairs were aligned to the above transcript reference by STAR version 2.7.6a (14). The read count of each gene and spike-in was calculated and normalized to TPM (transcript per million) by RSEM (v 1.3.1) (47). Spike-in normalization was done by the ratio of geometric mean of spike-in TPMs.

Conventional protein analyses

RIC samples were resolved on SDS-PAGE and analyzed by silver staining using EzWay Protein-Silver Staining Kit (KOMABIOTECH, cat#K14040D). For western blot analysis, the eluates of RIC were first concentrated with Amicon 30K Ultra-0.5 (Millipore) and treated with RNase A (Thermo Scientific, cat#EN0531) and Benzonase (Sigma-Aldrich, cat#E1014). The concentrated samples were then loaded on 10% Novex WedgeWell Tris-Glycine Mini Gel (Invitrogen). After transferring to a methanol-activated PVDF membrane (Millipore), the membrane was blocked in PBS-T containing 5% milk, probed with primary antibodies, and washed three times. Anti-mouse or anti-rabbit HRP-conjugated secondary antibodies (Jackson ImmunoResearch Laboratories) were incubated and washed three times again. Chemiluminescence was performed with West Pico Luminol reagents (Thermo), and the signals were detected by ChemiDoc XRS+ System (BioRad).

In detail, LARP1 (Bethyl, A302-087A), ALYREF (Bethyl, A302-892A), TDP-43 (ProteinTech, 10782-2-AP) and G3BP1 (BD Bioscience, 611126) were first detected, then the membrane was stripped with WSE-7240 EzReprobe (2332530) and restained with antibodies against hnRNPA1 (gift fromGideon Dreyfuss), SRSF7 (MBL, RN079PW) and FMR1 (MBL, RN016P). PABPN (Abcam, ab75855), PABPC4 (Bethyl, A301-466A), POLR2 (Santa Cruz, sc-56767), eIF4G2 (MBL, RN003P) were first detected, then the membrane was stripped and restained with IGF2BP3 (Santa Cruz, sc-365640).

Immunofluorescence and confocal microscopy

HeLa cells were cultured on 8-chamber slide glass (Thermo, 154461PK). The cells were labeled for 10 min with 4sU, followed by a 5 hrs chase with uridine-supplemented media, as previously described. To induce cellular stress, cells were treated with 0.5mM sodium arsenite for 1 hour. Subsequently, the cells were fixed using 4% paraformaldehyde for 10 min and permeabilized with 0.1% Triton X-100. After blocking with a 5% BSA buffer, the cells were incubated with anti-G3BP1 antibody (BD, 611127, mouse) for 2 hours at room temperature. Following washing steps, the cells were incubated with an anti-mouse Alexa Fluor 488-conjugated secondary antibody and DAPI (D9542) for 1 hour. Images were captured using a Nikon ECLIPSE Ti2 microscope.

Protein quantity processing and contaminant filtering

Following procedures were done to generate each protein's quantity dynamics from the triplicate experiments. First, protein quantities were divided by the pig trypsin (UniProt accession P00761) quantity of the regarding sample, to reduce the quantification bias from peptide sample preparation. Then, to remove the effect of non-specific binders, the intensity of no 4sU negative control was subtracted from the other channel's intensities. Pseudo intensity was set as the bottom 5% quantity of each replicate and added to all peptides' intensities to avoid division by zero. Protein intensities of each replicate were normalized so that the intensity sum of protein in each replicate is the same with median of summed

intensity. Normalized and log-transformed replicate quantities were merged and smoothed by univariate quadratic spline (from SciPy(https://scipy.org/)), using time points as independent variables and quantities as dependent variables. The univariate spline was unsuccessful on 18 proteins with very high variance among replicates, so those proteins were discarded. The peak binding time of RBP was found from the fitted spline line, interpolated at 0.1 min interval. Protein quantification quality was defined as the ratio between per replicate variation and per time-point variation. In practice, it was calculated as root mean squared error (RMSE) between measured quantities and merged protein quantity spline (per replicate variation) divided by standard deviation (std) of merged protein quantities (per time-point variation). Proteins with RMSE / std ratio above 1 were discarded. Before further analyzing data, proteins marked as common lab contaminants by cRAP database were discarded. Also, human keratin and histone proteins were removed before the analysis, because those proteins are less likely to act as real RBP, and show high variance between replicates.

To identify mRNA interacting proteins from one non-labeled (No4sU) and 10 crosslinked (CL) samples, we compared all 10 No4sU versus CL sample pairs and combined the results. For each pair, normalized and log-transformed triplicate quantities were tested for differential expression by the DEqMS package, which uses a moderated ANOVA test considering the number of quantified PSMs per protein group (89). P-values of all 10 NoCL versus CL differential expression tests were merged into one p-value by the empirical Brown's method (59). Resulting p-values of all protein groups were adjusted for multiple test correction by Benjamini-Hochberg method.

Previously identified mRNP list from RBP2GO

We adopted previously identified mRNP list from the meta analysis database, RBP2GO (11). All human RBP datasets were taken, except for in vitro experiments, in silico prediction, review or meta analysis, and non-poly(A) enrichment datasets. The RBP2GO identifiers of used datasets are following: Baltz_HEK293_2012, Castello_HeLa-S3_2012, Beckmann_HuH-7_2015, Castello_HeLa-

S3_2016, Conrad_K562_2016, Milek_MCF7_2017, Perez-Perri_Jurkat_RIC_2018, Perez-Perri_Jurkat_eRIC_2018, Garcia-Moreno_HEK293_2019, Backlund_HuH-7_Cytoplasmic_2020, Backlund_HuH-7_Nuclear_2020, Kramer_HeLa_2014, Panhale_HEK293_2019, Mullari_HEK293_2017.

Protein domain enrichment analysis

Taxon 9606 (human) protein domain annotations in Pfam database (version 32.0) was used for protein domain enrichment analysis. One-sided Fisher's exact test was applied to estimate the statistical enrichment of a particular domain among the quantified RBPs. Benjamini-Hochberg method was applied to the p-values for the multiple test correction.

Clustering analysis on temporal dynamics of RBPs

For the feature standardization, log-transformed quantities were z-score transformed for protein-wise direction, by the mean and standard deviation of all time points for each protein. Also, the maximal time of protein quantities were z-score transformed for feature-wise direction. K-means clustering using above normalized features were done by scipy version 1.4.1 (https://scipy.org/). The mean distortion of clustering result was calculated as the mean Euclidean distance between the feature values and the cluster centroids. The number of clusters were manually set to 7 after testing several cluster numbers ($5 \leq K \leq 10$), based on the mean distortion of clustering results.

Filtering out non-protein coding RNA binders and mitochondrial mRNA binders

Several RBPs in our data are primarily known as non-coding RNA or mitochondria-coded mRNA binders, even after we filtered RBPs with previously reported mRNP list. Thus, we defined annotation and knowledge based blacklist for the further analyses. First of all, mitochondrial mRNA binders were defined as genes annotated with GO "mitochondrial matrix" but not with GO "cytosol". Then, we added ribosomal proteins and mitochondrial ribosome proteins to the blacklist.

Next, GO "pre-snoRNP complex", "sno(s)RNA-containing ribonucleoprotein complex", and "preribosome" annotated genes were added to the blacklist. Lastly, three proteins (DCAF13, FTSJ3, NGDN) were removed from the blacklist and re-included to the mRNP list, as there are literatures supporting their binding on nuclear-coded mRNAs.

Gene Ontology (GO) and subcellular localization analysis

As previously described, ribosomal proteins, snoRNA related factors, and RBPs exclusively localized to the mitochondrial matrix were removed in this analysis. All GO gene annotations used in this study were obtained from the org.Hs.eg.db R package (version 3.14.0). To gain functional insights to each cluster, GO term enrichment analysis was done by Fisher's exact test, by setting all 1035 proteins identified by MS as the statistical background. P-values were adjusted for GO hierarchy and local dependencies by weight01 algorithm in topGO R package (2). To test GO terms enriched at a specific time point, we utilized pairwise distances between RBPs used in prior clustering analysis. Per each GO term, pairwise distances within RBPs annotated with GO term and not annotated with GO term were compared by Mann-Whitney U test. To remove redundantly enriched parent-child GO terms, the elim algorithm (described in (2)) was applied to adjusted p-values. We downloaded Human cell map database v1 (26) for deeper analysis of subcellular localizations and polished their data as described in (45).

Binding site mapping of RBPs

As previously described, ribosomal proteins, snoRNA related factors, and RBPs exclusively localized to the mitochondrial matrix were removed in this analysis. The binding locations of RNA-binding proteins (RBPs) were determined based on eCLIP peak locations provided by the ENCODE project (80; 79; 81). To generate non-redundant transcript annotations, we initially calculated read counts for duplicated RNA-seq data from HepG2 and K562 cell lines using RSEM, as previously described (ENCODE data accession: ENCFF002DKZ, ENCFF002DLC, ENCFF002DLE, ENCFF002DLG for HepG2; ENCFF001RDE, ENCFF001RCW,

ENCFF001RDD, ENCFF001RCV for K562). Subsequently, we selected the most abundant transcript for each protein-coding gene, based on TPM values calculated by RSEM. The transcript regions were then divided into subregions, including introns, 5' UTRs, CDS, and 3' UTRs. Finally, for all overlapping subregions, we selected the subregion from the most abundant transcript. In cases where TPM values were tied, which was very rare, we prioritized genes with the smallest RefSeq accession number. The overlap between eCLIP peaks and transcript annotations was determined using the intersectBed tool in Bedtools, with a minimum requirement of $\geq 50\%$ overlap relative to the span of the eCLIP peak (61).

Protein-protein interaction (PPI) network and protein complex analysis

As previously described, ribosomal proteins, snoRNA related factors, and RBPs exclusively localized to the mitochondrial matrix were removed in this analysis. We downloaded PPI data from the BioGRID database (release 4.2.191, (67)). Also, we considered only human PPIs (1) classified as physical interaction and (2) found from at least two different types of experiments, and (3) supported by at least two publications. The networkx python package was used for graph visualization. For the protein complex annotation, we utilized the CORUM database (release 3.0_03.09.2018_coreComplexes). To quantitatively measure the differences among the mRNA binding dynamics of protein within PPI pairs or protein complexes, we calculated Euclidean distances between mRNA binding dynamics vectors, defined as [log2 protein intensity at 0 min, log2 protein intensity at 15 min, ..., log2 protein intensity at 300 min, peak binding time]. Before calculating Euclidean distances, protein intensities and peak binding times were normalized as described in "Clustering analysis on temporal dynamics of RBPs" section.

mRNA binding dynamics prediction from GO annotations

As previously described, ribosomal proteins, snoRNA related factors, and RBPs exclusively localized to the mitochondrial matrix were removed in this analysis.

To generate a boolean table of RBPs versus GO, we utilized the org.Hs.eg.db R package (v3.14.0). Each cell in this table was marked as "true" if an RBP was annotated with a GO term, and "false" otherwise. To remove less informative annotations, we excluded GO terms with fewer than 7 annotated or unannotated RBPs. Subsequently, we performed multiple correspondence analysis (MCA) to convert the boolean table into numeric values and reduce its dimensionality. From the MCA transformed features, we selected the top 30% (323 features), which retained approximately 98% of the original boolean table's information. As the presence of imbalanced numbers of early and late binder RBPs could introduce prediction accuracy bias, we mitigated this bias by oversampling RBPs. This involved duplicating certain RBPs in clusters with fewer members, ensuring that all clusters contained an equal number of RBPs (200). For each time point, we trained a ridge regression model to predict the z-scores of individual RBPs using the MCA transformed features. To determine the optimal model parameters, we performed 5-fold cross-validation. The scikit-learn python package (v0.23.2, https://scikit-learn.org) was utilized for fitting the regression models and conducting cross-validation.

Cell fractionation RNA immunoprecipitation and qPCR

HeLa cell was washed with cold PBS and detached from the plate by scraping with a cell scraper. Cells were resuspended in cytosol fractionation buffer (50mM HEPES pH 7.6, 150mM NaCl, 0.1mM EDTA, 200ug/ml digitonin, 1mM DTT, SuperaseIn, proteinase inhibitor and phophatase inhibitor). After incubation at ice for 10 min, lysate was centrifuged at 2000 g for 10 min at 4°C and supernatant was used for RNA immunoprecipitation. For membrane and nuclear fractionation, subcellular protein fractionation kit for cultured cells (Thermo, 78840) was performed following manufacturer's instruction. Protein A sepharose bead were incubated with salmon sperm DNA overnight at 4°C and washed with cytosol fractionation buffer. 10ug Ab (Bethyl, A302-481A) was added to bead and incubated for 1 hr at 4°C for bead conjugation. Then the lysate and the Ab conjugated bead were subjected to

IP for 3 hrs at 4°C. After IP, the beads were washed with cytosol fractionation buffer.

After immunoprecipitation (IP) of CCDC86 from the cytoplasmic fraction, one-fourth of the sample was used for Western blot analysis, while the remaining sample was subjected to RNA isolation using TRIzol for subsequent qPCR analysis. The list of used oligos is shown in Table 2.7.

Knockdown RNA-seq

HeLa cell was plated in 60 mm dish and final 50 nM siRNAs were reverse-transfected using Lipofectamine 3000 (Invitrogen) and ON-TARGETplus SMART-pool siRNAs (Horizon Discovery) for 48 hrs. Total RNA was purified with TRIzol. RNA-seq reads were processed the same as the pulse-labeled RNA-seq, but without Pre-mRNA transcript models. From ENCODE shRNA-seq dataset, we downloaded fastq files with accession ENCFF541QLM, ENCFF791QXP, ENCFF232RVX, and ENCFF238SIB for shFAM120A of K562 cell line, ENCFF539FEL, ENCFF276RDY, ENCFF454RKS, and ENCFF224TRL for shFAM120A of K562 cell line. Also, ENCFF844XSA, ENCFF327PBI, ENCFF845TFX, and ENCFF841SLY were downloaded for HepG2 cell line shFAM120A, and ENCFF793WXG, ENCFF201DSF, ENCFF344ITC, and ENCFF314EUX were used for shNC of HepG2 cell line. To map spike-in sequences, ENCFF001RTP.fasta was also downloaded. Read counts calculated by RSEM (v1.3.1) were loaded to DESeq2 (v1.34.0) via tximport (v1.22.0). Differential gene expression was tested by DESeq2 with default parameters.

SUnSET assay

HeLa cell was plated in 6 well plate and final 50 nM siRNAs were reverse-transfected using Lipofectamine 3000 (Invitrogen) and ON-TARGETplus SMART-pool siRNAs (Horizon Discovery) for 72 hrs. Cells were incubated in final 0.54ug/ml puromycin for 30 min and then lysed with RIPA buffer (with proteinase inhibitor and phosphatase inhibitor). After BCA assay, same amount of lysate were loaded on 10% Novex WedgeWell Tris-Glycine Mini Gel (Invitrogen). After

transferring to a methanol-activated PVDF membrane (Millipore), the membrane was blocked in PBS-T containing 5% milk, probed with primary antibodies, and washed three times. Anti-mouse or anti-rabbit HRP-conjugated secondary antibodies (Jackson ImmunoResearch Laboratories) were incubated and washed three times again. Chemiluminescence was performed with West Pico Luminol reagents (Thermo), and the signals were detected by ChemiDoc XRS+ System (BioRad). Primary antibodies against puromycin (Sigma-Aldrich, MABE343), α-tubulin (Abcam, ab52866), GAPDH (Santa Cruz, sc-32233) were used.

2.5 Tables

Pfam domain	p-value	q-value	Quantified, w/ domain	Quantified, w/o domain	Not quantified, w/ domain	Not quantified, w/o domain
RRM_1	3E-117	2E-114	121	83	680	19419
Helicase_C	2E-36	7E-34	46	60	755	19442
DEAD	2E-34	4E-32	37	30	764	19472
KH_1	4E-18	7E-16	19	16	782	19486
zf-CCCH	3E-14	5E-12	16	18	785	19484
OB_NTP_bind	3E-12	4E-10	11	6	790	19496
SAP	3E-12	4E-10	11	6	790	19496
HA2	8E-12	8E-10	11	7	790	19495
dsrm	6E-11	5E-09	10	6	791	19496
S1	1E-09	8E-08	7	1	794	19501
G-patch	3E-09	2E-07	12	22	789	19480
RRM_5	4E-09	2E-07	6	0	795	19502
PWI	9E-08	4E-06	5	0	796	19502
Brix	9E-08	4E-06	5	0	796	19502
YTH	9E-08	4E-06	5	0	796	19502
zf-CCHC	9E-08	4E-06	10	19	791	19483
SPOC	5E-07	2E-05	5	1	796	19501
Surp	5E-07	2E-05	5	1	796	19501
La	2E-06	7E-05	5	2	796	19500
WD40	2E-06	7E-05	25	193	776	19309
PAP_assoc	2E-06	7E-05	5	2	796	19500
DUF4217	2E-06	8E-05	4	0	797	19502
Toprim	2E-06	8E-05	4	0	797	19502
RRM_8	2E-06	8E-05	4	0	797	19502
DZF	1E-05	4E-04	4	1	797	19501
zf-CCCH_4	2E-05	6E-04	5	5	796	19497
zf-RanBP	2E-05	6E-04	6	10	795	19492
AAA_12	4E-05	1E-03	5	6	796	19496
S4	6E-05	1E-03	3	0	798	19502
KH_9	6E-05	1E-03	3	0	798	19502
NOPS	6E-05	1E-03	3	0	798	19502
Nop	6E-05	1E-03	3	0	798	19502
zf-RNPHF	6E-05	1E-03	3	0	798	19502
CBF	6E-05	1E-03	3	0	798	19502
Ribosomal_L1	6E-05	1E-03	3	0	798	19502
BAT2_N	6E-05	1E-03	3	0	798	19502
FXMRP1_C_core	6E-05	1E-03	3	0	798	19502
LUC7	6E-05	1E-03	3	0	798	19502
AKAP95	6E-05	1E-03	3	0	798	19502
THRAP3_BCLAF1	6E-05	1E-03	3	0	798	19502
Agenet	6E-05	1E-03	3	0	798	19502
Tudor_FRX1	6E-05	1E-03	3	0	798	19502
Utp12	6E-05	1E-03	3	0	798	19502
CTD_bind	8E-05	1E-03	4	3	797	19499
zf-C2H2_jaz	1E-04	2E-03	5	9	796	19493
SNF2_N	2E-04	3E-03	7	25	794	19477
RRM_7	2E-04	4E-03	3	1	798	19501
OCRE	2E-04	4E-03	3	1	798	19501
CSRP_ZZ	2E-04	4E-03	3	1	798	19501
PHD	2E-04	4E-03	9	45	792	19457
KOW	3E-04	4E-03	4	5	797	19497
AAA_33	3E-04	4E-03	4	5	797	19497
MMR_HSR1	4E-04	6E-03	5	12	796	19490
zf-HC5HC2H	4E-04	6E-03	4	6	797	19496
RNase_T	4E-04	6E-03	4	6	797	19496
AAA_11	4E-04	6E-03	4	6	797	19496
AWS	6E-04	8E-03	3	2	798	19500
Ribosomal_L7Ae	6E-04	8E-03	4	7	797	19495
Rtt106	2E-03	1E-02	2	0	799	19502
Ribosomal_S9	2E-03	1E-02	2	0	799	19502
Ribosomal_S8e	2E-03	1E-02	2	0	799	19502
Ribosomal_S7	2E-03	1E-02	2	0	799	19502
Ribosomal_S5_C	2E-03	1E-02	2	0	799	19502
Ribosomal_S5	2E-03	1E-02	2	0	799	19502
Ribosomal_S4	2E-03	1E-02	2	0	799	19502
Ku_C	2E-03	1E-02	2	0	799	19502
Ribosomal_L44	2E-03	1E-02	2	0	799	19502
Ribosomal_L30_N	2E-03	1E-02	2	0	799	19502
Ribosomal_L28e	2E-03	1E-02	2	0	799	19502
Ribosomal_L27A	2E-03	1E-02	2	0	799	19502
Ribosomal_L24e	2E-03	1E-02	2	0	799	19502
Ribosomal_L22e	2E-03	1E-02	2	0	799	19502
Fcf1	2E-03	1E-02	2	0	799	19502
FXR_C1	2E-03	1E-02	2	0	799	19502
SM-ATX	2E-03	1E-02	2	0	799	19502
Suf	2E-03	1E-02	2	0	799	19502
zf-PARP	2E-03	1E-02	2	0	799	19502
DNA_gyraseB	2E-03	1E-02	2	0	799	19502
DNA_topoisoIV	2E-03	1E-02	2	0	799	19502
DTHCT	2E-03	1E-02	2	0	799	19502
zf-CCCH_2	1E-03	1E-02	3	3	798	19499
AARP2CN	2E-03	1E-02	2	0	799	19502
FoP_duplication	2E-03	1E-02	2	0	799	19502
tRNA_U5-meth_t	2E-03	1E-02	2	0	799	19502
A_deamin	1E-03	1E-02	3	3	798	19499
DUF1897	2E-03	1E-02	2	0	799	19502
DUF3697	2E-03	1E-02	2	0	799	19502

Pfam domain	p-value	q-value	Quantified, w/ domain	Quantified, w/o domain	Not quantified, w/ domain	Not quantified, w/o domain
Topoisom_bac	2E-03	1E-02	2	0	799	19502
TRM	2E-03	1E-02	2	0	799	19502
TOPRIM_C	2E-03	1E-02	2	0	799	19502
hnRNP_Q_AcD	2E-03	1E-02	2	0	799	19502
CSTF_C	2E-03	1E-02	2	0	799	19502
Ku_N	2E-03	1E-02	2	0	799	19502
CDH1_2_SANT_H	2E-03	1E-02	2	0	799	19502
NOP5NT	2E-03	1E-02	2	0	799	19502
MA3	1E-03	1E-02	3	3	798	19499
Gar1	2E-03	1E-02	2	0	799	19502
PPR	2E-03	1E-02	2	0	799	19502
PSP	2E-03	1E-02	2	0	799	19502
PUF	2E-03	1E-02	2	0	799	19502
GUCT	2E-03	1E-02	2	0	799	19502
CSTF2_hinge	2E-03	1E-02	2	0	799	19502
LsmAD	2E-03	1E-02	2	0	799	19502
RIBIOP_C	2E-03	1E-02	2	0	799	19502
Ku	2E-03	1E-02	2	0	799	19502
NUC153	2E-03	1E-02	2	0	799	19502
RNase_PH_C	1E-03	1E-02	3	3	798	19499
DBC1	2E-03	1E-02	2	0	799	19502
CBFNT	2E-03	1E-02	2	0	799	19502
RRM_3	2E-03	1E-02	2	0	799	19502
Nop52	2E-03	1E-02	2	0	799	19502
HHH_9	2E-03	1E-02	2	0	799	19502
RNase_PH	2E-03	1E-02	3	4	798	19498
Chromo	2E-03	1E-02	5	19	796	19483
PARP	3E-03	2E-02	4	12	797	19490
HATPase_c	3E-03	2E-02	4	12	797	19490
NTF2	3E-03	2E-02	3	5	798	19497
PAM2	3E-03	2E-02	3	5	798	19497
CSD	3E-03	2E-02	3	5	798	19497
Methyltr_RsmB-F	4E-03	2E-02	3	6	798	19496
DUF1087	5E-03	2E-02	2	1	799	19501
cwf21	5E-03	2E-02	2	1	799	19501
tRNA_m1G_MT	5E-03	2E-02	2	1	799	19501
DUF1086	5E-03	2E-02	2	1	799	19501
MIF4G	4E-03	2E-02	3	6	798	19496
CHDCT2	5E-03	2E-02	2	1	799	19501
WGR	5E-03	2E-02	2	1	799	19501
LSM14	5E-03	2E-02	2	1	799	19501
CHDNT	5E-03	2E-02	2	1	799	19501
CSHCH	5E-03	2E-02	2	1	799	19501
Staufen_C	5E-03	2E-02	2	1	799	19501
TruB_N	5E-03	2E-02	2	1	799	19501
Ribosomal_L3	5E-03	2E-02	2	1	799	19501
Ribosomal_L30	5E-03	2E-02	2	1	799	19501
PurA	5E-03	2E-02	2	1	799	19501
PARP_reg	5E-03	2E-02	2	1	799	19501
RmaAD	5E-03	2E-02	2	1	799	19501
S1-like	5E-03	2E-02	2	1	799	19501
S10_plectin	5E-03	2E-02	2	1	799	19501
Sas10_Utp3	5E-03	2E-02	2	1	799	19501
DUF4208	5E-03	2E-02	2	1	799	19501
FDF	5E-03	2E-02	2	1	799	19501
Cir_N	5E-03	2E-02	2	1	799	19501
HMG_box_2	6E-03	3E-02	3	7	798	19495
NTP_transf_2	8E-03	4E-02	3	8	798	19494
R3H	8E-03	4E-02	3	8	798	19494
ArgoN	9E-03	4E-02	2	2	799	19500
ArgoMid	9E-03	4E-02	2	2	799	19500
ArgoL2	9E-03	4E-02	2	2	799	19500
zf-CCCH_3	9E-03	4E-02	2	2	799	19500
WHIM1	9E-03	4E-02	2	2	799	19500

Table 2.1 Pfam protein domains enriched in mRNPs.

cluster	Primary gene name	Cluster membership (corr)	0m zscore	15m zscore	30m zscore	45m zscore	1h zscore	1.5h zscore	2h zscore	3h zscore	4h zscore	5h zscore	Maximal binding time
I	GAR1	0.99393153	1.225	0.953	0.729	0.544	0.386	0.12	-0.124	-0.67	-1.321	-1.841	7.11E-13
I	FBL	0.99947525	1.076	0.904	0.744	0.593	0.45	0.178	-0.086	-0.63	-1.25	-1.979	7.11E-13
I	SUPT5H	0.9925156	1.266	0.939	0.685	0.488	0.335	0.109	-0.078	-0.543	-1.241	-1.96	7.11E-13
I	NOP56	0.99948637	0.975	0.882	0.771	0.647	0.512	0.222	-0.082	-0.689	-1.287	-1.951	7.11E-13
I	CD3EAP	0.99335385	0.859	0.806	0.743	0.666	0.575	0.343	0.047	-0.695	-1.458	-1.886	7.11E-13
I	DKC1	0.99628987	0.882	0.821	0.736	0.634	0.519	0.266	-7E-04	-0.543	-1.17	-2.144	7.11E-13
I	SCAF4	0.99936634	0.988	0.893	0.775	0.64	0.494	0.188	-0.112	-0.654	-1.192	-2.019	7.11E-13
I	POLR2A	0.99295624	1.238	0.91	0.663	0.479	0.34	0.144	-0.022	-0.495	-1.255	-2.003	7.11E-13
I	POLR2B	0.985553	1.368	0.956	0.653	0.436	0.282	0.085	-0.067	-0.534	-1.301	-1.879	7.11E-13
I	DDX21	0.99789094	0.866	0.836	0.768	0.67	0.55	0.267	-0.038	-0.635	-1.228	-2.056	7.11E-13
I	SSRP1	0.99730611	0.989	0.91	0.801	0.669	0.519	0.192	-0.146	-0.766	-1.294	-1.875	7.11E-13
I	TCOF1	0.98317017	1.238	0.966	0.746	0.564	0.407	0.13	-0.147	-0.806	-1.48	-1.617	7.11E-13
I	NOLC1	0.98621488	1.283	0.995	0.753	0.548	0.37	0.069	-0.202	-0.758	-1.342	-1.714	7.11E-13
I	SPOUT1	0.99908032	0.918	0.865	0.778	0.665	0.533	0.237	-0.076	-0.671	-1.242	-2.006	7.11E-13
I	VIRMA	0.99047927	0.782	0.756	0.708	0.64	0.556	0.348	0.099	-0.493	-1.221	-2.175	7.11E-13
I	SUPT6H	0.98691466	1.335	0.934	0.641	0.432	0.285	0.102	-0.034	-0.474	-1.255	-1.964	7.11E-13
I	PHF3	0.98675369	1.169	0.82	0.587	0.439	0.351	0.259	0.163	-0.373	-1.363	-2.052	7.11E-13
I	PINX1	0.997316	0.988	0.858	0.739	0.625	0.511	0.27	-0.006	-0.685	-1.42	-1.879	7.11E-13
I	PPP1R10	0.99957972	1.026	0.881	0.74	0.601	0.465	0.2	-0.061	-0.594	-1.215	-2.043	7.11E-13
I	SCAF11	0.99155598	1.288	0.952	0.693	0.492	0.336	0.102	-0.095	-0.589	-1.289	-1.89	7.11E-13
I	FAM208A	0.99278231	0.886	0.804	0.709	0.606	0.497	0.268	0.033	-0.467	-1.123	-2.214	7.11E-13
I	SCAF8	0.99857406	0.996	0.912	0.795	0.656	0.501	0.171	-0.153	-0.71	-1.205	-1.963	7.11E-13
I	NOP58	0.99841456	0.887	0.855	0.781	0.674	0.544	0.244	-0.073	-0.662	-1.217	-2.034	7.11E-13
I	URB2	0.99738754	0.89	0.88	0.811	0.699	0.555	0.216	-0.134	-0.728	-1.207	-1.981	5.1
I	RPRD2	0.99455883	0.791	0.794	0.757	0.688	0.591	0.337	0.029	-0.647	-1.322	-2.017	8.3
I	URB1	0.99632874	0.857	0.865	0.813	0.713	0.578	0.247	-0.113	-0.754	-1.265	-1.942	9.2
I	CSTF3	0.99625602	0.815	0.823	0.78	0.697	0.584	0.295	-0.032	-0.676	-1.271	-2.016	9.6
I	ZNF579	0.98794034	0.831	0.856	0.798	0.682	0.529	0.179	-0.148	-0.573	-0.931	-2.224	11.3
I	SUPT16H	0.99617321	0.822	0.843	0.801	0.712	0.587	0.272	-0.077	-0.717	-1.254	-1.988	12
I	CSTF2T	0.99561948	0.801	0.833	0.797	0.711	0.586	0.272	-0.071	-0.679	-1.2	-2.049	14
I	FIP1L1	0.99221419	0.742	0.808	0.793	0.718	0.599	0.287	-0.054	-0.634	-1.135	-2.125	19.3
II	CSTF1	0.99309753	0.695	0.757	0.757	0.708	0.62	0.366	0.053	-0.602	-1.25	-2.103	22.4
II	CHERP	0.99126541	0.71	0.81	0.815	0.747	0.627	0.295	-0.074	-0.692	-1.166	-2.072	23.2
II	DDX50	0.99311544	0.699	0.779	0.783	0.728	0.628	0.341	0.002	-0.653	-1.235	-2.074	23.3
II	CSTF2	0.99294507	0.693	0.784	0.791	0.732	0.625	0.323	-0.022	-0.639	-1.172	-2.114	23.7
II	CHD2	0.99170695	0.657	0.706	0.71	0.678	0.613	0.413	0.145	-0.501	-1.245	-2.177	24.1
II	WDR33	0.99409234	0.678	0.758	0.768	0.722	0.632	0.365	0.038	-0.622	-1.244	-2.094	24.7
II	NOL11	0.98334056	0.72	0.847	0.863	0.793	0.66	0.279	-0.153	-0.867	-1.283	-1.859	24.9
II	LYAR	0.99413851	0.66	0.734	0.746	0.708	0.629	0.389	0.084	-0.575	-1.246	-2.129	25.6
II	DDX51	0.99400889	0.666	0.776	0.794	0.741	0.635	0.329	-0.022	-0.637	-1.154	-2.127	25.7
II	TTF1	0.99237553	0.685	0.787	0.805	0.755	0.654	0.348	-0.022	-0.733	-1.301	-1.978	26
II	NCL	0.99349206	0.669	0.781	0.805	0.758	0.659	0.353	-0.017	-0.724	-1.288	-1.995	27.1
II	NOL8	0.99150492	0.633	0.809	0.85	0.789	0.657	0.277	-0.134	-0.717	-1.056	-2.108	27.8
II	KRI1	0.9942171	0.657	0.773	0.801	0.759	0.662	0.361	-0.007	-0.715	-1.287	-2.004	27.9
II	WDR36	0.99357504	0.645	0.796	0.834	0.784	0.67	0.324	-0.077	-0.752	-1.213	-2.011	28.3
II	SETD2	0.99359745	0.611	0.738	0.769	0.728	0.634	0.35	0.024	-0.547	-1.077	-2.231	28.3
II	EPRS	0.9544017	0.664	0.854	0.909	0.856	0.721	0.291	-0.226	-1.103	-1.465	-1.501	29.5
II	NOP9	0.99130896	0.605	0.814	0.873	0.819	0.684	0.281	-0.161	-0.783	-1.091	-2.04	29.6
II	LUC7L2	0.99657928	0.616	0.754	0.794	0.757	0.663	0.365	0.006	-0.654	-1.201	-2.099	29.7
II	ZNF207	0.99617931	0.626	0.745	0.78	0.747	0.662	0.387	0.04	-0.656	-1.269	-2.063	29.7
II	DIDO1	0.99659306	0.616	0.755	0.796	0.76	0.665	0.366	0.003	-0.664	-1.21	-2.088	29.8
II	RAMAC	0.99376506	0.591	0.795	0.855	0.808	0.683	0.302	-0.121	-0.743	-1.094	-2.076	30.2
II	RBM39	0.99668549	0.612	0.754	0.798	0.764	0.671	0.371	0.005	-0.677	-1.231	-2.067	30.3
II	RBM15	0.99614066	0.58	0.738	0.789	0.755	0.66	0.359	0.007	-0.597	-1.103	-2.189	30.8
II	SF3A2	0.99708911	0.598	0.728	0.771	0.745	0.666	0.399	0.059	-0.623	-1.239	-2.106	31.3
II	SCAF1	0.99036985	0.55	0.807	0.89	0.842	0.702	0.273	-0.19	-0.786	-1.015	-2.072	31.3
II	RBM19	0.99735954	0.59	0.75	0.803	0.773	0.679	0.372	-6E-04	-0.678	-1.209	-2.08	31.4
II	SNRNP70	0.99782623	0.577	0.731	0.785	0.761	0.676	0.391	0.036	-0.638	-1.21	-2.111	32.2
II	DDX42	0.99501611	0.528	0.724	0.793	0.766	0.67	0.357	-0.002	-0.572	-1.024	-2.242	32.6
II	SUGP1	0.99207382	0.593	0.761	0.823	0.8	0.71	0.394	-0.014	-0.808	-1.374	-1.884	32.9
II	RBM10	0.99813083	0.567	0.729	0.788	0.767	0.684	0.397	0.037	-0.65	-1.223	-2.096	33
II	U2SURP	0.99817301	0.548	0.734	0.802	0.779	0.687	0.378	0.004	-0.647	-1.152	-2.133	33.1
II	SPEN	0.99800957	0.569	0.723	0.78	0.76	0.68	0.405	0.053	-0.637	-1.233	-2.101	33.1
II	CLTC	0.98762458	0.514	0.807	0.915	0.883	0.748	0.303	-0.203	-0.912	-1.153	-1.902	33.4
II	RBM5	0.99828832	0.56	0.723	0.784	0.766	0.686	0.404	0.047	-0.643	-1.227	-2.099	33.5
II	ZC3H4	0.99832234	0.557	0.724	0.789	0.771	0.691	0.407	0.044	-0.661	-1.246	-2.077	33.9
II	CPSF6	0.99819475	0.559	0.726	0.791	0.774	0.694	0.408	0.042	-0.672	-1.258	-2.062	33.9
II	U2AF1L5	0.99710298	0.559	0.738	0.808	0.791	0.707	0.404	0.015	-0.731	-1.296	-1.996	34.1
II	TUBB	0.98440713	0.418	0.79	0.932	0.903	0.753	0.263	-0.259	-0.829	-0.888	-2.083	34.3
II	WDR43	0.99472839	0.551	0.748	0.827	0.812	0.724	0.402	-0.012	-0.794	-1.335	-1.922	34.7
II	SMARCA5	0.99131677	0.449	0.779	0.908	0.886	0.754	0.31	-0.188	-0.834	-1.034	-2.029	34.8
II	RBM25	0.99891913	0.533	0.718	0.792	0.779	0.698	0.408	0.04	-0.653	-1.215	-2.1	34.8
II	BUD13	0.99105938	0.525	0.77	0.869	0.852	0.747	0.374	-0.089	-0.878	-1.308	-1.861	34.9
II	TAF15	0.99833948	0.542	0.703	0.769	0.758	0.688	0.427	0.083	-0.617	-1.243	-2.111	35
II	CCAR1	0.99907397	0.519	0.724	0.807	0.795	0.71	0.402	0.015	-0.683	-1.208	-2.081	35.1
II	ZNF106	0.99837477	0.487	0.737	0.837	0.823	0.723	0.372	-0.046	-0.709	-1.122	-2.101	35.1
II	PPHLN1	0.99760074	0.512	0.693	0.767	0.757	0.683	0.414	0.074	-0.564	-1.136	-2.201	35.3
II	PUF60	0.99915333	0.511	0.724	0.811	0.8	0.715	0.402	0.011	-0.691	-1.207	-2.076	35.4
II	UTP4	0.99904047	0.515	0.709	0.788	0.778	0.699	0.411	0.047	-0.629	-1.183	-2.134	35.4
II	CUSTOS	0.97104674	0.412	0.811	0.974	0.958	0.811	0.294	-0.3	-1.074	-1.165	-1.721	35.7
II	DHX15	0.99710509	0.548	0.686	0.745	0.739	0.68	0.45	0.131	-0.583	-1.28	-2.114	35.8
II	DDX60L	0.9838971	0.348	0.753	0.917	0.902	0.761	0.284	-0.225	-0.759	-0.81	-2.171	35.8
II	SF3B6	0.99863991	0.528	0.699	0.772	0.766	0.697	0.435	0.085	-0.629	-1.255	-2.097	36
II	EWSR1	0.99847454	0.507	0.689	0.767	0.761	0.693	0.43	0.088	-0.585	-1.188	-2.162	36.3
II	SMNDC1	0.99929263	0.473	0.721	0.826	0.819	0.729	0.397	-0.012	-0.7	-1.159	-2.093	36.3
II	PHRF1	0.99709958	0.541	0.682	0.743	0.739	0.683	0.456	0.136	-0.583	-1.286	-2.112	36.4
II	RBM7	0.99288498	0.552	0.653	0.698	0.695	0.652	0.471	0.202	-0.475	-1.252	-2.195	36.4
II	HNRNPH2	0.99918909	0.464	0.705	0.808	0.803	0.719	0.404	0.016	-0.642	-1.121	-2.154	36.6
II	ZCRB1	0.99843589	0.523	0.695	0.771	0.768	0.703	0.445	0.094	-0.64	-1.285	-2.073	36.7
II	FUBP1	0.99919438	0.505	0.703	0.789	0.786	0.714	0.433	0.061	-0.665	-1.254	-2.072	36.8
II	CPSF4	0.99656934	0.512	0.668	0.737	0.735	0.678	0.449	0.138	-0.527	-1.195	-2.195	36.9
II	CPSF7	0.99920432	0.504	0.702	0.788	0.786	0.714	0.434	0.063	-0.664	-1.255	-2.073	36.9
II	KHSRP	0.99931495	0.499	0.701	0.79	0.788	0.716	0.433	0.061	-0.663	-1.248	-2.077	37
II	CDK13	0.99924454	0.465	0.693	0.792	0.791	0.714	0.42	0.048	-0.617	-1.142	-2.163	37.1
II	PRPF38B	0.99517155	0.441	0.742	0.873	0.872	0.771	0.389	-0.082	-0.841	-1.222	-1.944	37.1
II	RBM4B	0.98813357	0.355	0.685	0.826	0.824	0.722	0.355	-0.054	-0.563	-0.832	-2.32	37.1
II	SF3A3	0.99911141	0.484	0.712	0.813	0.812	0.733	0.425	0.025	-0.716	-1.253	-2.034	37.2
II	THRAP3	0.99928395	0.476	0.69	0.784	0.783	0.71	0.428	0.064	-0.613	-1.169	-2.153	37.2
II	U2AF2	0.99881418	0.507	0.688	0.769	0.769	0.705	0.447	0.097	-0.623	-1.258	-2.1	37.3
II	DAZAP1	0.99935594	0.491	0.699	0.792	0.792	0.721	0.437	0.061	-0.671	-1.255	-2.068	37.4
II	BCLAF1	0.99942943	0.466	0.69	0.788	0.789	0.716	0.428	0.058	-0.62	-1.163	-2.151	37.5
II	SF3B2	0.99806854	0.493	0.708	0.805	0.806	0.734	0.44	0.046	-0.728	-1.311	-1.994	37.6
II	PHF5A	0.99978219	0.449	0.699	0.81	0.811	0.732	0.419	0.025	-0.664	-1.16	-2.121	37.6
II	LUC7L3	0.99877897	0.484	0.705	0.804	0.807	0.734	0.439	0.046	-0.714	-1.286	-2.019	37.8
II	PDCD6	0.97872546	0.405	0.764	0.924	0.929	0.817	0.377	-0.169	-1.023	-1.315	-1.709	37.8
II	FUS	0.99794728	0.452	0.674	0.773	0.776	0.706	0.431	0.079	-0.564	-1.112	-2.213	37.8
II	ANXA7	0.98095121	0.471	0.749	0.874	0.878	0.787	0.416	-0.074	-0.968	-1.436	-1.698	37.9
II	RBM6	0.99947865	0.468	0.683	0.78	0.784	0.717	0.443	0.08	-0.619	-1.202	-2.133	38.1
II	DDX46	0.99942461	0.476	0.684	0.778	0.782	0.717	0.447	0.086	-0.627	-1.227	-2.114	38.1
II	UTP23	0.99928945	0.454	0.705	0.818	0.823	0.746	0.432	0.023	-0.724	-1.245	-2.033	38.2
II	SF3B4	0.99879434	0.484	0.694	0.791	0.796	0.73	0.451	0.072	-0.69	-1.297	-2.031	38.3
II	ACOT7	0.99604921	0.412	0.726	0.867	0.875	0.781	0.408	-0.061	-0.828	-1.226	-1.954	38.3
II	KNOP1	0.99936221	0.41	0.69	0.816	0.824	0.743	0.419	0.014	-0.656	-1.111	-2.149	38.4
II	ZC3H13	0.998749	0.478	0.672	0.762	0.767	0.707	0.455	0.112	-0.589	-1.219	-2.145	38.4
II	SURF4	0.99313107	0.309	0.708	0.887	0.899	0.79	0.37	-0.119	-0.75	-0.961	-2.132	38.5
II	PQBP1	0.99553139	0.327	0.702	0.872	0.884	0.784	0.386	-0.085	-0.734	-1.007	-2.13	38.7
II	UBTF	0.99215086	0.565	0.657	0.704	0.708	0.673	0.5	0.216	-0.564	-1.41	-2.049	38.9
II	RPL30	0.99772585	0.445	0.66	0.759	0.768	0.707	0.45	0.11	-0.548	-1.14	-2.211	38.9
II	NHP2	0.99864663	0.369	0.693	0.841	0.854	0.767	0.413	-0.023	-0.702	-1.089	-2.123	39
II	DDX17	0.99888287	0.45	0.665	0.766	0.776	0.716	0.457	0.108	-0.584	-1.19	-2.162	39.2
II	HNRNPH3	0.99143244	0.323	0.654	0.806	0.822	0.739	0.405	0.01	-0.549	-0.903	-2.306	39.3
II	PATZ1	0.99642569	0.383	0.71	0.863	0.879	0.792	0.425	-0.043	-0.82	-1.23	-1.959	39.3
II	SRRM1	0.99900227	0.416	0.695	0.827	0.841	0.766	0.443	0.019	-0.744	-1.246	-2.016	39.4
II	TCF20	0.9498976	0.183	0.59	0.773	0.793	0.699	0.344	-0.027	-0.342	-0.474	-2.538	39.4
II	SART1	0.99864082	0.357	0.692	0.848	0.866	0.781	0.423	-0.025	-0.736	-1.129	-2.078	39.6
II	PRPF6	0.99953211	0.385	0.676	0.812	0.828	0.753	0.437	0.033	-0.654	-1.126	-2.143	39.6
II	ZC3H18	0.99717642	0.435	0.698	0.823	0.838	0.767	0.453	0.03	-0.774	-1.319	-1.952	39.6
II	PRPF40A	0.99861018	0.384	0.694	0.841	0.859	0.78	0.44	-0.002	-0.762	-1.219	-2.014	39.8
II	AKAP8L	0.99871705	0.437	0.659	0.764	0.777	0.719	0.462	0.113	-0.577	-1.182	-2.171	39.8
II	RBMX2	0.99982911	0.428	0.672	0.788	0.803	0.739	0.458	0.08	-0.645	-1.216	-2.107	39.8
II	WBP11	0.99976577	0.391	0.682	0.82	0.838	0.765	0.445	0.029	-0.704	-1.193	-2.075	39.9
II	DDX5	0.99917725	0.421	0.661	0.775	0.79	0.729	0.459	0.098	-0.596	-1.174	-2.163	40
II	GPATCH4	0.99944383	0.443	0.669	0.778	0.793	0.734	0.468	0.1	-0.64	-1.253	-2.092	40
II	RBM42	0.99848663	0.407	0.69	0.825	0.843	0.772	0.454	0.029	-0.754	-1.272	-1.994	40.1
II	CKAP4	0.9988302	0.447	0.675	0.786	0.802	0.743	0.472	0.093	-0.682	-1.303	-2.033	40.2
II	ZCCHC8	0.99771955	0.344	0.661	0.811	0.832	0.757	0.435	0.031	-0.618	-1.049	-2.202	40.2
II	UTP11	0.99946262	0.363	0.67	0.817	0.838	0.765	0.444	0.032	-0.666	-1.13	-2.132	40.3
II	MSN	0.98501699	0.182	0.668	0.896	0.928	0.821	0.377	-0.133	-0.718	-0.824	-2.197	40.3
II	RAB10	0.9923318	0.354	0.707	0.876	0.901	0.816	0.438	-0.054	-0.882	-1.285	-1.873	40.3
II	RBM4	0.99989785	0.404	0.668	0.796	0.814	0.75	0.46	0.071	-0.653	-1.201	-2.109	40.3
II	DUSP11	0.9984914	0.458	0.658	0.756	0.772	0.721	0.481	0.137	-0.604	-1.274	-2.105	40.5
II	SRFBP1	0.99939022	0.354	0.673	0.828	0.853	0.78	0.452	0.023	-0.711	-1.174	-2.077	40.7
II	HNRNPH1	0.99788044	0.376	0.646	0.776	0.798	0.737	0.459	0.093	-0.568	-1.103	-2.214	40.8
II	DDX31	0.99561845	0.264	0.67	0.864	0.896	0.809	0.425	-0.047	-0.727	-1.028	-2.124	40.8
II	TCERG1	0.99616758	0.293	0.653	0.825	0.854	0.777	0.435	0.01	-0.632	-1.007	-2.207	40.9
II	SF1	0.99881868	0.439	0.655	0.761	0.779	0.727	0.481	0.131	-0.602	-1.251	-2.119	40.9
II	SF3B1	0.99850318	0.371	0.649	0.784	0.806	0.744	0.46	0.085	-0.589	-1.116	-2.194	40.9
II	SNIP1	0.97518521	0.232	0.717	0.951	0.989	0.883	0.409	-0.186	-1.045	-1.226	-1.724	40.9
II	RTF1	0.9962013	0.312	0.687	0.868	0.898	0.816	0.442	-0.039	-0.811	-1.187	-1.986	40.9
II	RBM12	0.9990999	0.372	0.677	0.825	0.85	0.78	0.46	0.033	-0.733	-1.232	-2.031	40.9
II	RBM34	0.99969011	0.386	0.665	0.802	0.826	0.764	0.47	0.071	-0.681	-1.231	-2.072	41.1
II	ELOA	0.99724893	0.404	0.636	0.751	0.772	0.721	0.477	0.139	-0.536	-1.152	-2.212	41.3
II	DHX33	0.99720234	0.277	0.663	0.851	0.886	0.807	0.444	-0.016	-0.723	-1.085	-2.104	41.4
II	TRNAU1AP	0.99865849	0.432	0.657	0.77	0.791	0.741	0.489	0.126	-0.644	-1.299	-2.063	41.5
II	CIRBP	0.9996459	0.367	0.656	0.799	0.827	0.767	0.475	0.077	-0.663	-1.206	-2.097	41.6
II	NUDT21	0.9995176	0.385	0.651	0.784	0.81	0.753	0.478	0.099	-0.633	-1.211	-2.118	41.6
II	SRSF2	0.99964393	0.378	0.654	0.792	0.818	0.759	0.476	0.087	-0.648	-1.209	-2.107	41.6
II	SRSF1	0.99937805	0.399	0.651	0.777	0.801	0.747	0.481	0.111	-0.625	-1.228	-2.114	41.6
II	H1FX	0.9960981	0.255	0.664	0.864	0.902	0.821	0.444	-0.033	-0.754	-1.086	-2.077	41.6
II	MMTAG2	0.99769583	0.312	0.671	0.848	0.882	0.809	0.46	0.001	-0.769	-1.197	-2.016	41.6
II	SRSF5	0.99945631	0.385	0.65	0.782	0.808	0.753	0.48	0.103	-0.629	-1.211	-2.12	41.7
II	DDX10	0.998786	0.324	0.649	0.809	0.84	0.775	0.463	0.054	-0.644	-1.116	-2.153	41.7
II	CMSS1	0.99576498	0.242	0.657	0.861	0.901	0.821	0.445	-0.029	-0.737	-1.063	-2.1	41.8
II	XRN2	0.99579439	0.295	0.631	0.796	0.829	0.765	0.459	0.065	-0.576	-1.025	-2.239	41.9
II	HNRNPF	0.99915186	0.363	0.643	0.782	0.812	0.756	0.48	0.102	-0.614	-1.178	-2.146	42
II	TRA2B	0.99946417	0.361	0.648	0.791	0.821	0.764	0.48	0.091	-0.642	-1.197	-2.117	42
II	FSCN1	0.99351134	0.255	0.672	0.88	0.923	0.844	0.458	-0.045	-0.844	-1.194	-1.948	42.1
II	TRMT10C	0.99932889	0.358	0.655	0.804	0.836	0.777	0.482	0.076	-0.689	-1.236	-2.062	42.1
II	TRA2A	0.99931854	0.354	0.644	0.79	0.821	0.765	0.482	0.093	-0.634	-1.186	-2.128	42.2
II	AKAP8	0.99856586	0.392	0.637	0.761	0.789	0.74	0.491	0.136	-0.585	-1.21	-2.151	42.3
II	GRWD1	0.99617945	0.427	0.626	0.728	0.75	0.71	0.497	0.183	-0.516	-1.212	-2.194	42.3
II	HNRNPUL1	0.99375069	0.23	0.663	0.879	0.926	0.848	0.459	-0.044	-0.824	-1.155	-1.983	42.4
II	CCDC59	0.99498226	0.217	0.648	0.861	0.908	0.831	0.454	-0.025	-0.737	-1.056	-2.101	42.4
II	USP36	0.99797439	0.277	0.644	0.827	0.867	0.801	0.469	0.033	-0.683	-1.112	-2.123	42.4
II	HNRNPL	0.99839269	0.331	0.632	0.783	0.818	0.763	0.483	0.102	-0.6	-1.14	-2.173	42.6
II	HNRNPK	0.99903986	0.345	0.637	0.785	0.819	0.765	0.487	0.102	-0.622	-1.181	-2.138	42.6
II	SRSF8	0.9939778	0.229	0.623	0.819	0.863	0.795	0.459	0.033	-0.612	-0.985	-2.226	42.6
II	SNRNP200	0.99918861	0.349	0.647	0.798	0.833	0.778	0.49	0.088	-0.677	-1.236	-2.071	42.7
II	SLTM	0.99798962	0.377	0.629	0.757	0.787	0.74	0.493	0.143	-0.565	-1.186	-2.175	42.7
II	HNRNPUL2	0.99879838	0.355	0.634	0.776	0.809	0.758	0.49	0.116	-0.604	-1.183	-2.15	42.7
II	FAM133B	0.99720404	0.273	0.651	0.843	0.887	0.821	0.479	0.021	-0.756	-1.193	-2.026	42.8
II	HNRNPAB	0.9991709	0.333	0.641	0.797	0.834	0.778	0.489	0.089	-0.657	-1.2	-2.103	42.8
II	HNRNPA2B	0.99911012	0.342	0.638	0.788	0.823	0.77	0.49	0.101	-0.634	-1.195	-2.123	42.8
II	SNU13	0.99686793	0.434	0.649	0.762	0.789	0.746	0.509	0.15	-0.662	-1.366	-2.012	42.8
II	SRSF7	0.99907514	0.341	0.637	0.788	0.823	0.769	0.489	0.101	-0.631	-1.19	-2.128	42.8
II	HNRNPU	0.99827572	0.358	0.629	0.767	0.799	0.75	0.492	0.129	-0.58	-1.173	-2.171	42.8
II	CCAR2	0.99830663	0.344	0.629	0.773	0.807	0.757	0.489	0.119	-0.587	-1.159	-2.173	42.8
II	CHD1	0.9974369	0.378	0.624	0.75	0.78	0.736	0.497	0.154	-0.549	-1.183	-2.187	42.9
II	NONO	0.99859652	0.316	0.632	0.792	0.83	0.775	0.486	0.092	-0.623	-1.15	-2.151	42.9
II	RBM14	0.99826027	0.317	0.629	0.787	0.824	0.77	0.486	0.099	-0.606	-1.136	-2.17	42.9
II	KHDRBS1	0.99901363	0.362	0.641	0.785	0.82	0.77	0.498	0.111	-0.657	-1.254	-2.076	43
II	SRSF3	0.99867577	0.338	0.63	0.78	0.816	0.765	0.493	0.113	-0.609	-1.176	-2.15	43
II	HNRNPD	0.99876179	0.355	0.631	0.773	0.808	0.76	0.498	0.126	-0.61	-1.21	-2.132	43.1
II	HNRNPA1	0.99898014	0.344	0.634	0.783	0.819	0.768	0.495	0.111	-0.629	-1.205	-2.121	43.1
II	NCOA5	0.99738901	0.308	0.621	0.781	0.819	0.767	0.487	0.107	-0.581	-1.111	-2.198	43.1
II	RRP8	0.99770104	0.266	0.629	0.814	0.859	0.8	0.484	0.062	-0.656	-1.116	-2.14	43.2
II	HNRNPA3	0.99901727	0.331	0.636	0.792	0.831	0.778	0.495	0.099	-0.652	-1.211	-2.101	43.2
II	SON	0.99892505	0.341	0.638	0.791	0.829	0.779	0.5	0.105	-0.664	-1.242	-2.077	43.3
II	RBBP6	0.99699982	0.371	0.651	0.797	0.834	0.784	0.506	0.1	-0.729	-1.342	-1.973	43.3
II	HNRNPDL	0.99882878	0.341	0.639	0.793	0.832	0.781	0.501	0.102	-0.674	-1.252	-2.064	43.3
II	SUB1	0.99438694	0.376	0.659	0.806	0.844	0.793	0.508	0.088	-0.777	-1.392	-1.904	43.3
II	LUC7L	0.99866077	0.311	0.628	0.792	0.834	0.784	0.5	0.103	-0.644	-1.195	-2.113	43.6
II	RBM3	0.99881455	0.328	0.633	0.791	0.832	0.782	0.502	0.105	-0.659	-1.229	-2.087	43.6
II	SF3A1	0.99844357	0.373	0.635	0.773	0.809	0.764	0.509	0.135	-0.645	-1.285	-2.068	43.6
II	HNRNPA0	0.99785864	0.302	0.618	0.782	0.825	0.775	0.499	0.114	-0.6	-1.147	-2.167	43.7
II	HNRNPLL	0.99799386	0.305	0.619	0.782	0.825	0.776	0.5	0.115	-0.604	-1.156	-2.16	43.8
II	MFAP1	0.998026	0.272	0.628	0.813	0.861	0.807	0.499	0.075	-0.684	-1.182	-2.088	43.9
II	ZNF385A	0.99775856	0.26	0.626	0.815	0.865	0.81	0.498	0.07	-0.683	-1.167	-2.095	43.9
II	SRSF4	0.99796044	0.31	0.617	0.776	0.82	0.773	0.505	0.126	-0.599	-1.17	-2.157	44
II	ZNF326	0.99840985	0.328	0.622	0.776	0.818	0.773	0.51	0.131	-0.62	-1.217	-2.12	44.1
II	PABPN1	0.99583326	0.273	0.603	0.774	0.821	0.774	0.501	0.124	-0.561	-1.092	-2.217	44.3
II	PTBP2	0.99806724	0.284	0.618	0.793	0.841	0.793	0.507	0.106	-0.641	-1.181	-2.121	44.3
II	SRSF9	0.9982458	0.296	0.622	0.793	0.84	0.793	0.511	0.109	-0.656	-1.216	-2.093	44.3
II	BAZ1B	0.99822834	0.348	0.624	0.77	0.811	0.77	0.517	0.143	-0.63	-1.264	-2.089	44.3

II	RBMX	0.99793053	0.31	0.614	0.774	0.819	0.775	0.511	0.133	-0.602	-1.187	-2.146	44.4
II	ZCCHC17	0.99356945	0.264	0.64	0.839	0.894	0.84	0.513	0.048	-0.81	-1.312	-1.915	44.4
II	RPL10	0.98768235	0.258	0.573	0.737	0.784	0.742	0.496	0.16	-0.436	-0.972	-2.343	44.6
II	APOBEC3B	0.99780653	0.285	0.612	0.785	0.834	0.79	0.515	0.122	-0.626	-1.189	-2.127	44.7
II	SLC25A3	0.99737052	0.255	0.611	0.797	0.851	0.803	0.511	0.102	-0.642	-1.161	-2.127	44.7
II	SRRT	0.99807098	0.315	0.616	0.775	0.821	0.779	0.518	0.137	-0.622	-1.225	-2.114	44.7
II	SUGP2	0.99756222	0.277	0.609	0.785	0.835	0.791	0.514	0.121	-0.619	-1.174	-2.139	44.8
II	PSPC1	0.9976324	0.27	0.614	0.797	0.851	0.805	0.519	0.109	-0.666	-1.215	-2.084	44.9
II	PWP1	0.99541906	0.393	0.632	0.762	0.801	0.767	0.533	0.165	-0.678	-1.394	-1.98	44.9
II	SAFB	0.99785545	0.296	0.612	0.78	0.83	0.788	0.521	0.132	-0.632	-1.22	-2.108	45
II	SFPQ	0.99727431	0.264	0.604	0.785	0.84	0.797	0.521	0.125	-0.627	-1.184	-2.127	45.2
II	PARP1	0.99720864	0.266	0.603	0.783	0.837	0.796	0.523	0.129	-0.621	-1.185	-2.13	45.3
II	NAF1	0.99766578	0.314	0.612	0.772	0.821	0.783	0.528	0.148	-0.632	-1.257	-2.089	45.3
II	SLC16A3	0.99717239	0.264	0.602	0.783	0.839	0.798	0.525	0.13	-0.626	-1.192	-2.124	45.4
II	DEK	0.997481	0.311	0.612	0.774	0.825	0.787	0.531	0.147	-0.644	-1.272	-2.072	45.5
II	SLC16A1	0.99721514	0.279	0.601	0.775	0.829	0.791	0.529	0.144	-0.617	-1.212	-2.12	45.6
II	RBMXL1	0.99728801	0.299	0.603	0.768	0.82	0.783	0.532	0.156	-0.611	-1.233	-2.114	45.7
II	SF3B3	0.99675833	0.289	0.596	0.762	0.815	0.779	0.53	0.161	-0.583	-1.197	-2.152	45.7
II	SRSF6	0.99692183	0.268	0.597	0.775	0.832	0.794	0.532	0.146	-0.615	-1.206	-2.124	45.9
II	TIAL1	0.99701447	0.293	0.602	0.77	0.825	0.791	0.539	0.157	-0.631	-1.262	-2.084	46.1
II	SRSF10	0.99678701	0.291	0.599	0.767	0.823	0.791	0.542	0.163	-0.626	-1.263	-2.087	46.3
II	RPL29	0.98669192	0.393	0.556	0.655	0.7	0.696	0.568	0.32	-0.398	-1.264	-2.225	51
III	ENO1	0.80967395	-0.134	0.769	1.141	1.127	0.852	-0.056	-0.912	-1.143	0.073	-1.717	36.6
III	SRBD1	0.94734003	0.069	0.675	0.941	0.958	0.804	0.243	-0.324	-0.679	-0.382	-2.306	38.5
III	CHORDC1	0.92440622	0.112	0.775	1.076	1.102	0.931	0.261	-0.499	-1.298	-0.985	-1.475	39
III	NSD2	0.9881745	0.17	0.681	0.931	0.98	0.881	0.422	-0.145	-0.918	-1.082	-1.921	41.7
III	GAPDH	0.97943686	0.072	0.68	0.978	1.038	0.926	0.402	-0.232	-1.011	-1.014	-1.837	42
III	MRPL43	0.87280353	-0.225	0.67	1.11	1.203	1.045	0.303	-0.573	-1.464	-0.921	-1.147	42.2
III	GEMIN5	0.93988061	-0.268	0.591	1.009	1.098	0.957	0.313	-0.388	-0.87	-0.369	-2.073	42.4
III	SRRM2	0.99350816	0.216	0.661	0.883	0.933	0.854	0.46	-0.05	-0.832	-1.148	-1.978	42.5
III	MCM5	0.99513905	0.207	0.65	0.873	0.924	0.849	0.465	-0.032	-0.791	-1.116	-2.028	42.8
III	EEF1A1	0.97902278	0.152	0.677	0.942	1.003	0.913	0.452	-0.145	-1.033	-1.238	-1.723	42.8
III	FRG1	0.99282695	0.195	0.66	0.893	0.947	0.867	0.461	-0.064	-0.859	-1.152	-1.949	42.8
III	FAM50A	0.98740403	0.04	0.647	0.95	1.02	0.921	0.429	-0.173	-0.918	-0.967	-1.949	42.9
III	AP3D1	0.9434249	-0.024	0.669	1.019	1.104	0.993	0.419	-0.307	-1.255	-1.185	-1.434	43.2
III	RACK1	0.98980308	0.195	0.66	0.897	0.955	0.879	0.476	-0.06	-0.91	-1.23	-1.861	43.3
III	TECR	0.99228143	0.201	0.654	0.885	0.943	0.87	0.48	-0.039	-0.87	-1.214	-1.909	43.4
III	PKM	0.99235838	0.183	0.644	0.883	0.947	0.879	0.493	-0.028	-0.877	-1.233	-1.89	44
III	LDHA	0.95599708	-0.08	0.634	1.003	1.104	1.007	0.457	-0.253	-1.192	-1.159	-1.522	44.4
III	PUS7	0.99077122	0.231	0.641	0.857	0.918	0.861	0.513	0.021	-0.858	-1.318	-1.866	44.5
III	RAN	0.98908197	0.205	0.64	0.87	0.937	0.877	0.513	1E-03	-0.897	-1.324	-1.823	44.7
III	SNRPA	0.99555328	0.152	0.622	0.869	0.942	0.882	0.511	0.002	-0.833	-1.207	-1.939	44.9
III	YLPM1	0.99307108	0.223	0.587	0.777	0.832	0.786	0.505	0.12	-0.546	-1.038	-2.246	44.9
III	RCC2	0.99736824	0.198	0.615	0.835	0.9	0.846	0.513	0.052	-0.739	-1.183	-2.037	44.9
III	AP2M1	0.99757263	0.07	0.6	0.877	0.957	0.892	0.499	-0.02	-0.778	-1.049	-2.049	45
III	NOL7	0.99702331	0.219	0.605	0.809	0.869	0.82	0.514	0.088	-0.66	-1.145	-2.118	45
III	HSPA8	0.9908515	-0.032	0.599	0.929	1.026	0.951	0.493	-0.103	-0.913	-1.042	-1.909	45.1
III	SSB	0.99673626	0.148	0.615	0.862	0.936	0.878	0.514	0.014	-0.808	-1.19	-1.969	45.1
III	TCP1	0.9912274	0.104	0.624	0.898	0.979	0.914	0.51	-0.041	-0.917	-1.227	-1.842	45.1
III	RAB1A	0.98950973	0.11	0.626	0.898	0.979	0.915	0.513	-0.04	-0.934	-1.257	-1.81	45.1
III	ZNF512	0.9985483	0.118	0.599	0.852	0.926	0.868	0.508	0.023	-0.732	-1.082	-2.079	45.2
III	XRCC5	0.99625159	0.225	0.598	0.795	0.854	0.808	0.516	0.106	-0.622	-1.125	-2.155	45.2
III	ADARB2	0.99678421	0.231	0.607	0.806	0.866	0.82	0.52	0.096	-0.672	-1.182	-2.092	45.2
III	RBM15B	0.9952256	0.234	0.619	0.825	0.888	0.84	0.526	0.075	-0.76	-1.272	-1.977	45.3
III	DROSHA	0.99402831	0.156	0.574	0.794	0.859	0.811	0.504	0.094	-0.559	-0.977	-2.256	45.3
III	PRPF4B	0.99654377	0.236	0.605	0.801	0.861	0.816	0.523	0.106	-0.662	-1.187	-2.097	45.4
III	ESF1	0.99787949	0.052	0.581	0.859	0.943	0.884	0.505	0.007	-0.716	-0.996	-2.119	45.4
III	MPHOSPH1	0.99717081	0.198	0.609	0.829	0.896	0.848	0.526	0.07	-0.742	-1.219	-2.015	45.5
III	ACP1	0.99694772	0.095	0.574	0.826	0.903	0.85	0.508	0.053	-0.633	-0.98	-2.195	45.5
III	RPA1	0.99154371	0.216	0.626	0.847	0.915	0.865	0.53	0.047	-0.844	-1.333	-1.867	45.5
III	EFTUD2	0.99880018	0.093	0.589	0.852	0.932	0.876	0.514	0.025	-0.73	-1.069	-2.084	45.5
III	HEATR1	0.99878208	0.113	0.595	0.85	0.928	0.873	0.515	0.03	-0.738	-1.099	-2.066	45.5
III	SCAMP3	0.99858039	0.153	0.599	0.837	0.91	0.859	0.522	0.055	-0.729	-1.15	-2.055	45.6
III	SRP14	0.99541788	0.253	0.598	0.783	0.84	0.8	0.526	0.13	-0.62	-1.178	-2.134	45.6
III	USP42	0.99862179	0.121	0.585	0.831	0.907	0.855	0.517	0.056	-0.677	-1.062	-2.131	45.6
III	XPO5	0.99609199	0.231	0.594	0.787	0.848	0.806	0.525	0.123	-0.616	-1.149	-2.149	45.6
III	PNISR	0.99416307	0.118	0.563	0.798	0.871	0.823	0.51	0.09	-0.56	-0.951	-2.261	45.7
III	RBM45	0.99664493	0.221	0.593	0.792	0.855	0.813	0.527	0.118	-0.629	-1.152	-2.137	45.8
III	RBFOX2	0.99642932	0.232	0.606	0.807	0.87	0.827	0.533	0.105	-0.7	-1.236	-2.043	45.8
III	NCBP2	0.99599351	0.247	0.603	0.795	0.856	0.816	0.533	0.12	-0.671	-1.23	-2.069	45.8
III	SLC25A6	0.98466769	0.107	0.619	0.895	0.981	0.924	0.531	-0.027	-0.971	-1.332	-1.728	45.8
III	HMGA1	0.98813301	-0.007	0.599	0.922	1.023	0.958	0.52	-0.075	-0.964	-1.178	-1.799	45.8
III	SAFB2	0.99649492	0.229	0.594	0.791	0.853	0.812	0.529	0.122	-0.635	-1.173	-2.124	45.8
III	PWP2	0.99747956	0.015	0.569	0.861	0.952	0.894	0.511	0.006	-0.713	-0.971	-2.125	45.8
III	PLAA	0.99860768	0.117	0.581	0.828	0.905	0.855	0.519	0.062	-0.669	-1.058	-2.139	45.8
III	SLC1A5	0.98111003	-0.114	0.515	0.844	0.946	0.883	0.481	-0.015	-0.567	-0.661	-2.312	45.9
III	HSP90AB1	0.98431148	-0.054	0.592	0.936	1.045	0.978	0.521	-0.098	-0.999	-1.164	-1.757	46
III	NACA	0.99013636	-0.085	0.576	0.927	1.038	0.971	0.516	-0.088	-0.919	-1.05	-1.887	46
III	ZCCHC7	0.99753869	0.174	0.602	0.832	0.905	0.859	0.534	0.07	-0.753	-1.222	-2.001	46
III	DHX8	0.99500248	0.147	0.564	0.786	0.857	0.816	0.522	0.116	-0.557	-1.009	-2.243	46.2
III	HMGB3	0.97652913	-0.225	0.494	0.873	0.993	0.928	0.486	-0.058	-0.623	-0.609	-2.258	46.3
III	ELAVL1	0.99740696	0.204	0.588	0.796	0.864	0.825	0.537	0.12	-0.65	-1.177	-2.107	46.3
III	PRKDC	0.99552587	0.174	0.566	0.778	0.848	0.81	0.532	0.136	-0.561	-1.063	-2.219	46.5
III	PTBP1	0.99547396	0.227	0.58	0.772	0.836	0.801	0.538	0.152	-0.586	-1.154	-2.165	46.5
III	TKT	0.99885732	0.023	0.565	0.855	0.95	0.899	0.53	0.028	-0.727	-1.034	-2.088	46.5
III	DDX49	0.99688296	-0.012	0.549	0.849	0.946	0.894	0.522	0.027	-0.675	-0.94	-2.161	46.5
III	ZFR	0.99315558	0.243	0.574	0.754	0.814	0.782	0.536	0.173	-0.537	-1.129	-2.211	46.6
III	PRPF31	0.9968182	0.007	0.547	0.836	0.93	0.881	0.525	0.047	-0.645	-0.942	-2.186	46.6
III	RPS8	0.99822573	0.148	0.588	0.828	0.908	0.867	0.547	0.083	-0.744	-1.219	-2.006	46.7
III	UTP15	0.99904617	0.119	0.569	0.813	0.894	0.853	0.539	0.096	-0.656	-1.099	-2.129	46.7
III	RRP36	0.99689575	0.034	0.579	0.873	0.972	0.922	0.544	0.014	-0.834	-1.169	-1.936	46.8
III	AQR	0.99871406	0.148	0.573	0.804	0.882	0.844	0.544	0.113	-0.651	-1.138	-2.118	46.9
III	HNRNPM	0.99699645	0.203	0.578	0.783	0.853	0.819	0.547	0.143	-0.623	-1.179	-2.125	46.9
III	NKAP	0.99558667	0.243	0.59	0.781	0.847	0.815	0.551	0.151	-0.654	-1.256	-2.066	47
III	ARL6IP4	0.99832689	0.121	0.583	0.835	0.921	0.88	0.552	0.076	-0.762	-1.218	-1.988	47
III	RPS24	0.99646744	0.22	0.589	0.793	0.863	0.829	0.553	0.136	-0.681	-1.257	-2.044	47
III	DDX23	0.99582107	0.236	0.585	0.776	0.842	0.81	0.549	0.155	-0.629	-1.226	-2.1	47
III	RNMT	0.99342385	0.271	0.597	0.778	0.842	0.812	0.557	0.159	-0.68	-1.323	-2.012	47.1
III	TENT4B	0.99955173	0.108	0.57	0.823	0.909	0.869	0.55	0.091	-0.701	-1.149	-2.069	47.1
III	WDR75	0.99656133	0.199	0.591	0.807	0.881	0.846	0.556	0.119	-0.723	-1.277	-1.998	47.1
III	QKI	0.99880422	0.145	0.571	0.803	0.882	0.846	0.548	0.117	-0.653	-1.146	-2.112	47.1
III	CACTIN	0.99833929	0.161	0.579	0.809	0.889	0.854	0.556	0.115	-0.702	-1.22	-2.04	47.3
III	POP1	0.99870193	0.148	0.568	0.798	0.879	0.844	0.553	0.126	-0.649	-1.156	-2.11	47.3
III	PCBP4	0.99809377	0.172	0.571	0.791	0.869	0.837	0.556	0.138	-0.647	-1.187	-2.1	47.4
III	STRBP	0.99382462	0.146	0.545	0.763	0.839	0.808	0.542	0.16	-0.517	-1.027	-2.259	47.4
III	NKRF	0.99640447	0.197	0.567	0.771	0.843	0.813	0.553	0.163	-0.591	-1.163	-2.154	47.5
III	COPB2	0.9967426	0.164	0.557	0.774	0.85	0.82	0.553	0.157	-0.577	-1.117	-2.181	47.6
III	ZMAT2	0.99266709	0.107	0.585	0.85	0.944	0.907	0.569	0.063	-0.86	-1.328	-1.838	47.6
III	ISG20L2	0.99826565	-0.06	0.534	0.858	0.973	0.931	0.557	0.038	-0.742	-1.03	-2.059	47.7

III	NUMA1	0.98069786	-0.321	0.475	0.905	1.056	1.002	0.538	-0.066	-0.767	-0.75	-2.071	47.8
III	ZNF638	0.99739324	0.131	0.575	0.822	0.911	0.878	0.569	0.105	-0.759	-1.27	-1.962	47.8
III	HNRNPC	0.99611903	0.21	0.568	0.767	0.839	0.813	0.561	0.174	-0.601	-1.203	-2.127	47.9
III	XRCC6	0.99801581	0.157	0.56	0.783	0.864	0.835	0.562	0.152	-0.62	-1.165	-2.127	47.9
III	MATR3	0.99740305	0.174	0.562	0.777	0.855	0.827	0.561	0.16	-0.609	-1.172	-2.134	47.9
III	HNRNPR	0.99844228	0.145	0.558	0.788	0.871	0.842	0.564	0.147	-0.632	-1.167	-2.116	48
III	ADAR	0.99987562	0.046	0.544	0.819	0.918	0.884	0.564	0.102	-0.676	-1.101	-2.1	48
III	ILF2	0.99739524	0.161	0.557	0.776	0.855	0.827	0.56	0.16	-0.596	-1.148	-2.152	48
III	PPIL4	0.98470062	0.067	0.504	0.743	0.828	0.8	0.536	0.169	-0.415	-0.857	-2.375	48
III	PHF10	0.99281648	0.079	0.576	0.852	0.953	0.917	0.576	0.065	-0.863	-1.321	-1.833	48
III	RBM22	0.99919374	0.122	0.559	0.802	0.89	0.86	0.567	0.13	-0.671	-1.182	-2.077	48
III	HSP90AA1	0.97821468	-0.281	0.508	0.94	1.096	1.045	0.567	-0.089	-0.983	-1.039	-1.763	48.1
III	TOP1	0.99790073	0.139	0.569	0.809	0.897	0.868	0.574	0.127	-0.725	-1.262	-1.996	48.2
III	ADARB1	0.99942871	-0.023	0.533	0.838	0.949	0.913	0.567	0.074	-0.709	-1.064	-2.078	48.2
III	PRPF3	0.9998337	0.071	0.549	0.814	0.912	0.882	0.573	0.116	-0.693	-1.163	-2.061	48.3
III	SUMO3	0.98916908	0.269	0.594	0.78	0.851	0.828	0.579	0.168	-0.744	-1.429	-1.897	48.3
III	RAVER1	0.99606621	0.194	0.558	0.762	0.837	0.813	0.565	0.183	-0.58	-1.182	-2.15	48.3
III	RAVER2	0.99814336	0.153	0.557	0.783	0.866	0.84	0.569	0.158	-0.629	-1.187	-2.109	48.3
III	FARSA	0.99805732	0.092	0.563	0.826	0.923	0.892	0.577	0.103	-0.763	-1.251	-1.963	48.3
III	NKTR	0.99899578	0.123	0.553	0.794	0.882	0.855	0.571	0.144	-0.651	-1.178	-2.093	48.4
III	WDR74	0.99582282	-0.096	0.503	0.832	0.951	0.915	0.562	0.071	-0.642	-0.926	-2.171	48.4
III	RPS27	0.99861849	-0.036	0.533	0.85	0.967	0.934	0.582	0.069	-0.774	-1.141	-1.985	48.6
III	PCBP1	0.99865226	0.055	0.529	0.793	0.892	0.864	0.57	0.139	-0.606	-1.07	-2.165	48.6
III	RBM12B	0.99776219	0.079	0.529	0.78	0.874	0.849	0.57	0.157	-0.579	-1.074	-2.186	48.7
III	RPP25	0.99983537	0.023	0.538	0.825	0.933	0.904	0.581	0.104	-0.719	-1.154	-2.036	48.7
III	ILF3	0.99873036	0.072	0.531	0.788	0.884	0.86	0.575	0.151	-0.606	-1.099	-2.155	48.8
III	CDK11B	0.99742623	0.032	0.518	0.789	0.89	0.863	0.569	0.141	-0.579	-1.023	-2.201	48.8
III	DUS3L	0.9956229	0.143	0.536	0.757	0.84	0.818	0.568	0.188	-0.538	-1.104	-2.208	48.8
III	RALY	0.99487108	0.182	0.544	0.748	0.826	0.806	0.57	0.202	-0.538	-1.15	-2.191	48.9
III	DHX16	0.99758707	0.146	0.545	0.77	0.856	0.835	0.577	0.178	-0.599	-1.175	-2.134	48.9
III	HSPA5	0.98008825	-0.372	0.448	0.899	1.066	1.025	0.573	-0.036	-0.782	-0.797	-2.023	48.9
III	PCBP2	0.99802882	0.124	0.541	0.775	0.864	0.841	0.576	0.17	-0.598	-1.149	-2.145	48.9
III	DDX18	0.99937291	0.008	0.519	0.805	0.914	0.888	0.582	0.13	-0.639	-1.078	-2.129	49.1
III	PAK1IP1	0.9997745	-0.014	0.521	0.821	0.935	0.908	0.586	0.111	-0.69	-1.105	-2.074	49.1
III	TRMT1	0.99551279	0.028	0.506	0.774	0.876	0.853	0.573	0.163	-0.536	-0.998	-2.239	49.2
III	NVL	0.99683606	-0.14	0.494	0.847	0.982	0.952	0.589	0.069	-0.72	-1.01	-2.064	49.2
III	CELF1	0.99860388	0.116	0.541	0.781	0.873	0.852	0.583	0.168	-0.627	-1.182	-2.106	49.2
III	ZNF800	0.99902842	-0.056	0.517	0.838	0.961	0.933	0.593	0.091	-0.739	-1.119	-2.019	49.2
III	RBM27	0.99797798	0.128	0.54	0.772	0.862	0.842	0.582	0.178	-0.603	-1.171	-2.131	49.2
III	CDC5L	0.88421447	-0.099	0.347	0.587	0.674	0.656	0.458	0.229	0.059	-0.205	-2.708	49.2
III	DCAF13	0.9977872	-0.102	0.509	0.851	0.981	0.952	0.594	0.071	-0.761	-1.092	-2.002	49.2
III	BAZ2A	0.99534972	0.21	0.558	0.756	0.834	0.816	0.581	0.202	-0.605	-1.258	-2.094	49.2
III	TARDBP	0.99753208	0.134	0.538	0.767	0.856	0.837	0.582	0.185	-0.59	-1.168	-2.142	49.3
III	RBM28	0.99969342	-0.011	0.517	0.813	0.927	0.902	0.589	0.123	-0.669	-1.098	-2.093	49.3
III	RPL27	0.99916249	0.048	0.522	0.79	0.893	0.872	0.587	0.155	-0.62	-1.115	-2.132	49.4
III	DBR1	0.99176251	0.269	0.573	0.749	0.819	0.804	0.585	0.215	-0.635	-1.354	-2.024	49.4
III	MBNL1	0.99586923	0.191	0.551	0.756	0.837	0.82	0.584	0.203	-0.597	-1.24	-2.106	49.5
III	TOP2A	0.99956371	0.056	0.528	0.796	0.901	0.881	0.594	0.153	-0.661	-1.174	-2.074	49.6
III	WDR3	0.99953962	-0.011	0.521	0.821	0.938	0.916	0.599	0.121	-0.717	-1.164	-2.023	49.6
III	RPL12	0.99498509	-0.105	0.511	0.859	0.995	0.97	0.61	0.07	-0.831	-1.189	-1.891	49.7
III	DDX47	0.99758495	-0.127	0.492	0.84	0.977	0.953	0.604	0.09	-0.728	-1.065	-2.034	49.7
III	PARP2	0.99871292	-0.082	0.502	0.832	0.962	0.939	0.603	0.104	-0.724	-1.107	-2.029	49.7
III	HMGB1	0.99781607	0.035	0.533	0.817	0.931	0.911	0.608	0.133	-0.756	-1.263	-1.949	49.8
III	ARPC1B	0.9971954	0.114	0.526	0.761	0.854	0.838	0.588	0.196	-0.569	-1.148	-2.161	49.8
III	GTF2I	0.99895179	-0.044	0.512	0.827	0.952	0.931	0.607	0.115	-0.736	-1.164	-2	49.8
III	HLTF	0.99643717	0.16	0.538	0.755	0.842	0.827	0.59	0.208	-0.582	-1.209	-2.129	49.9
III	TRMT10A	0.97038111	0.142	0.572	0.825	0.928	0.912	0.616	0.116	-0.958	-1.579	-1.574	50
III	TOE1	0.9962827	0.066	0.509	0.76	0.86	0.844	0.588	0.193	-0.538	-1.073	-2.21	50
III	LENG8	0.99881843	-0.082	0.497	0.824	0.954	0.934	0.608	0.117	-0.704	-1.102	-2.047	50
III	NOL10	0.99827115	-0.105	0.493	0.832	0.965	0.944	0.608	0.107	-0.718	-1.091	-2.036	50
III	DHX36	0.98766742	-0.203	0.44	0.8	0.942	0.922	0.59	0.12	-0.544	-0.816	-2.25	50.1
III	NUFIP1	0.9995703	-0.016	0.51	0.81	0.929	0.911	0.607	0.14	-0.689	-1.153	-2.049	50.1
III	ISY1	0.99788877	0.048	0.532	0.809	0.921	0.904	0.61	0.146	-0.74	-1.27	-1.96	50.1
III	ABT1	0.99828625	-0.095	0.497	0.832	0.966	0.946	0.612	0.108	-0.734	-1.122	-2.01	50.1
III	DHX9	0.99632735	0.057	0.505	0.76	0.862	0.848	0.592	0.196	-0.538	-1.073	-2.208	50.2
III	NXF1	0.99713781	0.053	0.506	0.764	0.868	0.854	0.595	0.193	-0.556	-1.091	-2.187	50.3
III	TOP2B	0.99848308	0.088	0.524	0.774	0.877	0.863	0.605	0.19	-0.628	-1.207	-2.086	50.4
III	HP1BP3	0.98756679	-0.231	0.475	0.877	1.04	1.02	0.634	0.05	-0.888	-1.171	-1.807	50.5
III	MRPS7	0.98817697	-0.17	0.44	0.783	0.921	0.905	0.595	0.148	-0.514	-0.838	-2.27	50.5
III	UTP18	0.99738077	0.058	0.528	0.8	0.912	0.899	0.618	0.163	-0.73	-1.291	-1.957	50.5
III	PHF6	0.99891958	0.057	0.518	0.783	0.892	0.88	0.611	0.181	-0.652	-1.21	-2.061	50.6
III	METTL16	0.99288814	-0.063	0.466	0.766	0.888	0.876	0.598	0.181	-0.51	-0.946	-2.256	50.7
III	MTPAP	0.99199005	-0.203	0.442	0.807	0.955	0.94	0.611	0.128	-0.596	-0.904	-2.18	50.7
III	WDR46	0.99527388	-0.199	0.452	0.824	0.977	0.966	0.631	0.125	-0.686	-1.028	-2.061	51.1
III	RSL1D1	0.99693215	-0.146	0.462	0.81	0.954	0.944	0.628	0.145	-0.659	-1.051	-2.086	51.1
III	SERPINH1	0.98602433	-0.231	0.467	0.869	1.036	1.023	0.65	0.072	-0.894	-1.217	-1.774	51.1
III	C7orf50	0.99590899	-0.185	0.457	0.825	0.977	0.966	0.634	0.126	-0.703	-1.062	-2.036	51.1
III	DIMT1	0.99821981	-0.102	0.475	0.807	0.945	0.934	0.628	0.152	-0.671	-1.104	-2.064	51.1
III	RRP9	0.98876969	-0.321	0.425	0.851	1.027	1.016	0.643	0.086	-0.751	-0.99	-1.985	51.2
III	TFB2M	0.98817185	-0.156	0.433	0.768	0.906	0.897	0.607	0.177	-0.49	-0.863	-2.278	51.2
III	DDX56	0.99640601	-0.17	0.459	0.819	0.969	0.959	0.633	0.134	-0.689	-1.064	-2.05	51.2
III	ZFC3H1	0.99135746	-0.236	0.427	0.806	0.963	0.954	0.628	0.14	-0.604	-0.92	-2.157	51.3
III	SMARCA4	0.98817834	0.296	0.556	0.713	0.781	0.776	0.598	0.27	-0.561	-1.36	-2.071	51.3
III	UTP6	0.99751391	-0.129	0.465	0.807	0.95	0.941	0.633	0.154	-0.666	-1.088	-2.068	51.3
III	KRR1	0.98909006	-0.318	0.42	0.842	1.017	1.007	0.643	0.098	-0.718	-0.966	-2.024	51.4
III	REPIN1	0.98239425	0.056	0.534	0.817	0.938	0.931	0.642	0.149	-0.886	-1.487	-1.693	51.4
III	EIF2S3	0.99613092	-0.147	0.468	0.824	0.974	0.967	0.646	0.139	-0.746	-1.165	-1.961	51.5
III	VDAC2	0.97845601	-0.357	0.429	0.882	1.072	1.063	0.664	0.051	-0.914	-1.145	-1.744	51.5
III	ZC3H8	0.99849976	-0.064	0.479	0.794	0.928	0.923	0.636	0.177	-0.666	-1.161	-2.048	51.6
III	RPS6	0.9955715	-0.121	0.451	0.781	0.92	0.915	0.629	0.184	-0.577	-1.016	-2.166	51.7
III	RPL22	0.99719534	0.054	0.495	0.753	0.864	0.86	0.622	0.226	-0.569	-1.168	-2.138	51.8
III	SNW1	0.99248338	0.174	0.515	0.717	0.805	0.802	0.606	0.265	-0.5	-1.2	-2.185	51.8
III	FUBP3	0.99493993	-0.057	0.46	0.759	0.886	0.883	0.623	0.212	-0.529	-1.028	-2.208	51.8
III	SRSF11	0.99656447	0.058	0.51	0.777	0.893	0.891	0.638	0.208	-0.69	-1.311	-1.974	52
III	FEN1	0.97912413	-0.064	0.498	0.831	0.978	0.977	0.667	0.138	-0.923	-1.459	-1.644	52.2
III	NUSAP1	0.99794269	-0.055	0.469	0.776	0.909	0.909	0.642	0.205	-0.62	-1.148	-2.089	52.2
III	RPL31	0.99239132	0.169	0.511	0.715	0.805	0.804	0.612	0.272	-0.501	-1.211	-2.177	52.3
III	CEBPZ	0.99011171	-0.296	0.406	0.812	0.986	0.986	0.657	0.149	-0.649	-0.967	-2.082	52.3
III	RPS17	0.99360388	0.026	0.47	0.73	0.845	0.847	0.624	0.253	-0.487	-1.083	-2.225	52.6
III	NSUN2	0.99700681	9E-04	0.474	0.753	0.877	0.879	0.64	0.236	-0.571	-1.162	-2.127	52.7
III	PTCD1	0.98847923	-0.273	0.392	0.78	0.95	0.956	0.659	0.191	-0.561	-0.926	-2.169	52.9
III	CLK3	0.97656791	-0.356	0.408	0.858	1.057	1.063	0.699	0.106	-0.903	-1.225	-1.705	52.9
III	RPS4X	0.99341786	-0.073	0.442	0.744	0.877	0.882	0.64	0.241	-0.504	-1.036	-2.214	53
III	RRP12	0.9910492	-0.285	0.4	0.803	0.982	0.99	0.68	0.178	-0.667	-1.049	-2.033	53.2
III	EIF5A	0.99344691	-0.067	0.441	0.741	0.874	0.881	0.643	0.247	-0.502	-1.046	-2.212	53.2
III	FASTKD2	0.99311447	-0.039	0.447	0.733	0.862	0.868	0.64	0.256	-0.489	-1.057	-2.221	53.2
III	RRP1B	0.99124922	-0.239	0.401	0.776	0.943	0.953	0.668	0.207	-0.576	-0.993	-2.139	53.3
III	BUD23	0.99301784	-0.238	0.413	0.797	0.969	0.98	0.684	0.193	-0.675	-1.111	-2.011	53.4
III	APEX1	0.98192512	-0.281	0.419	0.836	1.024	1.035	0.704	0.146	-0.864	-1.278	-1.74	53.4

III	GRSF1	0.99248353	0.085	0.478	0.713	0.82	0.826	0.631	0.283	-0.476	-1.152	-2.207	53.4
III	PPIG	0.99547437	-0.064	0.446	0.749	0.885	0.893	0.654	0.247	-0.546	-1.11	-2.153	53.4
III	RPL24	0.9964968	-0.036	0.457	0.752	0.886	0.896	0.66	0.25	-0.584	-1.183	-2.097	53.6
III	MRTO4	0.99652751	0.008	0.473	0.751	0.879	0.887	0.659	0.252	-0.606	-1.243	-2.06	53.6
III	MEPCE	0.99655015	-0.045	0.456	0.757	0.895	0.905	0.667	0.247	-0.609	-1.21	-2.063	53.8
III	RBM26	0.98975618	-0.173	0.403	0.743	0.897	0.91	0.662	0.248	-0.491	-0.978	-2.22	53.9
III	ERI3	0.98117433	-0.194	0.381	0.72	0.873	0.887	0.649	0.261	-0.401	-0.861	-2.315	54
III	ZRANB2	0.99560521	-0.049	0.457	0.762	0.905	0.919	0.679	0.248	-0.654	-1.273	-1.993	54.2
III	TRMT2A	0.99559487	-0.101	0.436	0.759	0.909	0.925	0.682	0.251	-0.614	-1.196	-2.051	54.3
III	RPL22L1	0.99332951	0.101	0.482	0.715	0.826	0.838	0.65	0.296	-0.53	-1.257	-2.119	54.4
III	RPL11	0.98003545	-0.088	0.398	0.687	0.822	0.839	0.644	0.305	-0.344	-0.912	-2.35	54.9
III	RPL36A	0.99055929	0.113	0.471	0.693	0.803	0.822	0.658	0.328	-0.485	-1.258	-2.146	55.9
III	TRMT1L	0.99063951	-0.145	0.398	0.735	0.905	0.942	0.732	0.311	-0.617	-1.281	-1.98	57.1
III	SLC25A5	0.98837329	-0.04	0.434	0.734	0.887	0.921	0.725	0.313	-0.67	-1.415	-1.888	57.3
III	RPL7	0.98586108	-0.036	0.401	0.674	0.813	0.847	0.689	0.362	-0.399	-1.117	-2.234	57.9
III	ELAC2	0.93551825	0.097	0.375	0.549	0.641	0.669	0.596	0.427	-0.025	-0.766	-2.562	60.6
III	AKAP17A	0.98512049	-0.088	0.371	0.669	0.831	0.883	0.745	0.406	-0.459	-1.249	-2.109	60.8
III	CHD4	0.93365105	0.018	0.424	0.704	0.869	0.928	0.779	0.353	-0.892	-1.834	-1.349	61.8
III	ZBTB11	0.97909562	-0.101	0.37	0.683	0.861	0.925	0.788	0.413	-0.606	-1.466	-1.867	62.2
IV	PARP12	0.81067565	-0.716	0.205	0.68	0.829	0.758	0.302	-0.144	-0.036	0.618	-2.495	46.6
IV	ERAL1	0.95943467	-0.637	0.336	0.864	1.055	1.006	0.513	-0.093	-0.564	-0.254	-2.226	48.7
IV	PDCD11	0.98765157	-0.353	0.409	0.846	1.029	1.021	0.651	0.095	-0.735	-0.967	-1.995	51.6
IV	IK	0.9865971	-0.357	0.408	0.849	1.037	1.032	0.663	0.097	-0.77	-1.019	-1.94	51.9
IV	SRPK1	0.98975638	-0.55	0.321	0.818	1.027	1.024	0.642	0.092	-0.578	-0.638	-2.159	52
IV	IMP4	0.98819869	-0.319	0.389	0.798	0.973	0.973	0.65	0.157	-0.584	-0.876	-2.159	52.3
IV	CHD3	0.99157759	-0.4	0.368	0.812	1.002	1.003	0.658	0.137	-0.616	-0.846	-2.118	52.4
IV	REXO4	0.99116257	-0.389	0.382	0.827	1.019	1.02	0.666	0.125	-0.684	-0.927	-2.038	52.4
IV	LAS1L	0.99072574	-0.369	0.385	0.822	1.01	1.012	0.665	0.133	-0.672	-0.935	-2.052	52.4
IV	NOL6	0.98888155	-0.409	0.385	0.847	1.046	1.048	0.679	0.107	-0.773	-1.013	-1.918	52.5
IV	POLRMT	0.98421261	-0.263	0.39	0.769	0.934	0.938	0.647	0.196	-0.512	-0.87	-2.227	52.8
IV	ATP5F1A	0.97147454	-0.664	0.322	0.897	1.148	1.155	0.71	0.018	-0.985	-1.032	-1.568	52.8
IV	DDX52	0.99065487	-0.393	0.38	0.831	1.028	1.033	0.682	0.132	-0.725	-0.997	-1.971	52.8
IV	NOL9	0.9870462	-0.335	0.363	0.768	0.946	0.953	0.654	0.192	-0.498	-0.807	-2.235	53.1
IV	DIEXF	0.98004655	-0.412	0.385	0.854	1.063	1.073	0.706	0.111	-0.874	-1.163	-1.744	53.2
IV	RRP15	0.98755876	-0.37	0.386	0.831	1.029	1.039	0.697	0.144	-0.767	-1.089	-1.899	53.2
IV	ZCCHC9	0.99188035	-0.608	0.313	0.851	1.09	1.105	0.713	0.098	-0.794	-0.925	-1.843	53.4
IV	TPR	0.98227196	-0.313	0.351	0.739	0.911	0.923	0.651	0.226	-0.418	-0.765	-2.306	53.6
IV	PNPT1	0.99340347	-0.7	0.256	0.812	1.058	1.075	0.694	0.118	-0.609	-0.65	-2.055	53.6
IV	RPS19BP1	0.99445412	-0.58	0.312	0.835	1.07	1.088	0.717	0.126	-0.749	-0.924	-1.896	53.8
IV	AATF	0.9954545	-0.558	0.315	0.828	1.058	1.076	0.712	0.135	-0.72	-0.909	-1.938	53.8
IV	PA2G4	0.98661253	-0.435	0.363	0.836	1.05	1.067	0.719	0.144	-0.812	-1.121	-1.812	53.8
IV	DNTTIP2	0.99502956	-0.441	0.338	0.796	1.003	1.019	0.697	0.18	-0.617	-0.901	-2.074	53.9
IV	EMG1	0.99669035	-0.555	0.308	0.815	1.043	1.062	0.709	0.149	-0.67	-0.865	-1.998	53.9
IV	HTATSF1	0.80147968	-1.439	0.016	0.871	1.256	1.29	0.711	-0.186	-1.26	-0.684	-0.575	54
IV	NOM1	0.9956773	-0.583	0.303	0.826	1.063	1.085	0.724	0.143	-0.726	-0.92	-1.914	54.1
IV	DHX38	0.99398476	-0.454	0.318	0.772	0.978	0.998	0.692	0.202	-0.532	-0.811	-2.164	54.2
IV	PNO1	0.98790217	-0.318	0.383	0.8	0.991	1.01	0.708	0.198	-0.699	-1.114	-1.96	54.2
IV	LARP7	0.97601098	-0.823	0.239	0.867	1.153	1.181	0.754	0.065	-0.92	-0.94	-1.577	54.3
IV	MYBBP1A	0.99164805	-0.342	0.359	0.775	0.966	0.986	0.698	0.219	-0.585	-0.973	-2.103	54.4
IV	RPS16	0.99553628	-0.443	0.333	0.793	1.004	1.027	0.714	0.197	-0.635	-0.955	-2.034	54.5
IV	EXOSC9	0.9973432	-0.534	0.306	0.803	1.031	1.056	0.723	0.179	-0.657	-0.908	-1.998	54.5
IV	SNRPD1	0.9690228	-0.404	0.371	0.837	1.056	1.081	0.744	0.153	-0.923	-1.311	-1.603	54.6
IV	NOC2L	0.99509443	-0.421	0.332	0.779	0.986	1.01	0.711	0.214	-0.593	-0.936	-2.082	54.7
IV	YTHDC1	0.98909673	-0.347	0.337	0.743	0.931	0.954	0.688	0.248	-0.472	-0.861	-2.222	54.8
IV	PPAN	0.99148339	-0.356	0.359	0.786	0.986	1.011	0.72	0.219	-0.657	-1.07	-1.997	54.8
IV	UTP3	0.9963958	-0.536	0.305	0.806	1.039	1.069	0.739	0.185	-0.7	-0.98	-1.928	54.9
IV	RTCB	0.95114027	-1.052	0.071	0.725	1.021	1.057	0.681	0.13	-0.357	-0.135	-2.14	54.9
IV	ESRP2	0.98937756	-0.297	0.362	0.758	0.944	0.97	0.709	0.253	-0.566	-1.03	-2.104	55.2
IV	PTBP3	0.98910435	-0.297	0.368	0.767	0.955	0.982	0.715	0.247	-0.607	-1.077	-2.053	55.2
IV	RPL10A	0.98386434	-0.31	0.378	0.794	0.991	1.018	0.732	0.221	-0.738	-1.213	-1.873	55.2
IV	RRP7A	0.99721545	-0.595	0.276	0.798	1.046	1.085	0.76	0.202	-0.698	-0.977	-1.898	55.6
IV	NGDN	0.99766994	-0.526	0.294	0.786	1.02	1.056	0.75	0.22	-0.654	-0.98	-1.966	55.6
IV	TSR1	0.99214839	-0.347	0.343	0.759	0.957	0.989	0.725	0.259	-0.579	-1.033	-2.073	55.7
IV	NAT10	0.99785604	-0.505	0.296	0.777	1.005	1.041	0.744	0.23	-0.619	-0.959	-2.012	55.7
IV	RPF1	0.99695557	-0.493	0.302	0.781	1.009	1.047	0.751	0.232	-0.649	-1.011	-1.97	55.9
IV	NPM1	0.98906432	-0.361	0.347	0.778	0.987	1.023	0.75	0.25	-0.691	-1.171	-1.911	56.1
IV	RBM33	0.99800286	-0.512	0.28	0.757	0.985	1.024	0.743	0.253	-0.549	-0.894	-2.086	56.1
IV	RPL5	0.99306309	-0.365	0.331	0.753	0.957	0.993	0.735	0.271	-0.573	-1.035	-2.068	56.2
IV	RPS18	0.99860653	-0.72	0.213	0.773	1.04	1.087	0.767	0.22	-0.596	-0.797	-1.987	56.2
IV	EIF1AY	0.98713771	-0.267	0.354	0.732	0.916	0.95	0.721	0.297	-0.519	-1.055	-2.13	56.5
IV	DHX30	0.99328047	-0.443	0.286	0.726	0.938	0.977	0.726	0.285	-0.451	-0.846	-2.198	56.5
IV	SURF6	0.99959203	-0.674	0.224	0.765	1.027	1.077	0.773	0.241	-0.59	-0.851	-1.992	56.6
IV	LDHB	0.97682746	-1.051	0.071	0.741	1.061	1.122	0.771	0.195	-0.496	-0.445	-1.969	56.6
IV	UTP14A	0.99832399	-0.686	0.227	0.78	1.048	1.1	0.787	0.232	-0.665	-0.934	-1.89	56.7
IV	RPS11	0.99568322	-0.554	0.272	0.777	1.025	1.076	0.787	0.254	-0.693	-1.08	-1.864	57
IV	RPL19	0.98613751	-0.259	0.347	0.719	0.903	0.941	0.727	0.317	-0.492	-1.055	-2.147	57.1
IV	SUPV3L1	0.99530838	-0.701	0.189	0.726	0.987	1.041	0.761	0.273	-0.45	-0.692	-2.134	57.1
IV	NOC4L	0.99790326	-0.51	0.267	0.739	0.97	1.017	0.758	0.286	-0.52	-0.913	-2.094	57.1
IV	BYSL	0.99839977	-0.764	0.185	0.761	1.043	1.102	0.796	0.249	-0.601	-0.833	-1.937	57.2
IV	RRP1	0.99692316	-0.819	0.159	0.753	1.046	1.11	0.804	0.255	-0.585	-0.792	-1.931	57.5
IV	RBM38	0.98299316	-0.625	0.252	0.793	1.063	1.123	0.82	0.239	-0.826	-1.209	-1.63	57.5
IV	NOP2	0.99596532	-0.443	0.285	0.73	0.951	1	0.761	0.308	-0.518	-0.981	-2.093	57.6
IV	BMS1	0.98167281	-1.065	0.069	0.756	1.094	1.169	0.826	0.219	-0.625	-0.664	-1.779	57.6
IV	C1orf131	0.98410884	-0.993	0.105	0.773	1.105	1.179	0.84	0.222	-0.714	-0.831	-1.685	57.7
IV	EXOSC4	0.97867303	-0.996	0.107	0.781	1.117	1.194	0.85	0.216	-0.776	-0.907	-1.587	57.8
IV	DDX24	0.99957137	-0.606	0.23	0.744	1.001	1.062	0.799	0.297	-0.584	-0.973	-1.97	58
IV	RNPS1	0.99961736	-0.591	0.231	0.735	0.987	1.046	0.789	0.302	-0.541	-0.928	-2.03	58
IV	BRIX1	0.99684304	-0.469	0.276	0.735	0.965	1.02	0.779	0.312	-0.557	-1.031	-2.029	58
IV	EXOSC10	0.99683699	-0.825	0.15	0.747	1.045	1.116	0.822	0.276	-0.595	-0.84	-1.896	58.1
IV	RCL1	0.98127793	-1.055	0.049	0.72	1.052	1.131	0.818	0.259	-0.497	-0.554	-1.922	58.2
IV	DHX37	0.99953043	-0.699	0.192	0.74	1.016	1.084	0.816	0.3	-0.581	-0.926	-1.941	58.4
IV	EBNA1BP2	0.99868526	-0.546	0.243	0.73	0.978	1.04	0.797	0.321	-0.555	-1.003	-2.005	58.5
IV	PUM3	0.99984122	-0.658	0.2	0.729	0.997	1.064	0.809	0.314	-0.543	-0.918	-1.995	58.6
IV	RPL7L1	0.99948038	-0.686	0.187	0.724	0.994	1.063	0.806	0.315	-0.515	-0.865	-2.022	58.6
IV	TRMT6	0.99613851	-0.6	0.205	0.7	0.949	1.012	0.779	0.334	-0.42	-0.806	-2.154	58.6
IV	FCF1	0.99835804	-0.756	0.168	0.738	1.028	1.102	0.831	0.304	-0.595	-0.923	-1.896	58.7
IV	RBM47	0.99511902	-0.464	0.256	0.702	0.929	0.988	0.774	0.348	-0.451	-0.945	-2.137	58.8
IV	NIFK	0.99659552	-0.525	0.233	0.701	0.94	1.003	0.783	0.347	-0.447	-0.905	-2.129	58.9
IV	RPL15	0.9984099	-0.65	0.189	0.707	0.97	1.039	0.802	0.336	-0.464	-0.847	-2.082	59
IV	UTP20	0.98725531	-0.999	0.06	0.71	1.039	1.126	0.841	0.3	-0.501	-0.66	-1.914	59.1
IV	RP9	0.98757331	-0.549	0.202	0.664	0.899	0.962	0.759	0.363	-0.306	-0.722	-2.272	59.2
IV	IMP3	0.97917675	-1.008	0.079	0.752	1.096	1.189	0.881	0.273	-0.733	-0.938	-1.59	59.2
IV	NSUN5	0.99858463	-0.573	0.224	0.721	0.977	1.047	0.816	0.342	-0.552	-1.022	-1.979	59.3
IV	RPL18	0.99939991	-0.684	0.182	0.72	0.997	1.072	0.828	0.336	-0.545	-0.944	-1.962	59.4
IV	NOP14	0.98582208	-1.031	0.045	0.71	1.051	1.145	0.864	0.311	-0.542	-0.721	-1.832	59.6
IV	TBL3	0.99739603	-0.543	0.228	0.713	0.966	1.039	0.822	0.36	-0.549	-1.064	-1.973	59.9
IV	HMCES	0.99385029	-0.845	0.123	0.727	1.04	1.13	0.869	0.33	-0.622	-0.962	-1.791	59.9
IV	NOP16	0.99854785	-0.722	0.155	0.701	0.984	1.066	0.836	0.358	-0.49	-0.886	-2.002	60
IV	MRPL3	0.99285055	-0.884	0.087	0.689	1	1.089	0.845	0.35	-0.449	-0.732	-1.995	60.1

IV	RPL26	0.99622283	-0.492	0.24	0.7	0.942	1.013	0.811	0.373	-0.503	-1.049	-2.036	60.1
IV	RPS23	0.98154868	-1.084	0.017	0.699	1.052	1.154	0.877	0.323	-0.534	-0.704	-1.802	60.1
IV	RPL23	0.97321057	-1.17	-0.019	0.693	1.062	1.169	0.885	0.318	-0.535	-0.653	-1.75	60.2
IV	CRNKL1	0.99417409	-0.652	0.192	0.725	1.006	1.091	0.86	0.355	-0.641	-1.131	-1.804	60.3
IV	ACIN1	0.99855723	-0.689	0.162	0.696	0.977	1.062	0.844	0.375	-0.498	-0.944	-1.985	60.5
IV	RPS3A	0.98771368	-0.995	0.035	0.68	1.021	1.129	0.891	0.374	-0.498	-0.787	-1.851	61.2
IV	RPL7A	0.98199191	-0.96	0.028	0.644	0.966	1.067	0.848	0.388	-0.328	-0.587	-2.066	61.2
IV	GPATCH8	0.95622948	-0.395	0.286	0.73	0.975	1.056	0.856	0.359	-0.827	-1.536	-1.503	61.2
IV	GIGYF2	0.98630169	-0.34	0.281	0.682	0.903	0.978	0.817	0.417	-0.522	-1.23	-1.985	61.8
IV	RPL9	0.98918755	-0.898	0.051	0.649	0.968	1.073	0.869	0.411	-0.375	-0.725	-2.023	61.9
IV	RC3H1	0.97425579	-1.144	-0.043	0.649	1.017	1.14	0.909	0.393	-0.438	-0.659	-1.825	62
IV	RSL24D1	0.99626748	-0.652	0.151	0.662	0.938	1.032	0.853	0.427	-0.421	-0.942	-2.048	62.1
IV	NIP7	0.99658632	-0.717	0.132	0.673	0.967	1.067	0.876	0.42	-0.484	-0.988	-1.946	62.2
IV	DDX27	0.97727648	-1.11	-0.033	0.646	1.011	1.135	0.914	0.408	-0.437	-0.7	-1.833	62.3
IV	BOP1	0.98873192	-0.921	0.055	0.677	1.015	1.131	0.92	0.413	-0.554	-0.971	-1.764	62.4
IV	FAM98B	0.97230784	-0.723	0.084	0.59	0.861	0.953	0.798	0.445	-0.151	-0.555	-2.304	62.5
IV	RPL13A	0.9941184	-0.792	0.089	0.651	0.956	1.064	0.883	0.44	-0.414	-0.884	-1.993	62.7
IV	ALKBH5	0.99566852	-0.731	0.117	0.658	0.954	1.058	0.88	0.439	-0.442	-0.952	-1.98	62.7
IV	ZC3H11A	0.98482438	-0.988	0.003	0.633	0.977	1.1	0.911	0.446	-0.395	-0.767	-1.92	63.2
IV	RPL23A	0.99123063	-0.863	0.054	0.64	0.961	1.077	0.899	0.452	-0.403	-0.853	-1.964	63.2
IV	SAP18	0.97464195	-1.127	-0.054	0.63	1.004	1.14	0.94	0.442	-0.437	-0.752	-1.785	63.4
IV	RPL13	0.99402736	-0.74	0.1	0.642	0.943	1.055	0.894	0.466	-0.419	-0.963	-1.977	63.7
IV	RPL28	0.96268014	-0.182	0.288	0.593	0.764	0.828	0.735	0.471	-0.195	-0.94	-2.362	63.9
IV	EIF3H	0.99078005	-0.792	0.08	0.647	0.966	1.089	0.929	0.476	-0.498	-1.067	-1.831	64.3
IV	RPL36	0.99358505	-0.694	0.114	0.639	0.934	1.048	0.899	0.48	-0.432	-1.03	-1.959	64.3
IV	PNN	0.97695078	-1.069	-0.05	0.605	0.97	1.11	0.943	0.485	-0.369	-0.758	-1.866	64.6
IV	RPL17	0.99229681	-0.674	0.112	0.622	0.911	1.025	0.89	0.496	-0.37	-0.979	-2.033	64.8
IV	RPL18A	0.99138825	-0.548	0.164	0.63	0.896	1.002	0.876	0.495	-0.4	-1.084	-2.03	64.9
IV	RPL3	0.9857619	-0.875	0.019	0.599	0.925	1.055	0.917	0.509	-0.317	-0.823	-2.008	65.2
IV	ZC3H14	0.98819296	-0.798	0.048	0.599	0.913	1.041	0.915	0.521	-0.327	-0.897	-2.015	65.7
IV	RPSA	0.98844069	-0.748	0.063	0.595	0.902	1.03	0.916	0.534	-0.326	-0.945	-2.021	66.3
IV	RPUSD3	0.98489474	-0.569	0.119	0.584	0.864	0.993	0.92	0.575	-0.349	-1.14	-1.998	68.7
IV	RPL4	0.97412902	-0.822	-0.021	0.52	0.847	1.004	0.959	0.636	-0.189	-0.89	-2.043	70.9
IV	RPL37	0.96999599	-0.674	0.026	0.503	0.797	0.944	0.921	0.648	-0.115	-0.88	-2.17	72.4
V	KPNA2	0.9219617	-1.139	0.04	0.715	1.009	1.029	0.612	0.051	-0.296	0.131	-2.152	53.6
V	RPS13	0.90377159	-1.661	-0.167	0.689	1.063	1.093	0.581	-0.098	-0.389	0.516	-1.628	53.8
V	MRPL45	0.93566217	-1.306	-0.143	0.547	0.879	0.954	0.668	0.232	0.005	0.327	-2.164	58
V	PLEC	0.97715372	-1.542	-0.189	0.635	1.048	1.158	0.829	0.241	-0.381	-0.113	-1.686	59.3
V	CCDC137	0.96657586	-1.225	-0.038	0.693	1.066	1.17	0.871	0.294	-0.516	-0.557	-1.758	59.7
V	MRPL39	0.97320333	-1.694	-0.283	0.578	1.015	1.138	0.823	0.25	-0.295	0.067	-1.6	60.1
V	SPATS2L	0.97766388	-1.364	-0.111	0.662	1.059	1.174	0.878	0.301	-0.462	-0.422	-1.714	60.2
V	RPS15A	0.97191089	-1.298	-0.1	0.654	1.056	1.19	0.937	0.373	-0.526	-0.67	-1.614	62
V	MKI67	0.9717968	-1.324	-0.113	0.651	1.059	1.196	0.944	0.374	-0.537	-0.677	-1.575	62.1
V	RPL35A	0.98160504	-1.311	-0.121	0.627	1.026	1.161	0.923	0.391	-0.42	-0.546	-1.73	62.3
V	MAP4	0.89055386	-2.033	-0.469	0.518	1.049	1.232	0.936	0.263	-0.645	-0.289	-0.562	62.7
V	NSA2	0.99112124	-1.506	-0.237	0.57	1.01	1.172	0.961	0.434	-0.37	-0.453	-1.582	63.9
V	RPS9	0.98506415	-1.66	-0.312	0.548	1.02	1.197	0.981	0.428	-0.409	-0.42	-1.372	64.3
V	MAK16	0.98837724	-1.413	-0.2	0.576	1.006	1.17	0.977	0.464	-0.391	-0.579	-1.61	64.5
V	UPF3B	0.98469247	-1.524	-0.252	0.565	1.02	1.196	1.001	0.463	-0.441	-0.594	-1.435	64.9
V	RPS14	0.99228382	-1.329	-0.189	0.541	0.948	1.107	0.948	0.5	-0.232	-0.458	-1.836	65.3
V	MRPL1	0.98734	-1.746	-0.414	0.434	0.904	1.091	0.931	0.481	-0.09	-0.017	-1.574	65.9
V	MKRN2	0.99434966	-1.431	-0.26	0.488	0.905	1.07	0.926	0.509	-0.1	-0.236	-1.871	65.9
V	RPL32	0.98181347	-1.216	-0.14	0.56	0.96	1.125	0.988	0.537	-0.331	-0.72	-1.763	66.4
V	NOC3L	0.99660856	-1.597	-0.327	0.494	0.957	1.148	0.998	0.521	-0.257	-0.398	-1.541	66.5
V	DDX39B	0.97761174	-1.103	-0.112	0.532	0.901	1.056	0.944	0.557	-0.183	-0.601	-1.992	67.1
V	EIF4A3	0.97250268	-1.067	-0.088	0.552	0.92	1.076	0.962	0.559	-0.258	-0.729	-1.926	67.1
V	GADD45GIP	0.94890166	-0.982	-0.1	0.464	0.781	0.912	0.826	0.543	0.101	-0.236	-2.308	67.2
V	DDX54	0.9971334	-1.589	-0.334	0.481	0.947	1.144	1.012	0.547	-0.244	-0.428	-1.536	67.3
V	GNL3	0.97076767	-1.079	-0.1	0.547	0.926	1.093	0.994	0.585	-0.301	-0.83	-1.835	68.1
V	MRPL15	0.99817941	-1.63	-0.375	0.443	0.915	1.121	1.011	0.575	-0.164	-0.343	-1.554	68.3
V	RRS1	0.98929871	-1.748	-0.43	0.432	0.931	1.151	1.038	0.573	-0.235	-0.381	-1.332	68.5
V	HELZ2	0.96416078	-1.579	-0.415	0.331	0.755	0.937	0.861	0.556	0.232	0.225	-1.903	68.9
V	API5	0.99545266	-1.359	-0.249	0.482	0.909	1.101	1.013	0.608	-0.187	-0.568	-1.751	69
V	RPL35	0.99038372	-1.299	-0.217	0.499	0.92	1.11	1.023	0.613	-0.238	-0.678	-1.732	69.1
V	RPF2	0.99804109	-1.409	-0.279	0.465	0.898	1.093	1.007	0.609	-0.145	-0.484	-1.755	69.1
V	FTSJ3	0.99914148	-1.554	-0.35	0.443	0.907	1.118	1.032	0.613	-0.169	-0.453	-1.587	69.4
V	PES1	0.99356213	-1.718	-0.447	0.384	0.868	1.085	1.002	0.601	-0.052	-0.184	-1.539	69.5
V	MRPS5	0.98845909	-1.238	-0.199	0.49	0.897	1.085	1.011	0.626	-0.188	-0.661	-1.822	69.7
V	LRPPRC	0.99710185	-1.378	-0.276	0.451	0.879	1.076	1.005	0.629	-0.106	-0.479	-1.801	69.9
V	SARNP	0.99954515	-1.472	-0.322	0.437	0.884	1.09	1.019	0.631	-0.113	-0.445	-1.709	70
V	MRPS31	0.98906206	-1.244	-0.206	0.483	0.892	1.081	1.013	0.633	-0.175	-0.652	-1.825	70
V	MAGOH	0.99813502	-1.435	-0.301	0.45	0.895	1.101	1.032	0.637	-0.155	-0.534	-1.689	70.2
V	RPL6	0.98984391	-1.262	-0.227	0.466	0.882	1.08	1.029	0.66	-0.162	-0.671	-1.795	71
V	ALYREF	0.99716009	-1.615	-0.405	0.401	0.883	1.112	1.06	0.662	-0.135	-0.459	-1.503	71.2
V	SYNCRIP	0.98728254	-1.208	-0.21	0.457	0.858	1.05	1.007	0.663	-0.102	-0.619	-1.897	71.4
V	SLIRP	0.98782472	-1.219	-0.214	0.46	0.865	1.06	1.017	0.666	-0.123	-0.648	-1.863	71.4
V	MRPS9	0.99911637	-1.537	-0.381	0.389	0.85	1.071	1.033	0.674	-0.041	-0.386	-1.673	71.8
V	TBRG4	0.97947246	-1.115	-0.176	0.454	0.834	1.019	0.987	0.67	-0.061	-0.619	-1.994	71.9
V	TOP3B	0.92598022	-2.119	-0.706	0.232	0.792	1.062	1.027	0.627	-0.035	-0.013	-0.867	72.2
V	TRUB2	0.99200452	-1.721	-0.489	0.333	0.828	1.07	1.047	0.688	-0.003	-0.264	-1.489	72.7
V	NOL12	0.9912489	-1.722	-0.489	0.34	0.844	1.093	1.076	0.704	-0.063	-0.378	-1.405	73.1
V	MTREX	0.96030321	-1.854	-0.597	0.234	0.73	0.97	0.962	0.663	0.223	0.164	-1.495	73.4
V	TRIM56	0.96476889	-1.85	-0.601	0.231	0.732	0.981	0.989	0.692	0.207	0.088	-1.469	74.3
V	POLDIP3	0.99296178	-1.668	-0.481	0.323	0.819	1.071	1.081	0.741	-0.012	-0.397	-1.479	74.6
V	DDX1	0.98019194	-1.724	-0.532	0.265	0.749	0.992	1.006	0.715	0.182	-0.049	-1.604	74.7
V	TSNAX	0.98921198	-1.299	-0.303	0.372	0.787	1	1.011	0.73	0.071	-0.443	-1.926	74.9
V	FYTTD1	0.99451159	-1.384	-0.337	0.378	0.822	1.051	1.065	0.749	-0.03	-0.577	-1.737	75
V	CHTOP	0.99027777	-1.666	-0.488	0.317	0.819	1.081	1.107	0.768	-0.04	-0.485	-1.412	75.6
V	TUT7	0.95075696	-1.198	-0.296	0.305	0.668	0.851	0.875	0.688	0.345	-0.035	-2.204	75.9
V	GTPBP4	0.988205	-1.708	-0.525	0.282	0.785	1.048	1.085	0.773	0.055	-0.338	-1.457	76.2
V	RPL14	0.9470728	-1.995	-0.699	0.184	0.735	1.026	1.08	0.766	0.095	-0.13	-1.061	77
V	NCBP3	0.98936153	-1.664	-0.511	0.28	0.776	1.042	1.092	0.794	0.066	-0.38	-1.495	77.1
V	RBM8A	0.97938303	-1.782	-0.576	0.253	0.775	1.055	1.111	0.799	0.039	-0.369	-1.306	77.3
V	PTCD3	0.98880267	-1.419	-0.393	0.308	0.747	0.981	1.029	0.778	0.159	-0.343	-1.847	77.4
V	NFX1	0.97719065	-1.53	-0.464	0.256	0.702	0.936	0.985	0.756	0.278	-0.081	-1.839	77.5
V	DDX55	0.98998872	-1.557	-0.467	0.291	0.777	1.045	1.118	0.833	0.034	-0.546	-1.528	78.7
V	KIF1C	0.95698764	-1.877	-0.671	0.158	0.682	0.97	1.06	0.813	0.244	-0.058	-1.321	79.7
V	PRRC2B	0.98001211	-1.632	-0.523	0.257	0.767	1.057	1.158	0.874	0.005	-0.623	-1.341	80.3
V	CCDC9	0.96690626	-1.81	-0.64	0.177	0.707	1.008	1.125	0.872	0.152	-0.323	-1.27	81.3
V	NOP53	0.96181889	-1.629	-0.62	0.115	0.622	0.941	1.155	1.004	0.29	-0.448	-1.431	89.6
V	MSI2	0.91324689	-1.072	-0.362	0.212	0.651	0.963	1.231	1.089	-0.021	-1.317	-1.374	93.6
V	TEX10	0.95861727	-1.392	-0.525	0.13	0.603	0.919	1.174	1.066	0.286	-0.679	-1.583	94.1
VI	RPS19	0.95092869	-2.339	-0.875	0.094	0.671	0.949	0.925	0.552	0.046	0.334	-0.358	72.7
VI	RPS5	0.95019913	-2.182	-0.775	0.157	0.715	0.987	0.974	0.624	0.114	0.233	-0.849	73.2
VI	DHX57	0.95420643	-2.027	-0.76	0.096	0.624	0.903	0.972	0.735	0.348	0.295	-1.187	78.3
VI	ZC3H7B	0.96647158	-2.087	-0.812	0.065	0.622	0.929	1.039	0.802	0.282	0.117	-0.956	80.7
VI	MEX3D	0.98317886	-2.221	-0.915	-0.013	0.563	0.884	1.012	0.782	0.289	0.221	-0.602	81.7
VI	RPL27A	0.98709687	-2.196	-0.941	-0.058	0.523	0.864	1.046	0.858	0.329	0.134	-0.558	85.6
VI	CPEB4	0.99103298	-2.153	-0.935	-0.074	0.496	0.837	1.039	0.885	0.411	0.183	-0.687	87.8

VI	CASC3	0.96404932	-1.99	-0.825	0.007	0.567	0.907	1.115	0.95	0.344	-0.102	-0.971	88.1
VI	UNK	0.99481169	-2.183	-0.972	-0.128	0.424	0.749	0.94	0.82	0.537	0.485	-0.672	88.4
VI	RPS10	0.95668939	-1.904	-0.787	-0.008	0.502	0.802	0.98	0.868	0.561	0.305	-1.319	88.5
VI	TDRD3	0.99083218	-2.103	-0.921	-0.091	0.456	0.783	0.984	0.867	0.534	0.363	-0.873	89.3
VI	PUM2	0.97633841	-1.991	-0.859	-0.048	0.501	0.841	1.074	0.96	0.474	0.064	-1.017	91.4
VI	AGO3	0.99329651	-2.101	-0.937	-0.108	0.45	0.793	1.026	0.921	0.515	0.241	-0.801	91.6
VI	EDF1	0.99069443	-2.169	-1.02	-0.213	0.322	0.646	0.872	0.817	0.672	0.671	-0.599	94.4
VI	RPL34	0.99635468	-2.151	-1.02	-0.191	0.386	0.758	1.055	0.983	0.506	0.141	-0.467	96.3
VI	EIF4A1	0.98313072	-1.989	-0.903	-0.127	0.398	0.726	0.977	0.929	0.665	0.383	-1.059	96.8
VI	RPL21	0.99174732	-2.066	-0.963	-0.152	0.418	0.789	1.091	1.024	0.513	0.041	-0.695	97
VI	CCDC86	0.98600992	-2.232	-1.11	-0.291	0.278	0.646	0.948	0.906	0.567	0.393	-0.104	98.8
VI	EIF2S1	0.99868683	-2.108	-1.007	-0.2	0.365	0.733	1.041	0.997	0.583	0.206	-0.611	98.9
VI	OTUD4	0.986443	-1.993	-0.932	-0.145	0.412	0.781	1.097	1.053	0.56	0.023	-0.855	99.3
VI	RPL8	0.95469896	-1.814	-0.842	-0.103	0.438	0.81	1.158	1.133	0.538	-0.234	-1.083	101.8
VI	AGO2	0.99461085	-2.16	-1.078	-0.29	0.258	0.615	0.924	0.923	0.702	0.521	-0.414	103.6
VI	SDAD1	0.96378868	-1.841	-0.873	-0.134	0.409	0.784	1.144	1.137	0.581	-0.168	-1.04	103.6
VI	PUM1	0.99437152	-2.167	-1.091	-0.302	0.253	0.618	0.943	0.945	0.683	0.46	-0.34	104.1
VI	OASL	0.99801119	-2.085	-1.023	-0.245	0.299	0.657	0.973	0.975	0.711	0.412	-0.674	104.1
VI	EIF4G1	0.99100378	-2.138	-1.064	-0.289	0.245	0.589	0.885	0.893	0.753	0.634	-0.508	105
VI	CNBP	0.94624407	-1.743	-0.801	-0.102	0.395	0.729	1.038	1.047	0.708	0.119	-1.391	105.4
VI	EIF3G	0.93292685	-2.227	-1.178	-0.415	0.115	0.46	0.764	0.777	0.657	0.73	0.318	105.9
VI	PRRC2A	0.9890395	-2.17	-1.11	-0.332	0.216	0.579	0.909	0.928	0.718	0.538	-0.275	106.7
VI	CPEB3	0.96684972	-2.21	-1.161	-0.385	0.164	0.532	0.871	0.892	0.67	0.546	0.081	107
VI	RBMS1	0.98845667	-2.172	-1.117	-0.339	0.212	0.58	0.92	0.942	0.708	0.5	-0.233	107.1
VI	STAU1	0.87150666	-1.607	-0.903	-0.265	0.287	0.738	1.301	1.394	0.42	-0.969	-0.397	111
VI	YTHDF2	0.99354776	-2.113	-1.091	-0.331	0.212	0.581	0.938	0.983	0.767	0.485	-0.43	111
VI	YTHDF3	0.97700796	-2.17	-1.136	-0.376	0.16	0.518	0.855	0.898	0.762	0.649	-0.161	111.3
VI	CPEB2	0.95397708	-2.192	-1.182	-0.427	0.115	0.484	0.844	0.892	0.701	0.577	0.187	111.4
VI	GNL2	0.98140848	-1.895	-0.979	-0.259	0.288	0.685	1.117	1.187	0.715	-0.043	-0.816	111.9
VI	EIF4H	0.98239607	-2.118	-1.1	-0.355	0.169	0.519	0.853	0.91	0.826	0.696	-0.4	115.6
VI	ATXN2	0.95396167	-2.152	-1.193	-0.46	0.083	0.467	0.873	0.959	0.738	0.495	0.19	116.5
VI	ATXN2L	0.96975046	-2.145	-1.166	-0.428	0.11	0.484	0.871	0.952	0.785	0.572	-0.036	117.4
VI	CSDE1	0.95623348	-2.14	-1.179	-0.456	0.07	0.436	0.818	0.912	0.816	0.679	0.044	122.4
VI	PABPC1	0.95072827	-2.12	-1.196	-0.487	0.041	0.419	0.836	0.954	0.822	0.603	0.127	124.3
VI	NUFIP2	0.96121103	-2.135	-1.151	-0.425	0.091	0.441	0.792	0.875	0.844	0.784	-0.116	124.8
VI	LARP4	0.93306252	-2.125	-1.198	-0.498	0.014	0.374	0.761	0.875	0.835	0.76	0.203	130.6
VI	GNL3L	0.83520912	-1.148	-0.749	-0.334	0.073	0.453	1.063	1.395	1.082	-0.259	-1.577	135.5
VII	YBX3	0.99765936	-2.107	-1.211	-0.53	-0.028	0.33	0.725	0.855	0.842	0.792	0.332	137.7
VII	LSM14A	0.99778606	-2.118	-1.202	-0.512	-0.009	0.344	0.725	0.844	0.843	0.818	0.267	138.4
VII	STAU2	0.99140719	-2.094	-1.173	-0.478	0.029	0.387	0.778	0.906	0.901	0.788	-0.043	140.6
VII	RPS26	0.98857679	-2.054	-1.174	-0.498	0.008	0.375	0.8	0.959	0.947	0.741	-0.105	142.9
VII	IGF2BP1	0.99033965	-2.034	-1.185	-0.524	-0.02	0.353	0.801	0.982	0.967	0.718	-0.057	143.9
VII	PURB	0.99848025	-2.076	-1.217	-0.555	-0.057	0.306	0.727	0.885	0.884	0.782	0.32	143.9
VII	DDX3X	0.99838292	-2.068	-1.208	-0.545	-0.046	0.319	0.744	0.908	0.913	0.782	0.199	146.2
VII	PRRC2C	0.99762883	-2.084	-1.197	-0.522	-0.021	0.338	0.745	0.893	0.904	0.805	0.138	147.3
VII	PABPC4	0.99716377	-2.074	-1.222	-0.567	-0.076	0.281	0.693	0.847	0.861	0.813	0.444	147.7
VII	YBX1	0.99785058	-2.085	-1.217	-0.554	-0.061	0.293	0.696	0.841	0.858	0.825	0.405	148.5
VII	G3BP2	0.99697331	-2.004	-1.234	-0.616	-0.13	0.243	0.72	0.937	0.949	0.746	0.39	148.8
VII	IGF2BP3	0.99552383	-1.967	-1.224	-0.618	-0.131	0.251	0.758	1.005	1.021	0.714	0.191	149.8
VII	FAM120A	0.99878551	-1.998	-1.225	-0.61	-0.131	0.235	0.702	0.921	0.98	0.814	0.312	158.5
VII	UPF1	0.99699548	-1.967	-1.215	-0.61	-0.132	0.24	0.728	0.97	1.039	0.8	0.147	158.9
VII	IGF2BP2	0.99650628	-2.033	-1.194	-0.545	-0.053	0.309	0.745	0.93	0.976	0.818	0.048	159.3
VII	EIF3CL	0.99934584	-2.009	-1.221	-0.602	-0.126	0.232	0.68	0.887	0.97	0.865	0.323	170.8
VII	YTHDC2	0.98196729	-1.867	-1.171	-0.605	-0.147	0.217	0.724	1.013	1.17	0.866	-0.2	171
VII	FXR2	0.99367822	-2.071	-1.176	-0.499	-0.001	0.353	0.751	0.898	0.938	0.839	-0.032	171.1
VII	PURA	0.99454185	-1.905	-1.23	-0.674	-0.222	0.14	0.644	0.925	1.071	0.886	0.365	171.5
VII	HDLBP	0.98698684	-1.836	-1.237	-0.724	-0.29	0.071	0.606	0.928	1.107	0.894	0.482	171.5
VII	RPS2	0.9992086	-2.025	-1.221	-0.594	-0.116	0.24	0.676	0.87	0.945	0.866	0.359	172.4
VII	FXR1	0.99660438	-1.943	-1.228	-0.651	-0.191	0.168	0.651	0.905	1.033	0.885	0.37	172.6
VII	FMR1	0.99142892	-1.855	-1.223	-0.695	-0.256	0.103	0.623	0.935	1.133	0.93	0.306	176.8
VII	USP10	0.99937582	-2.015	-1.203	-0.575	-0.099	0.253	0.683	0.881	0.992	0.912	0.171	192.3
VII	EIF3L	0.98067554	-2.035	-1.137	-0.464	0.027	0.373	0.761	0.909	0.983	0.871	-0.288	193.3
VII	EIF3A	0.99635246	-2.05	-1.182	-0.524	-0.036	0.314	0.717	0.881	0.965	0.896	0.02	198.2
VII	EIF4G2	0.99130015	-1.927	-1.176	-0.59	-0.138	0.204	0.65	0.895	1.112	1.015	-0.045	200
VII	RPS3	0.99996645	-2.051	-1.209	-0.564	-0.081	0.27	0.683	0.855	0.933	0.892	0.273	200.3
VII	EIF3D	0.99959957	-2.077	-1.203	-0.539	-0.05	0.3	0.697	0.848	0.906	0.879	0.237	208.1
VII	UBAP2	0.99036072	-1.927	-1.224	-0.664	-0.224	0.116	0.568	0.814	1.007	0.996	0.54	209.7
VII	ZC3HAV1	0.9953308	-2.117	-1.179	-0.48	0.024	0.372	0.74	0.853	0.871	0.847	0.069	211.8
VII	UBAP2L	0.99473191	-2.004	-1.225	-0.618	-0.155	0.191	0.618	0.816	0.929	0.922	0.527	212.4
VII	SERBP1	0.98323827	-1.916	-1.229	-0.678	-0.243	0.095	0.547	0.791	0.968	0.972	0.693	213.4
VII	EIF4B	0.99863677	-2.038	-1.217	-0.585	-0.111	0.236	0.649	0.827	0.924	0.917	0.397	213.8
VII	G3BP1	0.99392885	-1.988	-1.222	-0.625	-0.17	0.171	0.595	0.801	0.948	0.968	0.522	220.8
VII	MOV10	0.91766268	-1.536	-1.167	-0.825	-0.511	-0.223	0.277	0.68	1.192	1.274	0.838	221
VII	YTHDF1	0.98113012	-2.09	-1.124	-0.422	0.069	0.396	0.721	0.818	0.919	0.966	-0.252	222.1
VII	CAPRIN1	0.99557979	-2.053	-1.22	-0.583	-0.107	0.237	0.636	0.797	0.874	0.905	0.514	229.7
VII	LSM14B	0.98383848	-1.929	-1.222	-0.664	-0.231	0.1	0.532	0.762	0.962	1.02	0.672	230.1
VII	ZNFX1	0.97473109	-2.21	-1.118	-0.34	0.185	0.515	0.782	0.78	0.728	0.824	-0.146	233
VII	FAM120C	0.99833869	-2.103	-1.193	-0.517	-0.033	0.301	0.656	0.775	0.868	0.964	0.281	233.5
VII	LARP4B	0.99426966	-2.069	-1.222	-0.575	-0.094	0.252	0.648	0.796	0.844	0.87	0.549	233.7
VII	RPS28	0.98800544	-1.977	-1.22	-0.633	-0.188	0.144	0.555	0.755	0.925	1.005	0.634	235.8
VII	LSG1	0.91636356	-2.217	-0.988	-0.154	0.372	0.663	0.801	0.68	0.602	0.832	-0.591	236.8
VII	SND1	0.993483	-2.138	-1.207	-0.515	-0.018	0.322	0.671	0.763	0.769	0.86	0.492	245.8
VII	PYM1	0.95229574	-1.84	-1.153	-0.644	-0.276	-0.012	0.317	0.527	0.982	1.404	0.695	247.2
VII	LARP1	0.96069278	-2.328	-1.104	-0.262	0.278	0.586	0.747	0.625	0.489	0.813	0.155	253.4

Table 2.2 Clustering analysis of mRNA binding dynamics of RBPs

Seed gene	Mean Euclidean distance to protein interactors	p-value
STAU1	3.514936384	5E-17
RC3H1	3.570607772	4.2E-10
MOV10	4.814208015	3E-09
PABPC1	3.099038955	1.2E-07
SYNCRIP	2.649187933	3.9E-07
G3BP1	2.25667873	6E-07
CDC5L	1.668116532	9.6E-07
YBX1	4.571605013	8.3E-06
EIF3H	4.926631762	7.1E-05
TDRD3	2.580645656	0.00017
IGF2BP3	4.183604071	0.00022
EIF4A3	1.805746514	0.00031
DDX3X	2.864823798	0.00078
ZC3HAV1	2.740612715	0.0014
UPF1	2.667313093	0.00165
AGO2	2.76530979	0.00323
NFX1	3.472777146	0.00331
IGF2BP2	3.38234806	0.00504
FAM120A	3.867572707	0.00736
ALYREF	2.686071455	0.00777
EIF3G	2.765964815	0.00806
LSM14A	3.859641045	0.00993
EIF4B	2.843241499	0.01019
LARP4B	5.951179865	0.01078
PABPC4	3.647435152	0.01176
PRRC2A	3.03863048	0.01208
PNN	1.609045357	0.01445
EIF4A1	2.29948521	0.01472
RBM34	3.068570891	0.01478
RBM8A	2.165362641	0.01507
DDX1	2.491991432	0.01864
RNPS1	1.21840251	0.0191
FXR1	2.272034676	0.0205
TRIM56	4.082956083	0.021
SND1	4.896067529	0.02156
FTSJ3	2.150053372	0.02382
FUBP3	2.902038782	0.02422
EIF4G1	2.321955574	0.02519
UPF3B	1.941961505	0.02713
FXR2	1.690211087	0.02929
CASC3	2.461836822	0.02958
VIRMA	1.612137369	0.03013
RBMS1	3.183959018	0.03058
PUM1	3.176821126	0.03075
LARP4	3.568905553	0.03125
YTHDF2	3.13967693	0.03125
NCBP3	2.993439739	0.03424
YTHDF3	2.693486365	0.04051
MTREX	2.793425759	0.04308
CHD3	1.525090136	0.04314
CSDE1	2.516511005	0.04743
FMR1	2.256762362	0.04841
CHD4	1.360576088	0.04854
YTHDF1	2.135125606	0.05159
STAU2	2.423407131	0.05187
PYM1	5.399110504	0.05411
IGF2BP1	2.189016861	0.05442
EIF4H	5.196179758	0.05755
SNRPD1	1.392042097	0.06017
OTUD4	2.211018098	0.0614
NCL	1.439160666	0.0625
NOL11	4.826023079	0.06283
GNL2	4.815482738	0.06325
LYAR	4.815482738	0.06325
SRPK1	1.150486903	0.06888
RRP8	4.24947421	0.07074
PWP1	4.190485099	0.0726
UTP15	4.102663372	0.07546
EIF2S1	4.075495337	0.07643
EIF2S3	4.075495337	0.07643
DHX36	3.900759525	0.08143
SERBP1	3.578440328	0.0896
G3BP2	1.222965774	0.09166
HTATSF1	3.124179642	0.0933

Seed gene	Mean Euclidean distance to protein interactors	p-value
LARP1	3.092452397	0.09387
DDX21	1.601006949	0.09486
TOP3B	2.314485577	0.09682
EIF3CL	2.966175169	0.09723
APEX1	2.203834876	0.09846
EIF4G2	2.942729847	0.09851
MSI2	2.886789892	0.10089
WDR43	2.707007892	0.10186
RPF2	1.911400538	0.10358
USP10	1.320298686	0.10401
YTHDC2	2.77297194	0.10454
EIF3D	2.068507543	0.10484
NOP53	1.73596523	0.10592
ATXN2	1.866233507	0.1064
DDX27	1.595337351	0.10873
SSRP1	1.30491813	0.10924
MAP4	2.689837347	0.10955
ZNFX1	2.604718263	0.11473
POLDIP3	1.853812975	0.11575
EIF3A	1.827277643	0.11751
RACK1	3.798786925	0.11907
DHX30	1.771116672	0.12003
NOL9	2.436533216	0.12283
TEX10	2.436533216	0.12283
HSPA5	1.21975002	0.1251
SCAF8	2.390694083	0.12633
UBAP2L	1.810216474	0.13424
FYTTD1	2.245316565	0.13572
NPM1	1.302022095	0.13899
NUFIP2	1.585532943	0.14062
PUM3	1.80639242	0.14079
DIMT1	2.486259303	0.14194
GTPBP4	1.483747494	0.14325
EIF3L	1.820493274	0.14331
DDX39B	1.417595783	0.14414
SRSF5	2.104416004	0.14793
SLIRP	2.094455977	0.1503
LARP7	1.292984667	0.15794
ZCCHC17	1.962117968	0.16588
AP3D1	1.936327479	0.16929
RBM28	1.814905348	0.17008
RBM15	1.585165316	0.1746
SNIP1	1.129530845	0.17575
MKRN2	1.822026798	0.1789
PARP12	1.822026798	0.1789
AQR	1.814987273	0.17979
PRRC2C	1.801018942	0.18248
LDHA	1.797975521	0.18338
LDHB	1.797975521	0.18338
PRRC2B	1.796064882	0.18428
UNK	1.796064882	0.18428
YBX3	1.752982118	0.19069
BCLAF1	3.332753579	0.20524
RTF1	1.637479679	0.20777
PA2G4	2.376691053	0.21857
SAP18	1.286052711	0.22245
DDX47	1.535179343	0.22675
SCAF4	1.527185316	0.2288
ELOA	1.504264523	0.24134
POLR2A	1.386629554	0.24194
RTCB	1.194681123	0.2454
CAPRIN1	1.262149697	0.25311
EXOSC10	1.217937382	0.25584
ELAC2	1.407706646	0.25862
SCAF11	1.406765665	0.25972
GEMIN5	1.403987405	0.26082
MAGOH	1.115913676	0.26317
CHD1	1.397661214	0.26526
TCP1	1.082414807	0.27027
LUC7L3	1.11341146	0.28475
SSB	1.059519141	0.28639
CRNKL1	1.229624097	0.29266
GNL3	1.198690028	0.29735
CLK3	0.887027857	0.30519

Seed gene	Mean Euclidean distance to protein interactors	p-value
SETD2	1.107947363	0.30923
SRSF8	1.068772218	0.31646
PINX1	1.068653422	0.31767
CHTOP	1.048182439	0.32497
ISY1	1.095911072	0.32775
ARL6IP4	1.038269713	0.32988
NOL8	1.037388399	0.33111
TRA2A	2.205720609	0.33315
SMARCA5	0.89592401	0.33458
NKRF	2.186889005	0.33561
ZCCHC8	1.445389592	0.33601
ZRANB2	1.01610221	0.33606
MEPCE	0.938156676	0.33648
YTHDC1	1.0112864	0.33979
EEF1A1	1.166262111	0.34453
ZC3H13	0.991089751	0.34478
RBM47	0.986708009	0.34604
RBM33	0.978822379	0.34981
SURF6	0.962460824	0.35612
USP36	0.959774	0.35739
SMARCA4	0.888030916	0.36332
DROSHA	0.94401025	0.36375
TPR	0.845635215	0.365
ATXN2L	1.461436056	0.36591
XRN2	1.971744912	0.3679
CHORDC1	0.842305371	0.36862
GPATCH8	0.933614759	0.37015
PNO1	0.907763753	0.38047
NXF1	0.895984528	0.38073
DCAF13	2.108021674	0.38875
HMGB1	0.904620366	0.38875
SARNP	0.870893323	0.39479
ZC3H11A	0.870893323	0.39479
HP1BP3	0.803034606	0.39521
LUC7L2	1.578849713	0.40254
CDK11B	0.819904857	0.4119
PRPF4B	1.577044155	0.42062
SUPT16H	0.874125952	0.42097
BAZ2A	0.794842402	0.42384
SNRPA	0.767517599	0.42462
FAM98B	0.780965385	0.42918
LUC7L	0.824214014	0.43647
CLTC	0.765863525	0.43854
ZNF106	0.758189956	0.44122
RAMAC	0.75128889	0.44659
RNMT	0.75128889	0.44659
TUBB	0.736160684	0.45197
RPRD2	0.726596075	0.45871
RBM7	0.820805814	0.46778
HSPA8	1.124302209	0.47181
PTBP3	0.695159219	0.47493
HMGA1	0.685915363	0.47763
RBM15B	0.683492881	0.4817
MFAP1	0.662814402	0.48983
HSP90AA1	1.067087477	0.49014
RBM6	0.630420547	0.50475
BAZ1B	0.626725963	0.50746
ILF2	1.740848989	0.51003
PHF10	0.589908618	0.52101
DHX8	0.770958934	0.52358
API5	0.582656924	0.52507
RBM12	0.580235673	0.52778
PTCD3	0.573555913	0.52913
DAZAP1	0.640799704	0.52924
PPHLN1	0.605938658	0.53402
BRIX1	1.267944515	0.54101
AKAP8L	0.561770277	0.54129
ZC3H18	1.015129272	0.54874
NSUN2	0.537667495	0.55207
EXOSC4	0.590996632	0.55309
GRWD1	0.56244969	0.55499
MCM5	0.746111452	0.55635
RAN	0.531255838	0.56012
RPA1	0.865115401	0.5667

Seed gene	Mean Euclidean distance to protein interactors	p-value
EXOSC9	0.578753513	0.57393
SNW1	1.247394847	0.57657
SRRT	0.661056421	0.5777
RRP12	0.506718378	0.58015
SRSF11	0.696557295	0.59319
IK	0.646189627	0.60015
GAPDH	0.623693374	0.60041
PPIG	0.829436104	0.60293
RBMX2	0.464307453	0.6039
SRSF10	0.871557065	0.607
ACIN1	0.752083209	0.61288
CPSF4	0.500957342	0.63228
SRRM2	0.858016306	0.63876
PHF3	0.433227004	0.6388
AGO3	0.542754064	0.6431
NKAP	0.511726884	0.66964
HNRNPU	1.271265553	0.69321
ADARB1	0.390409967	0.69673
STRBP	0.390409967	0.69673
NCOA5	0.386028079	0.70382
DHX15	0.596651302	0.71949
CHERP	0.537019606	0.72712
SUPT5H	0.892681262	0.73254
NOP2	0.620324142	0.73362
TOP2A	0.803829171	0.73372
PRPF3	0.612904654	0.73497
ESF1	0.356999938	0.73696
RBM39	0.88770982	0.73718
SUGP1	0.404356951	0.74156
U2SURP	0.339707277	0.7501
CSTF2	1.135342765	0.75819
WBP11	0.425054183	0.75912
PABPN1	0.327528494	0.76183
GTF2I	0.327281993	0.76393
PCBP2	1.82208576	0.76666
RBM3	2.466878109	0.76786
PRPF31	0.536504171	0.76892
DDX18	0.425419424	0.76948
THRAP3	0.751978243	0.77021
SRSF4	0.320353116	0.77222
WDR33	0.482842143	0.77441
MBNL1	0.313926259	0.77733
AATF	0.50720221	0.78455
DDX42	0.29727783	0.79028
HNRNPH3	0.508195099	0.79075
RBM5	0.477326005	0.79563
SRSF7	0.547935498	0.79829
XPO5	0.376351201	0.8174
DDX24	0.273235057	0.81752
PARP1	0.562045401	0.81984
NIFK	0.665930299	0.82205
PQBP1	0.269137247	0.82375
KHSRP	0.463922633	0.82389
HNRNPUL1	0.448891151	0.83373
UBAP2	0.465412726	0.84629
SRRM1	0.686966268	0.86448
AKAP8	0.219487486	0.87297
ADAR	0.219120732	0.87367
HSP90AB1	0.431722817	0.87697
YLPM1	0.214824176	0.87717
SF3A1	0.546389459	0.87887
RBM10	0.212079155	0.88059
SMNDC1	0.210850084	0.88261
CSTF1	0.440911153	0.88741
ILF3	1.056253094	0.89079
PCBP4	0.203161623	0.89109
HNRNPLL	0.289152497	0.89158
CELF1	1.357129245	0.89588
SNRNP70	0.677524463	0.8961
DHX9	0.708298018	0.90929
NGDN	0.16825777	0.9117
SRSF2	0.51553168	0.91254
CCAR1	0.153581553	0.91754
RBM14	0.257418549	0.91902

PRPF6	0.50412963	0.92045
SF3A2	0.608031844	0.92295
RAVER1	0.135499182	0.92454
EFTUD2	0.584631622	0.92588
CSTF3	0.378002757	0.92618
PSPC1	0.250149171	0.92767
FUBP1	0.418184548	0.92787
SRSF6	0.453248829	0.92874
DDX46	0.242909065	0.92996
TAF15	0.352723674	0.93075
SAFB2	0.242125095	0.93092
PTBP2	0.11597408	0.93331
TOP1	0.497167251	0.93437
NUDT21	0.285190036	0.93813
PCBP1	1.160627775	0.94171
TCERG1	0.481044858	0.94407
PRPF40A	0.511651547	0.94483
FIP1L1	0.330014232	0.94493
SRSF1	0.675797376	0.94589
TOP2B	0.084812686	0.94664
DDX5	0.929944691	0.94799
HNRNPC	0.795398226	0.94816
PHF5A	0.337157769	0.94898
SF3B6	0.505876188	0.94935
NCBP2	0.208096665	0.94939
HNRNPR	0.67870596	0.95586
POLR2B	0.204600852	0.95603
MATR3	0.963943455	0.95862
SF3B3	0.462652214	0.95898
PUF60	0.4834033	0.9591
SAFB	0.377408637	0.96068
TARDBP	0.814348659	0.96202
KHDRBS1	0.285139423	0.96553
ZFR	0.17596801	0.96858
RBM25	0.232554976	0.96908
SF3B2	0.474878748	0.97079
DDX23	0.297048068	0.9714
XRCC6	0.570083431	0.97162
SRSF9	0.50368231	0.97172
SART1	0.329033517	0.97436
SF3A3	0.2882199	0.97445
RBMX	0.565716565	0.97615
SF1	0.296316992	0.97638
SUPT6H	0.146991711	0.97671
RBFOX2	0.214872709	0.97793
HNRNPM	0.319181125	0.97858
CPSF7	0.29271725	0.97899
ZNF326	0.124942302	0.98052
SF3B4	0.342838589	0.98383
CPSF6	0.18571139	0.98462
CSTF2T	0.23235951	0.98465
TRA2B	0.582997878	0.98729
SRSF3	0.4580724	0.98762
SF3B1	0.437802929	0.98766
HNRNPH2	0.264697581	0.99013
SNRNP200	0.457151704	0.99225
EWSR1	0.62701859	0.99434
HNRNPAB	0.11087051	0.99563
RALY	0.233788581	0.99594
SFPQ	0.398811072	0.99689
FUS	0.78408873	0.99743
QKI	0.184016756	0.99766
PTBP1	0.847172762	0.99806
HNRNPDL	0.220319836	0.99851
DDX17	0.224824254	0.99932
HNRNPA3	0.262728168	0.99948
HNRNPL	0.673796126	0.9995
NONO	0.208977205	0.99955
ELAVL1	0.998787522	0.99958
HNRNPF	0.202534499	0.99982
HNRNPK	0.603109362	0.99988
HNRNPA2B1	0.628277453	0.99991
HNRNPA0	0.164643759	0.99991
HNRNPD	0.852686553	0.99998
U2AF2	0.517041145	1
HNRNPH1	0.445753745	1
HNRNPA1	0.564881052	1

Table 2.3 Mean Euclidean distance to protein interactors

gene name	cluster	Tier 1 Stress granule	Tier 1 P-body	Core viral interactome	SARS2 sgRNA (Lee)	OC43 sgRNA (Lee)	DENV (Ooi)	ZIKV (Ooi)	RV (Ooi)	HIV All (Knoener)	IAV, 1hr (Kim)	CHIKV - IFN, 1hr (Kim)
CSTF3	I	FALSE	FALSE	FALSE	FALSE	FALSE	TRUE	FALSE	FALSE	FALSE	FALSE	FALSE
DDX21	I	TRUE	FALSE	TRUE	FALSE	FALSE	TRUE	FALSE	TRUE	TRUE	FALSE	TRUE
FIP1L1	I	FALSE	FALSE	FALSE	FALSE	FALSE	TRUE	FALSE	FALSE	TRUE	FALSE	FALSE
POLR2A	I	FALSE	FALSE	FALSE	FALSE	FALSE	TRUE	FALSE	FALSE	FALSE	FALSE	FALSE
POLR2B	I	FALSE	FALSE	TRUE	FALSE	FALSE	TRUE	FALSE	FALSE	TRUE	FALSE	TRUE
PPP1R10	I	FALSE	FALSE	FALSE	FALSE	FALSE	FALSE	FALSE	FALSE	FALSE	TRUE	TRUE
RPRD2	I	FALSE	FALSE	FALSE	FALSE	FALSE	FALSE	FALSE	FALSE	FALSE	TRUE	FALSE
SCAF11	I	FALSE	FALSE	FALSE	FALSE	FALSE	FALSE	FALSE	TRUE	FALSE	FALSE	FALSE
SSRP1	I	FALSE	FALSE	FALSE	FALSE	FALSE	FALSE	FALSE	FALSE	TRUE	FALSE	TRUE
SUPT16H	I	FALSE	FALSE	TRUE	FALSE	FALSE	TRUE	FALSE	FALSE	TRUE	TRUE	TRUE
SUPT5H	I	FALSE	FALSE	FALSE	FALSE	FALSE	TRUE	FALSE	FALSE	FALSE	FALSE	FALSE
SUPT6H	I	FALSE	FALSE	FALSE	FALSE	FALSE	TRUE	FALSE	TRUE	FALSE	TRUE	FALSE
TCOF1	I	FALSE	FALSE	FALSE	FALSE	FALSE	FALSE	FALSE	FALSE	TRUE	TRUE	TRUE
VIRMA	I	FALSE	FALSE	FALSE	FALSE	FALSE	FALSE	FALSE	FALSE	FALSE	FALSE	TRUE
ACOT7	II	FALSE	FALSE	FALSE	FALSE	FALSE	FALSE	FALSE	FALSE	TRUE	FALSE	TRUE
AKAP8	II	FALSE	FALSE	FALSE	FALSE	TRUE	TRUE	FALSE	TRUE	FALSE	FALSE	FALSE
AKAP8L	II	FALSE	FALSE	FALSE	FALSE	FALSE	TRUE	FALSE	FALSE	FALSE	FALSE	FALSE
ANXA7	II	FALSE	FALSE	FALSE	FALSE	FALSE	FALSE	FALSE	TRUE	FALSE	FALSE	FALSE
APOBEC3B	II	FALSE	FALSE	FALSE	FALSE	FALSE	FALSE	FALSE	TRUE	FALSE	FALSE	FALSE
BAZ1B	II	FALSE	FALSE	FALSE	FALSE	FALSE	FALSE	FALSE	FALSE	TRUE	FALSE	FALSE
BCLAF1	II	FALSE	FALSE	TRUE	FALSE	FALSE	FALSE	TRUE	FALSE	TRUE	FALSE	TRUE
BUD13	II	FALSE	FALSE	FALSE	FALSE	FALSE	FALSE	FALSE	FALSE	FALSE	FALSE	TRUE
CCAR1	II	TRUE	FALSE	FALSE	FALSE	FALSE	TRUE	FALSE	TRUE	FALSE	TRUE	TRUE
CHD1	II	FALSE	FALSE	FALSE	FALSE	FALSE	FALSE	FALSE	FALSE	FALSE	TRUE	FALSE
CHERP	II	FALSE	FALSE	FALSE	FALSE	FALSE	FALSE	FALSE	TRUE	FALSE	FALSE	FALSE
CIRBP	II	TRUE	FALSE	FALSE	TRUE	TRUE	FALSE	FALSE	TRUE	FALSE	FALSE	FALSE
CKAP4	II	FALSE	FALSE	TRUE	FALSE	TRUE	TRUE	TRUE	FALSE	FALSE	FALSE	FALSE
CLTC	II	FALSE	FALSE	FALSE	FALSE	FALSE	FALSE	FALSE	FALSE	TRUE	FALSE	TRUE
CPSF6	II	FALSE	FALSE	FALSE	FALSE	FALSE	TRUE	FALSE	TRUE	FALSE	FALSE	FALSE
CPSF7	II	FALSE	FALSE	FALSE	FALSE	FALSE	TRUE	FALSE	TRUE	FALSE	FALSE	FALSE
DAZAP1	II	TRUE	FALSE	FALSE	TRUE	TRUE	TRUE	TRUE	TRUE	FALSE	FALSE	FALSE
DDX17	II	FALSE	FALSE	FALSE	TRUE	TRUE	TRUE	TRUE	TRUE	FALSE	FALSE	FALSE
DDX31	II	FALSE	FALSE	FALSE	FALSE	FALSE	FALSE	FALSE	FALSE	FALSE	FALSE	TRUE
DDX42	II	FALSE	FALSE	FALSE	FALSE	FALSE	TRUE	FALSE	TRUE	FALSE	TRUE	TRUE
DDX46	II	FALSE	FALSE	TRUE	FALSE	FALSE	TRUE	FALSE	TRUE	TRUE	FALSE	FALSE
DDX5	II	FALSE	FALSE	FALSE	TRUE	TRUE	TRUE	TRUE	TRUE	TRUE	FALSE	FALSE
DEK	II	FALSE	FALSE	FALSE	FALSE	FALSE	FALSE	FALSE	TRUE	FALSE	FALSE	FALSE
DHX15	II	FALSE	FALSE	TRUE	FALSE	FALSE	TRUE	TRUE	TRUE	TRUE	TRUE	TRUE
DHX33	II	TRUE	FALSE	FALSE	FALSE	FALSE	FALSE	FALSE	FALSE	FALSE	FALSE	FALSE
EPRS	II	TRUE	FALSE	FALSE	FALSE	FALSE	TRUE	FALSE	TRUE	TRUE	TRUE	TRUE
EWSR1	II	FALSE	FALSE	FALSE	TRUE	TRUE	TRUE	TRUE	TRUE	TRUE	FALSE	FALSE
FAM133B	II	FALSE	FALSE	FALSE	FALSE	FALSE	FALSE	FALSE	FALSE	TRUE	FALSE	FALSE
FSCN1	II	FALSE	FALSE	FALSE	FALSE	FALSE	TRUE	TRUE	TRUE	FALSE	FALSE	TRUE
FUBP1	II	TRUE	FALSE	TRUE	TRUE	TRUE	TRUE	TRUE	TRUE	TRUE	FALSE	FALSE
FUS	II	TRUE	FALSE	FALSE	TRUE	TRUE	TRUE	TRUE	TRUE	TRUE	FALSE	FALSE
H1FX	II	FALSE	FALSE	FALSE	FALSE	FALSE	FALSE	FALSE	FALSE	TRUE	FALSE	FALSE
HNRNPA0	II	FALSE	FALSE	FALSE	TRUE	TRUE	TRUE	TRUE	TRUE	TRUE	FALSE	FALSE
HNRNPA1	II	TRUE	FALSE	TRUE	TRUE	TRUE	TRUE	TRUE	TRUE	TRUE	FALSE	TRUE
HNRNPA2B1	II	FALSE	FALSE	TRUE	TRUE	TRUE	TRUE	TRUE	TRUE	TRUE	FALSE	TRUE
HNRNPA3	II	FALSE	FALSE	TRUE	TRUE	TRUE	TRUE	TRUE	TRUE	TRUE	FALSE	TRUE
HNRNPAB	II	TRUE	FALSE	TRUE	TRUE	TRUE	TRUE	TRUE	TRUE	TRUE	FALSE	FALSE
HNRNPD	II	FALSE	FALSE	TRUE	TRUE	TRUE	TRUE	TRUE	TRUE	TRUE	FALSE	FALSE
HNRNPDL	II	FALSE	FALSE	TRUE	TRUE	TRUE	TRUE	TRUE	TRUE	TRUE	FALSE	FALSE
HNRNPF	II	FALSE	FALSE	FALSE	FALSE	TRUE	TRUE	TRUE	TRUE	TRUE	FALSE	FALSE
HNRNPH1	II	FALSE	FALSE	TRUE	TRUE	TRUE	TRUE	TRUE	TRUE	TRUE	FALSE	FALSE
HNRNPH2	II	FALSE	FALSE	FALSE	FALSE	TRUE	TRUE	TRUE	TRUE	FALSE	FALSE	FALSE
HNRNPH3	II	FALSE	FALSE	FALSE	TRUE	TRUE	TRUE	TRUE	TRUE	TRUE	FALSE	FALSE
HNRNPK	II	TRUE	FALSE	TRUE	TRUE	TRUE	TRUE	TRUE	TRUE	TRUE	FALSE	FALSE
HNRNPL	II	FALSE	FALSE	TRUE	TRUE	TRUE	TRUE	TRUE	TRUE	TRUE	FALSE	TRUE
HNRNPLL	II	FALSE	FALSE	FALSE	FALSE	FALSE	FALSE	FALSE	TRUE	FALSE	FALSE	FALSE
HNRNPU	II	FALSE	FALSE	TRUE	TRUE	TRUE	TRUE	TRUE	TRUE	TRUE	TRUE	TRUE
HNRNPUL1	II	FALSE	FALSE	FALSE	FALSE	FALSE	TRUE	TRUE	TRUE	TRUE	FALSE	FALSE
HNRNPUL2	II	FALSE	FALSE	FALSE	TRUE	TRUE	TRUE	TRUE	TRUE	FALSE	TRUE	FALSE
KHDRBS1	II	TRUE	FALSE	FALSE	TRUE	TRUE	TRUE	TRUE	TRUE	TRUE	FALSE	FALSE
KHSRP	II	TRUE	FALSE	FALSE	TRUE	TRUE	TRUE	TRUE	TRUE	TRUE	FALSE	FALSE
LUC7L	II	FALSE	FALSE	FALSE	FALSE	FALSE	FALSE	FALSE	FALSE	TRUE	FALSE	FALSE
LUC7L2	II	FALSE	FALSE	FALSE	FALSE	FALSE	TRUE	TRUE	TRUE	TRUE	FALSE	FALSE
LUC7L3	II	FALSE	FALSE	FALSE	FALSE	FALSE	TRUE	FALSE	TRUE	TRUE	FALSE	FALSE
MSN	II	FALSE	FALSE	FALSE	FALSE	FALSE	FALSE	FALSE	FALSE	TRUE	FALSE	TRUE
NCL	II	FALSE	FALSE	TRUE	TRUE	TRUE	TRUE	TRUE	TRUE	TRUE	TRUE	TRUE
NCOA5	II	FALSE	FALSE	FALSE	FALSE	FALSE	TRUE	FALSE	TRUE	TRUE	FALSE	FALSE
NOL8	II	FALSE	FALSE	FALSE	FALSE	FALSE	FALSE	FALSE	FALSE	FALSE	TRUE	FALSE
NONO	II	FALSE	FALSE	TRUE	TRUE	TRUE	TRUE	TRUE	TRUE	TRUE	FALSE	TRUE
NUDT21	II	FALSE	FALSE	FALSE	FALSE	FALSE	TRUE	FALSE	TRUE	TRUE	FALSE	FALSE
PABPN1	II	FALSE	FALSE	FALSE	TRUE	FALSE	TRUE	FALSE	FALSE	FALSE	FALSE	FALSE
PARP1	II	FALSE	FALSE	TRUE	FALSE	FALSE	TRUE	TRUE	TRUE	TRUE	TRUE	TRUE
PDCD6	II	FALSE	TRUE	FALSE	FALSE	FALSE	FALSE	FALSE	TRUE	FALSE	FALSE	FALSE
PQBP1	II	TRUE	FALSE	FALSE	FALSE	FALSE	FALSE	FALSE	FALSE	FALSE	FALSE	FALSE
PRPF40A	II	FALSE	FALSE	FALSE	FALSE	FALSE	TRUE	FALSE	TRUE	TRUE	FALSE	FALSE
PRPF6	II	FALSE	FALSE	FALSE	FALSE	FALSE	TRUE	FALSE	TRUE	TRUE	FALSE	FALSE
PSPC1	II	TRUE	FALSE	FALSE	TRUE	TRUE	TRUE	TRUE	TRUE	FALSE	FALSE	FALSE
PUF60	II	FALSE	FALSE	TRUE	FALSE	TRUE	TRUE	FALSE	TRUE	TRUE	FALSE	FALSE
RAB10	II	FALSE	FALSE	FALSE	FALSE	FALSE	FALSE	FALSE	FALSE	FALSE	TRUE	TRUE
RBBP6	II	FALSE	FALSE	FALSE	FALSE	FALSE	FALSE	FALSE	FALSE	TRUE	FALSE	FALSE
RBM12	II	FALSE	FALSE	FALSE	FALSE	FALSE	TRUE	FALSE	TRUE	TRUE	FALSE	TRUE
RBM14	II	TRUE	FALSE	FALSE	TRUE	TRUE	TRUE	TRUE	TRUE	TRUE	FALSE	FALSE
RBM15	II	TRUE	FALSE	TRUE	FALSE	FALSE	TRUE	FALSE	TRUE	FALSE	TRUE	TRUE
RBM25	II	TRUE	FALSE	FALSE	FALSE	FALSE	TRUE	FALSE	TRUE	FALSE	FALSE	TRUE
RBM3	II	FALSE	FALSE	TRUE	TRUE	TRUE	TRUE	TRUE	TRUE	FALSE	FALSE	FALSE
RBM39	II	FALSE	FALSE	TRUE	FALSE	FALSE	TRUE	TRUE	TRUE	TRUE	FALSE	FALSE
RBM4	II	FALSE	FALSE	FALSE	FALSE	TRUE	TRUE	TRUE	TRUE	FALSE	FALSE	FALSE
RBM42	II	TRUE	FALSE	FALSE	FALSE	FALSE	FALSE	FALSE	FALSE	FALSE	FALSE	FALSE
RBM6	II	FALSE	FALSE	FALSE	FALSE	FALSE	TRUE	FALSE	FALSE	FALSE	FALSE	FALSE
RBMX	II	TRUE	FALSE	FALSE	FALSE	TRUE	TRUE	TRUE	TRUE	TRUE	FALSE	FALSE
SAFB	II	FALSE	FALSE	FALSE	TRUE	TRUE	TRUE	TRUE	TRUE	TRUE	FALSE	FALSE
SART1	II	FALSE	FALSE	FALSE	FALSE	FALSE	TRUE	FALSE	FALSE	TRUE	FALSE	FALSE
SF1	II	TRUE	FALSE	TRUE	TRUE	TRUE	TRUE	FALSE	TRUE	FALSE	FALSE	FALSE
SF3A1	II	FALSE	FALSE	FALSE	FALSE	FALSE	TRUE	FALSE	TRUE	TRUE	FALSE	FALSE
SF3A3	II	FALSE	FALSE	FALSE	FALSE	FALSE	TRUE	FALSE	FALSE	TRUE	FALSE	FALSE
SF3B1	II	FALSE	FALSE	TRUE	FALSE	FALSE	TRUE	TRUE	TRUE	TRUE	FALSE	FALSE
SF3B2	II	FALSE	FALSE	TRUE	FALSE	FALSE	TRUE	FALSE	TRUE	FALSE	FALSE	FALSE
SF3B3	II	FALSE	FALSE	FALSE	FALSE	FALSE	TRUE	TRUE	TRUE	TRUE	TRUE	TRUE
SFPQ	II	FALSE	FALSE	TRUE	TRUE	TRUE	TRUE	TRUE	TRUE	TRUE	FALSE	FALSE
SLC16A3	II	FALSE	FALSE	FALSE	FALSE	FALSE	FALSE	FALSE	FALSE	FALSE	TRUE	FALSE
SLC25A3	II	FALSE	FALSE	FALSE	FALSE	FALSE	FALSE	FALSE	FALSE	TRUE	FALSE	FALSE
SLTM	II	FALSE	FALSE	TRUE	FALSE	TRUE	TRUE	FALSE	TRUE	TRUE	FALSE	TRUE
SMARCA5	II	FALSE	FALSE	FALSE	FALSE	FALSE	TRUE	FALSE	FALSE	TRUE	FALSE	FALSE
SNRNP200	II	FALSE	FALSE	TRUE	FALSE	FALSE	TRUE	TRUE	TRUE	TRUE	TRUE	TRUE
SNRNP70	II	FALSE	FALSE	FALSE	FALSE	FALSE	TRUE	TRUE	TRUE	TRUE	FALSE	FALSE
SON	II	FALSE	FALSE	TRUE	FALSE	FALSE	TRUE	FALSE	FALSE	TRUE	FALSE	FALSE
SPEN	II	FALSE	FALSE	FALSE	FALSE	FALSE	FALSE	FALSE	FALSE	TRUE	FALSE	FALSE
SRRM1	II	FALSE	FALSE	FALSE	FALSE	FALSE	FALSE	FALSE	FALSE	FALSE	FALSE	TRUE
SRRT	II	FALSE	FALSE	FALSE	FALSE	FALSE	TRUE	TRUE	TRUE	TRUE	FALSE	FALSE
SRSF1	II	TRUE	FALSE	FALSE	TRUE	TRUE	TRUE	TRUE	TRUE	TRUE	FALSE	FALSE
SRSF10	II	FALSE	FALSE	FALSE	FALSE	TRUE	TRUE	FALSE	TRUE	FALSE	FALSE	FALSE
SRSF2	II	FALSE	FALSE	TRUE	TRUE	FALSE	TRUE	TRUE	TRUE	TRUE	FALSE	FALSE
SRSF3	II	TRUE	FALSE	FALSE	TRUE	TRUE	TRUE	TRUE	TRUE	TRUE	FALSE	FALSE
SRSF5	II	TRUE	FALSE	FALSE	FALSE	TRUE	FALSE	FALSE	TRUE	FALSE	FALSE	FALSE

gene name	cluster	Tier 1 Stress granule	Tier 1 P-body	Core viral interactome	SARS2 sgRNA (Lee)	OC43 sgRNA (Lee)	DENV (Ooi)	ZIKV (Ooi)	RV (Ooi)	HIV All (Knoener)	IAV, 1hr (Kim)	CHIKV - IFN, 1hr (Kim)
SRSF6	II	FALSE	FALSE	TRUE	TRUE	FALSE	TRUE	TRUE	TRUE	TRUE	FALSE	FALSE
SRSF7	II	TRUE	FALSE	FALSE	FALSE	TRUE	TRUE	TRUE	TRUE	TRUE	FALSE	FALSE
SRSF9	II	TRUE	FALSE	FALSE	FALSE	FALSE	TRUE	FALSE	TRUE	TRUE	FALSE	FALSE
SUB1	II	FALSE	FALSE	FALSE	FALSE	FALSE	FALSE	FALSE	FALSE	TRUE	FALSE	FALSE
SUGP2	II	FALSE	FALSE	FALSE	FALSE	FALSE	TRUE	TRUE	TRUE	FALSE	FALSE	FALSE
SURF4	II	FALSE	FALSE	FALSE	FALSE	FALSE	TRUE	TRUE	FALSE	FALSE	TRUE	TRUE
TAF15	II	FALSE	FALSE	FALSE	TRUE	TRUE	TRUE	TRUE	FALSE	TRUE	FALSE	FALSE
TCERG1	II	FALSE	FALSE	FALSE	FALSE	FALSE	TRUE	FALSE	TRUE	TRUE	FALSE	FALSE
THRAP3	II	FALSE	FALSE	TRUE	TRUE	TRUE	TRUE	TRUE	TRUE	TRUE	FALSE	TRUE
TIAL1	II	TRUE	FALSE	TRUE	TRUE	TRUE	TRUE	TRUE	TRUE	TRUE	FALSE	FALSE
TRA2A	II	FALSE	FALSE	FALSE	FALSE	TRUE	FALSE	TRUE	FALSE	TRUE	FALSE	FALSE
TRA2B	II	TRUE	FALSE	FALSE	TRUE	TRUE	TRUE	TRUE	TRUE	TRUE	FALSE	FALSE
TUBB	II	FALSE	FALSE	FALSE	FALSE	TRUE	FALSE	FALSE	TRUE	TRUE	TRUE	FALSE
U2AF1L5	II	FALSE	FALSE	FALSE	FALSE	FALSE	TRUE	FALSE	TRUE	FALSE	FALSE	FALSE
U2AF2	II	FALSE	FALSE	TRUE	TRUE	TRUE	TRUE	TRUE	TRUE	TRUE	FALSE	FALSE
U2SURP	II	FALSE	FALSE	FALSE	FALSE	FALSE	TRUE	FALSE	TRUE	FALSE	FALSE	FALSE
WBP11	II	FALSE	FALSE	FALSE	FALSE	FALSE	TRUE	FALSE	FALSE	FALSE	FALSE	FALSE
WDR33	II	FALSE	FALSE	FALSE	FALSE	FALSE	TRUE	FALSE	FALSE	FALSE	TRUE	TRUE
XRN2	II	TRUE	FALSE	TRUE	FALSE	FALSE	TRUE	TRUE	TRUE	TRUE	TRUE	FALSE
ZC3H4	II	FALSE	FALSE	FALSE	FALSE	FALSE	TRUE	FALSE	FALSE	FALSE	FALSE	FALSE
ZNF326	II	FALSE	FALSE	FALSE	FALSE	FALSE	TRUE	TRUE	TRUE	TRUE	TRUE	FALSE
ACP1	III	FALSE	FALSE	FALSE	FALSE	FALSE	FALSE	FALSE	FALSE	FALSE	TRUE	FALSE
ADAR	III	FALSE	FALSE	TRUE	FALSE	FALSE	TRUE	TRUE	TRUE	TRUE	TRUE	TRUE
AP2M1	III	FALSE	FALSE	FALSE	FALSE	FALSE	FALSE	FALSE	FALSE	FALSE	FALSE	TRUE
APEX1	III	FALSE	FALSE	FALSE	FALSE	FALSE	FALSE	FALSE	FALSE	TRUE	FALSE	FALSE
AQR	III	TRUE	FALSE	FALSE	FALSE	FALSE	TRUE	FALSE	FALSE	FALSE	FALSE	FALSE
ARPC1B	III	FALSE	FALSE	FALSE	FALSE	FALSE	FALSE	FALSE	FALSE	FALSE	FALSE	FALSE
CDC5L	III	FALSE	FALSE	FALSE	FALSE	FALSE	TRUE	FALSE	TRUE	FALSE	TRUE	FALSE
CELF1	III	TRUE	FALSE	TRUE	TRUE	TRUE	TRUE	TRUE	TRUE	TRUE	FALSE	FALSE
CHD4	III	FALSE	FALSE	FALSE	FALSE	FALSE	TRUE	FALSE	FALSE	FALSE	TRUE	FALSE
CHORDC1	III	FALSE	FALSE	FALSE	FALSE	FALSE	FALSE	FALSE	FALSE	FALSE	TRUE	TRUE
COPB2	III	FALSE	FALSE	TRUE	FALSE	FALSE	TRUE	TRUE	FALSE	FALSE	TRUE	TRUE
DCAF13	III	FALSE	FALSE	FALSE	FALSE	FALSE	FALSE	FALSE	FALSE	FALSE	FALSE	TRUE
DDX23	III	FALSE	FALSE	FALSE	FALSE	FALSE	TRUE	FALSE	TRUE	TRUE	FALSE	FALSE
DHX15	III	FALSE	FALSE	FALSE	FALSE	FALSE	TRUE	FALSE	FALSE	FALSE	TRUE	FALSE
DHX36	III	TRUE	FALSE	FALSE	FALSE	FALSE	TRUE	TRUE	TRUE	TRUE	FALSE	TRUE
DHX9	III	FALSE	FALSE	TRUE	TRUE	TRUE	TRUE	TRUE	TRUE	TRUE	TRUE	TRUE
DROSHA	III	TRUE	FALSE	FALSE	FALSE	FALSE	FALSE	FALSE	FALSE	FALSE	FALSE	FALSE
EEF1A1	III	FALSE	FALSE	FALSE	FALSE	FALSE	TRUE	FALSE	TRUE	TRUE	FALSE	FALSE
EFTUD2	III	FALSE	FALSE	FALSE	FALSE	FALSE	TRUE	TRUE	TRUE	TRUE	TRUE	FALSE
EIF2S3	III	FALSE	FALSE	FALSE	FALSE	FALSE	FALSE	FALSE	TRUE	TRUE	FALSE	FALSE
EIF5A	III	TRUE	TRUE	FALSE	FALSE	FALSE	TRUE	TRUE	FALSE	TRUE	FALSE	FALSE
ELAVL1	III	TRUE	FALSE	FALSE	TRUE	TRUE	TRUE	TRUE	TRUE	TRUE	FALSE	FALSE
ENO1	III	FALSE	FALSE	FALSE	TRUE	FALSE	FALSE	FALSE	TRUE	TRUE	FALSE	TRUE
FEN1	III	FALSE	FALSE	TRUE	FALSE	FALSE	TRUE	FALSE	TRUE	TRUE	TRUE	FALSE
FUBP3	III	TRUE	FALSE	TRUE	TRUE	TRUE	TRUE	TRUE	TRUE	TRUE	FALSE	FALSE
GAPDH	III	FALSE	FALSE	FALSE	TRUE	FALSE	FALSE	FALSE	TRUE	TRUE	TRUE	FALSE
GEMIN5	III	FALSE	TRUE	FALSE	TRUE	FALSE	TRUE	TRUE	FALSE	FALSE	TRUE	FALSE
GTF2I	III	FALSE	FALSE	FALSE	FALSE	FALSE	FALSE	FALSE	FALSE	FALSE	FALSE	FALSE
HMGA1	III	FALSE	FALSE	FALSE	FALSE	FALSE	FALSE	FALSE	FALSE	TRUE	FALSE	FALSE
HMGB1	III	FALSE	FALSE	FALSE	FALSE	FALSE	TRUE	FALSE	TRUE	TRUE	FALSE	FALSE
HNRNPC	III	FALSE	FALSE	TRUE	TRUE	TRUE	TRUE	TRUE	TRUE	TRUE	FALSE	FALSE
HNRNPM	III	FALSE	FALSE	TRUE	TRUE	TRUE	TRUE	TRUE	TRUE	TRUE	FALSE	FALSE
HNRNPR	III	FALSE	FALSE	FALSE	TRUE	TRUE	TRUE	TRUE	TRUE	TRUE	FALSE	FALSE
HP1BP3	III	FALSE	FALSE	FALSE	FALSE	FALSE	FALSE	FALSE	FALSE	TRUE	FALSE	FALSE
HSP90AA1	III	FALSE	FALSE	FALSE	FALSE	FALSE	FALSE	FALSE	FALSE	TRUE	TRUE	FALSE
HSP90AB1	III	FALSE	FALSE	TRUE	FALSE	FALSE	FALSE	FALSE	FALSE	TRUE	FALSE	TRUE
HSPA5	III	FALSE	FALSE	FALSE	FALSE	FALSE	TRUE	TRUE	TRUE	TRUE	FALSE	FALSE
HSPA8	III	FALSE	FALSE	TRUE	FALSE	FALSE	FALSE	FALSE	FALSE	TRUE	FALSE	FALSE
IF2	III	FALSE	FALSE	FALSE	TRUE	TRUE	TRUE	TRUE	TRUE	TRUE	FALSE	FALSE
ILF3	III	TRUE	FALSE	TRUE	TRUE	TRUE	TRUE	TRUE	TRUE	TRUE	TRUE	TRUE
LDHA	III	FALSE	FALSE	FALSE	FALSE	FALSE	TRUE	FALSE	TRUE	FALSE	TRUE	FALSE
MATR3	III	FALSE	TRUE	TRUE	TRUE	TRUE	TRUE	TRUE	TRUE	TRUE	TRUE	FALSE
MBNL1	III	TRUE	FALSE	FALSE	TRUE	FALSE	FALSE	FALSE	TRUE	TRUE	FALSE	FALSE
MCM5	III	FALSE	FALSE	FALSE	FALSE	FALSE	TRUE	FALSE	TRUE	TRUE	FALSE	TRUE
NACA	III	FALSE	FALSE	FALSE	FALSE	FALSE	FALSE	FALSE	FALSE	FALSE	TRUE	FALSE
NKRF	III	TRUE	FALSE	FALSE	FALSE	FALSE	FALSE	FALSE	FALSE	FALSE	FALSE	FALSE
NSUN2	III	FALSE	FALSE	FALSE	FALSE	FALSE	FALSE	FALSE	TRUE	TRUE	FALSE	FALSE
NUMA1	III	FALSE	FALSE	FALSE	FALSE	FALSE	FALSE	FALSE	FALSE	FALSE	TRUE	TRUE
NXF1	III	FALSE	FALSE	FALSE	FALSE	FALSE	TRUE	TRUE	TRUE	TRUE	FALSE	FALSE
PCBP1	III	TRUE	TRUE	TRUE	TRUE	TRUE	FALSE	FALSE	TRUE	TRUE	TRUE	FALSE
PCBP2	III	TRUE	TRUE	TRUE	TRUE	FALSE	TRUE	TRUE	FALSE	TRUE	FALSE	FALSE
PKM	III	FALSE	FALSE	FALSE	FALSE	FALSE	FALSE	FALSE	FALSE	FALSE	TRUE	FALSE
PLA	III	FALSE	FALSE	FALSE	FALSE	FALSE	FALSE	FALSE	FALSE	FALSE	FALSE	TRUE
PPIG	III	FALSE	FALSE	FALSE	FALSE	FALSE	FALSE	FALSE	FALSE	FALSE	FALSE	FALSE
PPIL4	III	FALSE	FALSE	FALSE	FALSE	FALSE	TRUE	FALSE	FALSE	FALSE	FALSE	FALSE
PRPF3	III	FALSE	FALSE	FALSE	FALSE	FALSE	FALSE	FALSE	FALSE	FALSE	FALSE	TRUE
PRPF31	III	FALSE	FALSE	FALSE	FALSE	FALSE	FALSE	FALSE	FALSE	FALSE	TRUE	FALSE
PTBP1	III	FALSE	FALSE	TRUE	TRUE	TRUE	TRUE	TRUE	TRUE	TRUE	FALSE	TRUE
QKI	III	TRUE	FALSE	FALSE	TRUE	FALSE	TRUE	TRUE	FALSE	TRUE	FALSE	FALSE
RAB1A	III	FALSE	FALSE	FALSE	FALSE	FALSE	FALSE	TRUE	FALSE	TRUE	FALSE	FALSE
RACK1	III	TRUE	FALSE	TRUE	FALSE	FALSE	TRUE	TRUE	TRUE	TRUE	FALSE	TRUE
RALY	III	FALSE	TRUE	FALSE	TRUE	TRUE	TRUE	TRUE	TRUE	TRUE	FALSE	FALSE
RAN	III	TRUE	FALSE	TRUE	FALSE	FALSE	TRUE	TRUE	TRUE	TRUE	FALSE	TRUE
RAVER1	III	FALSE	FALSE	FALSE	FALSE	FALSE	TRUE	FALSE	TRUE	FALSE	FALSE	FALSE
RBFOX2	III	TRUE	FALSE	FALSE	FALSE	TRUE	FALSE	FALSE	FALSE	FALSE	FALSE	FALSE
RBM12B	III	FALSE	FALSE	TRUE	FALSE	FALSE	TRUE	FALSE	TRUE	TRUE	TRUE	TRUE
RBM26	III	FALSE	FALSE	FALSE	FALSE	FALSE	FALSE	FALSE	FALSE	TRUE	FALSE	TRUE
RBM27	III	FALSE	FALSE	FALSE	FALSE	FALSE	FALSE	FALSE	FALSE	FALSE	FALSE	TRUE
RBM28	III	FALSE	FALSE	FALSE	FALSE	FALSE	FALSE	FALSE	FALSE	FALSE	FALSE	TRUE
RCC2	III	FALSE	FALSE	FALSE	FALSE	FALSE	FALSE	FALSE	FALSE	TRUE	TRUE	TRUE
RNMT	III	FALSE	FALSE	FALSE	FALSE	FALSE	TRUE	FALSE	TRUE	TRUE	FALSE	FALSE
RPA1	III	FALSE	FALSE	TRUE	FALSE	FALSE	TRUE	FALSE	TRUE	TRUE	FALSE	TRUE
RRP12	III	FALSE	FALSE	FALSE	FALSE	FALSE	FALSE	FALSE	FALSE	FALSE	FALSE	FALSE
SAFB2	III	TRUE	FALSE	TRUE	TRUE	TRUE	TRUE	TRUE	TRUE	TRUE	FALSE	TRUE
SCAMP3	III	FALSE	FALSE	FALSE	FALSE	FALSE	FALSE	FALSE	FALSE	FALSE	FALSE	FALSE
SERPINH1	III	FALSE	FALSE	FALSE	FALSE	FALSE	FALSE	FALSE	FALSE	FALSE	FALSE	TRUE
SLC1A5	III	FALSE	FALSE	FALSE	FALSE	FALSE	FALSE	FALSE	FALSE	FALSE	FALSE	FALSE
SLC25A6	III	FALSE	FALSE	FALSE	FALSE	FALSE	FALSE	FALSE	FALSE	FALSE	TRUE	TRUE
SMARCA4	III	FALSE	FALSE	FALSE	FALSE	FALSE	FALSE	FALSE	FALSE	FALSE	FALSE	FALSE
SNRPA	III	FALSE	FALSE	FALSE	FALSE	FALSE	FALSE	FALSE	FALSE	TRUE	TRUE	FALSE
SRP14	III	TRUE	FALSE	FALSE	FALSE	FALSE	FALSE	FALSE	FALSE	FALSE	TRUE	FALSE
SRRM2	III	FALSE	FALSE	FALSE	FALSE	FALSE	FALSE	FALSE	FALSE	TRUE	TRUE	FALSE
SRSF11	III	FALSE	FALSE	FALSE	FALSE	FALSE	FALSE	FALSE	FALSE	FALSE	TRUE	FALSE
SSB	III	FALSE	FALSE	TRUE	FALSE	FALSE	FALSE	FALSE	FALSE	TRUE	FALSE	FALSE
STRBP	III	FALSE	FALSE	FALSE	FALSE	FALSE	FALSE	FALSE	TRUE	FALSE	TRUE	FALSE
SUMO3	III	FALSE	FALSE	FALSE	FALSE	FALSE	FALSE	FALSE	FALSE	TRUE	FALSE	FALSE
TARDBP	III	TRUE	FALSE	TRUE	TRUE	TRUE	TRUE	TRUE	TRUE	TRUE	FALSE	TRUE
TCP1	III	FALSE	FALSE	FALSE	FALSE	TRUE	FALSE	FALSE	FALSE	TRUE	FALSE	FALSE
TECR	III	FALSE	FALSE	FALSE	FALSE	FALSE	FALSE	FALSE	FALSE	FALSE	TRUE	TRUE
TKT	III	FALSE	FALSE	TRUE	FALSE	FALSE	TRUE	FALSE	TRUE	TRUE	FALSE	TRUE
TOP1	III	FALSE	FALSE	TRUE	FALSE	TRUE	TRUE	TRUE	TRUE	TRUE	FALSE	FALSE
TOP2A	III	FALSE	FALSE	TRUE	FALSE	FALSE	TRUE	FALSE	FALSE	TRUE	TRUE	TRUE
TOP2B	III	FALSE	FALSE	FALSE	FALSE	FALSE	TRUE	FALSE	FALSE	TRUE	TRUE	TRUE
TRMT1	III	FALSE	FALSE	FALSE	FALSE	FALSE	FALSE	FALSE	TRUE	FALSE	FALSE	FALSE
UTP15	III	FALSE	FALSE	FALSE	FALSE	FALSE	FALSE	FALSE	FALSE	FALSE	FALSE	TRUE
WDR75	III	FALSE	FALSE	FALSE	FALSE	FALSE	FALSE	FALSE	FALSE	FALSE	TRUE	TRUE
XRCC6	III	FALSE	FALSE	TRUE	TRUE	TRUE	TRUE	TRUE	TRUE	TRUE	TRUE	FALSE

YLPM1	III	FALSE	FALSE	TRUE	FALSE	FALSE	TRUE	TRUE	TRUE	TRUE	TRUE	TRUE
ZFR	III	FALSE	FALSE	TRUE	FALSE	FALSE	TRUE	TRUE	TRUE	FALSE	TRUE	TRUE
ZNF638	III	FALSE	FALSE	TRUE	FALSE	FALSE	TRUE	TRUE	TRUE	FALSE	TRUE	FALSE
ACIN1	IV	FALSE	FALSE	FALSE	FALSE	FALSE	TRUE	FALSE	TRUE	TRUE	FALSE	FALSE
DDX24	IV	FALSE	FALSE	FALSE	FALSE	FALSE	FALSE	FALSE	FALSE	TRUE	FALSE	FALSE
DDX27	IV	FALSE	FALSE	FALSE	FALSE	FALSE	FALSE	FALSE	FALSE	FALSE	FALSE	TRUE
DHX30	IV	TRUE	FALSE	FALSE	TRUE	FALSE	FALSE	FALSE	TRUE	TRUE	TRUE	TRUE
DHX38	IV	FALSE	FALSE	FALSE	FALSE	FALSE	FALSE	FALSE	FALSE	FALSE	TRUE	TRUE
EIF3H	IV	TRUE	FALSE	FALSE	FALSE	FALSE	FALSE	FALSE	FALSE	TRUE	FALSE	FALSE
ESRP2	IV	FALSE	FALSE	FALSE	FALSE	TRUE	FALSE	FALSE	TRUE	FALSE	FALSE	FALSE
FAM98B	IV	FALSE	FALSE	FALSE	FALSE	FALSE	FALSE	FALSE	FALSE	TRUE	FALSE	FALSE
GIGYF2	IV	TRUE	TRUE	TRUE	FALSE	FALSE	TRUE	TRUE	FALSE	FALSE	FALSE	FALSE
LARP7	IV	FALSE	FALSE	FALSE	FALSE	TRUE	FALSE	FALSE	FALSE	FALSE	FALSE	FALSE
LDHB	IV	FALSE	FALSE	FALSE	FALSE	FALSE	FALSE	FALSE	FALSE	TRUE	FALSE	TRUE
MYBBP1A	IV	FALSE	FALSE	FALSE	FALSE	FALSE	FALSE	FALSE	FALSE	FALSE	FALSE	TRUE
NAT10	IV	FALSE	FALSE	FALSE	FALSE	FALSE	FALSE	FALSE	FALSE	TRUE	FALSE	TRUE
NOP2	IV	FALSE	FALSE	FALSE	FALSE	FALSE	FALSE	FALSE	FALSE	FALSE	FALSE	TRUE
NPM1	IV	FALSE	FALSE	TRUE	TRUE	FALSE	TRUE	FALSE	TRUE	TRUE	FALSE	TRUE
PA2G4	IV	FALSE	FALSE	FALSE	TRUE	FALSE	TRUE	TRUE	TRUE	TRUE	FALSE	FALSE
PARP12	IV	TRUE	FALSE	FALSE	TRUE	FALSE	FALSE	FALSE	FALSE	FALSE	FALSE	FALSE
PNN	IV	FALSE	FALSE	TRUE	FALSE	FALSE	TRUE	FALSE	TRUE	TRUE	FALSE	FALSE
PNPT1	IV	TRUE	FALSE	FALSE	FALSE	FALSE	FALSE	FALSE	FALSE	TRUE	FALSE	FALSE
PTBP3	IV	TRUE	FALSE	FALSE	TRUE	TRUE	TRUE	FALSE	FALSE	FALSE	FALSE	FALSE
RBM33	IV	FALSE	FALSE	FALSE	FALSE	FALSE	FALSE	FALSE	FALSE	FALSE	TRUE	TRUE
RBM47	IV	TRUE	FALSE	FALSE	TRUE	TRUE	TRUE	TRUE	TRUE	TRUE	FALSE	FALSE
RC3H1	IV	TRUE	TRUE	FALSE	FALSE	FALSE	FALSE	FALSE	FALSE	FALSE	FALSE	FALSE
RNPS1	IV	FALSE	FALSE	FALSE	FALSE	FALSE	FALSE	FALSE	FALSE	TRUE	FALSE	FALSE
RTCB	IV	FALSE	FALSE	TRUE	TRUE	TRUE	TRUE	TRUE	TRUE	TRUE	FALSE	FALSE
SAP18	IV	FALSE	FALSE	FALSE	FALSE	FALSE	FALSE	FALSE	TRUE	FALSE	FALSE	FALSE
SNRPD1	IV	FALSE	FALSE	FALSE	FALSE	FALSE	TRUE	FALSE	TRUE	TRUE	FALSE	TRUE
TPR	IV	FALSE	FALSE	FALSE	FALSE	FALSE	TRUE	FALSE	TRUE	TRUE	FALSE	TRUE
YTHDC1	IV	FALSE	FALSE	FALSE	FALSE	FALSE	TRUE	FALSE	FALSE	FALSE	FALSE	FALSE
ZC3H11A	IV	TRUE	FALSE	FALSE	FALSE	FALSE	TRUE	FALSE	TRUE	TRUE	TRUE	TRUE
ZC3H14	IV	FALSE	FALSE	FALSE	FALSE	FALSE	TRUE	FALSE	TRUE	FALSE	FALSE	FALSE
ALYREF	V	FALSE	FALSE	FALSE	TRUE	TRUE	TRUE	TRUE	TRUE	TRUE	FALSE	FALSE
API5	V	FALSE	FALSE	FALSE	FALSE	FALSE	TRUE	FALSE	TRUE	FALSE	FALSE	FALSE
CHTOP	V	FALSE	FALSE	TRUE	TRUE	TRUE	TRUE	TRUE	TRUE	TRUE	FALSE	FALSE
DDX1	V	TRUE	FALSE	TRUE	FALSE	TRUE	TRUE	TRUE	TRUE	TRUE	FALSE	TRUE
DDX39B	V	FALSE	FALSE	FALSE	FALSE	FALSE	TRUE	TRUE	TRUE	TRUE	FALSE	FALSE
DDX54	V	FALSE	FALSE	FALSE	FALSE	TRUE	FALSE	FALSE	FALSE	FALSE	FALSE	TRUE
EIF4A3	V	TRUE	FALSE	FALSE	FALSE	FALSE	TRUE	TRUE	TRUE	TRUE	FALSE	FALSE
FTSJ3	V	FALSE	FALSE	FALSE	FALSE	FALSE	FALSE	FALSE	FALSE	FALSE	TRUE	TRUE
GNL3	V	FALSE	FALSE	FALSE	FALSE	TRUE	FALSE	FALSE	FALSE	TRUE	FALSE	FALSE
GTPBP4	V	FALSE	FALSE	FALSE	FALSE	TRUE	FALSE	FALSE	FALSE	TRUE	FALSE	FALSE
HELZ2	V	FALSE	FALSE	FALSE	TRUE	TRUE	FALSE	FALSE	FALSE	FALSE	FALSE	FALSE
KIF1C	V	FALSE	FALSE	FALSE	FALSE	FALSE	TRUE	TRUE	FALSE	FALSE	TRUE	FALSE
KPNA2	V	TRUE	FALSE	TRUE	FALSE	FALSE	TRUE	FALSE	FALSE	TRUE	FALSE	FALSE
MAP4	V	FALSE	FALSE	TRUE	TRUE	TRUE	TRUE	TRUE	FALSE	TRUE	TRUE	TRUE
MKI67	V	FALSE	FALSE	TRUE	FALSE	FALSE	TRUE	FALSE	FALSE	FALSE	TRUE	FALSE
MKRN2	V	TRUE	FALSE	FALSE	FALSE	FALSE	FALSE	FALSE	FALSE	FALSE	FALSE	FALSE
MSI2	V	TRUE	FALSE	FALSE	FALSE	FALSE	FALSE	FALSE	FALSE	TRUE	FALSE	FALSE
MTREX	V	FALSE	FALSE	FALSE	FALSE	FALSE	TRUE	FALSE	FALSE	TRUE	FALSE	FALSE
NFX1	V	TRUE	FALSE	FALSE	FALSE	FALSE	FALSE	FALSE	FALSE	FALSE	TRUE	FALSE
NOL12	V	FALSE	TRUE	FALSE	FALSE	FALSE	FALSE	FALSE	FALSE	FALSE	FALSE	FALSE
PLEC	V	FALSE	FALSE	FALSE	FALSE	FALSE	FALSE	FALSE	TRUE	FALSE	TRUE	TRUE
POLDIP3	V	FALSE	FALSE	TRUE	FALSE	FALSE	TRUE	FALSE	TRUE	TRUE	FALSE	FALSE
PRRC2B	V	TRUE	TRUE	FALSE	FALSE	FALSE	FALSE	FALSE	FALSE	FALSE	TRUE	FALSE
PTCD3	V	FALSE	FALSE	FALSE	FALSE	FALSE	FALSE	FALSE	FALSE	TRUE	FALSE	FALSE
SARNP	V	FALSE	FALSE	FALSE	FALSE	FALSE	FALSE	FALSE	FALSE	TRUE	FALSE	FALSE
SLIRP	V	FALSE	FALSE	FALSE	TRUE	TRUE	FALSE	FALSE	FALSE	TRUE	FALSE	FALSE
SPATS2L	V	FALSE	FALSE	TRUE	FALSE	FALSE	TRUE	TRUE	FALSE	FALSE	FALSE	FALSE
SYNCRIP	V	TRUE	TRUE	FALSE	TRUE	TRUE	TRUE	TRUE	TRUE	TRUE	FALSE	FALSE
TOP3B	V	TRUE	FALSE	FALSE	FALSE	FALSE	FALSE	TRUE	FALSE	FALSE	TRUE	FALSE
TRIM56	V	TRUE	FALSE	FALSE	FALSE	FALSE	FALSE	TRUE	TRUE	FALSE	FALSE	FALSE
UPF3B	V	FALSE	TRUE	FALSE	FALSE	FALSE	FALSE	FALSE	FALSE	FALSE	FALSE	FALSE
AGO2	VI	TRUE	TRUE	TRUE	FALSE	FALSE	FALSE	TRUE	TRUE	FALSE	FALSE	FALSE
AGO3	VI	TRUE	TRUE	FALSE	FALSE	FALSE	FALSE	FALSE	FALSE	FALSE	FALSE	FALSE
ATXN2	VI	TRUE	FALSE	TRUE	TRUE	TRUE	TRUE	TRUE	FALSE	FALSE	FALSE	FALSE
ATXN2L	VI	TRUE	FALSE	TRUE	TRUE	TRUE	TRUE	TRUE	TRUE	TRUE	FALSE	TRUE
CASC3	VI	TRUE	TRUE	FALSE	FALSE	FALSE	FALSE	FALSE	FALSE	FALSE	FALSE	FALSE
CNBP	VI	FALSE	FALSE	TRUE	TRUE	TRUE	FALSE	FALSE	FALSE	FALSE	FALSE	FALSE
CPEB4	VI	TRUE	TRUE	FALSE	FALSE	FALSE	FALSE	FALSE	FALSE	FALSE	FALSE	FALSE
CSDE1	VI	TRUE	FALSE	TRUE	TRUE	TRUE	TRUE	TRUE	TRUE	TRUE	FALSE	FALSE
DHX57	VI	TRUE	FALSE	TRUE	FALSE	FALSE	TRUE	TRUE	FALSE	FALSE	TRUE	FALSE
EDF1	VI	FALSE	FALSE	FALSE	TRUE	FALSE	FALSE	FALSE	FALSE	FALSE	FALSE	FALSE
EIF2S1	VI	FALSE	FALSE	TRUE	FALSE	FALSE	TRUE	TRUE	FALSE	TRUE	FALSE	FALSE
EIF3G	VI	TRUE	FALSE	TRUE	TRUE	FALSE	TRUE	FALSE	FALSE	FALSE	FALSE	TRUE
EIF4A1	VI	TRUE	FALSE	TRUE	TRUE	FALSE	TRUE	TRUE	TRUE	TRUE	TRUE	FALSE
EIF4G1	VI	TRUE	FALSE	TRUE	TRUE	TRUE	TRUE	TRUE	TRUE	TRUE	FALSE	FALSE
EIF4H	VI	TRUE	FALSE	TRUE	TRUE	TRUE	TRUE	TRUE	TRUE	TRUE	FALSE	FALSE
LARP4	VI	TRUE	FALSE	TRUE	TRUE	TRUE	TRUE	TRUE	TRUE	FALSE	FALSE	FALSE
MEX3D	VI	TRUE	FALSE	FALSE	FALSE	FALSE	FALSE	FALSE	FALSE	FALSE	FALSE	FALSE
NUFIP2	VI	TRUE	FALSE	TRUE	TRUE	FALSE	TRUE	TRUE	FALSE	TRUE	FALSE	FALSE
OASL	VI	TRUE	FALSE	FALSE	FALSE	FALSE	FALSE	FALSE	FALSE	FALSE	FALSE	FALSE
OTUD4	VI	TRUE	FALSE	FALSE	FALSE	FALSE	FALSE	FALSE	FALSE	FALSE	FALSE	FALSE
PABPC1	VI	TRUE	FALSE	TRUE	TRUE	TRUE	TRUE	TRUE	TRUE	TRUE	FALSE	FALSE
PRRC2A	VI	TRUE	FALSE	TRUE	FALSE	TRUE	TRUE	TRUE	TRUE	TRUE	TRUE	FALSE
PUM1	VI	TRUE	TRUE	FALSE	TRUE	TRUE	TRUE	TRUE	TRUE	FALSE	FALSE	FALSE
PUM2	VI	TRUE	FALSE	TRUE	TRUE	FALSE	FALSE	TRUE	FALSE	FALSE	FALSE	FALSE
RBMS1	VI	TRUE	FALSE	TRUE	TRUE	FALSE	TRUE	FALSE	FALSE	FALSE	FALSE	FALSE
STAU1	VI	FALSE	FALSE	FALSE	FALSE	FALSE	TRUE	TRUE	FALSE	FALSE	TRUE	FALSE
TDRD3	VI	TRUE	FALSE	FALSE	FALSE	FALSE	FALSE	FALSE	FALSE	FALSE	FALSE	FALSE
YTHDF2	VI	TRUE	TRUE	TRUE	FALSE	FALSE	TRUE	TRUE	TRUE	FALSE	FALSE	TRUE
YTHDF3	VI	TRUE	FALSE	FALSE	FALSE	FALSE	TRUE	TRUE	FALSE	FALSE	FALSE	TRUE
ZC3H7B	VI	FALSE	FALSE	TRUE	FALSE	FALSE	TRUE	FALSE	FALSE	FALSE	FALSE	FALSE
CAPRIN1	VII	TRUE	FALSE	TRUE	TRUE	FALSE	TRUE	TRUE	TRUE	TRUE	FALSE	FALSE
DDX3X	VII	TRUE	FALSE	TRUE	TRUE	TRUE	TRUE	TRUE	TRUE	TRUE	TRUE	TRUE
EIF3A	VII	TRUE	FALSE	TRUE	TRUE	TRUE	TRUE	TRUE	TRUE	TRUE	TRUE	TRUE
EIF3CL	VII	FALSE	FALSE	FALSE	FALSE	FALSE	FALSE	TRUE	FALSE	FALSE	FALSE	FALSE
EIF3D	VII	TRUE	FALSE	TRUE	TRUE	TRUE	TRUE	FALSE	TRUE	FALSE	FALSE	FALSE
EIF3L	VII	FALSE	FALSE	FALSE	FALSE	FALSE	TRUE	TRUE	TRUE	TRUE	FALSE	FALSE
EIF4B	VII	TRUE	FALSE	TRUE	TRUE	TRUE	TRUE	TRUE	TRUE	FALSE	FALSE	FALSE
EIF4G2	VII	TRUE	FALSE	FALSE	FALSE	FALSE	TRUE	TRUE	FALSE	TRUE	FALSE	FALSE
FAM120A	VII	TRUE	FALSE	TRUE	TRUE	TRUE	TRUE	TRUE	TRUE	TRUE	FALSE	FALSE
FAM120C	VII	TRUE	FALSE	FALSE	TRUE	FALSE	FALSE	FALSE	FALSE	FALSE	FALSE	FALSE
FMR1	VII	TRUE	TRUE	FALSE	TRUE	FALSE	TRUE	TRUE	FALSE	FALSE	FALSE	FALSE
FXR1	VII	TRUE	FALSE	TRUE	TRUE	TRUE	TRUE	TRUE	TRUE	TRUE	FALSE	FALSE
FXR2	VII	TRUE	FALSE	TRUE	TRUE	TRUE	TRUE	TRUE	FALSE	FALSE	FALSE	FALSE
G3BP1	VII	TRUE	FALSE	TRUE	TRUE	TRUE	TRUE	TRUE	TRUE	TRUE	FALSE	FALSE
G3BP2	VII	TRUE	FALSE	FALSE	TRUE	TRUE	TRUE	TRUE	TRUE	TRUE	FALSE	FALSE
HDLBP	VII	FALSE	FALSE	TRUE	TRUE	TRUE	TRUE	TRUE	TRUE	TRUE	TRUE	TRUE
IGF2BP1	VII	TRUE	FALSE	TRUE	FALSE	FALSE	TRUE	TRUE	TRUE	TRUE	FALSE	FALSE
IGF2BP2	VII	TRUE	FALSE	TRUE	TRUE	FALSE	TRUE	TRUE	FALSE	FALSE	FALSE	FALSE
IGF2BP3	VII	TRUE	FALSE	TRUE	TRUE	TRUE	TRUE	TRUE	TRUE	TRUE	FALSE	FALSE
LARP1	VII	FALSE	FALSE	TRUE	TRUE	TRUE	TRUE	TRUE	TRUE	TRUE	TRUE	TRUE
LARP4B	VII	TRUE	FALSE	TRUE	TRUE	TRUE	TRUE	TRUE	FALSE	FALSE	FALSE	FALSE
LSM14A	VII	TRUE	TRUE	TRUE	TRUE	FALSE	TRUE	TRUE	FALSE	FALSE	FALSE	FALSE
LSM14B	VII	TRUE	TRUE	FALSE	FALSE	FALSE	TRUE	TRUE	FALSE	FALSE	FALSE	FALSE
MOV10	VII	TRUE	TRUE	TRUE	TRUE	TRUE	TRUE	TRUE	TRUE	TRUE	FALSE	TRUE
PABPC4	VII	TRUE	FALSE	TRUE	TRUE	TRUE	TRUE	TRUE	TRUE	TRUE	FALSE	TRUE
PRRC2C	VII	TRUE	FALSE	TRUE	FALSE	TRUE	TRUE	TRUE	FALSE	TRUE	TRUE	TRUE
PURA	VII	FALSE	FALSE	TRUE	TRUE	TRUE	TRUE	TRUE	FALSE	FALSE	FALSE	FALSE

PURB	VII	FALSE	FALSE	TRUE	TRUE	FALSE	TRUE	TRUE	FALSE	FALSE	FALSE	FALSE
SERBP1	VII	TRUE	FALSE	TRUE	TRUE	TRUE	TRUE	TRUE	TRUE	TRUE	FALSE	FALSE
SND1	VII	TRUE	FALSE	TRUE	TRUE	TRUE	TRUE	TRUE	TRUE	TRUE	TRUE	TRUE
STAU2	VII	TRUE	TRUE	FALSE	FALSE	FALSE	FALSE	FALSE	FALSE	TRUE	FALSE	FALSE
UBAP2	VII	TRUE	TRUE	FALSE	TRUE	TRUE	TRUE	TRUE	FALSE	FALSE	FALSE	FALSE
UBAP2L	VII	TRUE	FALSE	TRUE	TRUE	TRUE	TRUE	TRUE	TRUE	TRUE	FALSE	FALSE
UPF1	VII	TRUE	FALSE	TRUE	TRUE	TRUE	TRUE	TRUE	TRUE	TRUE	TRUE	TRUE
USP10	VII	TRUE	FALSE	TRUE	FALSE	TRUE	TRUE	TRUE	FALSE	TRUE	TRUE	TRUE
YBX1	VII	FALSE	TRUE	TRUE	TRUE	TRUE	TRUE	TRUE	TRUE	TRUE	FALSE	FALSE
YBX3	VII	TRUE	FALSE	TRUE	TRUE	TRUE	TRUE	TRUE	FALSE	TRUE	FALSE	FALSE
YTHDC2	VII	FALSE	FALSE	TRUE	FALSE	FALSE	FALSE	TRUE	FALSE	FALSE	FALSE	FALSE
YTHDF1	VII	TRUE	FALSE	FALSE	FALSE	FALSE	FALSE	FALSE	FALSE	FALSE	FALSE	FALSE
ZC3HAV1	VII	TRUE	FALSE	TRUE	TRUE	TRUE	TRUE	TRUE	TRUE	TRUE	TRUE	TRUE

Table 2.4 Stress granules, P-bodies, and viral proteins in mRNPs

Name of GO term	Contribution to									
	0 min	15 min	30 min	45 min	60 min	90 min	120 min	180 min	240 min	300 min
transcription elongation factor complex	16.54	8.058	2.196	-1.575	-3.733	-4.865	-3.969	-2.923	-5.747	-3.986
nucleotidyltransferase activity	12.88	6.222	1.642	-1.272	-2.895	-3.556	-2.538	-1.136	-3.779	-5.567
mRNA cleavage and polyadenylation specificity factor complex	12.62	6.859	2.678	-0.214	-2.084	-3.689	-3.722	-3.235	-4.565	-4.653
kinetochore	12.56	6.382	2.054	-0.796	-2.5	-3.609	-3.2	-2.629	-4.601	-3.657
transporter activity	12.04	7.142	3.517	0.914	-0.891	-2.884	-3.746	-5.109	-6.851	-4.133
mRNA cleavage factor complex	12.01	6.664	2.766	0.043	-1.748	-3.385	-3.588	-3.446	-4.773	-4.541
nucleosome binding	11.61	6.805	3.282	0.785	-0.918	-2.734	-3.479	-4.82	-6.691	-3.845
pre-mRNA cleavage required for polyadenylation	10.22	5.624	2.278	-0.049	-1.564	-2.886	-2.937	-2.544	-3.708	-4.431
viral RNA genome replication	9.986	5.421	2.226	0.122	-1.147	-2.05	-1.948	-2.325	-4.963	-5.322
transferase complex, transferring phosphorus-containing groups	9.877	2.657	-1.856	-4.264	-5.104	-3.908	-1.287	1.253	-1.227	3.86
transcription by RNA polymerase I	9.5	4.799	1.651	-0.297	-1.36	-1.893	-1.679	-2.773	-5.865	-2.084
RNA polymerase II complex binding	9.385	5.659	2.836	0.753	-0.739	-2.46	-3.192	-3.898	-4.748	-3.597
mRNA 3'-end processing	9.311	5.143	2.128	0.046	-1.301	-2.476	-2.568	-2.514	-3.841	-3.929
mRNA polyadenylation	9.24	4.668	1.437	-0.711	-2.011	-2.874	-2.531	-1.762	-2.844	-2.613
regulation of RNA export from nucleus	8.998	4.726	1.723	-0.262	-1.455	-2.253	-2	-1.728	-3.55	-4.198
actin cytoskeleton	8.871	6.203	4.086	2.406	1.067	-0.928	-2.441	-5.187	-7.513	-6.563
chromosome, centromeric region	8.822	4.795	1.944	0.033	-1.151	-2.07	-2.047	-2.237	-4.094	-3.994
mRNA cleavage	8.692	3.669	0.253	-1.876	-3.004	-3.261	-2.205	-0.432	-1.304	-0.532
transferase activity, transferring phosphorus-containing groups	8.544	4.928	2.271	0.396	-0.857	-2.055	-2.283	-2.391	-3.743	-4.809
cytoplasmic vesicle membrane	8.41	5.842	3.694	1.901	0.409	-1.867	-3.457	-5.357	-5.824	-3.752
fibrillar center	8.346	4.648	1.998	0.179	-0.999	-2.087	-2.354	-2.976	-4.386	-2.37
regulation of circadian rhythm	8.16	5.523	3.406	1.73	0.419	-1.366	-2.417	-3.675	-5.069	-6.71
transcription elongation from RNA polymerase II promoter	8.123	4.472	1.843	0.032	-1.142	-2.203	-2.385	-2.657	-3.773	-2.311
positive regulation of RNA splicing	8.043	4.143	1.477	-0.22	-1.184	-1.723	-1.481	-1.816	-4.092	-3.147
mRNA cis splicing, via spliceosome	7.84	4.603	2.261	0.633	-0.446	-1.515	-1.879	-2.749	-4.586	-4.163
ion transmembrane transport	7.729	4.939	2.724	0.993	-0.336	-2.076	-2.997	-3.736	-4.006	-3.235
positive regulation of transcription by RNA polymerase I	7.432	4.468	2.332	0.844	-0.155	-1.232	-1.783	-3.25	-5.255	-3.399
U2-type prespliceosome	7.368	3.733	1.218	-0.405	-1.343	-1.877	-1.576	-1.405	-3.014	-2.698
pre-mRNA binding	7.357	4.363	2.206	0.714	-0.27	-1.241	-1.591	-2.55	-4.548	-4.44
lysosome	7.279	5.799	4.207	2.577	0.976	-1.93	-4.172	-6.069	-5.006	-3.661
mRNA splice site selection	7.243	4.107	1.855	0.305	-0.702	-1.643	-1.887	-2.48	-3.913	-2.884
integral component of membrane	7.225	4.759	2.857	1.407	0.311	-1.154	-2.093	-3.691	-5.212	-4.409
ion transport	7.183	4.644	2.593	0.96	-0.318	-2.041	-2.976	-3.617	-3.602	-2.825
monocarboxylic acid metabolic process	7.173	6.224	4.782	3.036	1.151	-2.489	-5.284	-6.798	-4.059	-3.736
catalytic activity, acting on a tRNA	7.158	4.742	2.902	1.512	0.462	-0.987	-2.036	-4.135	-5.91	-3.707
negative regulation of cell population proliferation	7.085	5.483	3.981	2.578	1.278	-1.012	-2.882	-5.336	-6.068	-5.107
tRNA binding	7.034	5.323	3.839	2.534	1.371	-0.656	-2.427	-5.403	-6.926	-4.689
animal organ morphogenesis	7.01	5.242	3.623	2.162	0.86	-1.264	-2.774	-4.274	-4.716	-5.869
chromatin DNA binding	6.959	5.317	3.867	2.571	1.393	-0.711	-2.587	-5.71	-7.055	-4.044
positive regulation of chromosome organization	6.831	4.531	2.718	1.309	0.232	-1.195	-2.016	-3.077	-4.269	-5.063
cell cycle G2/M phase transition	6.809	3.507	1.302	-0.057	-0.793	-1.147	-0.99	-1.85	-4.358	-2.421
RNA polymerase binding	6.793	3.295	0.881	-0.67	-1.554	-2.006	-1.618	-1.153	-2.313	-1.653
mRNA processing	6.778	4.539	2.758	1.359	0.27	-1.225	-2.148	-3.375	-4.442	-4.514
positive regulation of mRNA splicing, via spliceosome	6.73	3.937	1.925	0.532	-0.384	-1.275	-1.569	-2.327	-3.966	-3.603
nucleobase-containing small molecule metabolic process	6.729	5.251	3.67	2.066	0.509	-2.24	-4.234	-5.435	-3.752	-2.565
negative regulation of transferase activity	6.72	5.14	3.533	1.961	0.476	-2.072	-3.872	-4.969	-3.705	-3.211
protein-containing complex disassembly	6.665	2.242	-0.74	-2.558	-3.466	-3.426	-2.112	0.483	0.811	2.103
regulation of nucleocytoplasmic transport	6.657	3.714	1.61	0.176	-0.739	-1.535	-1.65	-1.983	-3.323	-2.928
nucleosome organization	6.613	4.015	2.075	0.666	-0.326	-1.445	-1.939	-2.671	-3.758	-3.229
carboxylic acid metabolic process	6.598	5.947	4.767	3.242	1.532	-1.903	-4.687	-6.651	-4.57	-4.274
anatomical structure formation involved in morphogenesis	6.529	4.024	2.081	0.603	-0.496	-1.854	-2.506	-3.015	-3.244	-2.121
chromatin remodeling	6.472	4.049	2.252	0.945	0.01	-1.147	-1.871	-3.388	-4.818	-2.502
rhythmic process	6.455	4.461	2.818	1.477	0.394	-1.167	-2.154	-3.273	-4.115	-4.897
positive regulation of telomere maintenance	6.432	4.645	3.147	1.89	0.829	-0.849	-2.129	-4.056	-5.244	-4.666
protein domain specific binding	6.365	4.467	2.825	1.424	0.246	-1.506	-2.577	-3.326	-3.423	-4.496
protein-DNA complex subunit organization	6.303	3.55	1.592	0.263	-0.586	-1.349	-1.538	-2.155	-3.582	-2.497
intrinsic apoptotic signaling pathway by p53 class mediator	6.245	4.263	2.648	1.351	0.323	-1.1	-1.934	-2.817	-3.741	-5.241
rRNA transcription	6.213	3.033	1.018	-0.121	-0.639	-0.659	-0.407	-1.842	-5.059	-1.538
RNA 3'-end processing	6.208	3.984	2.254	0.934	-0.052	-1.289	-1.921	-2.628	-3.505	-3.986
protein-macromolecule adaptor activity	6.203	3.397	1.358	-0.071	-1.029	-2.005	-2.582	-2.813	-3.129	0.433
lysosomal membrane	6.189	4.802	3.37	1.944	0.57	-1.875	-3.731	-5.237	-4.072	-1.961
transmembrane transport	6.149	4.494	2.956	1.556	0.311	-1.674	-2.965	-3.713	-3.198	-3.915
regulation of intracellular transport	6.143	3.523	1.594	0.228	-0.688	-1.574	-1.754	-1.811	-2.635	-3.027
nuclear matrix	6.108	3.929	2.252	0.986	0.051	-1.106	-1.705	-2.517	-3.66	-4.338
gland development	6.08	4.773	3.559	2.441	1.421	-0.33	-1.719	-3.65	-5.144	-7.431
spindle	6.078	3.642	1.767	0.358	-0.673	-1.902	-2.434	-2.732	-2.753	-1.351
regulation of transport	6.074	3.343	1.374	0.018	-0.859	-1.641	-1.753	-1.89	-2.733	-1.934
chromatin binding	6.039	2.902	0.8	-0.492	-1.178	-1.42	-1.066	-1.19	-2.927	-1.469
forebrain development	5.983	3.388	1.578	0.386	-0.336	-0.881	-1.491	-1.489	-3.53	-3.499
response to light stimulus	5.832	3.831	2.3	1.147	0.286	-0.845	-1.567	-2.888	-4.284	-3.813
membrane-bounded organelle	5.813	4.188	2.885	1.841	0.999	-0.276	-1.263	-3.141	-5.107	-5.939
nucleobase-containing compound metabolic process	5.791	3.837	2.295	1.091	0.16	-1.108	-1.892	-2.962	-3.818	-3.395
negative regulation of catalytic activity	5.75	3.915	2.337	0.994	-0.134	-1.823	-2.871	-3.536	-2.951	-1.68
RNA processing	5.734	4.116	2.753	1.609	0.65	-0.828	-1.884	-3.3	-4.249	-4.601
endomembrane system organization	5.728	5.019	4.024	2.843	1.564	-0.988	-3.152	-5.339	-4.914	-4.785
RNA polymerase II cis-regulatory region sequence-specific DNA binding	5.725	3.738	2.26	1.18	0.398	-0.602	-1.28	-2.843	-4.656	-3.919
double-strand break repair via homologous recombination	5.724	3.745	2.241	1.113	0.274	-0.838	-1.578	-3.005	-4.384	-3.293
purine ribonucleotide metabolic process	5.716	4.777	3.554	2.168	0.72	-2.018	-4.118	-5.392	-3.378	-2.028
Golgi membrane	5.67	5.913	5.22	3.886	2.171	-1.546	-4.588	-6.189	-3.56	-6.976
cellular process	5.655	3.917	2.539	1.454	0.598	-0.633	-1.507	-3.016	-4.461	-4.547
intracellular membrane-bounded organelle	5.642	3.766	2.339	1.272	0.484	-0.532	-1.174	-2.472	-4.255	-5.07
chromosomal region	5.634	2.67	0.654	-0.616	-1.318	-1.628	-1.292	-1.09	-2.202	-0.812
protein-DNA complex assembly	5.62	3.683	2.237	1.171	0.388	-0.65	-1.398	-3.085	-4.753	-3.213
basal RNA polymerase II transcription machinery binding	5.607	2.977	1.062	-0.269	-1.131	-1.862	-1.837	-1.391	-1.659	-1.497
ubiquitin-like protein ligase binding	5.588	3.902	2.509	1.362	0.419	-0.998	-1.986	-3.291	-4.008	-3.496
RNA metabolic process	5.572	3.555	2.015	0.861	0.013	-1.043	-1.619	-2.49	-3.515	-3.348
nuclear periphery	5.543	3.709	2.259	1.13	0.264	-0.88	-1.532	-2.372	-3.456	-4.666
response to bacterium	5.542	3.118	1.422	0.297	-0.395	-0.955	-1.047	-1.668	-3.339	-2.976
circadian rhythm	5.524	3.78	2.38	1.268	0.394	-0.826	-1.595	-2.646	-3.724	-4.555
protein dimerization activity	5.496	3.045	1.234	-0.055	-0.931	-1.809	-2.023	-2.021	-2.178	-0.759
regulation of mRNA processing	5.489	3.477	1.952	0.822	0.005	-0.982	-1.495	-2.313	-3.433	-3.521
regulation of telomerase activity	5.448	4.115	2.815	1.573	0.409	-1.609	-3.128	-4.458	-3.645	-1.521
organic cyclic compound metabolic process	5.441	3.509	2.013	0.874	0.018	-1.09	-1.73	-2.635	-3.466	-2.934
bounding membrane of organelle	5.432	4.577	3.469	2.217	0.916	-1.524	-3.375	-4.53	-3.265	-3.918
regulation of defense response	5.37	3.604	2.208	1.116	0.27	-0.89	-1.617	-2.658	-3.639	-3.763
regulation of transcription by RNA polymerase I	5.357	3.179	1.675	0.686	0.071	-0.505	-0.815	-2.22	-4.413	-3.014
secretory granule lumen	5.32	3.947	2.71	1.597	0.601	-1.078	-2.378	-3.95	-4.133	-2.635
positive regulation of transport	5.319	3.558	2.116	0.953	0.032	-1.227	-1.92	-2.433	-2.782	-3.616
cellular component disassembly	5.311	1.887	-0.414	-1.813	-2.509	-2.487	-1.521	0.248	0.188	1.108
enzyme linked receptor protein signaling pathway	5.306	3.616	2.305	1.292	0.505	-0.629	-1.482	-3.128	-4.505	-3.281

Name of GO term	Contribution to									
	0 min	15 min	30 min	45 min	60 min	90 min	120 min	180 min	240 min	300 min
histone binding	5.186	2.01	-0.044	-1.219	-1.727	-1.551	-0.729	-0.1	-1.565	-0.251
cellular response to growth factor stimulus	5.137	3.562	2.191	1.021	0.045	-1.358	-2.119	-2.317	-2.175	-3.987
protein localization to chromosome	5.128	2.604	0.951	-0.028	-0.506	-0.557	-0.194	-0.559	-3.025	-3.814
cellular homeostasis	5.107	3.714	2.547	1.559	0.71	-0.702	-1.884	-3.844	-4.727	-2.481
ficolin-1-rich granule	5.086	3.365	2.039	1.025	0.249	-0.834	-1.604	-3.014	-4.043	-2.269
intracellular organelle lumen	5.05	4.303	3.469	2.585	1.683	-0.074	-1.636	-3.863	-5.071	-6.448
leukocyte mediated immunity	4.988	2.959	1.427	0.308	-0.476	-1.313	-1.557	-1.592	-2.078	-2.666
kinase activity	4.951	3.797	2.705	1.688	0.755	-0.833	-2.028	-3.312	-3.623	-4.1
cellular chemical homeostasis	4.949	3.479	2.265	1.259	0.417	-0.912	-1.943	-3.503	-4.08	-1.931
N-methyltransferase activity	4.927	3.138	1.782	0.777	0.049	-0.836	-1.305	-2.081	-3.149	-3.301
enzyme regulator activity	4.909	2.576	0.893	-0.273	-1.037	-1.757	-1.919	-2.045	-2.117	0.771
membrane protein complex	4.878	3.724	2.606	1.535	0.52	-1.306	-2.796	-4.48	-3.966	-0.714
U1 snRNP	4.868	3.375	2.226	1.34	0.643	-0.412	-1.305	-3.233	-4.739	-2.763
positive regulation of mRNA processing	4.866	3.139	1.829	0.853	0.137	-0.768	-1.31	-2.296	-3.414	-3.036
cis-regulatory region sequence-specific DNA binding	4.825	3.456	2.358	1.473	0.749	-0.382	-1.305	-3.055	-4.449	-3.671
molecular function regulator	4.81	2.284	0.533	-0.606	-1.279	-1.725	-1.615	-1.559	-1.915	1.073
biological_process	4.791	2.744	1.287	0.299	-0.332	-0.897	-1.034	-1.527	-2.785	-2.546
endoplasmic reticulum membrane	4.773	4.32	3.429	2.261	0.957	-1.594	-3.512	-4.278	-2.333	-4.024
negative regulation of immune response	4.704	3.876	3.059	2.257	1.476	-0.007	-1.356	-3.552	-4.956	-5.501
regulation of mRNA 3'-end processing	4.686	2.52	0.999	-0.006	-0.611	-1.027	-0.93	-0.925	-2.066	-2.639
response to radiation	4.678	3.029	1.762	0.804	0.092	-0.82	-1.348	-2.174	-3.083	-2.939
DNA-templated transcription, initiation	4.656	3.3	2.221	1.359	0.659	-0.428	-1.317	-3.021	-4.304	-3.124
precatalytic spliceosome	4.652	3.132	1.893	0.886	0.073	-1.118	-1.913	-2.861	-3.085	-1.659
exonuclease activity, active with either ribo- or deoxyribonucleic acids and producing 5'-phosphomonoesters	4.65	4.704	4.231	3.37	2.248	-0.351	-2.848	-5.821	-5.555	-4.63
protein methylation	4.638	2.427	0.846	-0.222	-0.882	-1.35	-1.195	-0.747	-1.348	-2.166
T cell activation	4.626	4.057	3.253	2.302	1.276	-0.75	-2.437	-4.06	-3.79	-4.477
histone modification	4.6	2.126	0.494	-0.483	-0.97	-1.037	-0.642	-0.628	-2.128	-1.332
lymphocyte differentiation	4.579	3.687	2.765	1.842	0.944	-0.696	-2.025	-3.537	-3.756	-3.801
intracellular organelle	4.566	3.145	2.035	1.172	0.497	-0.479	-1.206	-2.591	-3.844	-3.295
metal ion binding	4.555	2.988	1.743	0.775	0.041	-0.882	-1.315	-1.63	-2.295	-3.979
organelle subcompartment	4.548	3.558	2.501	1.436	0.412	-1.356	-2.577	-3.159	-2.279	-3.083
cellular metabolic process	4.538	3.078	1.873	0.889	0.096	-1.028	-1.699	-2.301	-2.587	-2.858
protein complex oligomerization	4.537	2.807	1.442	0.392	-0.391	-1.325	-1.675	-1.614	-1.675	-2.497
activation of immune response	4.536	3.51	2.558	1.679	0.874	-0.523	-1.646	-3.145	-3.834	-4.009
RNA splicing	4.528	3.196	2.088	1.17	0.413	-0.725	-1.51	-2.531	-3.218	-3.412
negative regulation of protein modification process	4.526	2.382	0.901	-0.056	-0.612	-0.952	-0.832	-0.951	-2.197	-2.209
ribose phosphate metabolic process	4.526	4.159	3.329	2.192	0.89	-1.75	-3.852	-4.995	-2.668	-1.832
nuclear chromosome segregation	4.508	2.992	1.807	0.89	0.188	-0.765	-1.369	-2.296	-3.132	-2.823
nuclear lumen	4.499	3.748	2.979	2.207	1.444	-0.01	-1.312	-3.33	-4.613	-5.612
secretory granule	4.497	3.433	2.475	1.608	0.817	-0.581	-1.777	-3.588	-4.235	-2.648
cellular response to insulin stimulus	4.429	2.337	0.854	-0.146	-0.776	-1.309	-1.379	-1.582	-2.127	-0.3
kinase binding	4.429	2.923	1.71	0.748	1E-03	-0.998	-1.528	-1.949	-2.331	-3.004
3'-5'-exoribonuclease activity	4.416	4.635	4.207	3.318	2.134	-0.571	-3.014	-5.266	-4.355	-5.506
intracellular protein transport	4.399	3.52	2.55	1.547	0.558	-1.217	-2.536	-3.452	-2.689	-2.678
response to growth factor	4.397	3.271	2.203	1.221	0.347	-1.02	-1.843	-2.122	-1.985	-4.468
chromosome, telomeric region	4.395	1.639	-0.167	-1.231	-1.738	-1.705	-1.103	-0.534	-1.159	1.603
apoptotic signaling pathway	4.385	2.89	1.633	0.594	-0.246	-1.407	-2.003	-2.102	-1.725	-2.021
response to lipopolysaccharide	4.362	2.015	0.486	-0.41	-0.836	-0.838	-0.439	-0.548	-2.237	-1.554
positive regulation of innate immune response	4.35	2.748	1.494	0.53	-0.192	-1.097	-1.532	-1.868	-2.184	-2.249
centrosome	4.348	3.415	2.548	1.735	0.971	-0.435	-1.689	-3.65	-4.391	-2.852
telomere maintenance via telomere lengthening	4.342	2.739	1.545	0.678	0.065	-0.655	-1.038	-1.808	-2.931	-2.936
regulation of RNA splicing	4.34	3.021	1.954	1.094	0.401	-0.619	-1.337	-2.424	-3.272	-3.159
enzyme binding	4.334	2.667	1.395	0.447	-0.243	-1.069	-1.459	-1.887	-2.336	-1.848
mitotic sister chromatid segregation	4.325	2.644	1.338	0.35	-0.374	-1.219	-1.535	-1.571	-1.752	-2.206
central nervous system development	4.291	3.294	2.456	1.744	1.126	0.076	-0.853	-2.681	-4.4	-5.053
organelle	4.272	2.99	1.981	1.189	0.566	-0.344	-1.026	-2.33	-3.629	-3.668
response to insulin	4.262	2.184	0.727	-0.237	-0.826	-1.268	-1.251	-1.347	-1.933	-0.312
nucleoplasm	4.247	3.43	2.651	1.911	1.212	-0.059	-1.16	-2.887	-4.134	-5.209
regulation of histone modification	4.246	1.491	-0.28	-1.277	-1.691	-1.419	-0.55	0.361	-0.744	-0.137
chromosome organization	4.236	3.531	2.787	2.023	1.255	-0.233	-1.573	-3.535	-4.346	-4.144
stem cell differentiation	4.232	1.975	0.617	-0.081	-0.328	-0.161	0.026	-1.552	-4.397	-0.331
regulation of mRNA polyadenylation	4.225	1.315	-0.497	-1.456	-1.778	-1.257	-0.172	0.757	-0.827	-0.31
negative regulation of cell cycle phase transition	4.089	2.394	1.19	0.382	-0.112	-0.462	-0.383	0.416	-1.943	-4.739
histone deacetylase binding	4.04	3.409	2.628	1.764	0.872	-0.806	-2.118	-3.198	-2.844	-3.747
heterochromatin	4.037	2.825	1.885	1.157	0.59	-0.242	-0.895	-2.267	-3.651	-3.439
nucleus	4.036	2.369	1.157	0.314	-0.24	-0.759	-0.871	-1.102	-2.076	-2.829
proteasome-mediated ubiquitin-dependent protein catabolic process	4.007	3.34	2.712	2.106	1.512	0.319	-0.907	-3.351	-5.105	-4.633
vesicle-mediated transport	4	2.561	1.44	0.579	-0.074	-0.933	-1.436	-2.08	-2.478	-1.579
mRNA metabolic process	3.987	2.539	1.416	0.563	-0.073	-0.876	-1.299	-1.803	-2.308	-2.146
mRNA splicing, via spliceosome	3.981	3.015	2.142	1.356	0.652	-0.529	-1.44	-2.606	-3.159	-3.411
response to inorganic substance	3.973	3.318	2.601	1.85	1.088	-0.385	-1.679	-3.398	-3.848	-3.518
spliceosomal complex assembly	3.964	2.655	1.659	0.909	0.348	-0.408	-0.933	-2.019	-3.209	-2.967
RNA splicing, via transesterification reactions	3.941	2.986	2.122	1.343	0.645	-0.528	-1.436	-2.604	-3.145	-3.324
membrane organization	3.927	3.487	2.786	1.912	0.939	-1.037	-2.716	-4.237	-3.251	-1.811
sister chromatid segregation	3.912	2.562	1.517	0.717	0.112	-0.691	-1.189	-1.969	-2.688	-2.285
regulation of transcription elongation from RNA polymerase II promoter	3.905	2.201	0.945	0.053	-0.554	-1.179	-1.374	-1.545	-1.806	-0.645
positive regulation of immune response	3.897	3.016	2.179	1.394	0.665	-0.607	-1.617	-2.841	-3.149	-2.937
chromatin assembly	3.895	3.467	2.839	2.076	1.235	-0.484	-2.001	-3.736	-3.726	-3.566
telomere maintenance via telomerase	3.895	2.316	1.216	0.486	0.028	-0.404	-0.613	-1.522	-3.04	-2.361
macromolecule metabolic process	3.877	2.34	1.167	0.295	-0.329	-1.031	-1.278	-1.359	-1.67	-2.013
cellular nitrogen compound metabolic process	3.861	2.351	1.23	0.421	-0.145	-0.785	-1.087	-1.619	-2.355	-1.871
regulation of lymphocyte activation	3.853	2.857	1.956	1.145	0.422	-0.78	-1.678	-2.684	-2.815	-2.276
organic substance metabolic process	3.828	2.273	1.087	0.21	-0.415	-1.103	-1.322	-1.316	-1.514	-1.729
gene expression	3.82	2.226	1.053	0.218	-0.35	-0.937	-1.131	-1.388	-1.942	-1.569
snRNA binding	3.813	3.01	2.175	1.343	0.545	-0.856	-1.89	-2.711	-2.455	-2.975
negative regulation of protein phosphorylation	3.801	3.552	2.974	2.172	1.24	-0.708	-2.373	-3.859	-3.211	-3.589
regulation of telomere maintenance via telomere lengthening	3.791	2.173	1.047	0.309	-0.137	-0.471	-0.498	-0.932	-2.35	-2.933
negative regulation of immune system process	3.775	3.267	2.708	2.112	1.492	0.226	-1.006	-3.114	-4.475	-4.984
histone methylation	3.763	1.481	0.029	-0.78	-1.114	-0.922	-0.334	-0.11	-1.517	-0.497
negative regulation of kinase activity	3.758	3.968	3.537	2.658	1.503	-1.069	-3.268	-4.723	-2.86	-3.503
response to metal ion	3.749	2.05	0.862	0.072	-0.417	-0.835	-0.941	-1.422	-2.295	-0.822
inflammatory response	3.722	3.499	3.072	2.503	1.848	0.46	-0.819	-2.619	-4.024	-7.644
protein localization to membrane	3.721	3.236	2.522	1.661	0.727	-1.11	-2.597	-3.722	-2.63	-1.808
primary metabolic process	3.714	2.383	1.334	0.522	-0.093	-0.883	-1.289	-1.652	-1.974	-2.061

U2-type precatalytic spliceosome	5.271	3.487	2.075	0.967	0.1	-1.116	-1.915	-3.038	-3.639	-2.192	
ubiquitin protein ligase binding	5.245	3.887	2.672	1.591	0.634	-0.943	-2.124	-3.518	-3.91	-3.535	
T cell differentiation	5.208	4.361	3.394	2.358	1.302	-0.716	-2.412	-4.346	-4.53	-4.619	
nucleic acid metabolic process	5.2	3.354	1.926	0.841	0.029	-1.014	-1.607	-2.444	-3.286	-3.001	
embryonic morphogenesis	5.198	2.436	0.596	-0.518	-1.082	-1.164	-0.663	-0.386	-2.042	-2.374	
organophosphate metabolic process	5.195	4.483	3.423	2.15	0.782	-1.853	-3.873	-4.959	-2.916	-2.431	
unfolded protein binding	3.712	4.052	3.782	3.062	2.034	-0.454	-2.866	-5.516	-4.641	-3.164	
response to lipid	3.709	2.141	1.045	0.32	-0.126	-0.49	-0.566	-1.074	-2.396	-2.562	
regulation of leukocyte mediated immunity	3.69	1.972	0.782	0.009	-0.446	-0.743	-0.676	-0.83	-1.87	-1.889	
transferase complex	3.664	0.802	-0.876	-1.652	-1.78	-0.942	0.252	0.704	-1.37	1.199	
regulation of cellular localization	3.644	2.316	1.3	0.536	-0.026	-0.73	-1.115	-1.675	-2.271	-1.979	
supramolecular fiber organization	3.628	3.807	3.429	2.658	1.638	-0.663	-2.697	-4.378	-3.278	-4.144	
cellular response to biotic stimulus	3.621	1.286	-0.218	-1.069	-1.425	-1.201	-0.461	0.343	-0.597	-0.278	
cytoplasmic vesicle	3.604	2.589	1.692	0.9	0.204	-0.94	-1.794	-2.736	-2.587	-0.933	
Golgi vesicle transport	3.6	2.66	1.858	1.168	0.57	-0.43	-1.256	-2.579	-3.262	-2.329	
organonitrogen compound catabolic process	3.595	2.805	2.035	1.297	0.603	-0.621	-1.586	-2.679	-2.825	-2.623	
lymphocyte activation	3.59	2.165	1.07	0.25	-0.349	-1.06	-1.37	-1.578	-1.688	-1.03	
regulation of transferase activity	3.583	2.78	1.96	1.15	0.373	-1	-2.039	-2.909	-2.386	-1.512	
protein kinase binding	3.566	2.675	1.863	1.133	0.489	-0.543	-1.252	-1.931	-2.319	-3.682	
regulation of innate immune response	3.507	2.342	1.418	0.692	0.127	-0.654	-1.146	-1.82	-2.346	-2.118	
positive regulation of intracellular transport	3.505	2.702	1.93	1.203	0.534	-0.59	-1.402	-2.157	-2.352	-3.373	
protein import	3.504	3.003	2.294	1.467	0.599	-1.008	-2.153	-2.556	-1.616	-3.534	
protein heterodimerization activity	3.498	-0.255	-2.402	-3.314	-3.324	-1.765	0.42	2.467	0.838	3.839	
mononuclear cell differentiation	3.487	2.902	2.266	1.601	0.928	-0.368	-1.503	-2.998	-3.352	-2.962	
tube morphogenesis	3.487	2.191	1.211	0.482	-0.05	-0.715	-1.097	-1.728	-2.304	-1.477	
positive regulation of nucleocytoplasmic transport	3.472	2.75	2.074	1.442	0.85	-0.217	-1.137	-2.548	-3.336	-3.352	
carbohydrate derivative metabolic process	3.465	3.457	2.957	2.118	1.073	-1.184	-3.09	-4.354	-2.529	-1.912	
import into nucleus	3.438	2.692	1.889	1.085	0.324	-0.931	-1.693	-1.728	-1.208	-3.868	
3'-UTR-mediated mRNA stabilization	3.394	2.169	1.29	0.672	0.241	-0.306	-0.738	-1.969	-3.208	-1.544	
cellular response to lipid	3.393	1.857	0.787	0.085	-0.336	-0.636	-0.616	-0.83	-1.82	-1.884	
negative regulation of phosphorylation	3.376	3.063	2.506	1.79	0.985	-0.645	-2.002	-3.173	-2.676	-3.224	
transmembrane receptor protein serine/threonine kinase signaling pathway	3.37	2.317	1.472	0.796	0.256	-0.537	-1.099	-1.967	-2.564	-2.043	
negative regulation of telomere maintenance via telomerase	3.36	1.458	0.31	-0.266	-0.43	-0.067	0.5	0.215	-2.24	-2.838	
regulation of localization	3.351	2.116	1.164	0.443	-0.096	-0.785	-1.173	-1.688	-2.052	-1.279	
leukocyte differentiation	3.332	2.577	1.886	1.252	0.67	-0.356	-1.219	-2.488	-3.055	-2.598	
microtubule organizing center	3.3	2.68	2.075	1.482	0.899	-0.234	-1.303	-3.047	-3.683	-2.168	
head development	3.28	2.322	1.535	0.894	0.374	-0.388	-0.904	-1.637	-2.368	-3.108	
negative regulation of mitotic cell cycle	3.257	0.896	-0.532	-1.237	-1.41	-0.803	0.219	0.973	-0.687	-0.676	
negative regulation of phosphate metabolic process	3.243	2.751	2.138	1.454	0.744	-0.611	-1.701	-2.691	-2.459	-2.87	
regulation of immune effector process	3.242	2.37	1.629	1.002	0.474	-0.347	-0.939	-1.76	-2.46	-3.211	
U4/U6 x U5 tri-snRNP complex	3.219	2.669	2.081	1.469	0.845	-0.387	-1.521	-3.15	-3.417	-1.809	
brain development	3.218	2.428	1.746	1.158	0.649	-0.185	-0.845	-1.892	-2.788	-3.488	
regulation of vesicle-mediated transport	3.204	1.532	0.374	-0.378	-0.818	-1.001	-0.983	-0.877	-1.199	0.237	
proteasomal protein catabolic process	3.202	2.35	1.7	1.199	0.8	0.154	-0.473	-2.065	-3.665	-3.202	
DNA binding	3.197	1.902	0.937	0.242	-0.236	-0.735	-0.886	-1.018	-1.516	-1.887	
ncRNA transcription	3.192	1.985	1.171	0.64	0.301	-0.113	-0.537	-2.146	-3.713	-0.781	
negative regulation of telomere maintenance via telomere lengthening	3.182	1.217	0.059	-0.488	-0.596	-0.085	0.628	0.486	-1.997	-2.406	
protein homodimerization activity	3.167	2.1	1.16	0.349	-0.334	-1.325	-1.847	-1.766	-0.922	-0.581	
nuclear protein-containing complex	3.152	2.102	1.287	0.659	0.178	-0.49	-0.947	-1.742	-2.402	-1.796	
negative regulation of cell cycle process	3.151	1.757	0.813	0.223	-0.097	-0.228	-0.085	-0.266	-1.787	-3.48	
cell surface receptor signaling pathway involved in cell-cell signaling	3.101	1.291	0.051	-0.739	-1.187	-1.418	-1.235	-0.942	-0.838	1.916	
tube development	3.085	1.855	0.948	0.297	-0.157	-0.682	-0.956	-1.484	-2.01	-0.896	
positive regulation of immune system process	3.075	2.528	1.943	1.341	0.74	-0.396	-1.366	-2.576	-2.795	-2.494	
transcription by RNA polymerase II	3.06	1.816	0.88	0.198	-0.281	-0.806	-0.993	-1.131	-1.432	-1.311	
nucleobase-containing compound biosynthetic process	3.043	1.783	0.857	0.2	-0.247	-0.716	-0.888	-1.163	-1.65	-1.221	
regulation of telomere maintenance via telomerase	3.033	1.438	0.455	-0.064	-0.251	-0.08	0.239	-0.272	-2.316	-2.18	
establishment of protein localization to organelle	3.027	2.561	1.935	1.221	0.477	-0.902	-1.909	-2.375	-1.555	-2.481	
protein kinase activity	3.007	2.792	2.369	1.803	1.15	-0.227	-1.457	-2.853	-2.967	-3.617	
transcription regulator complex	2.989	2.389	1.801	1.225	0.66	-0.422	-1.415	-2.904	-3.15	-1.174	
regulation of T cell differentiation	2.964	3.339	3.194	2.666	1.878	-0.067	-1.961	-4.063	-3.759	-4.192	
response to peptide hormone	2.963	1.917	1.06	0.374	-0.16	-0.845	-1.139	-1.096	-1.067	-2.007	
cellular response to peptide hormone stimulus	2.951	1.644	0.673	-0.019	-0.483	-0.915	-0.943	-0.704	-0.864	-1.341	
response to organic cyclic compound	2.93	2.58	2.071	1.464	0.811	-0.458	-1.47	-2.31	-2.148	-3.471	
negative regulation of mRNA processing	2.929	2.25	1.702	1.251	0.865	0.197	-0.452	-1.939	-3.38	-3.425	
animal organ development	2.909	1.808	0.979	0.37	-0.066	-0.579	-0.835	-1.236	-1.767	-1.583	
regulation of protein transport	2.863	2.222	1.624	1.069	0.556	-0.342	-1.076	-2.071	-2.479	-2.366	
embryo development	2.857	1.636	0.749	0.128	-0.287	-0.712	-0.869	-1.173	-1.61	-0.72	
peptidyl-lysine modification	2.854	0.403	-0.902	-1.35	-1.198	0.047	1.426	1.552	-1.737	-1.095	
protein folding	2.847	2.594	2.025	1.249	0.366	-1.404	-2.769	-3.287	-1.303	-0.319	
transcription, DNA-templated	2.814	1.646	0.79	0.183	-0.228	-0.652	-0	-1.035	-1.504	-1.214	
regulation of chromosome organization	2.789	1.435	0.518	-0.057	-0.371	-0.505	-0.361	-0.411	-1.364	-1.673	
chromosome	2.769	2.389	1.952	1.474	0.972	-0.052	-1.024	-2.521	-3.139	-2.818	
magnesium ion binding	2.765	3.316	3.114	2.382	1.318	-1.152	-3.25	-4.245	-1.73	-2.518	
regulation of cellular component size	2.749	1.727	1.008	0.522	0.209	-0.107	-0.284	-0.991	-2.067	-2.566	
intrinsic apoptotic signaling pathway	2.73	1.631	0.726	0.002	-0.554	-1.214	-1.379	-0.801	-0.142	-0.998	
positive regulation of catalytic activity	2.73	2.312	1.832	1.313	0.773	-0.296	-1.255	-2.531	-2.75	-2.127	
negative regulation of DNA metabolic process	2.727	1.317	0.46	0.02	-0.121	0.086	0.417	-0.038	-2.126	-2.742	
DNA-templated transcription, elongation	2.713	2.464	1.992	1.366	0.647	-0.868	-2.203	-3.462	-2.454	-0.195	
nuclear chromosome	2.708	2.369	1.931	1.423	0.872	-0.266	-1.322	-2.748	-2.929	-2.038	
cellular response to inorganic substance	2.692	2.023	1.49	1.064	0.722	0.2	-0.225	-1.186	-2.579	-4.201	
tissue development	2.687	1.687	0.873	0.224	-0.282	-0.939	-1.24	-1.234	-0.967	-0.809	
axonogenesis	2.677	1.432	0.549	-0.038	-0.392	-0.615	-0.497	-0.271	-0.872	-1.973	
regulation of catalytic activity	2.664	1.96	1.315	0.729	0.203	-0.671	-1.31	-1.927	-1.798	-1.167	
DNA helicase activity	2.663	1.076	0.037	-0.576	-0.874	-0.897	-0.638	-0.584	-1.117	0.908	
U2-type spliceosomal complex	2.645	2.234	1.771	1.271	0.751	-0.294	-1.261	-2.63	-2.843	-1.644	
neuron apoptotic process	2.625	2.646	2.403	1.966	1.397	0.073	-1.222	-2.919	-3.263	-3.705	
plasma membrane region	2.605	2.547	2.051	1.279	0.37	-1.404	-2.587	-2.178	0.109	-2.792	
cell surface receptor signaling pathway	2.594	1.491	0.724	0.216	-0.102	-0.401	-0.543	-1.129	-1.969	-0.88	
protein import into nucleus	2.589	2.154	1.546	0.851	0.147	-1.062	-1.747	-1.284	-0.07	-3.123	
small molecule metabolic process	2.565	1.894	1.184	0.474	-0.206	-1.367	-2.139	-2.256	-0.819	0.67	
regulation of cytoskeleton organization	2.564	1.904	1.343	0.869	0.47	-0.146	-0.587	-1.236	-1.982	-3.199	
autophagy	2.551	0.851	-0.343	-1.12	-1.561	-1.719	-1.303	-0.065	0.788	1.92	
regulation of lymphocyte differentiation	2.532	2.706	2.511	2.047	1.403	-0.124	-1.581	-3.188	-2.983	-3.324	
regulation of protein catabolic process	2.511	2.042	1.595	1.164	0.745	-0.064	-0.836	-2.171	-2.855	-2.131	
alternative mRNA splicing, via spliceosome	2.473	1.694	1.101	0.656	0.325	-0.112	-0.407	-1.059	-2.007	-2.665	
regulation of DNA repair	2.472	1.635	0.952	0.402	-0.035	-0.646	-1.005	-1.317	-1.37	-1.087	
endosome	2.457	1.494	0.76	0.206	-0.212	-0.784	-1.178	-1.798	-1.778	0.834	
response to UV	2.442	1.66	1.146	0.823	0.621	0.357	0.011	-1.48	-3.305	-2.277	
telomere maintenance	2.438	1.258	0.488	0.027	-0.213	-0.324	-0.319	-0.905	-1.969	-0.482	
vesicle	2.427	1.876	1.352	0.855	0.388	-0.448	-1.137	-2.005	-2.081	-1.227	
regulation of establishment of protein localization	2.414	1.768	1.197	0.693	0.246	-0.499	-1.081	-1.818	-1.914	-1.007	
microtubule cytoskeleton	2.41	1.581	0.956	0.487	0.13	-0.385	-0.803	-1.697	-2.23	-0.449	
tRNA modification	2.38	2.403	2.229	1.901	1.459	0.37	-0.798	-2.711	-3.576	-3.658	
3'-5' exonuclease activity	2.365	3.214	3.353	2.962	2.201	0.113	-2.015	-4.337	-3.74	-4.116	
ion binding	2.364	1.662	1.066	0.572	0.172	-0.378	-0.657	-0.783	-1.131	-2.887	
negative regulation of mRNA metabolic process	2.332	1.296	0.587	0.132	-0.135	-0.321	-0.336	-0.674	-1.545	-1.337	

regulation of cell migration	2.239	1.946	1.561	1.116	0.637	-0.329	-1.185	-2.194	-2.157	-1.634	
positive regulation of response to DNA damage stimulus	2.235	0.482	-0.613	-1.188	-1.365	-0.956	-0.111	1.038	0.485	-0.005	
positive regulation of transferase activity	2.206	1.857	1.457	1.023	0.572	-0.33	-1.145	-2.219	-2.251	-1.169	
RNA stabilization	2.199	1.305	0.646	0.176	-0.145	-0.483	-0.605	0.798	1.191	-1.104	
response to unfolded protein	2.197	2.778	2.796	2.394	1.698	-0.141	-2.001	-4.047	-3.308	-2.367	
molecular adaptor activity	2.185	0.921	0.093	-0.403	-0.658	-0.741	-0.639	-0.835	-1.226	1.304	
regulation of response to DNA damage stimulus	2.144	0.614	-0.363	-0.903	-1.109	-0.882	-0.287	0.502	0.08	0.204	
positive regulation of cellular component organization	2.141	0.657	-0.293	-0.821	-1.025	-0.812	-0.238	0.519	0.028	-0.157	
intracellular steroid hormone receptor signaling pathway	2.117	1.299	0.757	0.42	0.223	0.039	-0.126	-1.02	-2.274	-1.435	
ATP-dependent chromatin remodeler activity	2.092	1.791	1.529	1.281	1.027	0.445	-0.283	-2.085	-3.463	-2.335	
methylation	2.08	1.343	0.802	0.415	0.142	-0.19	-0.404	-0.951	-1.68	-1.557	
spliceosomal snRNP assembly	2.061	2.251	1.996	1.435	0.69	-0.943	-2.263	-2.737	-0.972	-1.518	
cellular anatomical entity	2.054	0.444	-0.501	-0.938	-1.005	-0.499	0.242	0.674	-0.538	0.067	
cellular_component	2.054	0.551	-0.394	-0.905	-1.09	-0.859	-0.319	0.248	-0.185	0.899	
cellular response to hormone stimulus	2.043	1.202	0.596	0.179	-0.092	-0.348	-0.418	-0.621	-1.179	-1.362	
regulation of intrinsic apoptotic signaling pathway	2.02	0.96	0.124	-0.506	-0.949	-1.344	-1.222	-0.11	0.896	0.131	
establishment of protein localization	1.998	1.481	0.987	0.527	0.109	-0.57	-1.02	-1.264	-1.023	-1.226	
negative regulation of chromosome organization	1.989	1.18	0.665	0.372	0.24	0.238	0.304	-0.203	-1.775	-3.011	
regulation of transcription by RNA polymerase II	1.979	1.372	0.859	0.43	0.076	-0.445	-0.772	-1.067	-1.163	-1.268	
positive regulation of DNA metabolic process	1.971	2.102	2.04	1.82	1.477	0.539	-0.557	-2.549	-3.56	-3.284	
organelle membrane	1.953	2.312	2.196	1.746	1.085	-0.458	-1.784	-2.545	-1.44	-3.063	
protein catabolic process	1.95	1.728	1.403	1.01	0.579	-0.29	-1.037	-1.82	-1.735	-1.788	
protein-containing complex subunit organization	1.895	0.872	0.14	-0.351	-0.65	-0.834	-0.697	-0.237	-0.115	-0.023	
response to nitrogen compound	1.883	1.477	1.045	0.607	0.184	-0.559	-1.094	-1.425	-1.064	-1.053	
meiotic cell cycle	1.874	-0.304	-1.549	-2.068	-2.047	-1.023	0.455	2.176	1.264	1.224	
regulation of gene silencing	1.873	0.976	0.355	-0.044	-0.267	-0.359	-0.213	-0.02	-0.598	-1.703	
angiogenesis	1.86	0.762	0.06	-0.337	-0.511	-0.463	-0.247	-0.284	-0.937	0.097	
cell cycle phase transition	1.806	0.486	-0.308	-0.696	-0.784	-0.427	0.157	0.577	-0.39	-0.42	
negative regulation of RNA splicing	1.785	1.869	1.789	1.578	1.264	0.442	-0.488	-2.129	-2.997	-3.114	
cellular response to steroid hormone stimulus	1.781	0.947	0.428	0.144	0.023	0.034	0.081	-0.492	-1.723	-1.223	
regulation of mRNA metabolic process	1.759	0.802	0.162	-0.228	-0.43	-0.478	-0.326	0.242	-0.682	-0.335	
identical protein binding	1.758	1.391	1.092	0.842	0.621	0.213	-0.217	-1.251	-2.24	-2.208	
mitotic spindle	1.756	1.924	1.746	1.323	0.745	-0.573	-1.719	-2.483	-1.398	-1.321	
chromatin organization	1.753	1.196	0.73	0.342	0.022	-0.45	-0.752	-1.034	-1.045	-0.762	
cellular response to organic cyclic compound	1.732	1.708	1.469	1.086	0.621	-0.354	-1.139	-1.603	-1.131	-2.391	
nuclear body	1.726	1.663	1.495	1.252	0.958	0.301	-0.342	-1.34	-2.105	-3.607	
mRNA stabilization	1.725	0.818	0.192	-0.211	-0.442	-0.562	-0.461	-0.319	-0.542	-0.197	
mitotic nuclear division	1.722	1.15	0.643	0.203	-0.171	-0.719	-1.016	-0.992	-0.526	-0.295	
mitotic cell cycle phase transition	1.712	1.323	1.031	0.802	0.609	0.239	-0.205	-1.428	-2.496	-1.587	
cytoskeleton	1.694	1.026	0.538	0.188	-0.061	-0.378	-0.604	-1.112	-1.395	0.105	
protein transport	1.685	1.337	0.958	0.57	0.192	-0.472	-0.943	-1.21	-0.918	-1.197	
macromolecule methylation	1.684	1.118	0.712	0.427	0.231	-0.014	-0.207	-0.813	-1.621	-1.516	
regulation of DNA biosynthetic process	1.679	1.377	1.112	0.871	0.645	0.208	-0.246	-1.239	-2.133	-2.275	
midbody	1.666	1.045	0.596	0.272	0.036	-0.303	-0.609	-1.373	-1.742	0.411	
extracellular exosome	1.665	1.335	0.98	0.615	0.25	-0.432	-0.993	-1.57	-1.339	-0.512	
cellular protein localization	1.656	1.573	1.334	0.99	0.582	-0.278	-1.018	-1.681	-1.423	-1.736	
RNA phosphodiester bond hydrolysis	1.649	1.037	0.512	0.074	-0.276	-0.724	-0.868	-0.523	-0.078	-0.803	
RNA modification	1.646	1.839	1.803	1.59	1.247	0.336	-0.651	-2.156	-2.686	-2.967	
positive regulation of transcription, DNA-templated	1.645	1.145	0.733	0.4	0.136	-0.221	-0.411	-0.574	-0.909	-1.944	
spliceosomal snRNP complex	1.639	1.95	1.888	1.544	1.002	-0.394	-1.806	-3.382	-2.473	0.032	
U12-type spliceosomal complex	1.634	0.088	-0.77	-1.117	-1.107	-0.528	0.146	0.174	-0.903	2.382	
regulation of cell cycle phase transition	1.631	0.878	0.387	0.099	-0.037	-0.033	0.098	0.015	-0.993	2.013	
response to endogenous stimulus	1.63	1.383	1.091	0.773	0.444	-0.194	-0.74	-1.381	-1.471	-1.536	
spliceosomal complex	1.627	1.369	1.113	0.856	0.596	0.067	-0.47	-1.469	-2.055	-1.634	
programmed cell death	1.62	1.326	1.02	0.705	0.387	-0.236	-0.806	-1.619	-1.701	-0.697	
carbohydrate metabolic process	1.614	3.06	3.323	2.74	1.611	-1.296	-3.81	-4.498	-0.532	-2.212	
microtubule cytoskeleton organization	1.614	1.828	1.678	1.27	0.696	-0.63	-1.788	-2.523	-1.271	-0.874	
positive regulation of protein transport	1.597	1.384	1.13	0.849	0.551	-0.05	-0.604	-1.4	-1.71	-1.747	
vasculature development	1.595	0.748	0.162	-0.217	-0.44	-0.582	-0.539	-0.51	-0.62	0.403	
response to stimulus	1.595	1.085	0.667	0.326	0.05	-0.345	-0.594	-0.861	-0.988	-0.934	
neuron death	1.577	1.958	1.995	1.774	1.372	0.29	-0.823	-2.198	-2.401	-3.542	
apoptotic process	1.576	1.242	0.921	0.613	0.318	-0.237	-0.732	-1.46	-1.584	-0.658	
peptidyl-amino acid modification	1.569	0.828	0.365	0.11	-7E-04	0.003	0.039	-0.46	-1.502	-0.951	
cellular response to endogenous stimulus	1.547	1.31	1.026	0.713	0.389	-0.24	-0.772	-1.359	-1.348	-1.267	
regulation of leukocyte differentiation	1.544	1.942	1.984	1.757	1.335	0.177	-1.05	-2.628	-2.618	-2.444	
anatomical structure morphogenesis	1.536	0.447	-0.302	-0.772	-1.017	-1.028	-0.671	0.222	0.65	0.937	
negative regulation of mRNA catabolic process	1.534	0.567	-0.069	-0.443	-0.619	-0.584	-0.321	0.02	-0.217	0.132	
regulation of cellular component movement	1.533	1.336	1.048	0.704	0.334	-0.383	-0.948	-1.351	-1.027	-1.245	
mitotic cell cycle process	1.499	1.207	0.924	0.646	0.372	-0.166	-0.682	-1.523	-1.721	-0.555	
nuclear speck	1.496	1.591	1.528	1.345	1.078	0.404	-0.303	-1.415	-2.158	-1.565	
chordate embryonic development	1.494	0.367	-0.341	-0.724	-0.866	-0.709	-0.335	0.033	-0.178	1.257	
regulation of telomere maintenance	1.492	0.326	-0.339	-0.626	-0.642	-0.222	0.327	0.497	-0.636	-0.177	
positive regulation of nucleobase-containing compound metabolic process	1.487	0.911	0.477	0.161	-0.059	-0.29	-0.357	-0.401	-0.692	-1.236	
cell cycle checkpoint signaling	1.484	1.176	0.934	0.752	0.625	0.498	0.473	0.278	-1.088	-5.132	
positive regulation of RNA metabolic process	1.473	0.8	0.33	0.024	-0.157	-0.263	-0.205	-0.172	-0.626	-1.204	
cell death	1.466	1.146	0.843	0.556	0.284	-0.22	-0.665	-1.317	-1.443	-0.65	
negative regulation of mRNA splicing, via spliceosome	1.465	1.626	1.635	1.517	1.297	0.635	-0.193	-1.85	-2.946	-3.185	
regulation of response to stress	1.458	0.84	0.313	-0.124	-0.47	-0.903	-1.021	-0.557	0.215	0.248	
amide binding	1.456	1.914	1.81	1.33	0.636	-0.878	-1.932	-1.441	0.623	-3.519	
establishment of cell polarity	1.454	3.029	3.534	3.235	2.369	-0.248	-2.966	-5.515	-3.333	-1.559	
positive regulation of establishment of protein localization	1.447	1.37	1.192	0.938	0.631	-0.067	-0.761	-1.748	-1.86	-1.142	
maturation of 5.8S rRNA from tricistronic rRNA transcript (SSU-rRNA, 5.8S rRNA, LSU-rRNA)	1.444	1.972	1.948	1.536	0.879	-0.691	-2.007	-2.432	-0.657	-1.991	
protein-containing complex assembly	1.44	0.836	0.376	0.035	-0.208	-0.479	-0.569	-0.56	-0.545	-0.326	
regulation of type I interferon production	1.437	0.727	0.142	-0.323	-0.673	-1.057	-1.075	-0.364	0.581	0.604	
cell cycle	1.434	0.906	0.477	0.134	-0.136	-0.495	-0.676	-0.731	-0.595	-0.318	
extracellular region	1.433	0.906	0.491	0.169	-0.083	-0.436	-0.671	-0.978	-0.958	0.128	
homeostasis of number of cells	1.418	2.522	3.012	3.017	2.654	1.227	-0.577	-3.53	-4.57	-5.173	
response to organonitrogen compound	1.404	1.136	0.815	0.464	0.106	-0.556	-1.057	-1.347	-0.79	-0.176	
regulation of protein localization to nucleus	1.402	1.299	1.105	0.838	0.517	-0.221	-0.979	-2.084	-1.957	0.081	
regulation of apoptotic signaling pathway	1.399	1.031	0.589	0.125	-0.321	-1.026	-1.343	-0.699	0.613	-0.369	
negative regulation of RNA metabolic process	1.348	1.019	0.749	0.525	0.336	0.029	0.234	0.766	-1.333	1.675	
positive regulation of response to stimulus	1.342	1.005	0.697	0.421	0.177	-0.214	-0.482	-0.736	-0.868	-1.343	
cellular response to DNA damage stimulus	1.337	0.68	0.244	-0.019	-0.154	-0.186	-0.098	-0.158	-0.725	-0.921	
system development	1.333	0.515	-0.03	-0.359	-0.523	-0.533	-0.35	-0.106	-0.243	0.297	
nuclear division	1.331	1.006	0.69	0.392	0.117	-0.348	-0.68	-0.94	-0.819	-0.749	
negative regulation of nucleobase-containing compound metabolic process	1.309	1.001	0.753	0.551	0.382	0.103	-0.151	-0.73	-1.402	-1.816	
regulation of cellular component organization	1.3	0.419	-0.198	-0.599	-0.824	-0.9	-0.678	-0.026	0.433	1.072	
negative regulation of transcription, DNA-templated	1.283	1.047	0.792	0.53	0.271	-0.206	-0.588	-0.988	-1.011	-1.131	
cellular response to oxygen-containing compound	1.28	1.02	0.727	0.422	0.124	-0.394	-0.745	-0.864	-0.57	-1	
organelle inner membrane	1.276	2.724	3.182	2.929	2.207	0.162	-1.689	-2.503	-1.111	-7.177	
negative regulation of cellular component organization	1.273	0.624	0.233	0.031	-0.041	0.002	0.049	-0.436	-1.343	-0.392	
negative regulation of RNA catabolic process	1.266	0.735	0.371	0.138	0.002	-0.091	-0.099	-0.304	-0.886	-1.131	
double-strand break repair	1.239	1.688	1.782	1.605	1.234	0.173	-0.963	-2.391	-2.285	-2.081	
mitochondrion	1.214	2.17	2.546	2.476	2.083	0.74	-0.795	-2.842	-3.144	4.448	
response to steroid hormone	1.213	0.612	0.266	0.104	0.066	0.156	0.217	-0.348	-1.47	-0.816	
stem cell population maintenance	1.198	1.396	1.475	1.439	1.299	0.741	-0.1	-2.092	-3.331	-2.025	

I-kappaB kinase/NF-kappaB signaling	2.299	0.667	-0.408	-1.036	-1.315	-1.173	-0.57	0.492	0.465	0.578
telomeric DNA binding	2.293	-0.094	-1.515	-2.188	-2.304	-1.527	-0.266	1.226	0.914	3.463
immune effector process	2.291	2.317	2.035	1.545	0.935	-0.359	-1.404	-2.016	-1.513	-3.83
embryo development ending in birth or egg hatching	2.291	0.925	0.026	-0.51	-0.773	-0.795	-0.547	-0.388	-0.799	0.57
response to oxygen-containing compound	2.29	1.817	1.31	0.797	0.3	-0.574	-1.209	-1.644	-1.37	-1.718
transferase activity	2.288	2.193	1.884	1.435	0.908	-0.173	-1.047	-1.707	-1.688	-4.094
response to hormone	2.281	1.39	0.737	0.273	-0.045	-0.392	-0.551	-0.895	-1.456	-1.343
regulation of stem cell differentiation	2.281	1.768	1.366	1.043	0.772	0.301	-0.184	-1.424	-2.791	-3.132
methyltransferase complex	1.196	0.481	0.197	0.213	0.414	0.99	1.329	0.198	-2.575	-2.443
heterochromatin organization	1.194	0.674	0.243	-0.097	-0.345	-0.582	-0.516	0.144	0.494	-1.208
exonuclease activity	1.182	2.437	2.915	2.8	2.262	0.481	-1.484	-3.748	-3.226	-3.618
positive regulation of cell migration	1.178	1.355	1.292	1.053	0.694	-0.188	-1.03	-1.86	-1.418	-1.077
rRNA metabolic process	1.176	1.611	1.69	1.502	1.129	0.102	-0.941	-2.073	-1.84	-2.355
DNA biosynthetic process	1.13	0.481	0.062	-0.181	-0.293	-0.285	-0.169	-0.184	-0.551	-0.011
mitotic cell cycle	1.125	0.931	0.683	0.407	0.124	-0.392	-0.758	-0.886	-0.504	-0.731
protein-DNA complex	1.121	1.109	1.002	0.817	0.568	-0.054	-0.741	-1.849	-1.89	-0.084
leukocyte cell-cell adhesion	1.087	2.281	2.683	2.492	1.889	0.045	-1.855	-3.597	-2.348	-2.677
posttranscriptional gene silencing	1.081	0.208	-0.314	-0.561	-0.604	-0.317	0.144	0.598	0.036	-0.271
transition metal ion binding	1.076	0.876	0.691	0.523	0.371	0.116	-0.088	-0.438	-0.974	-2.152
immune system development	1.053	0.495	0.115	-0.125	-0.258	-0.32	-0.258	-0.213	-0.398	-0.092
regulation of rRNA processing	1.044	0.925	0.793	0.644	0.475	0.083	-0.369	-1.281	-1.683	-0.63
extracellular space	1.04	0.618	0.292	0.041	-0.15	-0.414	-0.588	-0.804	-0.664	0.629
regulation of protein localization	1.033	0.972	0.845	0.669	0.458	-0.023	-0.507	-1.227	-1.36	-0.86
negative regulation of cell cycle	1.017	-0.222	-0.883	-1.097	-0.982	-0.173	0.855	1.844	0.602	-0.961
cellular protein-containing complex assembly	1.001	0.476	0.097	-0.162	-0.325	-0.446	-0.405	-0.216	-0.126	0.106
cellular response to stimulus	1.001	0.78	0.57	0.373	0.187	-0.147	-0.429	-0.811	-0.902	-0.622
oxidoreductase activity	0.999	2.856	3.576	3.438	2.692	0.223	-2.425	-5.008	-3.287	-3.065
DNA packaging	0.996	1.361	1.434	1.289	0.991	0.162	-0.69	-1.657	-1.6	-2.288
protein localization to organelle	0.994	0.947	0.816	0.628	0.407	-0.058	-0.459	-0.856	-0.892	-1.528
rRNA processing	0.94	1.462	1.606	1.467	1.128	0.139	-0.891	-2.009	-1.719	-2.122
cell division	0.936	1.006	0.907	0.689	0.395	-0.272	-0.856	-1.278	-0.785	-0.741
response to temperature stimulus	0.935	2.266	2.76	2.623	2.04	0.161	-1.841	-3.821	-2.609	-2.515
transcription regulatory region nucleic acid binding	0.935	0.271	-0.137	-0.343	-0.397	-0.215	0.118	0.484	0.003	-0.719
regulation of alternative mRNA splicing, via spliceosome	0.933	0.625	0.406	0.258	0.163	0.071	0.027	-0.192	-0.766	-1.524
post-transcriptional gene silencing by RNA	0.929	-0.044	-0.615	-0.871	-0.89	-0.484	0.15	0.961	0.599	0.265
spindle organization	0.923	1.419	1.446	1.139	0.617	-0.677	-1.798	-2.206	-0.463	-0.402
methyltransferase activity	0.906	0.941	0.877	0.74	0.551	0.092	-0.373	-1.029	-1.235	-1.47
positive regulation of protein localization to nucleus	0.881	1	0.963	0.801	0.543	-0.154	-0.928	-2.044	-1.731	0.67
regulation of cell population proliferation	0.869	1.271	1.444	1.434	1.28	0.683	-0.1	-1.563	-2.402	-2.915
sequence-specific double-stranded DNA binding	0.862	0.25	-0.145	-0.364	-0.445	-0.328	-0.031	0.449	0.244	-0.493
phosphate-containing compound metabolic process	0.858	0.981	0.903	0.685	0.379	-0.313	-0.891	-1.161	-0.517	-0.925
catalytic complex	0.855	0.876	0.851	0.786	0.685	0.397	0.025	-0.825	-1.596	-2.053
Sm-like protein family complex	0.831	1.546	1.728	1.509	1.009	-0.429	-1.897	-3.224	-1.69	0.616
ncRNA 3'-end processing	0.831	1.994	2.488	2.465	2.063	0.595	-1.125	-3.354	-3.127	-2.829
response to organic substance	0.815	0.496	0.255	0.079	-0.044	-0.181	-0.233	-0.29	-0.416	-0.481
small nuclear ribonucleoprotein complex	0.801	1.554	1.782	1.609	1.148	-0.248	-1.744	-3.327	-2.078	0.505
positive regulation of signal transduction	0.784	0.756	0.662	0.524	0.36	0.013	-0.287	-0.6	-0.719	-1.493
regulation of response to external stimulus	0.775	0.485	0.299	0.193	0.144	0.144	0.169	-0.023	-0.694	-1.493
regulation of organelle organization	0.775	0.331	0.049	-0.111	-0.183	-0.179	-0.122	-0.225	-0.51	0.174
regulation of DNA-templated transcription, elongation	0.769	1.349	1.468	1.241	0.773	-0.526	-1.825	-2.924	-1.369	1.044
heart development	0.762	0.723	0.573	0.365	0.142	-0.211	-0.306	0.299	0.608	-2.955
regulation of RNA metabolic process	0.76	0.472	0.265	0.122	0.027	-0.071	-0.114	-0.251	-0.536	-0.675
cellular macromolecule localization	0.758	1.142	1.236	1.113	0.841	0.07	-0.715	-1.516	-1.248	-1.681
positive regulation of protein-containing complex assembly	0.755	0.119	-0.247	-0.401	-0.392	-0.071	0.4	0.926	0.244	-1.333
DNA recombination	0.755	1.239	1.365	1.23	0.919	0.053	-0.778	-1.417	-0.986	-2.38
condensed chromosome	0.749	1.086	1.204	1.15	0.964	0.343	-0.408	-1.613	-1.909	-1.565
regulation of mitotic cell cycle phase transition	0.743	0.84	0.874	0.848	0.767	0.457	-0.007	-1.129	-1.921	-1.471
intracellular anatomical structure	0.739	-0.053	-0.468	-0.602	-0.536	-0.088	0.419	0.62	-0.241	0.209
system process	0.728	1.751	2.139	2.058	1.654	0.367	-2.939	-2.018	-1.497	-4.244
muscle structure development	0.726	-0.439	-1.077	-1.313	-1.254	-0.628	0.191	1.042	0.71	2.041
positive regulation of transcription by RNA polymerase II	0.714	0.464	0.277	0.146	0.062	-3E-04	0.024	0.078	-0.272	-1.493
transcription cis-regulatory region binding	0.711	0.224	-0.081	-0.241	-0.289	-0.168	0.079	0.393	0.059	-0.689
positive regulation of cell death	0.71	1.135	1.286	1.226	1.014	0.328	-0.444	-1.48	-1.629	-2.148
circulatory system development	0.704	0.62	0.481	0.312	0.136	-0.172	-0.351	-0.257	-0.093	-1.38
DNA repair	0.699	0.243	-0.054	-0.225	-0.299	-0.256	-0.097	0.129	-0.012	-0.128
cytoskeletal protein binding	0.695	1.496	1.749	1.603	1.188	-0.01	-1.148	-1.845	-0.909	-2.819
sequence-specific DNA binding	0.694	0.213	-0.083	-0.235	-0.278	-0.159	0.066	0.296	-0.049	-0.465
regulation of microtubule-based process	0.694	1.359	1.489	1.234	0.727	-0.596	-1.763	-2.161	-0.336	-0.646
response to chemical	0.691	0.46	0.293	0.176	0.095	-0.002	-0.07	-0.281	-0.615	-0.747
homeostatic process	0.681	0.782	0.883	0.959	0.993	0.885	0.497	-0.998	-2.557	-2.125
regulation of biological process	0.671	0.373	0.162	0.016	-0.084	-0.204	-0.288	-0.495	-0.553	0.401
regulation of kinase activity	0.663	0.977	1.005	0.824	0.501	-0.339	-1.134	-1.713	-0.789	0.004
establishment of localization in cell	0.653	0.912	0.955	0.84	0.616	0.014	-0.576	-1.127	-0.897	-1.39
regulation of posttranscriptional gene silencing	0.652	0.432	0.275	0.163	0.083	-0.034	-0.15	-0.482	-0.749	-0.188
negative regulation of multicellular organismal process	0.648	0.259	0.07	0.018	0.046	0.165	0.158	-0.579	-1.43	0.645
negative regulation of molecular function	0.648	-0.171	-0.614	-0.773	-0.731	-0.313	0.187	0.511	0.033	1.223
regulation of protein stability	0.647	0.216	0.033	0.022	0.114	0.392	0.53	-0.165	-1.469	-0.318
chromosome organization	0.641	0.406	0.224	0.085	-0.022	-0.171	-0.274	-0.432	-0.466	0.01
positive regulation of cell cycle process	0.637	0.325	0.158	0.092	0.094	0.178	0.224	-0.147	-0.906	-0.654
positive regulation of apoptotic process	0.636	1.278	1.536	1.501	1.251	0.383	-0.613	-1.895	-1.88	-2.198
biological regulation	0.604	0.307	0.103	-0.03	-0.113	-0.197	-0.251	-0.434	-0.498	0.508
regulation of anatomical structure morphogenesis	0.576	-0.473	-1.115	-1.431	-1.495	-1.116	-0.408	0.928	1.641	2.894
regulation of protein ubiquitination	0.562	-0.572	-1.076	-1.119	-0.849	0.129	1.063	1.199	-0.464	1.127
nucleolus	0.561	0.984	1.181	1.196	1.067	0.518	-0.221	-1.554	-2.047	-1.684
positive regulation of intracellular signal transduction	0.538	0.955	1.111	1.069	0.888	0.303	-0.329	-1.063	-1.152	-2.32
negative regulation of catabolic process	0.519	0.213	0.057	0.011	0.04	0.205	0.359	0.21	-0.572	-1.04
regulation of cell differentiation	0.517	0.343	0.2	0.083	-0.012	-0.149	-0.234	-0.307	-0.291	-0.15
cellular component organization or biogenesis	0.505	0.13	-0.143	-0.332	-0.451	-0.534	-0.479	-0.175	0.293	1.187
cell migration	0.503	1.021	1.213	1.159	0.929	0.188	-0.614	-1.487	-1.25	-1.662
regulation of cell cycle	0.502	0.406	0.296	0.18	0.064	-0.144	-0.297	-0.39	-0.287	-0.329
positive regulation of biological process	0.501	0.237	0.055	-0.061	-0.125	-0.142	-0.084	0.023	-0.076	-0.329
regulation of cellular protein localization	0.499	0.718	0.791	0.749	0.62	0.194	-0.315	-1.115	-1.258	-0.884
intracellular protein-containing complex	0.488	-0.539	-1.145	-1.417	-1.431	-0.96	-0.186	1.132	1.598	2.46
protein localization to nucleus	0.487	0.804	0.876	0.766	0.533	-0.113	-0.745	-1.26	-0.72	-0.628
regulation of muscle cell differentiation	0.481	-0.296	-0.688	-0.793	-0.701	-0.216	0.298	0.484	-0.115	1.546
DNA modification	0.478	0.903	1.204	1.374	1.411	1.096	0.326	-1.964	-3.525	-1.301
RNA stem-loop binding	0.465	0.046	-0.191	-0.296	-0.311	-0.209	-0.101	-0.226	-0.407	1.229
cellular response to chemical stimulus	0.44	0.407	0.357	0.294	0.221	0.054	-0.123	-0.439	-0.618	-0.592
tRNA metabolic process	0.422	1.642	2.21	2.279	1.986	0.776	-0.656	-2.428	-2.406	-3.826
perikaryon	0.404	-0.412	-0.909	-1.157	-1.215	-0.969	-0.505	0.339	1.065	3.359
multicellular organismal process	0.398	0.223	0.078	-0.04	-0.131	-0.24	-0.267	-0.15	0.041	0.086
regulation of nucleobase-containing compound metabolic process	0.392	0.342	0.283	0.221	0.156	0.033	-0.073	-0.226	-0.378	-0.751
negative regulation of cellular catabolic process	0.384	0.073	-0.068	-0.084	-0.015	0.242	0.479	0.405	-0.436	-0.981
regulation of multicellular organismal development	0.382	0.483	0.487	0.419	0.299	-0.02	-0.344	-0.709	-0.589	-0.408
multicellular organism development	0.38	0.01	-0.235	-0.377	-0.438	-0.394	-0.229	0.134	0.368	0.781
lipid binding	0.36	-0.899	-1.601	-1.864	-1.798	-1.046	0.036	1.676	2.031	3.107
zinc ion binding	0.286	0.338	0.356	0.351	0.331	0.273	0.215	0.087	-0.358	-1.879
RNA methylation	0.28	0.615	0.82	0.91	0.901	0.645	0.17	-1.002	-1.807	-1.531
Cajal body	0.265	-0.238	-0.714	-1.121	-1.425	-1.636	-1.25	1.011	3.388	1.72
double-stranded RNA binding	0.263	-0.191	-0.354	-0.306	-0.117	0.448	0.953	0.943	-0.43	-1.209
positive regulation of gene expression	0.248	-0.215	-0.502	-0.645	-0.67	-0.473	-0.991	0.695	0.985	0.669
signal transduction	0.246	0.312	0.307	0.252	0.167	-0.034	-0.2	-0.266	-0.143	-0.642
anatomical structure development	0.245	-0.064	-0.247	-0.331	-0.341	-0.228	-0.05	0.182	0.199	0.634
cellular response to organic substance	0.242	0.243	0.213	0.161	0.096	-0.047	-0.168	-0.261	-0.196	-0.284
neuron projection morphogenesis	0.239	-0.894	-1.588	-1.918	-1.955	-1.396	-0.354	1.875	3.045	2.947
negative regulation of organelle organization	0.231	0.54	0.742	0.846	0.862	0.671	0.254	0.892	-1.771	-1.483
nuclear envelope	0.226	0.556	0.727	0.77	0.715	0.41	-0.018	-0.791	-1.162	-1.433
positive regulation of type I interferon production	0.214	0.116	-0.068	-0.293	-0.523	-0.876	-0.955	-0.107	1.357	1.135
intracellular transport	0.19	0.607	0.783	0.78	0.65	0.192	-0.3	-0.768	-0.626	-1.507
behavior	0.19	0.844	1.2	1.314	1.238	0.703	-0.083	-1.514	-2.032	-1.859
regulation of multicellular organismal process	0.188	0.043	-0.065	-0.143	-0.197	-0.246	-0.242	-0.131	0.121	0.672
positive regulation of macromolecule metabolic process	0.17	0.093	0.022	-0.04	-0.089	-0.139	-0.121	0.071	0.223	-0.189
regulation of response to stimulus	0.168	0.08	-0.006	-0.083	-0.148	-0.227	-0.226	-0.007	0.287	0.161
tubulin binding	0.166	0.657	0.843	0.804	0.611	-9E-04	-0.61	-1.013	-0.433	-1.023
translational elongation	0.152	0.321	0.461	0.559	0.603	0.511	0.177	-0.961	-1.723	-0.101
positive regulation of cell projection organization	0.123	-0.506	-0.882	-1.049	-1.048	-0.691	-0.073	1.173	1.674	1.28
cellular response to nitrogen compound	0.09	0.28	0.312	0.231	0.077	-0.314	-0.644	-0.658	0.13	0.496
positive regulation of mRNA metabolic process	0.081	-0.089	-0.169	-0.18	-0.142	0.012	0.181	0.303	0.072	-0.069
regulation of cell morphogenesis	0.077	-2.146	-3.367	-3.798	-3.63	-2.149	-0.027	3.424	4.649	6.968
adenyl ribonucleotide binding	0.071	0.478	0.655	0.662	0.549	0.141	-0.29	-0.639	-0.406	-1.22
ncRNA metabolic process	0.066	0.981	1.405	1.458	1.245	0.377	-0.612	-1.63	-1.218	-2.073
cellular protein catabolic process	0.063	0.506	0.722	0.762	0.673	0.27	-0.224	-0.85	-0.814	-1.107
double-stranded DNA binding	0.05	-0.169	-0.302	-0.361	-0.36	-0.221	0.029	0.555	0.698	0.08
epithelium development	0.048	0.663	0.879	0.809	0.555	-0.175	-0.789	-0.731	0.343	-1.603
ossification	0.044	0.229	0.381	0.496	0.571	0.596	0.458	-0.216	-1.082	-1.476
carbohydrate derivative biosynthetic process	0.041	1.605	2.177	2.027	1.392	-0.537	-2.333	-2.9	-0.037	-1.436
regulation of signal transduction by p53 class mediator	0.034	0.265	0.522	0.774	0.989	1.223	1.106	-0.223	-2.178	-2.511
regulation of cellular protein catabolic process	0.018	0.583	0.96	1.169	1.228	0.971	0.348	-1.338	-2.447	-1.492
positive regulation of lymphocyte activation	0.018	0.837	1.206	1.225	0.984	0.039	-1.086	-2.42	-1.539	0.736
cell communication	0.01	0.14	0.207	0.227	0.211	0.117	-0.004	-0.169	-0.224	-0.516
regulation of protein kinase activity	0.007	0.862	1.219	1.199	0.912	-0.088	-1.159	-2.054	-0.882	-0.016
positive regulation of cellular metabolic process	-5E-04	-0.039	-0.068	-0.086	-0.093	-0.077	-0.025	0.134	0.23	0.025
innate immune response	-0.002	-0.315	-0.488	-0.548	-0.519	-0.281	0.076	0.711	0.853	0.514
positive regulation of multicellular organismal process	-0.004	0.088	0.086	0.019	-0.089	-0.342	-0.535	-0.442	0.285	0.932
positive regulation of molecular function	-0.01	-0.266	-0.397	-0.432	-0.396	-0.197	0.055	0.39	0.439	0.814
positive regulation of nitrogen compound metabolic process	-0.013	-0.053	-0.078	-0.091	-0.092	-0.063	-0.003	0.15	0.222	0.021
ubiquitin-dependent protein catabolic process	-0.015	0.529	0.824	0.921	0.867	0.47	-0.089	-0.985	-1.188	-1.334
regulation of gene expression	-0.018	-0.118	-0.172	-0.193	-0.188	-0.133	-0.056	0.07	0.191	0.617
nucleic acid phosphodiester bond hydrolysis	-0.018	-0.181	-0.323	-0.434	-0.505	-0.506	-0.309	0.526	1.265	0.485
ribonucleoprotein complex subunit organization	-0.018	-0.119	-0.192	-0.239	-0.259	-0.234	-0.135	0.192	0.499	0.507
regulation of protein-containing complex assembly	-0.02	-0.185	-0.223	-0.166	-0.046	0.286	0.6	0.745	0.04	-1.032
RNA polymerase II-specific DNA-binding transcription factor binding	-0.032	0.294	0.494	0.587	0.589	0.382	-0.004	-0.863	-1.177	-0.27
ncRNA processing	-0.04	0.934	1.408	1.503	1.325	0.511	-0.443	-1.462	-1.21	2.524
ribonucleoprotein complex biogenesis	-0.047	0.29	0.454	0.488	0.426	0.142	-0.195	-0.554	-0.403	-0.6
ribonucleoprotein complex assembly	-0.059	-0.135	-0.193	-0.232	-0.251	-0.23	-0.138	0.196	0.53	0.513
cellular response to heat	-0.062	1.591	2.305	2.314	1.822	0.046	-1.865	-3.43	-1.533	-1.188
positive regulation of cell cycle phase transition	-0.063	-0.622	-0.821	-0.762	-0.533	0.139	0.727	0.778	-0.155	1.312
protein-containing complex binding	-0.07	-0.196	-0.315	-0.417	-0.492	-0.54	-0.429	0.226	1.066	1.167
regulation of immune system process	-0.074	-0.04	-0.003	0.035	0.073	0.143	0.194	0.198	-0.008	-0.518
signaling	-0.078	0.055	0.132	0.166	0.168	0.113	0.03	-0.082	-0.118	-0.386
regulation of immune response	-0.084	-0.182	-0.162	-0.062	0.079	0.375	0.548	0.241	-0.558	-0.196
microtubule-based process	-0.085	0.607	0.908	0.915	0.714	-0.019	-0.805	-1.423	-0.556	-0.256
DNA duplex unwinding	-0.086	-0.419	-0.584	-0.62	-0.563	-0.293	0.03	0.426	0.558	1.55
positive regulation of cell communication	-0.089	-0.175	-0.162	-0.081	0.041	0.31	0.498	0.358	-0.301	-0.398
DNA geometric change	-0.096	-0.246	-0.343	-0.396	-0.41	-0.345	-0.188	0.259	0.714	1.051
cellular component organization	-0.123	-0.517	-0.734	-0.81	-0.78	-0.516	-0.133	0.552	1.021	2.041
chemical homeostasis	-0.124	-0.655	-0.755	-0.556	-0.174	0.755	1.433	0.972	-1.043	0.149
developmental process involved in reproduction	-0.153	0.212	0.406	0.47	0.444	0.243	0.005	-0.192	-0.172	-1.263
cellular component biogenesis	-0.17	-0.014	0.055	0.062	0.029	-0.093	-0.199	-0.132	0.24	0.222
spermatogenesis	-0.178	0.21	0.407	0.46	0.412	0.15	-0.151	-0.384	-0.17	-0.753
positive regulation of cell differentiation	-0.185	0.08	0.23	0.29	0.281	0.132	-0.087	-0.39	-0.299	-0.051
protein-containing complex	-0.185	-0.231	-0.21	-0.149	-0.07	0.072	0.119	-0.136	-0.321	1.112
negative regulation of cell differentiation	-0.203	-0.09	0.023	0.128	0.218	0.331	0.338	0.044	-0.406	-0.383
proteolysis involved in cellular protein catabolic process	-0.206	0.131	0.342	0.45	0.475	0.357	0.117	-0.369	-0.596	-0.7
phosphorylation	-0.212	0.179	0.337	0.327	0.204	-0.192	-0.547	-0.523	0.316	0.11
regulation of autophagy	-0.226	-1.743	-2.595	-2.908	-2.8	-1.73	-0.089	2.971	4.324	4.797
positive regulation of hydrolase activity	-0.231	0.246	0.506	0.592	0.54	0.167	-0.368	-1.182	-0.911	0.641
cell growth	-0.234	0.603	0.966	0.979	0.751	-0.059	-0.868	-1.232	-0.093	-0.814
negative regulation of cell death	-0.248	0.577	0.961	1.012	0.827	0.073	-0.762	-1.434	-0.558	-0.447
carbohydrate derivative binding	-0.25	0.155	0.358	0.413	0.367	0.124	-0.126	-0.178	0.117	-0.979
ATP binding	-0.256	0.246	0.502	0.573	0.515	0.191	-0.176	-0.423	-0.136	-1.035
regulation of cell development	-0.256	-1.084	-1.472	-1.519	-1.312	-0.436	0.641	2.095	1.93	1.413
positive regulation of cellular process	-0.259	-0.394	-0.429	-0.39	-0.299	-0.035	0.24	0.54	0.465	0.561
cytoskeleton-dependent intracellular transport	-0.273	-0.439	-0.548	-0.605	-0.612	-0.499	-0.246	0.504	1.237	1.479
cell motility	-0.275	0.652	1.149	1.314	1.232	0.625	-0.184	-1.247	-1.244	-2.021
protein localization	-0.281	-0.046	0.088	0.147	0.153	0.079	-0.013	-0.014	0.153	-0.266
catalytic step 2 spliceosome	-0.288	0.511	0.98	1.188	1.197	0.832	0.24	-0.775	-1.295	-2.591
regulation of cell growth	-0.301	0.396	0.688	0.687	0.49	-0.165	-0.758	-0.746	0.431	-0.721
RNA export from nucleus	-0.312	0.381	0.838	1.097	1.192	1.019	0.538	-0.697	-1.689	-2.366
regulation of neuron projection development	-0.332	-0.283	-0.352	-0.485	-0.634	-0.837	-0.751	0.475	2.103	1.097
positive regulation of cellular protein localization	-0.338	0.139	0.442	0.6	0.64	0.465	0.095	-0.687	-0.939	-0.418
U2-type catalytic step 2 spliceosome	-0.348	0.6	1.115	1.293	1.222	0.635	-0.15	-1.159	-1.139	-2.069
tRNA processing	-0.351	0.934	1.627	1.865	1.771	0.995	-0.026	-1.311	-1.526	-3.979
cell junction organization	-0.352	-0.025	0.228	0.405	0.506	0.488	0.219	-0.711	-1.197	0.437
response to oxidative stress	-0.362	-0.379	-0.153	0.208	0.609	1.243	1.333	-0.452	-2.747	0.699
regulation of cell cycle process	-0.369	-0.252	-0.161	-0.091	-0.04	0.023	0.053	0.097	0.225	0.515
regulation of hemopoiesis	-0.38	0.287	0.596	0.639	0.5	0.044	-0.588	0.741	0.182	-0.45
regulation of response to biotic stimulus	-0.398	-0.207	-0.026	0.137	0.276	0.46	0.501	0.183	-0.388	-0.539
regulation of macromolecule metabolic process	-0.401	-0.302	-0.226	-0.169	-0.125	-0.057	0.007	0.187	0.443	0.642
cellular localization	-0.421	0.29	0.681	0.827	0.792	0.401	-0.124	-0.728	-0.562	-1.154
signaling receptor binding	-0.423	0.158	0.44	0.498	0.398	-0.051	-0.54	-0.794	0.031	0.283
ribosome biogenesis	-0.441	0.489	0.995	1.172	1.108	0.549	-0.194	-1.089	-0.927	-1.662
gamete generation	-0.449	0.008	0.275	0.401	0.425	0.306	0.137	0.055	0.101	-1.258
developmental process	-0.457	-0.341	-0.214	-0.087	0.029	0.2	0.261	0.083	-0.11	0.635
multicellular organism reproduction	-0.46	0.026	0.301	0.418	0.424	0.262	0.064	0.022	0.184	-1.241
regulation of molecular function	-0.466	-0.637	-0.675	-0.614	-0.484	-0.118	0.26	0.7	0.747	1.285
negative regulation of transcription by RNA polymerase II	-0.468	-1.007	-1.241	-1.24	-1.064	-0.402	0.39	1.498	1.627	1.907
positive regulation of cell population proliferation	-0.484	-0.073	0.25	0.496	0.673	0.848	0.826	0.334	-0.658	-2.211
positive regulation of developmental process	-0.493	-0.002	0.303	0.455	0.484	0.281	-0.107	-0.811	-0.706	0.597
DNA conformation change	-0.496	0.146	0.488	0.599	0.542	0.142	-0.354	-0.787	-0.234	-0.047
cell population proliferation	-0.499	0.019	0.363	0.563	0.646	0.56	0.279	-0.379	-0.735	-0.817
negative regulation of cellular process	-0.499	-0.55	-0.509	-0.403	-0.255	0.089	0.397	0.649	0.471	0.61

regulation of developmental process	0.359	0.275	0.192	0.107	0.02	-0.159	-0.34	-0.606	-0.462	0.614
muscle organ development	0.358	-0.774	-1.383	-1.587	-1.496	-0.791	0.133	1.28	1.315	2.946
hemopoiesis	0.349	0.19	0.078	0.005	-0.04	-0.073	-0.072	-0.092	-0.182	-0.164
gene silencing by miRNA	0.334	-0.461	-0.889	-1.03	-0.956	-0.413	0.322	1.3	1.076	0.717
positive regulation of cytokine production	0.299	0.104	-0.086	-0.257	-0.398	-0.556	-0.522	0.065	0.822	0.527
cellular response to radiation	0.288	-0.144	-0.357	-0.401	-0.324	0.038	0.458	0.807	0.203	-0.568
regulation of cellular process	0.287	0.204	0.142	0.092	0.049	-0.034	-0.13	-0.358	-0.429	0.176
biological process involved in interaction with symbiont	-0.505	-1.68	-2.185	-2.179	-1.803	-0.435	1.113	2.849	2.278	2.547
regulation of mitotic cell cycle	-0.507	-0.145	0.111	0.278	0.37	0.386	0.258	-0.129	-0.355	-0.268
negative regulation of transcription, DNA-templated	-0.517	-0.3	-0.137	-0.017	0.067	0.159	0.189	0.197	0.215	0.144
negative regulation of nitrogen compound metabolic process	-0.519	-0.297	-0.119	0.021	0.127	0.256	0.301	0.235	0.082	-0.086
establishment of localization	-0.527	-0.351	-0.198	-0.07	0.033	0.172	0.23	0.182	0.125	0.404
endoplasmic reticulum	-0.543	0.094	0.476	0.658	0.691	0.482	0.132	-0.342	-0.398	-1.25
developmental growth	-0.564	0.308	0.819	1.047	1.062	0.694	0.113	-0.74	-0.898	-1.842
maturation of 5.8S rRNA	-0.574	0.847	1.518	1.625	1.336	0.138	-1.153	-1.994	-0.483	-1.259
regulation of metabolic process	-0.575	-0.464	-0.368	-0.284	-0.209	-0.073	0.057	0.341	0.657	0.918
regulation of protein modification process	-0.584	-0.502	-0.347	-0.151	0.061	0.441	0.665	0.467	-0.189	0.139
regulation of cell death	-0.601	0.073	0.47	0.649	0.661	0.37	-0.091	-0.727	-0.544	-0.26
cytoskeleton organization	-0.611	0.086	0.424	0.496	0.384	-0.116	-0.624	-0.705	0.398	0.269
DNA replication	-0.62	-0.735	-0.715	-0.605	-0.444	-0.092	0.158	0.16	0.218	2.676
locomotion	-0.62	0.319	0.842	1.046	1.017	0.552	-0.076	-0.753	-0.565	-1.761
ATP-dependent activity, acting on DNA	-0.631	-0.164	0.154	0.349	0.446	0.432	0.261	-0.136	-0.304	-0.407
focal adhesion	-0.64	-0.267	-0.109	-0.105	-0.197	-0.49	-0.691	-0.231	1.163	1.567
regulation of DNA metabolic process	-0.65	-0.125	0.21	0.396	0.47	0.404	0.216	-0.053	-0.094	-0.774
RNA polymerase II transcription regulatory region sequence-specific DNA binding	-0.653	-0.683	-0.663	-0.594	-0.48	-0.136	0.319	1.259	1.547	0.082
negative regulation of cellular metabolic process	-0.654	-0.545	-0.398	-0.23	-0.055	0.269	0.504	0.582	0.281	0.245
growth	-0.677	0.53	1.127	1.267	1.086	0.217	-0.74	-1.319	-0.195	-1.296
DNA-binding transcription factor binding	-0.699	-0.56	-0.404	-0.245	-0.093	0.159	0.313	0.321	0.253	0.955
ATP hydrolysis activity	-0.701	-0.293	-0.007	0.182	0.298	0.382	0.369	0.31	0.176	-0.715
cell cycle process	-0.704	-0.585	-0.469	-0.358	-0.252	-0.059	0.11	0.396	0.704	1.217
negative regulation of apoptotic process	-0.715	0.164	0.63	0.779	0.698	0.143	-0.543	-1.124	-0.274	0.241
transport	-0.727	-0.515	-0.322	-0.147	0.005	0.241	0.383	0.425	0.305	0.353
response to abiotic stimulus	-0.729	0.19	0.657	0.78	0.656	0.003	-0.75	-1.264	-0.111	0.569
response to external stimulus	-0.75	-0.358	-0.13	-0.021	0.009	-0.041	-0.077	0.258	0.877	0.232
protein localization to nucleolus	-0.756	0.014	0.531	0.825	0.93	0.696	0.071	-1.409	-1.717	0.815
regulation of cellular response to stress	-0.764	-0.614	-0.58	-0.615	-0.677	-0.755	-0.623	0.507	2.134	1.987
positive regulation of macromolecule biosynthetic process	-0.783	-0.568	-0.397	-0.257	-0.141	0.051	0.225	0.581	0.821	0.468
DNA metabolic process	-0.786	-0.345	-0.032	0.176	0.302	0.383	0.339	0.189	0.095	-0.321
RNA methyltransferase activity	-0.788	0.072	0.655	1.001	1.148	0.993	0.452	-0.926	-1.643	-0.964
catalytic activity	-0.796	0.126	0.633	0.827	0.799	0.38	-0.135	-0.432	0.069	-1.473
peptidyl-serine modification	-0.802	0.162	0.723	0.961	0.952	0.447	-0.338	-1.493	-1.101	0.488
S-adenosylmethionine-dependent methyltransferase activity	-0.805	0.024	0.563	0.864	0.974	0.789	0.301	-0.736	-1.111	-0.863
regulation of nitrogen compound metabolic process	-0.812	-0.346	-0.039	0.145	0.236	0.239	0.143	0.063	0.26	0.11
modification-dependent macromolecule catabolic process	-0.814	0.502	1.224	1.494	1.439	0.775	-0.079	-0.889	-0.625	-3.027
generation of precursor metabolites and energy	-0.826	1.584	2.66	2.749	2.162	-0.008	-2.183	-3.09	-0.08	-2.969
cellular developmental process	-0.834	-0.676	-0.49	-0.29	-0.092	0.257	0.495	0.569	0.362	0.699
osteoblast differentiation	-0.836	-0.575	-0.279	0.023	0.309	0.761	0.971	0.573	-0.424	-0.524
positive regulation of cellular biosynthetic process	-0.836	-0.564	-0.372	-0.239	-0.146	-0.014	0.121	0.556	0.99	0.504
cell differentiation	-0.858	-0.798	-0.654	-0.456	-0.228	0.229	0.588	0.787	0.515	0.874
macromolecule modification	-0.865	-0.002	0.528	0.796	0.868	0.647	0.229	-0.348	-0.402	-1.452
regulatory RNA binding	-0.865	-0.483	-0.199	0.009	0.162	0.365	0.507	0.741	0.63	-0.866
purine ribonucleotide binding	-0.87	-0.114	0.322	0.514	0.535	0.291	-0.033	-0.138	0.331	-0.838
cell development	-0.881	-0.473	-0.193	-0.012	0.093	0.168	0.173	0.282	0.547	0.295
cell-cell signaling	-0.889	-1.239	-1.303	-1.159	-0.872	-0.098	0.657	1.373	1.203	2.327
cellular response to organonitrogen compound	-0.898	-0.359	-0.048	0.09	0.104	-0.074	-0.307	-0.285	0.568	1.208
catalytic activity, acting on RNA	-0.909	-0.411	-0.063	0.168	0.309	0.419	0.42	0.417	0.346	-0.695
regulation of apoptotic process	-0.929	-0.204	0.253	0.495	0.571	0.398	0.028	-0.521	-0.3	0.209
small molecule binding	-0.934	-0.149	0.305	0.509	0.534	0.289	-0.044	-0.158	0.352	-0.704
organelle envelope	-0.941	0.55	1.349	1.624	1.524	0.703	-0.298	-1.109	-0.491	-2.912
cellular response to stress	-0.968	-0.496	-0.167	0.049	0.174	0.241	0.183	0.093	0.304	0.589
intracellular non-membrane-bounded organelle	-0.97	-0.627	-0.33	-0.08	0.118	0.363	0.473	0.19	-0.074	0.96
regulation of cell adhesion	-0.977	0.295	1.061	1.422	1.47	0.95	0.049	-1.44	-1.564	-1.266
reproduction	-0.982	-0.604	-0.317	-0.104	0.052	0.25	0.368	0.551	0.644	0.142
cellular nitrogen compound biosynthetic process	-0.989	-0.994	-0.901	-0.736	-0.523	-0.034	0.435	1.026	1.167	1.549
cellular component assembly	-0.994	-0.836	-0.681	-0.53	-0.38	-0.087	0.198	0.735	1.172	1.404
intracellular signal transduction	-0.997	-0.828	-0.673	-0.524	-0.378	-0.075	0.251	0.931	1.368	0.926
regulation of phosphate metabolic process	-0.997	-0.538	-0.261	-0.116	-0.064	-0.094	-0.128	0.243	1.058	0.898
regulation of cellular metabolic process	-1	-0.526	-0.195	0.022	0.153	0.242	0.225	0.236	0.453	0.39
regulation of biological quality	-1.021	-0.988	-0.829	-0.587	-0.298	0.294	0.757	0.97	0.56	1.141
response to nutrient levels	-1.025	0.451	1.218	1.449	1.299	0.378	-0.696	-1.434	-0.25	-1.39
protein binding	-1.03	-0.583	-0.18	0.172	0.464	0.855	0.978	0.519	-0.405	-0.789
microtubule binding	-1.031	0.479	1.271	1.516	1.363	0.381	-0.823	-1.898	-0.694	-0.565
spermatid development	-1.036	-0.709	-0.438	-0.208	-0.005	0.354	0.685	1.227	1.094	-0.964
regulation of DNA recombination	-1.05	-0.049	0.393	0.447	0.259	-0.361	-0.735	0.405	2.407	-1.717
positive regulation of cell cycle	-1.054	-1.302	-1.274	-1.047	-0.688	0.2	1.02	1.68	1.113	1.352
positive regulation of cellular component biogenesis	-1.055	-2.127	-2.56	-2.497	-2.065	-0.542	1.252	3.701	3.519	2.374
germ cell development	-1.056	-0.383	0.094	0.425	0.649	0.911	1.069	1.278	0.567	-3.554
reproductive system development	-1.083	-1.577	-1.701	-1.552	-1.216	-0.271	0.675	1.635	1.615	3.473
gene silencing by RNA	-1.084	-1.494	-1.603	-1.482	-1.192	-0.318	0.658	2.023	2.211	2.279
gene silencing	-1.096	-1.315	-1.335	-1.199	-0.947	-0.232	0.572	1.805	2.071	1.675
cellular response to starvation	-1.097	0.319	1.179	1.598	1.68	1.189	0.308	-1.138	-1.5	-2.538
nucleoside-triphosphatase activity	-1.11	-0.672	-0.352	-0.123	0.038	0.232	0.353	0.621	0.832	0.181
regulation of phosphorylation	-1.123	-0.827	-0.583	-0.383	-0.217	0.041	0.241	0.602	0.983	1.267
regulation of growth	-1.158	-0.178	0.335	0.501	0.431	-0.057	-0.549	-0.37	1.025	0.019
purine ribonucleoside triphosphate binding	-1.164	-0.322	0.185	0.436	0.504	0.336	0.07	0.055	0.573	-0.672
structural molecule activity	-1.166	1.499	2.822	3.132	2.723	0.739	-1.517	-3.286	-1.309	-3.637
cellular protein modification process	-1.169	-0.346	0.176	0.467	0.588	0.528	0.329	0.213	0.36	-1.147
nucleotide binding	-1.179	-0.229	0.332	0.595	0.644	0.38	-0.008	-0.184	0.382	-0.732
biosynthetic process	-1.203	-1.038	-0.842	-0.627	-0.403	0.031	0.407	0.895	1.14	1.64
organic substance biosynthetic process	-1.226	-1.075	-0.883	-0.663	-0.43	0.033	0.439	0.957	1.184	1.664
melanosome	-1.229	-0.263	0.182	0.243	0.041	-0.735	-1.466	-1.261	1.328	3.16
regulation of intracellular signal transduction	-1.233	-0.895	-0.6	-0.343	-0.12	0.241	0.51	0.838	0.92	0.682
regulation of signal transduction	-1.239	-0.756	-0.385	-0.106	0.096	0.335	0.436	0.503	0.585	0.53
cell adhesion	-1.24	0.526	1.533	1.946	1.912	1.02	-0.284	-2.007	-1.638	-1.768
anion binding	-1.24	-0.333	0.208	0.473	0.54	0.344	0.047	0.03	0.616	-0.684
regulation of DNA-binding transcription factor	-1.244	-3.034	-3.707	-3.549	-2.817	-0.484	1.91	3.969	2.784	6.173
cellular biosynthetic process	-1.249	-1.093	-0.894	-0.669	-0.429	0.045	0.458	0.976	1.189	1.665
mitotic spindle organization	-1.274	-0.268	0.218	0.321	0.16	-0.541	-1.221	-1.04	1.254	2.39
endomembrane system	-1.318	-0.365	0.262	0.627	0.788	0.704	0.354	-0.261	-0.279	-0.512
cell morphogenesis involved in differentiation	-1.338	-1.017	-0.773	-0.581	-0.42	-0.12	0.223	1.127	1.863	1.036
macromolecule biosynthetic process	-1.348	-1.193	-0.984	-0.74	-0.478	0.049	0.514	1.098	1.314	1.77
hydrolase activity, acting on acid anhydrides, in phosphorus-containing anhydrides	-1.359	-0.744	-0.315	-0.029	0.151	0.318	0.386	0.635	0.926	0.03
cellular macromolecule biosynthetic process	-1.372	-1.211	-0.996	-0.746	-0.477	0.061	0.533	1.117	1.32	1.77
biological adhesion	-1.376	0.477	1.535	1.971	1.941	1.019	-0.33	-2.077	-1.591	-1.568
signal transduction by p53 class mediator	-1.478	-1.144	-0.765	-0.369	0.018	0.684	1.112	1.112	0.4	0.431
localization	-1.482	-0.737	-0.193	0.187	0.434	0.64	0.617	0.391	0.256	-0.112
3'-UTR-mediated mRNA destabilization	-1.488	-2.026	-2.183	-2.056	-1.732	-0.771	0.249	1.601	2.459	5.947
negative regulation of metabolic process	-1.491	-1.203	-0.909	-0.617	-0.334	0.183	0.604	1.109	1.256	1.403
nervous system process	-1.499	0.289	1.345	1.832	1.893	1.233	0.181	1.193	-1.143	-2.938
catalytic activity, acting on a nucleic acid	-1.515	-0.704	-0.138	0.233	0.454	0.595	0.537	0.417	0.452	-0.331
nervous system development	-1.521	-1.321	-1.071	-0.788	-0.488	0.113	0.646	1.327	1.5	1.603
muscle cell differentiation	-1.53	-0.908	-0.477	-0.192	-0.016	0.145	0.22	0.576	1.199	0.982
regulation of macromolecule biosynthetic process	-1.53	-0.98	-0.556	-0.235	0.002	0.298	0.455	0.666	0.922	0.96
myeloid cell differentiation	-1.549	-1.404	-1.194	-0.938	-0.651	-0.047	0.523	1.355	1.753	2.153
sexual reproduction	-1.552	-0.876	-0.382	-0.032	0.208	0.467	0.578	0.754	0.865	-0.029
presynapse	-1.553	-1.695	-1.691	-1.565	-1.342	-0.688	0.12	1.753	2.972	1.689
negative regulation of biological process	-1.554	-1.342	-1.085	-0.798	-0.497	0.098	0.623	1.296	1.51	1.749
regulation of cellular macromolecule biosynthetic process	-1.556	-0.999	-0.568	-0.241	0.003	0.311	0.475	0.686	0.928	0.961
transcription corepressor activity	-1.574	-0.104	0.819	1.304	1.447	1.049	0.213	-1.206	-1.222	-0.725
ncRNA catabolic process	-1.578	-0.815	-0.348	-0.095	0.011	0.019	0.036	0.733	1.773	0.263
protein stabilization	-1.582	-0.698	-0.047	0.401	0.675	0.806	0.556	-0.331	-0.616	0.836
response to stress	-1.619	-1.031	-0.588	-0.262	-0.029	0.242	0.371	0.586	0.992	1.338
proteolysis	-1.619	-0.483	0.239	0.634	0.779	0.593	0.135	-0.449	-0.025	0.198
regulation of protein phosphorylation	-1.623	-1.041	-0.605	-0.286	-0.06	0.207	0.345	0.618	1.083	1.361
hydrolase activity	-1.643	-0.791	-0.202	0.179	0.403	0.545	0.502	0.49	0.675	-0.159
catalytic activity, acting on DNA	-1.645	-0.466	0.306	0.747	0.927	0.753	0.219	-0.727	-0.55	0.436
positive regulation of response to biotic stimulus	-1.647	-1.194	-0.798	-0.452	-0.152	0.334	0.692	1.116	1.204	0.896
regulation of gene silencing by miRNA	-1.659	-1.582	-1.348	-1.003	-0.591	0.296	1.083	1.855	1.563	1.388
RNA helicase activity	-1.686	-1.253	-0.877	-0.544	-0.243	0.301	0.796	1.616	1.76	0.131
modulation by host of symbiont process	-1.69	-2.978	-3.387	-3.134	-2.413	-0.226	2.083	4.535	3.559	3.651
organelle organization	-1.699	-1.068	-0.597	-0.254	-0.014	0.253	0.367	0.566	1.01	1.437
protein phosphorylation	-1.699	-0.802	-0.194	0.185	0.39	0.465	0.341	0.251	0.636	0.428
miRNA binding	-1.72	-1.119	-0.643	-0.267	0.033	0.475	0.797	1.269	1.296	-0.122
cell part morphogenesis	-1.735	-1.206	-0.865	-0.649	-0.505	-0.269	0.092	1.466	2.771	0.899
response to biotic stimulus	-1.761	-1.317	-0.942	-0.621	-0.343	0.129	0.535	1.253	1.716	1.35
cellular process involved in reproduction in multicellular organism	-1.766	-0.771	-0.059	0.436	0.767	1.121	1.277	1.437	0.794	-3.236
microtubule cytoskeleton organization involved in mitosis	-1.769	-0.708	-0.098	0.174	0.208	-0.103	-0.481	-0.234	1.382	1.63
response to other organism	-1.775	-1.347	-0.974	-0.646	-0.355	0.147	0.577	1.289	1.699	1.385
nitrogen compound transport	-1.79	-0.973	-0.356	0.093	0.402	0.703	0.73	0.489	0.349	0.354
immune response	-1.829	-1.23	-0.748	-0.365	-0.062	0.366	0.639	0.988	1.208	1.032
regulation of neuron death	-1.834	-0.346	0.641	1.223	1.49	1.376	0.811	-0.365	-0.912	-2.084
miRNA 3'-UTR AU-rich region binding	-1.834	0.029	1.166	1.721	1.825	1.139	-0.098	-2.064	-1.763	-0.122
catalytic activity, acting on a protein	-1.847	-0.067	0.957	1.409	1.455	0.873	0.092	-0.277	0.472	-3.068
helicase activity	-1.848	-1.277	-0.81	-0.426	-0.107	0.396	0.788	1.385	1.53	0.368
endoribonuclease activity, producing 5'-phosphomonoesters	-1.867	-1.03	-0.268	0.394	0.934	1.594	1.667	0.359	-1.389	-0.395
movement of cell or subcellular component	-1.869	-0.491	0.367	0.818	0.965	0.696	0.143	-0.432	0.124	-0.322
nuclear receptor binding	-1.882	-1.219	-0.669	-0.218	0.144	0.648	0.92	1.018	0.807	0.449
regulation of cell communication	-1.887	-1.405	-0.94	-0.504	-0.108	0.532	0.945	1.13	0.905	1.331
synapse	-1.893	-2.138	-2.073	-1.778	-1.323	-0.174	0.98	2.422	2.612	3.364
plasma membrane bounded cell projection organization	-1.893	-1.711	-1.514	-1.301	-1.068	-0.541	0.068	1.457	2.825	3.677
U2 snRNP	-1.897	0.469	1.713	2.088	1.818	0.132	-2.005	-4.155	-1.447	3.284
organic substance transport	-1.941	-1.294	-0.744	-0.286	0.086	0.603	0.864	0.884	0.733	1.095
protein C-terminus binding	-1.948	-2.58	-2.698	-2.431	-1.898	-0.421	1.095	2.873	3.04	4.968
postsynapse	-1.964	-2.02	-1.94	-1.741	-1.44	-0.597	0.45	2.588	3.801	2.864
ribosomal small subunit biogenesis	-1.991	1.373	3.076	3.524	3.078	0.731	-1.964	-3.939	-1.042	-2.846
cell-cell adhesion	-1.995	-0.349	0.667	1.187	1.33	0.902	0.081	-0.993	-0.487	-0.342
GTPase binding	-1.996	-1.862	-1.825	-1.84	-1.867	-1.821	-1.474	0.547	4.168	7.97
production of miRNAs involved in gene silencing by miRNA	-2.01	-1.375	-0.829	-0.356	0.055	0.727	1.237	1.801	1.445	-0.695
neuron projection development	-2.029	-1.596	-1.265	-1.006	-0.795	-0.431	-0.038	1.094	2.573	3.491
immune system process	-2.04	-1.583	-1.163	-0.776	-0.421	0.199	0.708	1.432	1.803	1.84
generation of neurons	-2.073	-1.422	-0.953	-0.619	-0.382	-0.065	0.208	1.046	2.135	2.126
neuron differentiation	-2.088	-1.415	-0.944	-0.622	-0.406	-0.141	0.092	0.95	2.203	2.371
regulation of neurogenesis	-2.088	-2.496	-2.501	-2.198	-1.671	-0.246	1.276	3.351	3.51	3.063
negative regulation of developmental process	-2.091	-1.802	-1.401	-0.934	-0.443	0.478	1.163	1.548	1.202	2.28
regulation of nervous system development	-2.099	-2.063	-1.821	-1.429	-0.938	0.167	1.209	2.439	2.372	2.162
defense response	-2.099	-1.447	-0.903	-0.452	-0.077	0.492	0.887	1.355	1.439	0.804
distal axon	-2.104	-1.621	-1.207	-0.851	-0.544	-0.039	0.373	1.112	1.942	2.94
ATP-dependent activity	-2.116	-1.296	-0.672	-0.205	0.139	0.578	0.833	1.196	1.332	0.21
nuclear export	-2.128	-0.982	-0.119	0.503	0.921	1.285	1.216	0.504	-0.265	-0.935
nuclear organization	-2.13	-1.689	-1.371	-1.129	-0.92	-0.476	0.136	1.971	3.582	2.026
regulation of plasma membrane bounded cell projection organization	-2.164	-1.484	-1.036	-0.759	-0.596	-0.428	-0.232	0.837	2.623	3.24
positive regulation of posttranscriptional gene silencing	-2.171	-1.688	-1.202	-0.73	-0.287	0.473	1.019	1.443	1.353	1.789
biological process involved in interspecies interaction between organisms	-2.173	-1.589	-1.096	-0.679	-0.321	0.26	0.728	1.472	1.901	1.498
nuclear membrane	-2.177	-1.36	-0.694	-0.162	0.25	0.774	0.989	0.888	0.65	0.841
regulation of cytokine production	-2.185	-2.338	-2.245	-1.962	-1.538	-0.444	0.742	2.63	3.453	3.886
cell morphogenesis involved in neuron differentiation	-2.211	-1.659	-1.25	-0.939	-0.686	-0.231	0.297	1.765	3.064	1.85
microtubule	-2.221	-1.286	-0.693	-0.353	-0.189	-0.133	-0.11	0.685	2.254	0.496
regulation of cellular component biogenesis	-2.243	-2.287	-2.078	-1.683	-1.162	0.052	1.225	2.665	2.723	2.788
regulation of proteolysis	-2.3	-1.036	-0.184	0.336	0.594	0.581	0.216	-0.34	0.307	1.825
transport along microtubule	-2.311	-1.904	-1.472	-1.032	-0.602	0.186	0.82	1.562	1.913	2.841
cell morphogenesis	-2.313	-2.095	-1.841	-1.547	-1.214	-0.439	0.453	2.325	3.606	3.066
catabolic process	-2.341	-1.517	-0.9	-0.447	-0.122	0.28	0.521	1.031	1.722	1.773
cell body	-2.353	-2.397	-2.142	-1.682	-1.099	0.165	1.234	2.069	1.903	4.303
signal transduction in response to DNA damage	-2.357	-2.437	-2.178	-1.669	-0.992	0.586	2.081	3.633	2.709	0.625
positive regulation of growth	-2.365	-1.612	-0.99	-0.482	-0.069	0.528	0.907	1.302	1.459	1.321
neurogenesis	-2.369	-1.432	-0.773	-0.328	-0.04	0.25	0.404	0.967	1.853	1.467
response to starvation	-2.4	-0.264	1.01	1.613	1.718	1.015	-0.121	-1.35	-0.42	-0.801
regulation of catabolic process	-2.409	-2.043	-1.623	-1.172	-0.71	0.184	0.953	1.921	2.239	2.66
regulation of cell projection organization	-2.425	-2.379	-2.235	-2.006	-1.704	-0.921	0.028	2.127	4.069	5.446
cellular response to oxidative stress	-2.442	-1.927	-1.177	-0.32	0.537	1.918	2.493	0.895	-1.804	1.828
in utero embryonic development	-2.459	-2.232	-1.904	-1.501	-1.05	-0.088	0.837	2.228	2.882	3.287
transcription factor binding	-2.461	-1.849	-1.296	-0.797	-0.349	0.413	1.014	1.789	-2	1.536
regulation of RNA stability	-2.481	-2.012	-1.538	-1.07	-0.618	0.208	0.895	1.792	2.197	2.626
RNA destabilization	-2.487	-1.514	-0.786	-0.254	0.125	0.574	0.804	1.174	1.529	0.834
positive regulation of cellular catabolic process	-2.511	-1.753	-1.146	-0.663	-0.276	0.296	0.715	1.43	2.031	1.877
regulation of cellular catabolic process	-2.511	-2.139	-1.705	-1.233	-0.745	0.201	1.019	2.037	2.341	2.736
macromolecule localization	-2.537	-1.506	-0.706	-0.101	0.343	0.862	1.055	1.031	0.928	0.631
defense response to other organism	-2.542	-1.886	-1.297	-0.771	-0.305	0.461	1.03	1.68	1.858	1.772
cell periphery	-2.55	-1.897	-1.359	-0.913	-0.541	0.048	0.52	1.394	2.314	2.983
positive regulation of viral genome replication	-2.566	-1.972	-1.285	-0.578	0.089	1.118	1.564	0.727	-0.409	3.31
mRNA destabilization	-2.574	-1.612	-0.872	-0.312	0.103	0.626	0.906	1.248	1.501	0.986
ribosome	-2.6	-1.003	0.127	0.869	1.294	1.453	1.058	-0.1	-0.602	-0.496
multi-organism reproductive process	-2.603	-1.545	-0.757	-0.187	0.215	0.671	0.881	1.181	1.471	0.673
negative regulation of response to stimulus	-2.616	-2.173	-1.697	-1.208	-0.723	0.177	0.923	1.846	2.284	3.186
ribonucleoprotein complex	-2.621	-1.837	-1.148	-0.555	-0.056	0.666	1.059	1.153	1.103	2.236
cellular catabolic process	-2.644	-1.8	-1.125	-0.59	-0.169	0.423	0.806	1.352	1.834	1.912
anchoring junction	-2.657	-1.985	-1.437	-0.986	-0.611	-0.005	0.508	1.542	2.595	3.035
regulation of cell-cell adhesion	-2.671	-0.773	0.471	1.19	1.498	1.287	0.532	-0.774	-0.611	-0.149

nucleocytoplasmic transport	-1.377	-0.377	0.287	0.684	0.875	0.85	0.56	0.024	-0.189	-1.338	
cellular response to nutrient levels	-1.379	-0.064	0.76	1.196	1.338	1.061	0.459	-0.468	-0.685	-2.219	
heterochromatin assembly	-1.417	-1.353	-1.297	-1.217	-1.091	-0.639	0.117	2.246	3.649	1.002	
cellular macromolecule metabolic process	-1.432	-0.872	-0.464	-0.176	0.022	0.245	0.365	0.653	1.013	0.646	
positive regulation of cell growth	-1.438	-0.514	0.088	0.439	0.604	0.591	0.403	0.265	0.441	-0.878	
hematopoietic progenitor cell differentiation	-1.45	-0.706	-0.155	0.235	0.492	0.712	0.681	0.364	0.095	-0.267	
mRNA metabolic process	-1.452	-0.326	0.329	0.632	0.687	0.405	0.036	0.133	0.902	-1.344	
negative regulation of macromolecule metabolic process	-1.456	-1.126	-0.816	-0.528	-0.263	0.191	0.543	0.964	1.142	1.35	
chromosome segregation	-2.686	-0.922	0.211	0.844	1.097	0.873	0.231	-0.552	0.207	0.697	
rRNA modification	-2.686	-0.097	1.506	2.328	2.553	1.847	0.46	-1.672	-1.684	-2.556	
cell junction	-2.693	-2.703	-2.475	-2.07	-1.54	-0.287	0.981	2.844	3.594	4.349	
regulation of gene expression, epigenetic	-2.719	-2.213	-1.769	-1.361	-0.964	-0.144	0.769	2.753	3.897	1.752	
transcription regulator activity	-2.721	-1.325	-0.393	0.182	0.495	0.651	0.589	0.894	1.646	-0.018	
negative regulation of macromolecule biosynthetic process	-2.727	-2.043	-1.422	-0.864	-0.367	0.458	1.073	1.785	2.02	2.086	
maturation of LSU-rRNA from tricistronic rRNA transcript (SSU-rRNA, 5.8S rRNA, LSU-rRNA)	-2.731	-1.513	-0.589	0.093	0.579	1.12	1.3	1.237	0.917	-0.413	
organic substance catabolic process	-2.735	-1.646	-0.858	-0.309	0.056	0.429	0.579	0.974	1.747	1.763	
ameboidal-type cell migration	-2.75	-1.199	-0.19	0.394	0.659	0.593	0.214	-0.012	1.013	1.278	
transcription coregulator activity	-2.753	-1.269	-0.267	0.359	0.7	0.848	0.695	0.666	1.164	-0.144	
snRNA metabolic process	-2.768	-0.228	1.26	1.934	2.007	1.079	-0.316	-1.666	-0.333	-0.968	
negative regulation of cellular macromolecule biosynthetic process	-2.782	-2.084	-1.45	-0.878	-0.367	0.48	1.111	1.828	2.042	2.1	
biological process involved in symbiotic interaction	-2.789	-1.759	-0.988	-0.424	-0.02	0.468	0.741	1.262	1.901	1.608	
regulation of hydrolase activity	-2.839	-1.563	-0.64	-0.009	0.39	0.695	0.636	0.433	0.942	1.955	
transcription coactivator activity	-2.86	-1.249	-0.18	0.467	0.799	0.887	0.676	0.667	1.261	-0.466	
positive regulation of protein modification process	-2.861	-1.887	-1.075	-0.413	0.115	0.82	1.153	1.165	1.089	1.895	
positive regulation of proteolysis	-2.88	-2.276	-1.816	-1.457	-1.157	-0.607	0.03	1.861	3.951	4.35	
supramolecular fiber	-2.886	-1.257	-0.319	0.11	0.189	-0.175	-0.56	0.317	2.864	1.717	
regulation of response to cytokine stimulus	-2.916	-1.924	-1.077	-0.371	0.201	0.972	1.317	1.16	0.83	1.808	
maturation of SSU-rRNA	-2.935	0.656	2.579	3.233	2.973	0.926	-1.576	-3.449	-0.556	-1.851	
regulation of mRNA stability	-2.941	-2.359	-1.78	-1.218	-0.682	0.28	1.06	2.042	2.492	3.107	
regulation of viral genome replication	-2.944	-2.703	-2.225	-1.595	-0.886	0.531	1.657	2.437	2.007	3.721	
single-stranded DNA binding	-2.958	-2.033	-1.266	-0.635	-0.117	0.654	1.175	1.787	1.98	1.412	
cellular response to extracellular stimulus	-2.963	-0.631	0.816	1.577	1.829	1.407	0.538	-0.33	0.197	-2.442	
positive regulation of viral process	-2.985	-1.78	-0.874	-0.212	0.253	0.764	0.947	1.09	1.413	1.383	
DNA-binding transcription factor activity, RNA polymerase II-specific	-3.042	-2.231	-1.63	-1.171	-0.795	-0.11	0.683	2.797	4.285	1.213	
mRNA export from nucleus	-3.067	-1.242	0.047	0.9	1.409	1.707	1.468	0.685	0.062	-1.971	
posttranscriptional regulation of gene expression	-3.149	-2.314	-1.586	-0.955	-0.409	0.469	1.12	1.957	2.39	2.478	
GTPase activity	-3.149	-2.832	-2.46	-2.04	-1.582	-0.578	0.489	2.591	4.303	5.257	
glutamatergic synapse	-3.15	-2.019	-1.102	-0.376	0.181	0.874	1.146	1.058	1.093	2.294	
gonad development	-3.156	-2.897	-2.397	-1.744	-1.013	0.439	1.587	2.408	2.179	4.592	
neuron development	-3.169	-2.25	-1.56	-1.046	-0.661	-0.115	0.342	1.555	3.149	3.756	
organelle localization	-3.176	-2.243	-1.478	-0.859	-0.368	0.307	0.693	1.14	1.966	4.019	
cell projection	-3.275	-2.076	-1.096	-0.316	0.287	1.043	1.335	1.161	0.984	1.954	
positive regulation of phosphate metabolic process	-3.275	-2.432	-1.788	-1.292	-0.898	-0.261	0.359	1.975	3.76	3.852	
multi-organism process	-3.304	-1.91	-0.921	-0.246	0.196	0.654	0.89	1.592	2.391	0.657	
regulation of viral process	-3.319	-2.229	-1.387	-0.742	-0.25	0.429	0.897	1.761	2.592	2.247	
Golgi apparatus	-3.327	-1.161	0.242	1.05	1.409	1.287	0.71	0.119	0.69	-1.018	
neuronal cell body	-3.364	-3.236	-2.764	-2.065	-1.238	0.476	1.872	2.874	2.439	5.006	
cellular response to cytokine stimulus	-3.398	-2.659	-1.964	-1.313	-0.705	0.384	1.301	2.597	3.099	2.659	
membrane	-3.438	-2.297	-1.398	-0.697	-0.154	0.597	1.084	1.821	2.42	2.064	
regulation of protein modification by small protein conjugation or removal	-3.474	-2.756	-1.853	-0.863	0.126	1.833	2.867	2.463	0.286	1.372	
regulation of mRNA catabolic process	-3.52	-2.809	-2.115	-1.448	-0.817	0.308	1.225	2.418	3.021	3.737	
negative regulation of intracellular signal transduction	-3.535	-3.938	-3.844	-3.373	-2.63	-0.687	1.377	4.415	5.498	6.717	
plasma membrane bounded cell projection	-3.558	-2.263	-1.206	-0.362	0.291	1.115	1.444	1.293	1.124	2.122	
maturation of LSU-rRNA	-3.576	-1.991	-0.791	0.092	0.718	1.411	1.645	1.607	1.278	-0.393	
poly-pyrimidine tract binding	-3.577	-3.257	-2.555	-1.62	-0.582	1.389	2.734	2.686	0.828	3.956	
neuron projection	-3.588	-2.237	-1.149	-0.294	0.355	1.139	1.407	1.458	1.913	2.197	
macromolecule catabolic process	-3.598	-2.314	-1.323	-0.573	-0.015	0.69	1.077	1.617	2.226	2.213	
negative regulation of gene expression	-3.627	-2.662	-1.838	-1.136	-0.537	0.417	1.134	2.165	2.89	3.192	
mRNA binding	-3.663	-2.718	-1.879	-1.139	-0.491	0.56	1.331	2.253	2.696	3.05	
viral life cycle	-3.669	-2.183	-1.154	-0.482	-0.078	0.229	0.278	0.849	2.533	3.678	
hydrolase activity, acting on ester bonds	-3.677	-1.549	-0.161	0.656	1.048	1.06	0.695	0.648	1.622	-0.342	
viral genome replication	-3.694	-2.69	-1.833	-1.115	-0.522	0.335	0.849	1.377	2.277	5.016	
cytokine-mediated signaling pathway	-3.703	-3.169	-2.501	-1.752	-0.965	0.568	1.856	3.225	3.168	3.274	
positive regulation of protein phosphorylation	-3.729	-3.434	-2.933	-2.289	-1.556	-0.005	1.423	3.302	3.993	5.229	
negative regulation of cell communication	-3.733	-3.107	-2.427	-1.721	-1.017	0.302	1.4	2.738	3.266	4.298	
plasma membrane	-3.734	-2.758	-1.947	-1.27	-0.702	0.202	0.919	2.166	3.303	3.822	
ribosome assembly	-3.766	-0.929	0.863	1.839	2.202	1.787	0.769	-0.419	0.092	-2.439	
positive regulation of mRNA catabolic process	-3.767	-2.559	-1.589	-0.816	-0.204	0.67	1.246	2.045	2.619	2.355	
negative regulation of signal transduction	-3.773	-3.035	-2.296	-1.573	-0.882	0.355	1.347	2.555	3.124	4.178	
negative regulation of protein metabolic process	-3.831	-2.885	-2.031	-1.263	-0.578	0.562	1.428	2.493	2.949	3.156	
nucleobase-containing compound transport	-3.837	-2.352	-1.143	-0.184	0.554	1.471	1.807	1.483	0.927	1.274	
positive regulation of gene silencing by miRNA	-3.843	-2.95	-2.078	-1.245	-0.465	0.886	1.906	2.876	2.688	2.226	
organonitrogen compound metabolic process	-3.849	-2.444	-1.379	-0.588	-0.011	0.71	1.122	1.822	2.569	2.048	
protein-containing complex localization	-3.87	-2.294	-1.067	-0.133	0.558	1.387	1.725	1.747	1.471	0.476	
protein modification by small protein conjugation	-3.879	-1.764	-0.275	0.712	1.306	1.697	1.529	1.036	0.853	-1.214	
dendrite	-3.898	-2.628	-1.509	-0.544	0.263	1.471	1.98	1.806	1.099	2.02	
polymeric cytoskeletal fiber	-3.913	-1.862	-0.54	0.223	0.581	0.594	0.335	0.809	2.556	1.216	
protein ubiquitination	-3.923	-1.765	-0.282	0.667	1.209	1.503	1.309	1.076	1.307	-1.1	
RNA transport	-3.948	-2.413	-1.17	-0.186	0.567	1.502	1.853	1.568	1.027	1.2	
positive regulation of protein metabolic process	-3.949	-2.546	-1.473	-0.67	-0.079	0.654	1.055	1.688	2.534	2.787	
DNA-dependent DNA replication	-4.019	-2.648	-1.572	-0.753	-0.152	0.534	0.76	0.822	1.818	5.212	
nuclear-transcribed mRNA catabolic process, deadenylation-dependent decay	-4.026	-1.849	-0.376	0.546	1.055	1.297	1.109	1.126	1.765	-0.646	
epithelial cell differentiation	-4.08	-2.108	-0.829	-0.071	0.318	0.493	0.5	1.584	3.451	0.742	
response to type I interferon	-4.088	-2.63	-1.515	-0.679	-0.061	0.722	1.172	1.901	2.708	2.471	
RNA localization	-4.088	-2.327	-0.964	0.06	0.797	1.601	1.792	1.367	0.93	0.832	
nucleobase-containing compound catabolic process	-4.109	-2.719	-1.623	-0.77	-0.113	0.771	1.302	2.008	2.643	2.609	
growth cone	-4.116	-3.482	-2.76	-1.99	-1.203	0.315	1.622	3.282	3.838	4.494	
ribonuclease activity	-4.121	-1.494	0.213	1.198	1.639	1.5	0.805	0.102	0.908	-0.749	
negative regulation of cellular protein metabolic process	-4.128	-3.203	-2.321	-1.493	-0.725	0.605	1.64	2.852	3.232	3.54	
mitochondrial envelope	-4.136	0.497	2.994	3.894	3.676	1.473	-1.059	-1.918	1.417	-6.837	
positive regulation of cellular protein metabolic process	-4.138	-2.687	-1.572	-0.731	-0.108	0.684	1.133	1.84	2.709	2.873	
cellular macromolecule catabolic process	-4.14	-2.687	-1.555	-0.687	-0.032	0.821	1.303	1.937	2.56	2.48	
regulation of protein metabolic process	-4.17	-2.747	-1.622	-0.746	-0.071	0.83	1.354	1.999	2.572	2.6	
epidermis development	-4.18	-2.482	-1.397	-0.767	-0.449	-0.284	-0.151	1.502	4.444	3.763	
neuron projection cytoplasm	-4.191	-3.168	-2.28	-1.503	-0.816	0.357	1.347	2.965	3.929	3.359	
regulation of viral life cycle	-4.21	-3.248	-2.361	-1.545	-0.797	0.51	1.581	3.06	3.672	3.337	
ribosomal large subunit biogenesis	-4.231	-2.085	-0.453	0.739	1.562	2.345	2.337	1.239	-0.065	-1.388	
regulation of chromosome segregation	-4.248	-1.135	0.8	1.816	2.149	1.559	0.352	-0.814	0.477	-0.955	
viral gene expression	-4.292	-3.268	-2.36	-1.556	-0.845	0.335	1.256	2.579	3.576	4.575	
protein metabolic process	-4.301	-2.748	-1.562	-0.672	-0.014	0.825	1.318	2.115	2.873	2.166	
rRNA binding	-4.34	-1.324	0.712	1.963	2.603	2.657	1.88	0.271	-0.527	-3.895	
positive regulation of binding	-4.357	-3.395	-2.516	-1.712	-0.971	0.346	1.478	3.236	4.162	3.729	
response to cytokine	-4.384	-3.451	-2.561	-1.717	-0.921	0.521	1.745	3.457	4.035	3.277	
cytoplasmic region	-4.416	-1.974	-0.519	0.196	0.391	-0.044	-0.629	0.283	3.7	3.012	
regulation of binding	-4.418	-3.277	-2.213	-1.235	-0.351	1.116	2.168	3.088	2.831	2.292	
ribonucleoprotein complex binding	-4.443	-3.613	-2.869	-2.186	-1.544	-0.32	0.891	3.337	5.321	5.427	
RNA catabolic process	-4.528	-3.014	-1.816	-0.879	-0.154	0.835	1.443	2.263	2.969	2.88	
cellular protein metabolic process	-4.529	-2.97	-1.758	-0.826	-0.116	0.839	1.441	2.367	3.127	2.424	
regulation of cellular protein metabolic process	-4.544	-3.054	-1.853	-0.896	-0.141	0.912	1.557	2.311	2.849	2.859	
viral process	-4.59	-3.07	-1.919	-1.066	-0.444	0.336	0.808	1.813	3.426	4.706	
mRNA transport	-4.637	-2.678	-1.148	0.016	0.872	1.861	2.182	1.87	1.256	0.406	
intracellular receptor signaling pathway	-4.647	-3.48	-2.351	-1.286	-0.31	1.305	2.405	3.077	2.518	2.771	
ribonucleoprotein complex localization	-4.791	-2.718	-1.128	0.056	0.907	1.864	2.173	2.003	1.543	0.092	
lipid metabolic process	-4.797	-4.766	-4.279	-3.462	-2.423	-0.055	2.21	5.08	5.645	6.847	
cellular response to abiotic stimulus	-4.85	-3.663	-2.599	-1.647	-0.794	0.651	1.799	3.372	4.056	3.675	
response to virus	-4.868	-3.326	-2.128	-1.204	-0.489	0.526	1.266	2.682	4.021	3.52	
axon	-4.87	-2.336	-0.631	0.423	0.985	1.177	0.848	0.774	2.114	1.517	
somatodendritic compartment	-4.874	-3.514	-2.275	-1.169	-0.206	1.272	2.164	2.54	2.277	3.784	
response to decreased oxygen levels	-4.881	-1.904	-0.038	0.967	1.333	0.913	-0.031	-0.484	1.857	2.27	
filopodium	-4.909	-4.593	-4.047	-3.32	-2.454	-0.466	1.626	5.197	6.886	6.08	
single-stranded RNA binding	-4.987	-3.857	-2.698	-1.558	-0.481	1.361	2.645	3.404	2.723	3.447	
modification-dependent protein binding	-5.077	-4.202	-3.192	-2.109	-1.005	1.079	2.773	4.423	3.976	3.334	
striated muscle tissue development	-5.127	-2.981	-1.402	-0.278	0.49	1.304	1.612	2.07	2.745	1.566	
nucleic acid binding	-5.142	-3.326	-1.915	-0.835	-0.02	1.04	1.65	2.476	3.229	2.843	
regulation of organelle assembly	-5.188	-3.277	-1.899	-0.945	-0.315	0.32	0.588	1.501	3.659	5.555	
asymmetric synapse	-5.191	-4.894	-4.222	-3.283	-2.175	0.226	2.446	5.175	5.588	6.331	
mRNA catabolic process	-5.212	-3.506	-2.161	-1.111	-0.299	0.813	1.516	2.566	3.602	3.793	
cell adhesion molecule binding	-5.213	-4.715	-4.085	-3.355	-2.551	-0.822	0.938	4.136	6.684	8.984	
ribonucleoprotein complex export from nucleus	-5.214	-2.976	-1.258	0.025	0.95	1.995	2.339	2.165	1.701	0.274	
nuclear-transcribed mRNA catabolic process	-5.226	-2.624	-0.844	0.291	0.94	1.321	1.189	1.413	2.618	0.924	
GTP binding	-5.24	-2.88	-1.256	-0.198	0.442	0.968	1.129	2.071	3.638	1.325	
positive regulation of translation	-5.361	-4.005	-2.805	-1.747	-0.817	0.708	1.865	3.376	4.195	4.591	
regulation of cytokine-mediated signaling pathway	-5.366	-3.734	-2.321	-1.119	-0.117	1.339	2.167	2.555	2.542	4.054	
heterocyclic compound binding	-5.464	-3.33	-1.787	-0.711	0.01	0.765	1.107	2.041	3.703	3.666	
organic cyclic compound binding	-5.488	-3.362	-1.821	-0.742	-0.014	0.762	1.13	2.1	3.759	3.676	
postsynaptic specialization	-5.501	-4.196	-3.096	-2.151	-1.315	0.165	1.548	4.247	6.035	4.263	
poly(U) RNA binding	-5.574	-4.766	-3.634	-2.325	-0.964	1.519	3.23	3.662	2.32	6.53	
defense response to virus	-5.595	-3.88	-2.474	-1.328	-0.397	0.974	1.904	3.127	3.919	3.752	
cellular response to chemical stress	-5.65	-4.235	-2.816	-1.458	-0.214	1.779	2.966	3.024	1.961	4.643	
protein modification by small protein conjugation or removal	-5.655	-3.431	-1.692	-0.359	0.638	1.878	2.453	2.721	2.496	0.95	
cytoplasm	-5.718	-3.979	-2.535	-1.345	-0.368	1.085	2.061	3.242	3.873	3.683	
regulation of translation	-5.754	-4.045	-2.616	-1.428	-0.445	1.031	2.035	3.252	3.946	4.023	
organonitrogen compound biosynthetic process	-5.769	-4.031	-2.609	-1.452	-0.511	0.879	1.838	3.183	4.189	4.283	
establishment of organelle localization	-5.78	-3.696	-2.105	-0.92	-0.064	0.942	1.393	1.989	3.276	4.966	
microtubule-based movement	-5.781	-2.721	-0.592	0.78	1.557	1.881	1.344	0.28	1.029	2.222	
plasma membrane bounded cell projection cytoplasm	-5.823	-3.241	-1.44	-0.259	0.449	0.946	0.897	1.258	3.149	4.064	
mRNA 3'-UTR binding	-5.852	-4.602	-3.416	-2.306	-1.279	0.498	1.898	3.695	4.799	6.565	
cellular amide metabolic process	-5.864	-4.184	-2.764	-1.57	-0.569	0.965	2.037	3.375	4.162	4.414	
cadherin binding	-5.879	-5.285	-4.546	-3.698	-2.773	-0.806	1.165	4.655	7.348	9.821	
nuclease activity	-5.891	-3.008	-1.013	0.28	1.042	1.542	1.434	1.609	2.809	1.196	
RNA binding	-5.907	-3.97	-2.429	-1.212	-0.252	1.113	2.033	3.377	4.222	3.023	
supramolecular complex	-6.056	-5.133	-4.092	-2.984	-1.855	0.321	2.205	4.674	5.733	7.187	
amide biosynthetic process	-6.161	-4.398	-2.908	-1.655	-0.604	1.009	2.143	3.571	4.405	4.6	
translation	-6.204	-4.444	-2.952	-1.691	-0.63	1.009	2.169	3.633	4.467	4.644	
RNA phosphodiester bond hydrolysis, endonucleolytic	-6.244	-3.822	-1.982	-0.621	0.357	1.493	1.989	2.516	3.268	3.045	
negative regulation of viral process	-6.316	-4.129	-2.549	-1.429	-0.637	0.393	1.223	3.565	6.072	3.807	
non-membrane-bounded organelle assembly	-6.328	-4.201	-2.551	-1.284	-0.316	1.008	1.89	3.392	4.693	3.696	
organelle assembly	-6.368	-3.949	-2.155	-0.86	0.048	1.094	1.624	2.673	4.164	3.728	
synaptic signaling	-6.424	-4.222	-2.399	-0.907	0.298	2.005	2.999	3.648	3.234	1.767	
regulation of translational initiation	-6.458	-4.839	-3.371	-2.045	-0.852	1.164	2.728	4.645	5.066	3.961	
dendrite development	-6.478	-5.633	-4.668	-3.616	-2.509	-0.237	1.956	5.55	7.585	8.049	
viral translation	-6.489	-5.162	-3.908	-2.734	-1.64	0.3	1.915	4.287	5.906	7.524	
cellular response to virus	-6.513	-5.006	-3.553	-2.177	-0.901	1.291	2.937	4.569	4.615	4.738	
negative regulation of translation	-6.597	-4.884	-3.396	-2.104	-0.982	0.845	2.244	4.188	5.302	5.381	
cytosol	-7.223	-5.34	-3.709	-2.297	-1.078	0.885	2.363	4.389	5.684	6.327	
N6-methyladenosine-containing RNA binding	-7.235	-5.899	-4.546	-3.195	-1.86	0.694	2.994	6.367	7.39	5.289	
poly-purine tract binding	-7.614	-5.971	-4.4	-2.916	-1.531	0.905	2.863	5.356	6.366	6.942	
mRNA 5'-UTR binding	-7.748	-6.36	-4.941	-3.521	-2.126	0.498	2.785	6.027	7.487	7.899	
translation repressor activity	-8.033	-6.484	-4.814	-3.114	-1.462	1.458	3.603	5.279	5.175	8.393	
ribosome binding	-8.071	-7.238	-6.172	-4.93	-3.564	-0.644	2.266	7.149	10.05	11.16	
ribonucleoprotein granule	-8.106	-6.882	-5.446	-3.89	-2.293	0.765	3.328	6.284	7.073	9.166	
perinuclear region of cytoplasm	-8.175	-5.85	-3.857	-2.158	-0.719	1.504	3.04	4.774	5.56	5.879	
ribosomal small subunit binding	-8.289	-5.746	-3.811	-2.344	-1.218	0.421	1.767	4.86	7.916	6.445	
cytoplasmic ribonucleoprotein granule	-8.325	-6.964	-5.442	-3.839	-2.225	0.806	3.306	6.186	7.083	9.413	
isomerase activity	-8.491	-3.687	-0.49	1.436	2.397	2.462	1.454	0.474	2.519	1.925	
immune response-regulating signaling pathway	-8.656	-6.309	-4.145	-2.186	-0.449	2.32	4.142	5.311	4.678	5.294	
translational initiation	-8.868	-6.823	-4.95	-3.237	-1.673	1.046	3.269	6.374	7.735	7.124	
cytoplasmic stress granule	-8.942	-7.429	-5.754	-4.005	-2.258	0.988	3.616	6.506	7.307	7.972	
regulation of cytoplasmic translation	-9.034	-5.996	-3.508	-1.498	0.103	2.319	3.577	4.537	4.774	4.725	
polysome	-9.35	-7.108	-4.943	-2.905	-1.037	2.07	4.23	5.851	5.595	7.598	
endoribonuclease activity	-9.411	-5.664	-2.773	-0.599	0.983	2.822	3.519	3.656	3.862	3.605	
poly(A) binding	-9.877	-7.591	-5.451	-3.47	-1.658	1.435	3.812	6.606	7.621	8.573	
translation regulator activity, nucleic acid binding	-9.923	-8.065	-6.165	-4.276	-2.66	0.927	3.721	7.278	8.704	10.24	
translation regulator activity	-9.974	-8.394	-6.61	-4.712	-2.777	0.943	4.135	8.115	9.194	10.08	
cytoplasmic translation	-10.11	-7.53	-5.226	-3.177	-1.365	1.609	3.827	6.485	7.557	7.925	
translation factor activity, RNA binding	-10.49	-8.376	-6.274	-4.224	-2.264	1.265	4.134	7.658	8.83	9.738	
cytoplasmic translational initiation	-10.62	-8.539	-6.481	-4.479	-2.559	0.944	3.89	7.887	9.625	10.33	
endonuclease activity	-10.74	-7.198	-4.315	-1.998	-0.158	2.394	3.886	5.3	6.153	6.676	
exon-exon junction complex	-11.25	-6.969	-3.732	-1.349	0.353	2.316	3.181	4.296	6.22	6.931	
response to interleukin-1	-11.29	-10.23	-8.507	-6.336	-3.904	1.112	5.528	10.48	10.74	12.4	
translation initiation factor activity	-11.44	-9.182	-6.922	-4.705	-2.571	1.326	4.57	8.737	10.08	10.11	
pattern recognition receptor signaling pathway	-11.91	-8.987	-6.192	-3.58	-1.191	2.795	5.617	7.907	7.399	8.146	
P-body	-12.02	-10.38	-8.456	-6.356	-4.17	0.158	4.046	9.531	12.28	15.37	
stress granule assembly	-12.69	-10.7	-8.429	-6.003	-3.529	1.2	5.196	9.985	11.32	13.65	
regulation of pattern recognition receptor signaling pathway	-12.88	-9.166	-5.826	-2.869	-0.299	3.688	6.214	7.668	6.565	6.903	
nuclear-transcribed mRNA catabolic process, nonsense-mediated decay	-13.11	-7.74	-3.818	-1.056	0.81	2.753	3.51	5.031	7.668	5.955	
RNA cap binding	-13.19	-6.94	-2.627	0.164	1.806	2.918	2.811	3.769	7.183	4.11	
messenger ribonucleoprotein complex	-13.47	-10.58	-7.813	-5.215	-2.811	1.331	4.527	8.38	10.6	15.05	
eukaryotic 48S preinitiation complex	-13.48	-10.8	-8.155	-5.598	-3.167	1.188	4.733	9.301	11.55	14.43	

Table 2.5 Contribution of each GO term to mRNA binding dynamics prediction

cluster	gene name	Expected cluster	Expected peak binding time	Slope of error	RMSE
I	ZNF579	IV	64.1	-0.2074	0.651
I	URB2	IV	59	-0.1487	0.498
I	DDX21	III	56	-0.0995	0.407
I	SCAF11	II	41.1	-0.0445	0.388
I	PHF3	II	45.1	-0.0895	0.359
I	URB1	III	49.8	-0.0979	0.359
I	POLR2B	I	7.11E-13	-0.0653	0.240
I	SSRP1	II	35.3	-0.0706	0.236
I	FAM208A	II	37.1	-0.0782	0.234
I	SCAF4	I	20.6	-0.0733	0.214
I	VIRMA	II	47	-0.0367	0.191
I	SPOUT1	II	31.4	-0.0483	0.161
I	POLR2A	I	7.11E-13	-0.0227	0.112
I	TCOF1	I	7.11E-13	-0.0149	0.109
I	CSTF2T	II	29.6	-0.0135	0.081
I	SUPT5H	I	7.11E-13	-0.0172	0.068
I	PINX1	I	7.11E-13	-0.0217	0.068
I	CSTF3	II	26.2	-0.0112	0.068
I	FIP1L1	II	21.6	-0.0178	0.054
I	PPP1R10	I	7.11E-13	-0.0131	0.052
I	SUPT6H	I	7.11E-13	0.00211	0.052
I	SCAF8	I	7.11E-13	-0.0135	0.042
I	SUPT16H	I	7.9	-0.0084	0.036
I	CD3EAP	I	7.11E-13	-0.0079	0.028
I	RPRD2	I	7.11E-13	0.00779	0.025
II	DDX50	V	71.9	-0.2701	0.838
II	DDX42	V	73.6	-0.2632	0.806
II	KHSRP	V	74.1	-0.2687	0.805
II	HNRNPDL	V	76.8	-0.2673	0.777
II	EPRS	V	65.2	-0.2413	0.737
II	DDX60L	V	67.8	-0.2345	0.722
II	ZNF385A	V	75.3	-0.2302	0.683
II	CMSS1	V	68.9	-0.2271	0.667
II	FAM133B	V	67.8	-0.2253	0.660
II	PPHLN1	V	69.2	-0.2176	0.640
II	DDX31	V	68.1	-0.1958	0.619
II	FSCN1	V	65.2	-0.212	0.614
II	KNOP1	V	66.6	-0.2016	0.606
II	CIRBP	V	71.9	-0.2066	0.600
II	FUBP1	IV	65.8	-0.1955	0.586
II	HNRNPUL2	IV	66.4	-0.1875	0.553
II	GPATCH4	IV	64.5	-0.1816	0.538
II	EWSR1	IV	66.8	-0.1752	0.532
II	CCDC59	IV	65.5	-0.1779	0.528
II	RBM34	IV	62.9	-0.1682	0.515
II	DHX33	IV	67.6	-0.1683	0.508
II	CHD1	IV	66.9	-0.1723	0.504
II	TTF1	IV	67.3	-0.1717	0.501
II	TRNAU1AP	IV	64.8	-0.1611	0.496
II	HNRNPA3	IV	69.1	-0.1697	0.495
II	APOBEC3B	IV	64.3	-0.1715	0.494
II	SPEN	IV	60.2	-0.1643	0.489
II	CKAP4	IV	59.9	-0.164	0.484
II	DEK	IV	57.7	-0.1606	0.480
II	ZC3H4	IV	60.4	-0.1536	0.471
II	HNRNPH2	IV	62	-0.1583	0.465
II	ZCCHC17	IV	65.6	-0.1403	0.453
II	PQBP1	IV	50.6	-0.1522	0.443
II	CCAR1	IV	58.2	-0.0983	0.423
II	HNRNPF	IV	62.7	-0.134	0.405
II	TCERG1	IV	60.5	-0.1326	0.397
II	RBM4	IV	62.3	-0.1339	0.389
II	DDX51	IV	54.4	-0.1114	0.387
II	MMTAG2	IV	60	-0.1277	0.386
II	RAB10	IV	51.6	-0.128	0.382
II	HNRNPH1	IV	63.1	-0.1128	0.377
II	DDX17	IV	59.2	-0.1159	0.377
II	ANXA7	III	50.2	-0.1153	0.367
II	HNRNPAB	IV	59	-0.1242	0.359
II	PARP1	II	32.5	0.12283	0.356
II	TUBB	IV	51.1	-0.1161	0.356
II	CHD2	III	59.6	-0.1182	0.355
II	NOL8	III	52.4	-0.0848	0.354
II	AKAP8	IV	59.8	-0.1121	0.347
II	ZC3H18	IV	55.8	-0.1094	0.347
II	U2SURP	III	55.6	-0.1024	0.325
II	PRPF6	IV	55.5	-0.0949	0.320
II	USP36	IV	58.3	-0.1061	0.318
II	CUSTOS	III	51.2	-0.0798	0.318
II	NCL	III	50.4	-0.1086	0.316
II	TRA2B	II	32.7	0.10732	0.316
II	PRPF38B	III	52.9	-0.1044	0.313
II	RRP8	IV	54.4	-0.0954	0.312
II	NUDT21	I	7.11E-13	0.09048	0.308
II	HNRNPUL1	IV	56.7	-0.098	0.305
II	SLC16A3	IV	55.7	-0.1043	0.304
II	RBMX2	III	51.2	-0.0902	0.303
II	SUGP1	III	52.8	-0.0847	0.303
II	MSN	IV	53	-0.1008	0.302
II	DAZAP1	III	56.8	-0.1034	0.300
II	FUS	III	56.3	-0.101	0.299
II	DDX10	IV	54.8	-0.1006	0.295
II	NOL11	III	47.3	-0.0388	0.285
II	SF3B6	III	49.4	-0.0752	0.285
II	SMNDC1	III	53.1	-0.0936	0.284
II	RBBP6	III	51.6	-0.02	0.283
II	ZCCHC8	IV	56.1	-0.0812	0.282
II	SRSF3	IV	57.4	-0.0528	0.280
II	BAZ1B	II	33.7	0.09538	0.279
II	SRSF5	I	14.2	0.08685	0.275
II	RAMAC	III	48.8	-0.0903	0.273
II	RBM12	III	55	-0.0878	0.272
II	CLTC	III	44.6	-0.0821	0.267
II	HNRNPA1	II	45.4	0.07037	0.263
II	ZNF106	III	52.9	-0.0702	0.263
II	TAF15	III	51.8	-0.0784	0.259
II	RBM39	II	32.5	0.07624	0.254
II	RBM10	III	44.3	0.03329	0.248
II	ZCRB1	III	53.6	-0.0792	0.243
II	TCF20	III	48.9	-0.0132	0.242
II	CHERP	II	34.7	0.05545	0.240
II	WDR43	II	35.9	0.06771	0.237
II	SNIP1	III	45.6	-0.0395	0.237
II	SF3B2	III	50.5	-0.0551	0.232
II	HNRNPH3	III	52.3	-0.0547	0.232
II	HNRNPLL	III	51.9	-0.0785	0.229
II	PTBP2	III	53.1	-0.0782	0.227
II	SF1	III	55.6	-0.0774	0.227
II	SRRT	III	54.3	-0.0767	0.227
II	RBM42	III	52.9	-0.0683	0.221
II	LYAR	II	31.3	0.06485	0.220
II	RBM3	III	55.7	-0.0696	0.220
II	DUSP11	III	49.3	-0.0388	0.206
II	RTF1	I	8.5	0.01131	0.206
II	SUB1	III	53.8	-0.0438	0.204
II	SART1	II	41.5	0.03754	0.203
II	SURF4	II	35.7	0.05909	0.202
II	SRSF9	II	36	0.06861	0.198
II	U2AF2	III	55.6	-0.0333	0.198
II	RBM5	II	37.5	0.04759	0.192
II	ZNF326	II	35.3	0.0535	0.192
II	DHX15	III	51.7	-0.0417	0.191
II	NONO	II	38.5	0.06239	0.188
II	RBM14	III	52.5	-0.0599	0.187
II	GRWD1	III	47.8	-0.059	0.185
II	ZNF207	III	44.5	-0.0425	0.183
II	KHDRBS1	III	55.1	-0.0616	0.181
II	PABPN1	III	46.7	0.04427	0.181
II	RBM25	III	48.5	-0.0289	0.180
II	SRSF10	II	39.4	0.05332	0.176
II	SF3B3	III	47.7	-0.0117	0.176
II	DIDO1	II	38.8	-0.0596	0.174
II	CSTF2	I	13.5	0.06018	0.174
II	RBM19	III	46.3	-0.0273	0.172
II	SFPQ	II	40.2	0.05869	0.172
II	CPSF4	I	15.6	0.05294	0.169
II	RBM4B	II	39.2	0.03654	0.167
II	CSTF1	II	44.1	-0.0266	0.165
II	SRRM1	III	49.8	-0.0333	0.165
II	SON	II	39.1	0.04987	0.164
II	THRAP3	II	37	0.04534	0.164
II	BCLAF1	III	46.6	-0.0306	0.163
II	BUD13	III	45	-0.0302	0.163
II	SCAF1	II	35.4	-0.0459	0.163
II	SF3B1	III	47.9	-0.0445	0.163
II	SRSF7	III	50.4	0.00816	0.162
II	PUF60	II	39.5	-0.0528	0.161
II	LUC7L	III	47.9	-0.0511	0.161
II	RBMXL1	II	33.5	-0.0135	0.160
II	CPSF7	I	7.3	0.01869	0.159
II	U2AF1L5	II	44	-0.0255	0.157
II	WDR33	II	26.7	0.04669	0.156
II	ELOA	II	33.8	0.03208	0.156
II	SF3A2	II	41.7	-0.0139	0.155
II	RBM7	II	44.3	-0.0311	0.154
II	SMARCA5	III	44.8	-0.0244	0.152
II	RBM6	III	46.2	-0.0509	0.152
II	SAFB	II	31.8	0.0417	0.148
II	SRSF8	III	51.2	-0.0461	0.146
II	ZC3H13	III	50.4	-0.014	0.146
II	HNRNPA2B1	III	49.4	-0.0478	0.145
II	PHF5A	II	39.5	0.02919	0.145
II	CPSF6	I	4.6	0.03707	0.144
II	SF3A3	III	45.2	-0.0151	0.141
II	PATZ1	II	32.5	0.02996	0.135
II	LUC7L2	II	42.6	-0.0188	0.132
II	H1FX	III	47.8	-0.0442	0.131
II	TIAL1	III	50.6	-0.0376	0.128
II	SETD2	II	37.5	0.02135	0.127
II	PSPC1	II	39.2	0.04178	0.126
II	SRSF6	II	39	0.0379	0.126
II	DDX46	III	43.4	-0.0238	0.125
II	ACOT7	II	40.4	0.0218	0.125
II	SRSF4	II	41.4	0.03822	0.122
II	XRN2	II	42.2	0.02896	0.121
II	SNRNP70	II	34.3	0.03073	0.120
II	NCOA5	III	49.9	-0.0307	0.119
II	HNRNPK	II	34.2	0.00266	0.112
II	HNRNPU	III	46.8	-0.0334	0.109
II	SNRNP200	III	49.5	-0.0144	0.109
II	PHRF1	II	31.2	-0.0232	0.106
II	RBM15	II	41.7	-0.0291	0.104
II	SRSF1	III	49.9	-0.0029	0.101
II	CDK13	II	34.1	0.03073	0.101
II	WBP11	III	44.5	-0.0318	0.099
II	HNRNPL	III	46.6	-0.0333	0.099
II	SUGP2	III	48.1	-0.0329	0.098
II	SRSF2	III	43.6	0.00969	0.097
II	HNRNPD	II	37.8	0.0141	0.092
II	SF3A1	II	39.9	0.00869	0.086
II	AKAP8L	II	40	0.02105	0.085
II	SF3B4	II	33.9	0.02822	0.081
II	HNRNPA0	III	46.3	0.00922	0.078
II	TRA2A	II	42.1	0.01737	0.076
II	SLC25A3	III	46.5	-0.0153	0.074
II	SLTM	II	44	-0.0034	0.073
II	MFAP1	II	40.2	0.01871	0.073
II	PDCD6	II	41.8	-0.0033	0.069
II	UBTF	II	31.6	0.00505	0.069
II	SLC16A1	II	44.4	-0.008	0.068
II	RBMX	III	49.2	-0.0022	0.067
II	PWP1	III	48.5	0.00221	0.067
II	PRPF40A	II	40	-0.015	0.063
II	LUC7L3	II	41	0.00132	0.063
II	DDX5	II	39.8	-0.01	0.035
III	EIF2S3	VI	101	-0.4008	1.167
III	ILF3	VI	80.3	-0.3395	0.998
III	NXF1	V	82.5	-0.2943	0.879
III	PNISR	V	79	-0.2708	0.780
III	ZCCHC7	V	70.3	-0.2076	0.614
III	RBM45	V	72.1	-0.2042	0.598
III	PUS7	V	65.4	-0.1867	0.583
III	PCBP1	V	70.3	-0.1924	0.561
III	YLPM1	V	68.4	-0.1909	0.559
III	SRBD1	IV	63	-0.1612	0.549
III	NKTR	V	67.3	-0.1875	0.547
III	C7orf50	V	68.9	-0.188	0.543
III	TOP1	V	64.7	-0.1877	0.542
III	SSB	V	68.3	-0.1735	0.538
III	NOL7	IV	65.6	-0.1741	0.527
III	ENO1	IV	48.5	-0.1636	0.526
III	ACP1	V	67.1	-0.1719	0.501
III	ZFR	IV	68.9	-0.169	0.493
III	PPIL4	V	64	-0.1602	0.492
III	GEMIN5	IV	58.5	-0.1443	0.481
III	RAB1A	IV	58.1	-0.1611	0.474
III	EIF5A	IV	66.2	-0.1513	0.469
III	DCAF13	V	63.9	-0.1603	0.468
III	NACA	IV	64.5	-0.151	0.464
III	HNRNPR	IV	66.1	-0.1515	0.449
III	ZNF512	IV	63.6	-0.1497	0.437
III	HP1BP3	II	35.2	0.14481	0.435
III	ELAC2	IV	65.4	-0.1033	0.419
III	MCM5	IV	59.9	-0.1383	0.416
III	LENG8	IV	66.2	-0.1394	0.413
III	NUSAP1	IV	62.1	-0.1374	0.399
III	ELAVL1	IV	60.5	-0.1379	0.399
III	USP42	IV	62.4	-0.126	0.395
III	MEPCE	IV	64	-0.1359	0.395
III	ZNF800	IV	62.1	-0.1308	0.392
III	HLTF	IV	59.7	-0.0985	0.390
III	CHD4	II	37.7	0.09905	0.387
III	PAK1IP1	IV	68.7	-0.1283	0.380
III	HMGB3	IV	60.6	-0.113	0.367
III	CACTIN	IV	69.4	-0.1141	0.364
III	QKI	IV	58.8	-0.1238	0.358
III	FUBP3	IV	63	-0.119	0.354
III	RBM22	II	33.7	0.12101	0.349
III	PCBP4	IV	57.8	-0.1186	0.346
III	CEBPZ	IV	61.9	-0.1072	0.342
III	SRP14	IV	59.9	-0.1133	0.339

III	NCBP2	IV	58.5	-0.1088	0.338
III	ERI3	II	40.7	0.08882	0.326
III	MTPAP	II	33	0.09146	0.322
III	CHORDC1	IV	47.3	-0.0925	0.321
III	TRMT2A	IV	61.5	-0.1062	0.313
III	RBM15B	IV	58.4	-0.0365	0.312
III	GTF2I	IV	60.8	-0.0919	0.303
III	CELF1	IV	61.6	-0.1008	0.296
III	STRBP	IV	59.8	-0.0895	0.290
III	DBR1	IV	58.4	-0.0867	0.288
III	RBFOX2	IV	55.5	-0.0751	0.275
III	BAZ2A	IV	57.8	-0.0921	0.272
III	RALY	IV	60	-0.0909	0.269
III	HSPA8	II	33.1	0.07719	0.265
III	RAN	III	49.8	-0.0888	0.265
III	AP3D1	III	42.4	0.07104	0.260
III	TRMT10A	III	48	0.04401	0.253
III	ADARB1	II	37.6	0.08475	0.252
III	GAPDH	IV	48.8	-0.0856	0.249
III	MBNL1	III	53	-0.067	0.246
III	NKRF	IV	58	-0.0816	0.241
III	CLK3	III	49.6	0.05123	0.240
III	HNRNPM	IV	57.4	-0.0776	0.235
III	PHF6	II	30.2	0.02061	0.232
III	AQR	IV	57.2	-0.0609	0.228
III	ZC3H8	II	44	0.07688	0.222
III	HMGA1	III	52.4	-0.0695	0.222
III	BUD23	IV	61	-0.0752	0.221
III	EEF1A1	III	46.3	-0.0525	0.216
III	SUMO3	III	57.1	-0.057	0.215
III	PRPF4B	III	44.3	0.05377	0.215
III	PARP2	III	44.7	0.07387	0.214
III	ZFC3H1	III	49.7	-0.0041	0.213
III	RRP12	IV	57.5	-0.0576	0.211
III	RNMT	III	57.5	-0.0689	0.211
III	FARSA	IV	53.7	-0.0688	0.210
III	ZBTB11	III	47.8	0.01276	0.207
III	DDX47	II	42.2	0.06544	0.202
III	NUMA1	III	42.3	0.05122	0.201
III	PTBP1	IV	56	-0.0452	0.201
III	TARDBP	III	54.3	-0.0676	0.200
III	SLC1A5	III	46.5	-0.0177	0.198
III	ABT1	IV	50.4	-0.0561	0.193
III	DDX56	IV	55	-0.0623	0.190
III	PHF10	III	48.8	-0.0077	0.189
III	SERPINH1	IV	52.9	-0.0484	0.188
III	XPO5	III	51.6	-0.0572	0.185
III	TRMT1L	III	45.8	0.05315	0.185
III	DDX49	IV	53.4	-0.0627	0.183
III	AP2M1	II	39.7	-0.0245	0.182
III	NSD2	II	44.3	-0.0266	0.181
III	SLC25A6	III	50.5	-0.0317	0.181
III	NVL	IV	55.3	-0.0593	0.180
III	RBM26	III	51.4	-0.023	0.179
III	TRMT1	III	45.3	0.05672	0.178
III	RBM12B	III	55	-0.0593	0.178
III	HSPA5	III	43.7	0.05363	0.174
III	TENT4B	III	48.8	-0.022	0.172
III	REPIN1	II	42.4	0.03407	0.171
III	NKAP	III	52.5	-0.0476	0.169
III	ZNF638	III	50.3	-0.0314	0.166
III	DHX36	III	52.7	-0.0381	0.162
III	CDC5L	III	51.6	0.00094	0.159
III	DUS3L	III	52.2	-0.0346	0.158
III	HSP90AB1	III	46.8	0.03119	0.157
III	DIMT1	IV	56	-0.0486	0.149
III	PPIG	IV	54.9	-0.0459	0.148
III	DROSHA	III	52.8	-0.0498	0.148
III	RBM28	III	52.8	-0.0459	0.147
III	COPB2	III	46	0.0246	0.146
III	ZRANB2	III	48	-0.0036	0.146
III	FRG1	III	46.6	-0.041	0.146
III	XRCC6	III	50.1	-0.0449	0.145
III	LDHA	II	40.2	0.03267	0.145
III	FAM50A	III	48	-0.0202	0.144
III	DHX8	III	53	-0.0485	0.142
III	PRPF3	III	47	-0.0363	0.141
III	AKAP17A	III	52.4	-0.0119	0.141
III	RPA1	II	40.8	-0.0159	0.141
III	TOE1	III	45.9	0.03763	0.141
III	ADAR	III	45.6	0.04299	0.141
III	ARPC1B	III	54.1	-0.0405	0.136
III	ESF1	III	49.7	-0.0397	0.135
III	DDX23	III	46.5	0.01212	0.134
III	PKM	II	38.9	0.03233	0.129
III	HNRNPC	III	53.9	-0.0136	0.128
III	RAVER1	III	49.5	-0.0391	0.127
III	ZMAT2	II	40.4	0.02507	0.127
III	RAVER2	III	47.7	-0.0347	0.123
III	RACK1	III	46.8	-0.0415	0.122
III	SMARCA4	II	46.7	-0.0209	0.121
III	HSP90AA1	III	45.4	0.02863	0.121
III	APEX1	III	55.2	0.02218	0.120
III	SRRM2	III	47.7	-0.0269	0.118
III	ADARB2	III	50.4	-0.0352	0.110
III	TOP2B	III	53.5	-0.0367	0.109
III	FEN1	III	51.2	0.00734	0.109
III	SRSF11	III	49.6	-0.0119	0.107
III	PRPF31	III	45	0.00283	0.107
III	PLAA	II	39.8	0.01423	0.103
III	DDX18	III	52.4	-0.0194	0.102
III	SCAMP3	III	49.2	-0.0083	0.098
III	ARL6IP4	III	50.4	-0.0224	0.096
III	ISY1	III	46.7	-0.002	0.095
III	MATR3	III	47.1	0.00463	0.094
III	SNW1	II	46.2	0.02973	0.093
III	RCC2	II	40.3	0.01303	0.089
III	UTP15	II	43.4	0.01399	0.085
III	METTL16	III	51	-0.0044	0.083
III	TKT	III	47.3	-0.003	0.082
III	CDK11B	III	45.2	0.00702	0.079
III	ISG20L2	III	51.2	-0.0244	0.076
III	SNRPA	III	48.4	-0.0034	0.074
III	NSUN2	III	50.4	0.02175	0.073
III	RBM27	III	48.6	-0.0175	0.071
III	EFTUD2	III	47.5	-0.0179	0.064
III	TCP1	III	47.3	-0.0147	0.061
III	HMGB1	III	48.1	-0.0007	0.052
III	ILF2	III	48.4	-0.0017	0.051
III	WDR75	II	44	-0.0003	0.050
III	PCBP2	III	48.4	-0.0055	0.049
III	TECR	III	43.4	-0.0065	0.047
III	DHX16	III	47.4	0.00644	0.040
III	DHX9	III	52.1	-0.004	0.028
III	SAFB2	III	47.2	-0.0026	0.024
III	TOP2A	III	48.1	0.00431	0.023
IV	EIF1AY	VI	87.8	-0.2808	0.815
IV	EIF3H	V	87.5	-0.2175	0.640
IV	IK	II	32.3	0.18257	0.549
IV	PNO1	V	70	-0.1691	0.495
IV	GPATCH8	V	68.4	-0.1225	0.484
IV	GIGYF2	V	79.3	-0.1652	0.480
IV	PARP12	IV	59.7	0.00253	0.460
IV	RPS19BP1	V	69.5	-0.1408	0.435
IV	RBM33	V	67.8	-0.1457	0.433
IV	DHX30	V	74.3	-0.1479	0.430
IV	ESRP2	II	36.7	0.1292	0.402
IV	HTATSF1	IV	51.6	0.09479	0.384
IV	DDX27	III	53.4	0.09189	0.351
IV	ERAL1	V	60.5	-0.1062	0.347
IV	RBM38	IV	62.6	-0.0648	0.345
IV	C1orf131	V	65.6	-0.0775	0.327
IV	RBM47	IV	66.1	-0.0933	0.323
IV	ZCCHC9	IV	63.3	-0.0771	0.297
IV	RTCB	IV	54.9	0.06601	0.288
IV	NOM1	IV	60	-0.0819	0.273
IV	SAP18	IV	58	0.07634	0.272
IV	CRNKL1	III	50.7	0.06171	0.263
IV	REXO4	IV	61.3	-0.0868	0.255
IV	PNN	IV	58.5	0.0614	0.242
IV	RP9	III	51.1	0.04089	0.238
IV	LDHB	IV	54	0.06568	0.222
IV	ACIN1	IV	59.9	-0.0093	0.216
IV	CHD3	III	49.6	0.06471	0.212
IV	RNPS1	IV	63.3	-0.071	0.211
IV	NOP16	IV	65	-0.0537	0.205
IV	PUM3	IV	64.5	-0.065	0.200
IV	DDX24	IV	60.4	-0.0386	0.191
IV	HMCES	IV	53.8	0.04691	0.183
IV	RCL1	IV	56.8	0.04098	0.182
IV	LARP7	IV	50.9	0.04737	0.178
IV	ZC3H14	IV	64.1	-0.0094	0.177
IV	FAM98B	IV	57.4	0.01062	0.174
IV	ALKBH5	IV	63.3	-0.0519	0.170
IV	PTBP3	III	54.2	-0.0303	0.169
IV	ZC3H11A	V	70.9	-0.049	0.169
IV	SNRPD1	III	54.3	-0.0091	0.165
IV	TRMT6	IV	57.1	0.02474	0.158
IV	EXOSC9	IV	56.6	-0.0435	0.156
IV	EXOSC10	IV	62.3	-0.0485	0.150
IV	TPR	III	48.8	0.04877	0.143
IV	DNTTIP2	III	54.7	-0.0027	0.142
IV	NIFK	IV	57.1	0.0082	0.137
IV	NOL9	III	50.6	0.0056	0.134
IV	PNPT1	IV	58.7	-0.0362	0.131
IV	DHX37	IV	54.8	0.04321	0.126
IV	RC3H1	V	64.8	-0.0349	0.118
IV	DHX38	III	53.9	0.02241	0.108
IV	RSL24D1	IV	58.8	0.02089	0.106
IV	SURF6	IV	59.8	-0.0199	0.100
IV	EXOSC4	IV	58.2	0.00264	0.091
IV	NAT10	IV	52.8	0.02655	0.083
IV	NOP2	IV	60.4	-0.026	0.082
IV	MYBBP1A	III	52.7	0.02567	0.077
IV	BRIX1	IV	56.4	-0.0086	0.076
IV	YTHDC1	IV	56.6	0.00307	0.073
IV	DDX52	IV	52.3	-0.0072	0.068
IV	AATF	IV	52.3	0.01654	0.064
IV	SRPK1	IV	53.2	0.00297	0.054
IV	NGDN	IV	57.2	-0.0179	0.054
IV	PA2G4	IV	54.3	-0.0098	0.052
IV	NSUN5	IV	57.3	0.00987	0.043
IV	NPM1	IV	56.4	-0.0035	0.018
V	MTREX	IV	55.5	0.24664	0.738
V	TOP3B	V	63.4	0.16881	0.501
V	TEX10	IV	68.4	0.12074	0.428
V	NOC3L	IV	62.5	0.09964	0.410
V	RPF2	IV	58.3	0.13129	0.405
V	FTSJ3	IV	60.3	0.12641	0.402
V	CCDC9	V	68.9	0.08714	0.360
V	MSI2	V	88.8	-0.0866	0.357
V	TRIM56	V	68.8	0.09396	0.322
V	DDX54	IV	63	0.09625	0.314
V	PRRC2B	V	70.7	0.05724	0.310
V	NOL12	V	68.3	0.08278	0.305
V	SPATS2L	V	69.4	-0.04	0.297
V	CCDC137	IV	62.1	0.01521	0.281
V	POLDIP3	V	82.2	-0.074	0.230
V	UPF3B	V	70.7	-0.0709	0.227
V	NCBP3	V	71.7	0.06355	0.220
V	TUT7	V	67.1	0.05912	0.217
V	DDX55	V	71.1	0.02508	0.213
V	SYNCRIP	V	74.1	-0.035	0.207
V	API5	V	69.5	0.01042	0.185
V	ALYREF	V	66.6	0.05577	0.185
V	MAP4	V	67	-0.0329	0.176
V	HELZ2	V	68	0.03019	0.170
V	SARNP	V	77.6	-0.0487	0.168
V	DDX1	V	71.9	0.03416	0.163
V	PTCD3	V	67	0.02092	0.162
V	NOP53	V	83.6	0.05135	0.151
V	TSNAX	V	75	-0.0438	0.145
V	NFX1	V	72.6	0.03937	0.139
V	MKRN2	V	65.9	0.01986	0.133
V	EIF4A3	V	69.9	-0.0436	0.126
V	MKI67	IV	62.2	0.00661	0.111
V	CHTOP	V	77.3	-0.0196	0.097
V	KPNA2	IV	54.6	0.01709	0.096
V	MAGOH	V	70.6	-0.0177	0.095
V	RBM8A	V	76.3	0.02107	0.090
V	FYTTD1	V	72	0.01795	0.089
V	GNL3	IV	67.4	0.02116	0.086
V	GTPBP4	V	75.2	0.02198	0.071
V	SLIRP	V	68.9	0.01264	0.064
V	DDX39B	V	68.1	-0.0101	0.044
V	KIF1C	V	78.3	-0.0072	0.043
V	PLEC	V	59.2	0.00934	0.032
VI	CCDC86	IV	64	0.32253	0.928
VI	ZC3H7B	IV	57.7	0.26841	0.851
VI	PRRC2A	V	76.4	0.24881	0.717
VI	GNL2	V	65.9	0.21966	0.683
VI	TDRD3	V	73.6	0.19319	0.580
VI	NUFIP2	VI	87.6	0.16977	0.508
VI	RBMS1	VI	91.9	0.16301	0.479
VI	DHX57	V	68.4	0.14696	0.462
VI	EDF1	V	82.8	0.15078	0.446
VI	PUM2	VI	110.4	-0.1428	0.420
VI	SDAD1	V	78.6	0.12177	0.384
VI	MEX3D	V	79.3	0.1062	0.338
VI	ATXN2L	VI	106.5	0.09864	0.288
VI	GNL3L	V	106.7	0.04632	0.284
VI	ATXN2	VI	107.6	0.08135	0.235
VI	STAU1	VI	109.4	-0.0414	0.211
VI	OASL	VI	96.6	0.0626	0.184
VI	EIF4H	VII	144.4	-0.0548	0.177
VI	CNBP	V	94.5	0.04062	0.161
VI	EIF2S1	VI	104.4	-0.0492	0.146
VI	YTHDF3	VI	112.6	-0.0448	0.135
VI	AGO2	VI	101.3	0.03723	0.109
VI	CASC3	V	82	0.02817	0.107
VI	CSDE1	VI	128	-0.0341	0.104
VI	EIF4A1	VI	89.3	0.02199	0.104
VI	EIF3G	VI	129.3	0.00201	0.103
VI	CPEB2	VI	109	0.03395	0.102
VI	UNK	VI	87.9	0.0274	0.101
VI	CPEB3	VI	104.4	0.02924	0.085
VI	PUM1	VI	99.9	0.01881	0.085
VI	CPEB4	VI	89	-0.0286	0.084
VI	AGO3	VI	91	0.01838	0.071
VI	EIF4G1	VI	106.7	0.01184	0.042
VI	LARP4	VI	123.3	0.00852	0.032
VI	OTUD4	VI	97.3	0.00318	0.023
VI	PABPC1	VI	121.6	-0.001	0.019

VI	YTHDF2	VI	112.1	0.00278	0.013
VII	LSM14B	V	68.5	0.35314	1.080
VII	FAM120C	V	68.4	0.33196	0.966
VII	PURB	V	75.9	0.29207	0.845
VII	STAU2	V	74.2	0.28439	0.827
VII	UBAP2L	V	86.3	0.23182	0.723
VII	FAM120A	V	82.1	0.23827	0.708
VII	PYM1	VI	87.2	0.21211	0.665
VII	LARP4B	VI	88	0.21476	0.662
VII	ZNFX1	V	87.9	0.19828	0.590
VII	USP10	VI	102.6	0.16231	0.471
VII	UBAP2	VI	114.9	0.15809	0.464
VII	EIF4B	VI	116.9	0.1238	0.373
VII	YBX1	VI	105.9	0.1219	0.354
VII	IGF2BP3	VI	107.1	0.1084	0.342
VII	LSG1	VI	83.5	0.10981	0.336
VII	EIF3CL	VI	108.3	0.10442	0.324
VII	ZC3HAV1	VI	98.5	0.10995	0.320
VII	IGF2BP2	VI	106.9	0.10332	0.313
VII	G3BP2	VI	119.6	0.10586	0.307
VII	PRRC2C	VI	107	0.10317	0.302
VII	EIF3L	VI	108.4	0.0848	0.284
VII	FXR1	VI	138.3	0.09015	0.263
VII	MOV10	VII	217.3	0.03518	0.229
VII	SND1	VI	100.1	0.06515	0.228
VII	EIF3D	VII	235.4	-0.0448	0.224
VII	SERBP1	VII	197.9	0.07631	0.222
VII	PURA	VI	133.8	0.0659	0.222
VII	HDLBP	VII	140.5	0.03487	0.201
VII	YTHDC2	VI	144.4	0.05182	0.183
VII	G3BP1	VII	209.7	0.04701	0.137
VII	FMR1	VII	166.2	0.04163	0.124
VII	FXR2	VII	193.7	0.01564	0.098
VII	PABPC4	VI	130	0.02546	0.097
VII	EIF4G2	VII	200.9	0.02789	0.092
VII	DDX3X	VI	128.3	-0.0066	0.091
VII	EIF3A	VII	213.6	0.02315	0.079
VII	LARP1	VII	249.8	-0.0158	0.064
VII	YBX3	VI	131.6	0.01832	0.054
VII	CAPRIN1	VII	188.6	0.00714	0.047
VII	LSM14A	VI	130.6	0.00994	0.036
VII	UPF1	VII	157.6	0.01131	0.035
VII	YTHDF1	VII	222.7	-0.0094	0.034
VII	IGF2BP1	VII	140.4	-0.0015	0.024

Table 2.6 Accuracy of mRNA binding dynamics prediction using GO annotations

Sequence ID	
IVT_A10	GATGGCTTCCAAGGTGTACGACCCCGAGCAAGCTGACTCATAGATAGCACTACACACTCTGACAGAC AGTGTCATGCACACGGATCCCTAGATACTGCACTCAGAGTATGTGATGTCTAGATGTAGCTGTACACT CTATGTCTCATGATAGCATGATGCAGATGAGACTCATCTACTGATCTATAGAGCCGG
IVT_A30	GATGGCTTCCAAGGTGTACGACCCCGAGCAAGCTGACTCATAGATAGCACTACACACTCTGACAGAC AGTGTCATGCACACGGATCCTGCACTACAGAGACAGTAGTGTGAGCAGATATGTATGACTACGTAGCA TACGCTATGACTGACGAGCATATATATGATATGAGACTAGTGTATCACTGTAGCCGG
IVT_A60	GATGGCTTCCAAGGTGTACGACCCCGAGCAAGCTGACTCATAGATAGCACTACACACTCTGACAGAC AGTGTCATGCACACGGATCCCTCTCGCATAGACATCTCTGTAGTCTGCTCAGAGCGTGTCTCTGCATGA GTATATGTGTGTAGAGACTACTGTGCTGATACATATATACATAGACTGAGCGCCGG
IVT_A90	GATGGCTTCCAAGGTGTACGACCCCGAGCAAGCTGACTCATAGATAGCACTACACACTCTGACAGAC AGTGTCATGCACACGGATCCGACACAGTGCTCTATGCTGTCTGTATCTATCTGAGTATAGCTAGTCTAC TCAGAGATCTCATCACAGTGCACATATATGACATACAGTCTGATCTCATGTGCCGG
IVT_A120	GATGGCTTCCAAGGTGTACGACCCCGAGCAAGCTGACTCATAGATAGCACTACACACTCTGACAGAC AGTGTCATGCACACGGATCCGACATGAGTCTATGATCTGTGATGTGCGTGACTATCTGCAGCTCATACT CTGTGTATCATGATCACTCAGCATGAGATCTATGTGTCATCTGAGAGACAGGCCGG
IVT_A150	GATGGCTTCCAAGGTGTACGACCCCGAGCAAGCTGACTCATAGATAGCACTACACACTCTGACAGAC AGTGTCATGCACACGGATCCGCATGCTCATAGTCACTGTGCACACTATATACAGATGTGTGACATGCA GCGTAGAGACATCAGCACAGACATATATCTGAGTATGACTCGTATCATCTGCGCCGG
IVT_A180	GATGGCTTCCAAGGTGTACGACCCCGAGCAAGCTGACTCATAGATAGCACTACACACTCTGACAGAC AGTGTCATGCACACGGATCCTCTCGCTATCTGTCAGTGTACACAGCTCTACTACAGCTCACACTCTAGT CTCATCTACGACAGATCTATGTGTGATATATGTAGTCTAGCAGTGCTCTGAGCCGG

Sequencing adaptors	
Read 1 3′ adaptor	AAGTCGGAGGCCAAGCGGTCTTAGGAAGACAA
Read 2 3′ adaptor	AAGTCGGATCGTAGCCATGTCGTTCTGTGAGCCAAGGAGTTG

qPCR primer	
18S_fwd	CTCAACACGGGAAACCTCAC
18S_rev	CGCTCCACCAACTAAGAACG
28S_fwd	CTAAATACCGGCACGAGACC
28S_rev	TTCACGCCCTCTTGAACTCT
CHAC1_fwd	GTGTGGTGACGCTCCTTGAA
CHAC1_rev	ACTTCAGGGCCTTGCTTACC
CSPG4_fwd	GCTGCAGCTCTACTCTGGAC
CSPG4_rev	GATGGAGTCACTCAGCAGCG
GAPDH_fwd	GTGGAGATTGTTGCCATCAACGA
GAPDH_rev	CCCATTCTCGGCCTTGACTGT
HSPA1A_fwd	CCCCACCATTGAGGAGGTAG
HSPA1A_rev	AGGAAATGCAAAGTCTTGAAGCTC
PCBP1_fwd	GGACAACACACCATTTCTCCGC
PCBP1_rev	AGCCTTTCACCTCTGGAGAGCT
PCNA_fwd	GCCAGAGCTCTTCCCTTACG
PCNA_rev	TAGCTGGTTTCGGCTTCAGG
PLOD2_fwd	GACAGCGTTCTCTTCGTCCTCA
PLOD2_rev	CTCCAGCCTTTTCGTGGTGACT
SLC7A11_fwd	TGCCCAGATATGCATCGTCC
SLC7A11_rev	GAGGGAAAGGGCAACCATGA
SPINK4_fwd	TGTTGTGGACAGGGAAGTGC
SPINK4_rev	GCAGACCAGGTTGGACATCT

Table 2.7 Oligo and spike-in sequences utilized in this study

3. Conclusion

During the life cycle of mRNA, which includes processes such as transcription, processing, translation, and eventual decay, it interacts with a multitude of RNA-binding proteins (RBPs). These RBPs play a crucial role in determining the fate of mRNA, influencing not only its processing stages but also stability, localization, and functions. Therefore, understanding the mRNA interactome and its remodeling is essential for understanding mRNA.

In this study, a novel method was developed to investigate the mRNA binding dynamics of RBPs by combining metabolic labeling with RNA interactome capture method. mRNA binding dynamics of over 700 RBPs were identified over a 5-hour period following transcription. The sequence of peak binding times of these RBPs aligned with the order of mRNA life cycle, including co-transcriptional processing, splicing, nuclear export, and translation. By introducing a temporal dimension into previous studies on RBPs' localization, functions, and protein-protein interactions, we have significantly expanded understanding of mRNP remodeling and their roles in mRNA regulation. Notably, stress granule proteins exhibited late binding dynamics, suggesting their involvement in the terminal stage of the mRNA life cycle. Some RBPs such as CCDC86 and FAM120A/C displayed unexpected mRNA binding that deviated from their previously suggested functions. The mRNA binding dynamics uncovered in this study provide a critical basis for future investigations into the yet unknown functions and regulatory mechanisms of these proteins.

In conclusion, using a time-resolved mRNP capture method, this study has provided valuable insights into the molecular chronology of mRNP remodeling throughout the mRNA life cycle. It is anticipated that these findings will contribute

to further advancements in our understanding of mRNA regulation and cellular processes.

국문초록

mRNA-단백질 상호작용에 대한 시계열 분석

mRNA는 수많은 RNA 결합 단백질들과 결합하며 mRNA의 일생 동안 결합 단백질 조합은 지속적으로 변경된다. 하지만 이렇게 시간적으로 mRNA 결합 단백질의 종류와 조합이 변하는 것을 알고 있는데도 불구하고 지금까지 mRNA-단백질 복합체(mRNP)에 대한 연구는 어떤 단백질이 mRNA에 결합하는지에 대한 정보를 위주로 이뤄져 왔고 이러한 단백질들이 어떤 순서로 어떻게 결합하는지에 대해서는 많은 연구가 이뤄지지 않았다.

본 연구에서는 4-thiouridine을 이용한 RNA 표지법과 UVA 크로스링킹, RNA 분리 및 질량 분광법을 결합하여 mRNA의 일생동안 시간대별로 mRNA와 상호작용하는 단백질체에 대한 역학 데이터를 얻었다. 구체적으로는 mRNA가 전사되고 5시간이 지나기까지 10개의 시점 동안 700개 이상의 mRNA 결합 단백질의 변화를 정량적으로 관찰할 수 있었다. 이렇게 확인한 mRNA 결합 단백질들의 mRNA 결합 순서는 기존 연구들을 통해 일반적으로 알려진 단백질의 기능, 세포 내 위치 및 상호작용과 대체적으로 일치하였다. 흥미롭게도 stress granule과 바이러스 RNA에 연관된 단백질들이 오래된 시점까지 mRNA와 결합하는 것으로 발견되었으며 이는 이러한 단백질들이 mRNA 생명주기의 마지막 단계에서 아직 구체적으로 밝혀지지 않은 어떤 역할을 할 수도 있다는 것을 시사한다. 이 연구에서는 또한 기존에 연구되어 왔던 RNA 결합단백질들의 기능연구를 바탕으로 다양한 RNA 결합 단백질들의 mRNA의 결합 역학 예측값을 계산하고 이를 실제 관측한 mRNA 결합 역학값과 비교하였다. 이러한 비교를 통해 밝혀낸 예상치 못한 mRNA 결합 역학을 가진 다수의 RNA 결합 단백질들의 존재는 이 단백질들이 아직 알려지지 않은 기능과 조절 메커니즘을 가지고 있을 수도 있다는 것을 시사한다. 이 연구는 기존의 mRNA 결합 단백질체 데이터에 새롭게 시간적 차원을 도입함으로써 mRNP 리모델링에 대한 독특한 자원과 통찰력을 제공한다.

Bibliography

[1] Adusumilli, R. & Mallick, P. (2017). Data conversion with proteowizard msconvert. *Methods in molecular biology (Clifton, N.J.)*, 1550, 339–368.

[2] Alexa, A., Rahnenführer, J., & Lengauer, T. (2006). Improved scoring of functional groups from gene expression data by decorrelating go graph structure. *Bioinformatics (Oxford, England)*, 22, 1600–1607.

[3] Almada, A. E., Wu, X., Kriz, A. J., Burge, C. B., & Sharp, P. A. (2013). Promoter directionality is controlled by U1 snRNP and polyadenylation signals. *Nature*, 499(7458), 360–363.

[4] Ascano, M., Hafner, M., Cekan, P., Gerstberger, S., & Tuschl, T. (2012). Identification of rna-protein interaction networks using par-clip. *Wiley interdisciplinary reviews. RNA*, 3, 159–177.

[5] Baltz, A. G., Munschauer, M., Schwanhäusser, B., Vasile, A., Murakawa, Y., Schueler, M., Youngs, N., Penfold-Brown, D., Drew, K., Milek, M., Wyler, E., Bonneau, R., Selbach, M., Dieterich, C., & Landthaler, M. (2012). The mRNA-bound proteome and its global occupancy profile on protein-coding transcripts. *Mol. Cell*, 46(5), 674–690.

[6] Bao, X., Guo, X., Yin, M., Tariq, M., Lai, Y., Kanwal, S., Zhou, J., Li, N., Lv, Y., Pulido-Quetglas, C., Wang, X., Ji, L., Khan, M. J., Zhu, X., Luo, Z., Shao, C., Lim, D.-H., Liu, X., Li, N., Wang, W., He, M., Liu, Y.-L., Ward, C., Wang, T., Zhang, G., Wang, D., Yang, J., Chen, Y., Zhang, C., Jauch, R., Yang, Y.-G., Wang, Y., Qin, B., Anko, M.-L., Hutchins, A. P., Sun, H., Wang, H., Fu, X.-D., Zhang, B., & Esteban, M. A. (2018). Capturing the interactome of newly transcribed rna. *Nature methods*, 15, 213–220.

[7] Bidet, K., Dadlani, D., & Garcia-Blanco, M. A. (2014). G3BP1, G3BP2 and CAPRIN1 are required for translation of interferon stimulated mRNAs and are targeted by a dengue virus non-coding RNA. *PLoS Pathog.*, 10(7), e1004242.

[8] Bosco, D. A. (2018). Translation dysregulation in neurodegenerative disorders. *Proceedings of the National Academy of Sciences of the United States of America*, 115, 12842–12844.

[9] Castella, S., Bernard, R., Corno, M., Fradin, A., & Larcher, J.-C. (2015). Ilf3 and NF90 functions in RNA biology. *Wiley Interdiscip. Rev. RNA*, 6(2), 243–256.

[10] Castello, A., Fischer, B., Eichelbaum, K., Horos, R., Beckmann, B. M., Strein, C., Davey, N. E., Humphreys, D. T., Preiss, T., Steinmetz, L. M., Krijgsveld, J., & Hentze, M. W. (2012). Insights into RNA biology from an atlas of mammalian mRNA-binding proteins. *Cell*, 149(6), 1393–1406.

[11] Caudron-Herger, M., Jansen, R. E., Wassmer, E., & Diederichs, S. (2021). RBP2GO: a comprehensive pan-species database on RNA-binding proteins, their interactions and functions. *Nucleic Acids Res.*, 49(D1), D425–D436.

[12] Caudron-Herger, M., Rusin, S. F., Adamo, M. E., Seiler, J., Schmid, V. K., Barreau, E., Kettenbach, A. N., & Diederichs, S. (2019). R-deep: Proteome-wide and quantitative identification of rna-dependent proteins by density gradient ultracentrifugation. *Molecular cell*, 75, 184–199.e10.

[13] De Leeuw, F., Zhang, T., Wauquier, C., Huez, G., Kruys, V., & Gueydan, C. (2007). The cold-inducible rna-binding protein migrates from the nucleus to cytoplasmic stress granules by a methylation-dependent mechanism and acts as a translational repressor. *Experimental cell research*, 313, 4130–4144.

[14] Dobin, A., Davis, C. A., Schlesinger, F., Drenkow, J., Zaleski, C., Jha, S., Batut, P., Chaisson, M., & Gingeras, T. R. (2013). Star: ultrafast universal rna-seq aligner. *Bioinformatics (Oxford, England)*, 29, 15–21.

[15] Dreyfuss, G. (1986). Structure and function of nuclear and cytoplasmic ribonucleoprotein particles. *Annu. Rev. Cell Biol.*, 2, 459–498.

[16] Duffy, E. E., Schofield, J. A., & Simon, M. D. (2019). Gaining insight into transcriptome-wide RNA population dynamics through the chemistry of 4-thiouridine. *Wiley Interdiscip. Rev. RNA*, 10(1), e1513.

[17] Duffy, E. E. & Simon, M. D. (2016). Enriching s4 u-rna using methane thiosulfonate (mts) chemistry. *Current protocols in chemical biology*, 8, 234–250.

[18] Faustino, N. A. & Cooper, T. A. (2003). Pre-mrna splicing and human disease. *Genes development*, 17, 419–437.

[19] Finn, R. D., Bateman, A., Clements, J., Coggill, P., Eberhardt, R. Y., Eddy, S. R., Heger, A., Hetherington, K., Holm, L., Mistry, J., Sonnhammer, E. L. L., Tate, J., & Punta, M. (2014). Pfam: the protein families database. *Nucleic Acids Res.*, 42(Database issue), D222–30.

[20] Fu, K., Tian, S., Tan, H., Wang, C., Wang, H., Wang, M., Wang, Y., Chen, Z., Wang, Y., Yue, Q., Xu, Q., Zhang, S., Li, H., Xie, J., Lin, M., Luo, M., Chen, F., Ye, L., & Zheng, K. (2019). Biological and RNA regulatory function of MOV10 in mammalian germ cells. *BMC Biol.*, 17(1), 39.

[21] Fu, Y., Dominissini, D., Rechavi, G., & He, C. (2014). Gene expression regulation mediated through reversible m6a RNA methylation. *Nat. Rev. Genet.*, 15(5), 293–306.

[22] Gall, J. G. (1956). Small granules in the amphibian oocyte nucleus and their relationship to RNA. *J. Biophys. Biochem. Cytol.*, 2(4 Suppl), 393–396.

[23] Garcia-Moreno, M., Noerenberg, M., Ni, S., Järvelin, A. I., González-Almela, E., Lenz, C. E., Bach-Pages, M., Cox, V., Avolio, R., Davis, T., Hester, S., Sohier, T. J. M., Li, B., Heikel, G., Michlewski, G., Sanz, M. A., Carrasco, L., Ricci, E. P., Pelechano, V., Davis, I., Fischer, B., Mohammed, S., & Castello, A.

(2019). System-wide profiling of RNA-Binding proteins uncovers key regulators of virus infection. *Mol. Cell*, 74(1), 196–211.e11.

[24] Gerstberger, S., Hafner, M., & Tuschl, T. (2014). A census of human RNA-binding proteins. *Nat. Rev. Genet.*, 15(12), 829–845.

[25] Giurgiu, M., Reinhard, J., Brauner, B., Dunger-Kaltenbach, I., Fobo, G., Frishman, G., Montrone, C., & Ruepp, A. (2019). CORUM: the comprehensive resource of mammalian protein complexes-2019. *Nucleic Acids Res.*, 47(D1), D559–D563.

[26] Go, C. D., Knight, J. D. R., Rajasekharan, A., Rathod, B., Hesketh, G. G., Abe, K. T., Youn, J.-Y., Samavarchi-Tehrani, P., Zhang, H., Zhu, L. Y., Popiel, E., Lambert, J.-P., Coyaud, É., Cheung, S. W. T., Rajendran, D., Wong, C. J., Antonicka, H., Pelletier, L., Palazzo, A. F., Shoubridge, E. A., Raught, B., & Gingras, A.-C. (2021). A proximity-dependent biotinylation map of a human cell. *Nature*, 595(7865), 120–124.

[27] Grasso, G., Higuchi, T., Mac, V., Barbier, J., Helsmoortel, M., Lorenzi, C., Sanchez, G., Bello, M., Ritchie, W., Sakamoto, S., & Kiernan, R. (2020). NF90 modulates processing of a subset of human pri-miRNAs. *Nucleic Acids Res.*, 48(12), 6874–6888.

[28] Hafner, M., Landthaler, M., Burger, L., Khorshid, M., Hausser, J., Berninger, P., Rothballer, A., Ascano, Jr, M., Jungkamp, A.-C., Munschauer, M., Ulrich, A., Wardle, G. S., Dewell, S., Zavolan, M., & Tuschl, T. (2010). Transcriptome-wide identification of RNA-binding protein and microRNA target sites by PAR-CLIP. *Cell*, 141(1), 129–141.

[29] Herzog, V. A., Reichholf, B., Neumann, T., Rescheneder, P., Bhat, P., Burkard, T. R., Wlotzka, W., von Haeseler, A., Zuber, J., & Ameres, S. L. (2017). Thiol-linked alkylation of rna to assess expression dynamics. *Nature methods*, 14, 1198–1204.

[30] Huang, Y., Gattoni, R., Stévenin, J., & Steitz, J. A. (2003). Sr splicing factors serve as adapter proteins for tap-dependent mrna export. *Molecular cell*, 11, 837–843.

[31] Iselin, L., Palmalux, N., Kamel, W., Simmonds, P., Mohammed, S., & Castello, A. (2022). Uncovering viral RNA-host cell interactions on a proteome-wide scale. *Trends Biochem. Sci.*, 47(1), 23–38.

[32] Jain, S., Wheeler, J. R., Walters, R. W., Agrawal, A., Barsic, A., & Parker, R. (2016). ATPase-Modulated stress granules contain a diverse proteome and substructure. *Cell*, 164(3), 487–498.

[33] Jelínek, O. & Tāle, I. A. (1975). Thermoluminescence and long afterglow of adenine in the solid state. 10, 371–379.

[34] Jiang, X., Liu, B., Nie, Z., Duan, L., Xiong, Q., Jin, Z., Yang, C., & Chen, Y. (2021). The role of m6a modification in the biological functions and diseases. *Signal transduction and targeted therapy*, 6, 74.

[35] Kamieniarz-Gdula, K. & Proudfoot, N. J. (2019). Transcriptional control by premature termination: A forgotten mechanism. *Trends Genet.*, 35(8), 553–564.

[36] Kelly, T. J., Suzuki, H. I., Zamudio, J. R., Suzuki, M., & Sharp, P. A. (2019). Sequestration of microRNA-mediated target repression by the ago2-associated RNA-binding protein FAM120A. *RNA*, 25(10), 1291–1297.

[37] Kenny, P. J., Zhou, H., Kim, M., Skariah, G., Khetani, R. S., Drnevich, J., Arcila, M. L., Kosik, K. S., & Ceman, S. (2014). MOV10 and FMRP regulate AGO2 association with microRNA recognition elements. *Cell Rep.*, 9(5), 1729–1741.

[38] Kim, B., Arcos, S., Rothamel, K., Jian, J., Rose, K. L., McDonald, W. H., Bian, Y., Reasoner, S., Barrows, N. J., Bradrick, S., Garcia-Blanco, M. A., & Ascano, M. (2020). Discovery of widespread host protein interactions with the pre-replicated genome of CHIKV using VIR-CLASP. *Mol. Cell*, 78(4), 624–640.e7.

[Kim et al.] Kim, S., Kim, S., Chang, H. R., Kim, D., Park, J., Son, N., Park, J., Yoon, M., Chae, G., Kim, Y.-K., Kim, V. N., Kim, Y. K., Nam, J.-W., Shin, C., & Baek, D. The regulatory impact of rna-binding proteins on microrna targeting. 12.

[40] Kim, S. & Pevzner, P. A. (2014). Ms-gf+ makes progress towards a universal database search tool for proteomics. *Nature communications*, 5, 5277.

[41] Kim, V. N., Kataoka, N., & Dreyfuss, G. (2001). Role of the nonsense-mediated decay factor hupf3 in the splicing-dependent exon-exon junction complex. *Science (New York, N.Y.)*, 293, 1832–1836.

[42] Kleiner, R. E. (2021). Interrogating the transcriptome with metabolically incorporated ribonucleosides. *Mol Omics*, 17(6), 833–841.

[43] Knoener, R., Evans, 3rd, E., Becker, J. T., Scalf, M., Benner, B., Sherer, N. M., & Smith, L. M. (2021). Identification of host proteins differentially associated with HIV-1 RNA splice variants. *Elife*, 10.

[44] Kobayashi, Y., Suzuki, K., Kobayashi, H., Ohashi, S., Koike, K., Macchi, P., Kiebler, M., & Anzai, K. (2008). C9orf10 protein, a novel protein component of puralpha-containing mRNA-protein particles (Puralpha-mRNPs): characterization of developmental and regional expressions in the mouse brain. *J. Histochem. Cytochem.*, 56(8), 723–731.

[45] Lee, S., Lee, Y.-S., Choi, Y., Son, A., Park, Y., Lee, K.-M., Kim, J., Kim, J.-S., & Narry Kim, V. (2021). The SARS-CoV-2 RNA interactome.

[46] Lee, S. C.-W. & Abdel-Wahab, O. (2016). Therapeutic targeting of splicing in cancer. *Nature medicine*, 22, 976–986.

[47] Li, B. & Dewey, C. N. (2011). Rsem: accurate transcript quantification from rna-seq data with or without a reference genome. *BMC bioinformatics*, 12, 323.

[48] Mallam, A. L., Sae-Lee, W., Schaub, J. M., Tu, F., Battenhouse, A., Jang, Y. J., Kim, J., Wallingford, J. B., Finkelstein, I. J., Marcotte, E. M., & Drew, K.

(2019). Systematic discovery of endogenous human ribonucleoprotein complexes. *Cell Rep.*, 29(5), 1351–1368.e5.

[49] Markmiller, S., Soltanieh, S., Server, K. L., Mak, R., Jin, W., Fang, M. Y., Luo, E.-C., Krach, F., Yang, D., Sen, A., Fulzele, A., Wozniak, J. M., Gonzalez, D. J., Kankel, M. W., Gao, F.-B., Bennett, E. J., Lécuyer, E., & Yeo, G. W. (2018). Context-Dependent and Disease-Specific diversity in protein interactions within stress granules. *Cell*, 172(3), 590–604.e13.

[Martin] Martin, M. Cutadapt removes adapter sequences from high-throughput sequencing reads. 17, 10.

[51] Mateju, D., Eichenberger, B., Voigt, F., Eglinger, J., Roth, G., & Chao, J. A. (2020). Single-molecule imaging reveals translation of mrnas localized to stress granules. *Cell*, 183, 1801–1812.e13.

[52] Mitchell, S. F. & Parker, R. (2014). Principles and properties of eukaryotic mRNPs. *Mol. Cell*, 54(4), 547–558.

[53] Mor, A., Suliman, S., Ben-Yishay, R., Yunger, S., Brody, Y., & Shav-Tal, Y. (2010). Dynamics of single mRNP nucleocytoplasmic transport and export through the nuclear pore in living cells. *Nat. Cell Biol.*, 12(6), 543–552.

[54] Moy, T. I., Boettner, D., Rhodes, J. C., Silver, P. A., & Askew, D. S. (2002). Identification of a role for saccharomyces cerevisiae cgr1p in pre-rrna processing and 60s ribosome subunit synthesis. *Microbiology (Reading, England)*, 148, 1081–1090.

[55] Onomoto, K., Yoneyama, M., Fung, G., Kato, H., & Fujita, T. (2014). Antiviral innate immunity and stress granule responses. *Trends Immunol.*, 35(9), 420–428.

[56] Ooi, Y. S., Majzoub, K., Flynn, R. A., Mata, M. A., Diep, J., Li, J. K., van Buuren, N., Rumachik, N., Johnson, A. G., Puschnik, A. S., Marceau, C. D., Mlera, L., Grabowski, J. M., Kirkegaard, K., Bloom, M. E., Sarnow, P.,

Bertozzi, C. R., & Carette, J. E. (2019). An RNA-centric dissection of host complexes controlling flavivirus infection. *Nat Microbiol*, 4(12), 2369–2382.

[57] Perez-Perri, J. I., Rogell, B., Schwarzl, T., Stein, F., Zhou, Y., Rettel, M., Brosig, A., & Hentze, M. W. (2018). Discovery of RNA-binding proteins and characterization of their dynamic responses by enhanced RNA interactome capture. *Nat. Commun.*, 9(1), 4408.

[58] Perez-Riverol, Y., Csordas, A., Bai, J., Bernal-Llinares, M., Hewapathirana, S., Kundu, D. J., Inuganti, A., Griss, J., Mayer, G., Eisenacher, M., Pérez, E., Uszkoreit, J., Pfeuffer, J., Sachsenberg, T., Yilmaz, S., Tiwary, S., Cox, J., Audain, E., Walzer, M., Jarnuczak, A. F., Ternent, T., Brazma, A., & Vizcaíno, J. A. (2019). The pride database and related tools and resources in 2019: improving support for quantification data. *Nucleic acids research*, 47, D442–D450.

[59] Poole, W., Gibbs, D. L., Shmulevich, I., Bernard, B., & Knijnenburg, T. A. (2016). Combining dependent p-values with an empirical adaptation of brown's method. *Bioinformatics (Oxford, England)*, 32, i430–i436.

[60] Queiroz, R. M. L., Smith, T., Villanueva, E., Marti-Solano, M., Monti, M., Pizzinga, M., Mirea, D.-M., Ramakrishna, M., Harvey, R. F., Dezi, V., Thomas, G. H., Willis, A. E., & Lilley, K. S. (2019). Comprehensive identification of rna-protein interactions in any organism using orthogonal organic phase separation (oops). *Nature biotechnology*, 37, 169–178.

[61] Quinlan, A. R. & Hall, I. M. (2010). Bedtools: a flexible suite of utilities for comparing genomic features. *Bioinformatics (Oxford, England)*, 26, 841–842.

[62] Replogle, J. M., Saunders, R. A., Pogson, A. N., Hussmann, J. A., Lenail, A., Guna, A., Mascibroda, L., Wagner, E. J., Adelman, K., Lithwick-Yanai, G., Iremadze, N., Oberstrass, F., Lipson, D., Bonnar, J. L., Jost, M., Norman, T. M., & Weissman, J. S. (2022). Mapping information-rich genotype-phenotype landscapes with genome-scale perturb-seq. *Cell*, 185, 2559–2575.e28.

[63] Schlautmann, L. P. & Gehring, N. H. (2020). A day in the life of the exon junction complex. *Biomolecules*, 10.

[64] Schmidt, E. K., Clavarino, G., Ceppi, M., & Pierre, P. (2009). Sunset, a nonradioactive method to monitor protein synthesis. *Nature methods*, 6, 275–277.

[65] Silvera, D., Formenti, S. C., & Schneider, R. J. (2010). Translational control in cancer. *Nature reviews. Cancer*, 10, 254–266.

[66] Singh, G., Pratt, G., Yeo, G. W., & Moore, M. J. (2015). The clothes make the mrna: Past and present trends in mrnp fashion. *Annual review of biochemistry*, 84, 325–354.

[67] Stark, C., Breitkreutz, B.-J., Reguly, T., Boucher, L., Breitkreutz, A., & Tyers, M. (2006). Biogrid: a general repository for interaction datasets. *Nucleic acids research*, 34, D535–D539.

[68] Svitkin, Y. V., Yanagiya, A., Karetnikov, A. E., Alain, T., Fabian, M. R., Khoutorsky, A., Perreault, S., Topisirovic, I., & Sonenberg, N. (2013). Control of translation and miRNA-dependent repression by a novel poly(a) binding protein, hnRNP-Q. *PLoS Biol.*, 11(5), e1001564.

[69] Sysoev, V. O., Fischer, B., Frese, C. K., Gupta, I., Krijgsveld, J., Hentze, M. W., Castello, A., & Ephrussi, A. (2016). Global changes of the RNA-bound proteome during the maternal-to-zygotic transition in drosophila. *Nat. Commun.*, 7, 12128.

[70] Tafforeau, L., Zorbas, C., Langhendries, J.-L., Mullineux, S.-T., Stamatopoulou, V., Mullier, R., Wacheul, L., & Lafontaine, D. L. J. (2013). The complexity of human ribosome biogenesis revealed by systematic nucleolar screening of pre-rrna processing factors. *Molecular cell*, 51, 539–551.

[71] Tanaka, M., Sasaki, K., Kamata, R., Hoshino, Y., Yanagihara, K., & Sakai, R. (2009). A novel RNA-binding protein, Ossa/C9orf10, regulates activity of

src kinases to protect cells from oxidative stress-induced apoptosis. *Mol. Cell. Biol.*, 29(2), 402–413.

[72] Tang, P., Yang, Y., Li, G., Huang, L., Wen, M., Ruan, W., Guo, X., Zhang, C., Zuo, X., Luo, D., Xu, Y., Fu, X.-D., & Zhou, Y. (2022). Alternative polyadenylation by sequential activation of distal and proximal polya sites. *Nature structural molecular biology*, 29, 21–31.

[73] Tani, H., Mizutani, R., Salam, K. A., Tano, K., Ijiri, K., Wakamatsu, A., Isogai, T., Suzuki, Y., & Akimitsu, N. (2012). Genome-wide determination of RNA stability reveals hundreds of short-lived noncoding transcripts in mammals. *Genome Res.*, 22(5), 947–956.

[74] Thompson, A., Schäfer, J., Kuhn, K., Kienle, S., Schwarz, J., Schmidt, G., Neumann, T., Johnstone, R., Mohammed, A. K. A., & Hamon, C. (2003). Tandem mass tags: a novel quantification strategy for comparative analysis of complex protein mixtures by MS/MS. *Anal. Chem.*, 75(8), 1895–1904.

[75] Thul, P. J., Åkesson, L., Wiking, M., Mahdessian, D., Geladaki, A., Ait Blal, H., Alm, T., Asplund, A., Björk, L., Breckels, L. M., Bäckström, A., Danielsson, F., Fagerberg, L., Fall, J., Gatto, L., Gnann, C., Hober, S., Hjelmare, M., Johansson, F., Lee, S., Lindskog, C., Mulder, J., Mulvey, C. M., Nilsson, P., Oksvold, P., Rockberg, J., Schutten, R., Schwenk, J. M., Sivertsson, Å., Sjöstedt, E., Skogs, M., Stadler, C., Sullivan, D. P., Tegel, H., Winsnes, C., Zhang, C., Zwahlen, M., Mardinoglu, A., Pontén, F., von Feilitzen, K., Lilley, K. S., Uhlén, M., & Lundberg, E. (2017). A subcellular map of the human proteome. *Science*, 356(6340).

[76] Ting, L., Rad, R., Gygi, S. P., & Haas, W. (2011). MS3 eliminates ratio distortion in isobaric multiplexed quantitative proteomics. *Nat. Methods*, 8(11), 937–940.

[77] Trendel, J., Schwarzl, T., Horos, R., Prakash, A., Bateman, A., Hentze, M. W., & Krijgsveld, J. (2019). The human rna-binding proteome and its dynamics during translational arrest. *Cell*, 176, 391–403.e19.

[78] Uhlén, M., Fagerberg, L., Hallström, B. M., Lindskog, C., Oksvold, P., Mardinoglu, A., Sivertsson, , Kampf, C., Sjöstedt, E., Asplund, A., Olsson, I., Edlund, K., Lundberg, E., Navani, S., Szigyarto, C. A.-K., Odeberg, J., Djureinovic, D., Takanen, J. O., Hober, S., Alm, T., Edqvist, P.-H., Berling, H., Tegel, H., Mulder, J., Rockberg, J., Nilsson, P., Schwenk, J. M., Hamsten, M., von Feilitzen, K., Forsberg, M., Persson, L., Johansson, F., Zwahlen, M., von Heijne, G., Nielsen, J., & Pontén, F. (2015). Proteomics. tissue-based map of the human proteome. *Science (New York, N.Y.)*, 347, 1260419.

[79] Van Nostrand, E. L., Freese, P., Pratt, G. A., Wang, X., Wei, X., Xiao, R., Blue, S. M., Chen, J.-Y., Cody, N. A. L., Dominguez, D., Olson, S., Sundararaman, B., Zhan, L., Bazile, C., Bouvrette, L. P. B., Bergalet, J., Duff, M. O., Garcia, K. E., Gelboin-Burkhart, C., Hochman, M., Lambert, N. J., Li, H., McGurk, M. P., Nguyen, T. B., Palden, T., Rabano, I., Sathe, S., Stanton, R., Su, A., Wang, R., Yee, B. A., Zhou, B., Louie, A. L., Aigner, S., Fu, X.-D., Lécuyer, E., Burge, C. B., Graveley, B. R., & Yeo, G. W. (2020a). A large-scale binding and functional map of human RNA-binding proteins. *Nature*, 583(7818), 711–719.

[80] Van Nostrand, E. L., Pratt, G. A., Shishkin, A. A., Gelboin-Burkhart, C., Fang, M. Y., Sundararaman, B., Blue, S. M., Nguyen, T. B., Surka, C., Elkins, K., Stanton, R., Rigo, F., Guttman, M., & Yeo, G. W. (2016). Robust transcriptome-wide discovery of RNA-binding protein binding sites with enhanced CLIP (eCLIP). *Nat. Methods*, 13(6), 508–514.

[81] Van Nostrand, E. L., Pratt, G. A., Yee, B. A., Wheeler, E. C., Blue, S. M., Mueller, J., Park, S. S., Garcia, K. E., Gelboin-Burkhart, C., Nguyen, T. B., Rabano, I., Stanton, R., Sundararaman, B., Wang, R., Fu, X.-D., Graveley, B. R., & Yeo, G. W. (2020b). Principles of RNA processing from analysis of enhanced CLIP maps for 150 RNA binding proteins. *Genome Biol.*, 21(1), 90.

[82] Weidensdorfer, D., Stöhr, N., Baude, A., Lederer, M., Köhn, M., Schierhorn, A., Buchmeier, S., Wahle, E., & Hüttelmaier, S. (2009). Control of c-myc mRNA stability by IGF2BP1-associated cytoplasmic RNPs. *RNA*, 15(1), 104–115.

[83] Wellmann, S., Bührer, C., Moderegger, E., Zelmer, A., Kirschner, R., Koehne, P., Fujita, J., & Seeger, K. (2004). Oxygen-regulated expression of the rna-binding proteins rbm3 and cirp by a hif-1-independent mechanism. *Journal of cell science*, 117, 1785–1794.

[84] Yang, C. & Carrier, F. (2001). The UV-inducible RNA-binding protein A18 (a18 hnRNP) plays a protective role in the genotoxic stress response. *J. Biol. Chem.*, 276(50), 47277–47284.

[85] Yang, P., Mathieu, C., Kolaitis, R.-M., Zhang, P., Messing, J., Yurtsever, U., Yang, Z., Wu, J., Li, Y., Pan, Q., Yu, J., Martin, E. W., Mittag, T., Kim, H. J., & Taylor, J. P. (2020). G3BP1 is a tunable switch that triggers phase separation to assemble stress granules. *Cell*, 181(2), 325–345.e28.

[86] Youn, J.-Y., Dyakov, B. J. A., Zhang, J., Knight, J. D. R., Vernon, R. M., Forman-Kay, J. D., & Gingras, A.-C. (2019). Properties of stress granule and P-Body proteomes. *Mol. Cell*, 76(2), 286–294.

[87] Zhang, Z., Liu, T., Dong, H., Li, J., Sun, H., Qian, X., & Qin, W. (2021). An RNA tagging approach for system-wide RNA-binding proteome profiling and dynamics investigation upon transcription inhibition. *Nucleic Acids Res.*, 49(11), e65.

[88] Zhou, Z., Luo, M. J., Straesser, K., Katahira, J., Hurt, E., & Reed, R. (2000). The protein aly links pre-messenger-rna splicing to nuclear export in metazoans. *Nature*, 407, 401–405.

[89] Zhu, Y., Orre, L. M., Tran, Y. Z., Mermelekas, G., Johansson, H. J., Malyutina, A., Anders, S., & Lehtiö, J. (2020). Deqms: A method for accurate variance estimation in differential protein expression analysis. 19, 1047–1057.

감 사 의 글

박사 학위 과정을 졸업 논문으로 남기며 제 인생에서 짧지도, 길지도 않았던 7년의 지난한 시간들이 비로소 마무리되는 것 같습니다. 때로는 후회하고 좌절하기도 했지만 결국 새로이 알아가는 즐거움과 내가 쌓아온 시간에 대한 뿌듯함 덕분에 이렇게 박사 학위 논문을 작성하는 순간까지 도달할 수 있었던 것 같습니다. 지금까지 많은 사람들의 도움이 있어 미숙했던 제가 한 사람의 박사로 성장할 수 있었기에 이 자리를 빌려 짧게나마 감사의 마음을 기록하고자 합니다.

먼저 제 연구 생활을 시작했을 때부터 오랫동안 지원해주신 지도교수님이신 김빛내리 교수님과 그 동안 저와 인연을 맺었던 많은 연구실 선후배님들과 대학원 동기들에게도 감사드립니다. 처음 자연대라는 낯선 환경에서 낯선 공부를 시작할 때 이 분들의 조언과 지지가 무엇보다도 큰 힘이 되었습니다. 또한 바쁘신 와중에도 저의 박사 학위 심사를 맡아주신 노유선 교수님, 이현우 교수님, 장혜식 교수님, 김유식 교수님, 김종서 교수님께도 진심으로 감사의 인사를 드립니다.

나보다도 더 나를 믿어주고 응원해준 친구들과 나리, 민영언니, 한결이에게도 감사의 인사를 하고 싶습니다. 훌륭한 이들 곁에서 부끄럽지 않은 친구로 남을 수 있도록 더 열심히 살겠습니다.

연구실 생활에서 때로는 날카로운 비평을 해주는 연구자로 때로는 따뜻한 이해자로서 제 곁을 지켜준 남편, 김동완 박사에게도 감사의 인사를 전합니다. 앞으로도 서로 이해하고 존중하는 동반자로서 함께 살아갈 수 있도록 저도 더 노력하도록 하겠습니다. 남편과 함께 새로운 가족이 되어 응원해주신 시부모님과 가족들에게도 감사드립니다.

마지막으로 사랑하는 저의 가족에게 고맙다는 말을 하고 싶습니다. 제가 세상에서 가장 존경하는 엄훈, 장효순 두 분의 박사님 덕분에 연구를 시작하고 여기까지 올 수 있었습니다. 학위 과정을 겪고 나서야 부모님이 저를 아끼고 사랑하며 길러주셨기에 제가 모든 힘든 과정들을 견뎌내고 이겨낼 수 있었다는 걸 깨달을 수

있었습니다. 학위 과정을 시작할 때만 해도 초등학생이었는데 어느새 자라 제 든든한 지지자가 된 두 동생, 재형이와 재연이에게도 고맙다는 말을 하고 싶습니다. 무엇보다도 저의 대학원 진학을 가장 많이 응원해주셨던 아빠에게 기쁜 마음으로 박사가 되었음을 말하고 가족들 모두 함께 그 사실을 즐길 수 있어 감사합니다.

지금의 제가 있도록 도움을 주신 모든 분들께 감사드리며 이 논문을 마칩니다.

엄부연 올림